SCAPHOID FRACTURES

INCREASING DIAGNOSTIC EFFICIENCY AND TREATMENT FUNCTIONALITY

Anne Eva J. Bulstra

SCAPHOID FRACTURES

INCREASING DIAGNOSTIC EFFICIENCY AND TREATMENT FUNCTIONALITY

Anne Eva J. Bulstra

Provided by thesis specialist Ridderprint, ridderprint.nl

Printing Ridderprint
Layout and design Indah Hijmans, persoonlijkproefschrift.nl
Cover design Anne Eva en Diederick Bulstra

The research described in this thesis was supported by grants from Flinders University, Amsterdam UMC - Department of Orthopaedic Surgery, Prins Bernhard Cultuurfonds, Marti-Keuning Eckhardt Stichting, Stichting Prof. Michaël-van Vloten Fonds, Traumaplatform, Anna Fonds, Jo Kolk Studiefonds, KNAW van Leersum Beurs.

Printing of this thesis was financially supported by Amsterdam UMC, Department of Orthopaedic Surgery, Nederlandse Vereniging van Plastische Chirurgie, Traumaplatform, Chipsoft, Flinders University, ABN AMRO, Anna Fonds

SCAPHOID FRACTURES

INCREASING DIAGNOSTIC EFFICIENCY AND TREATMENT FUNCTIONALITY

ACADEMISCH PROEFSCHRIFT

ter verkrijging van de graad van doctor
aan de Universiteit van Amsterdam
op gezag van de Rector Magnificus
prof. dr. ir. P.P.C.C. Verbeek
ten overstaan van een door het College voor Promoties ingestelde commissie,
in het openbaar te verdedigen in de Agnietenkapel
op vrijdag 9 februari 2024, te 16.00 uur

door

Anne Eva Juliette Bulstra
geboren te Apeldoorn

Promotiecommissie

Promotores:	prof. dr. G.M.M.J. Kerkhoffs	AMC-UvA
	prof. dr. R.L. Jaarsma	Flinders University
Copromotores:	dr. M.C. Obdeijn	AMC-UvA
	prof. dr. J.N. Doornberg	Rijksuniversiteit Groningen
Overige leden:	prof. dr. M.J.P.F. Ritt	Vrije Universiteit Amsterdam
	dr. H.A. Rakhorst	Medisch Spectrum Twente
	prof. dr. M. Maas	AMC-UvA
	dr. C.M. Lameijer	AMC-UvA
	prof. dr. B.J. van Royen	Vrije Universiteit Amsterdam
	prof. dr. J.A.M. Bramer	AMC-UvA

Faculteit der Geneeskunde

Dit proefschrift is tot stand gekomen binnen een samenwerkingsverband tussen de Universiteit van Amsterdam en Flinders University met als doel het behalen van een gezamenlijk doctoraat. Het proefschrift is voorbereid aan de Faculteit der Geneeskunde van de Universiteit van Amsterdam en aan het College of Medicine and Public Health van Flinders University.

This thesis was prepared within the partnership between the University of Amsterdam and Flinders University with the purpose of obtaining a joint doctorate degree. The thesis was prepared in the Faculty of Medicine of the University of Amsterdam and in the College of Medicine and Public Health of Flinders University.

SCAPHOID FRACTURES
–
INCREASING DIAGNOSTIC EFFICIENCY AND TREATMENT FUNCTIONALITY

By

Anne Eva J. Bulstra
MD MSc

Thesis
Submitted to Flinders University
for the degree of

Doctor of Philosophy
College of Medicine and Public Health
14th of March 2024

Voor mijn ouders

TABLE OF CONTENTS

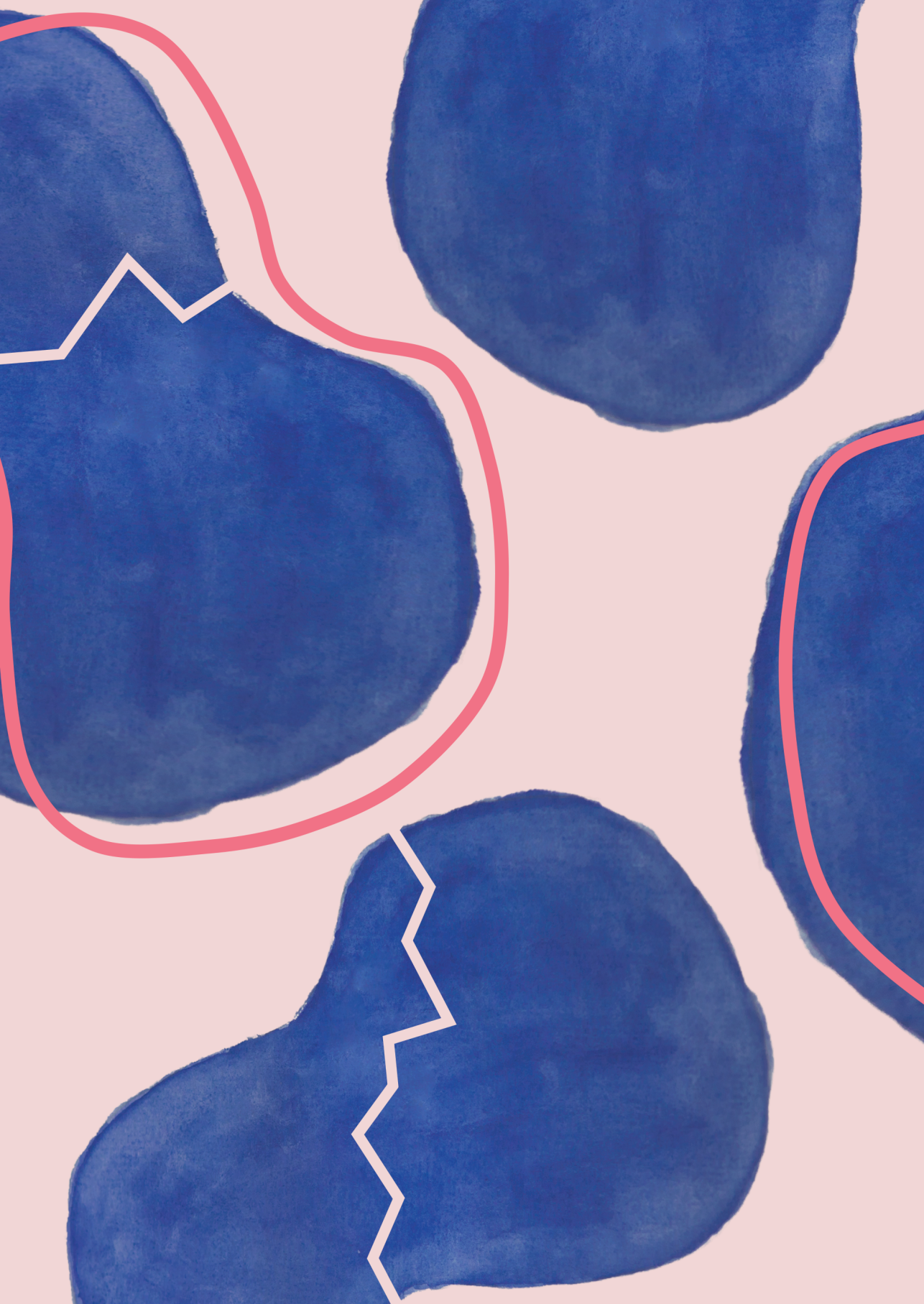

PART I

SCAPHOID FRACTURES: WHAT IS THE PROBLEM?

CHAPTER 1

General Introduction and Outline of this Thesis

GENERAL INTRODUCTION

Scaphoid fractures are common injuries that are notorious for their difficult diagnosis and the associated fear of nonunion when left undiagnosed or undertreated. It is estimated that 1 in every 5 scaphoid fractures is missed on acute radiographs.[1] Patients with tenderness of the scaphoid after a fall onto the outstretched hand and negative radiographs are therefore considered to have a clinically suspected scaphoid fracture.

There is a theoretical and undefined risk of nonunion associated with scaphoid fractures not visible on radiographs that are left untreated.[1-5] Traditionally, this risk has resulted in defensive treatment protocols around the globe.[4,5] Patients with scaphoid tenderness and inconclusive radiographs are typically immobilized until repeat radiographs or advanced imaging (magnetic resonance imaging [MRI] or computed tomography [CT]) are completed.[6-9] It has been reported that up to 5 in every 6 patients with a suspected scaphoid fracture are immobilized unnecessarily.[1,10,11] Patients with a confirmed scaphoid fracture may be treated with up to 12 weeks of cast immobilization.[12-14] Up until 1990, this even entailed wearing an above-elbow cast including the thumb.[15-17]

Fortunately, many advances have been made to improve diagnostic efficiency and treatment functionality. MRI and CT are currently considered the best available modalities to detect occult scaphoid fractures.[1] Immediate MRI or CT in patients with scaphoid tenderness but negative radiographs can aid in reducing unhelpful immobilization and hospital visits.[6,8,18,19] It is therefore considered a cost- and clinically effective diagnostic pathway.[6,8,18,19] Unfortunately, both modalities can display physiological and anatomical variations that can be misinterpreted as a fracture which may lead to overtreatment.[11,20] To date, a consensus reference standard for the diagnosis of acute scaphoid fractures is still lacking.[21]

As for treatment, an increased understanding of risk factors associated with nonunion has allowed for more tailored and functional treatment options.[5,22-24] Displaced and proximal pole fractures are at a higher risk of nonunion and benefit most from internal fixation.[5,22-26] Contrarily, the most commonly occurring fracture involving the scaphoid waist, is known to heal with cast immobilization if nondisplaced.[12,27-32] Screw fixation helps people with a CT-confirmed nondisplaced waist fracture avoid cast wear, but it does not improve union rates or long term functional outcomes.[28,33] Recent evidence suggests that these fractures heal with less rigid and shorter types of immobilization.[12,29,31,32,34] As such, current practice allows patients with a CT-confirmed nondisplaced waist fracture to be treated in a below-elbow cast, excluding the thumb. Shorter periods of immobilization (4-6 weeks) are also under consideration.[12,31,35] (Figure 1)

Despite these advances, the fear of undertreatment among surgeons continues to hinder our quest towards efficient diagnostics and functional treatment. The potential consequences of an undiagnosed or undertreated fracture – i.e. symptomatic nonunion - largely account for this fear of undertreatment. However, surgeons' fear of medicolegal consequences may also play a role. In an increasingly litigious medico-legal climate, doctors use advanced imaging such as MRI and CT to rule out the presence of a scaphoid

fracture more frequently.[36,37] Due to the low specificity of clinical exam (i.e. the inability to rule out a fracture based on clinical exam), many patients without a fracture undergo advanced imaging.[1,6,8,11,18,38] As a consequence, the prevalence of a true scaphoid fracture among patients with suspected fracture, may be as low as 5%.[39] Such low probability circumstances render the diagnosis of a fracture more challenging, even when relying on advanced imaging such as MRI or CT.[36,37] Therefore, strategies to increase the prevalence of true fractures by improving the selection of patients that require advanced imaging merit further investigation.

The adoption of shorter immobilization times for nondisplaced scaphoid waist fractures may equally be hindered by surgeons' fear of undertreatment. In the absence of reliable methods to confirm scaphoid union between 4 to 12 weeks after injury, surgeons tend to practice defensively.[40-42] This may lead to prolonged immobilization in a substantial proportion of patients. This contradicts the increasing evidence that nondisplaced scaphoid waist fractures heal predictably with shorter immobilization duration.[12,31,32,43]

To further increase diagnostic efficiency and treatment functionality in our daily practice, future strategies should be aimed at 1) reducing unhelpful imaging and immobilization in patients with a suspected scaphoid fracture and 2) reduce overtreatment of patients with a confirmed scaphoid fracture. Considering the relative frequency of scaphoid fractures, occurring predominantly in a young and active population, such strategies may greatly improve patient functionality (e.g. enabling earlier return to work and/or sports), reduce health care consumption and societal costs. [2,3,19]

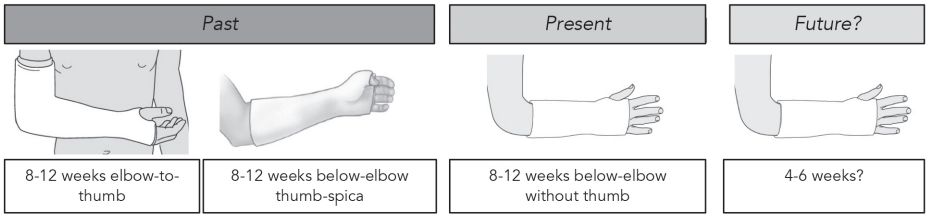

Figure 1. Past & future perspectives for nonoperative treatment of scaphoid waist fractures

OUTLINE OF THIS THESIS

In this thesis, the overdiagnosis and overtreatment of acute nondisplaced scaphoid waist fractures is addressed. The overall goal is to reduce unhelpful imaging and immobilization in patients with a suspected or confirmed scaphoid waist fracture. To increase diagnostic efficiency and treatment functionality safely and effectively, we need to (Figure 2):

1. Improve efficiency and accuracy of acute scaphoid fracture diagnosis
   (Part II - Clinical Presentation and Diagnosis of the [Suspected] Scaphoid Fracture);

2. Differentiate fractures that heal predictably from those that are at an increased risk of nonunion
   (Part III - Scaphoid Fracture Characteristics);

3. Gain a better understanding of factors associated with surgeon recommendation for prolonged cast immobilization of a nondisplaced waist fracture
   (Part IV Immobilization Duration of a Nondisplaced Scaphoid Waist Fracture).

Part I – Scaphoid Fractures: What is the Problem?

In **Part I** of this thesis, the core issues accounting for the fear of undertreatment among clinicians are addressed: scaphoid anatomy and scaphoid nonunion. In **Chapter 2** the scaphoid's complex anatomy is reviewed. Both the scaphoid's difficult diagnostics and the high risk of nonunion can be attributed to its anatomy. In **Chapter 3** the subject of surgeons' fear of undertreatment is reviewed: scaphoid nonunion. Risk factors associated with nonunion and preferred management options for scaphoid nonunion and scaphoid nonunion advanced collapse (SNAC) are discussed through a systematic literature review.

Part II – Diagnosis of a (Suspected) Scaphoid Fracture

In **Part II** of this thesis, we focus on the diagnostic work up of patients presenting with clinical signs of a scaphoid fracture. In **Chapter 4** a clinical prediction rule is devised using a Machine Learning (ML) algorithm. The clinical prediction rule aims to selectively identify patients with a suspected scaphoid injury that require advanced imaging, while reducing unnecessary imaging and immobilization in others. This strategy can also increase the prevalence of true fractures among patients with a suspected fractures undergoing advanced imaging. In **Chapter 5** the diagnostic potential of a deep learning algorithm for automated diagnosis of scaphoid fractures on radiographs is explored. If a deep learning algorithm proves more accurate than physician-based diagnosis of scaphoid fractures on radiographs, this may reduce the need for advanced imaging. In **Chapter 6** MRI signal characteristics among patients with a suspected scaphoid fracture are investigated. By evaluating patterns of MRI signal change, we aim to identify signal changes that likely represent scaphoid waist fractures. We also investigate the reliability of

differentiating between patterns of signal change, including anatomical and physiological variations.

Part III – Scaphoid Fracture Characteristics

To safely reduce the overtreatment of patients with a confirmed scaphoid fracture, we need to differentiate fractures that heal predictably from those that are at an increased risk of nonunion. In **Part III** we seek to identify recurring scaphoid fracture patterns including fracture characteristics associated with a higher risk of nonunion. In **Chapter 7** patterns in acute scaphoid fracture morphology are identified using three-dimensional (3D) CT. In **Chapter 8** the association between fracture morphology and displacement – the biggest risk factor for nonunion - is investigated using 3DCT analysis. Insight into recurring fracture patterns and their correlation with displacement may aid surgeons in diagnosing acute fractures and displacement.

Part IV - Immobilization Duration of a Nondisplaced Scaphoid Fracture

There is increasing evidence that shorter and less rigid types of support suffice for the treatment of nondisplaced waist fractures. In clinical practice, adoption of shorter immobilization times may be hindered by surgeons' fear of undertreatment. In **Chapter 9** we aim to identify factors associated with surgeon recommendation for additional cast immobilization after 8 and 12 weeks of completed cast wear through an international survey. In **Chapter 10** we investigate patient demographic, clinical, radiological and psychological factors associated with surgeon recommendation for additional cast immobilization of a nondisplaced scaphoid waist fracture in a prospective single centre study.

Part V - General Discussion

Chapter 11 summarizes the findings of this thesis. In **Chapter 12** the conclusion of this thesis and future perspectives for research and clinical practice are discussed.

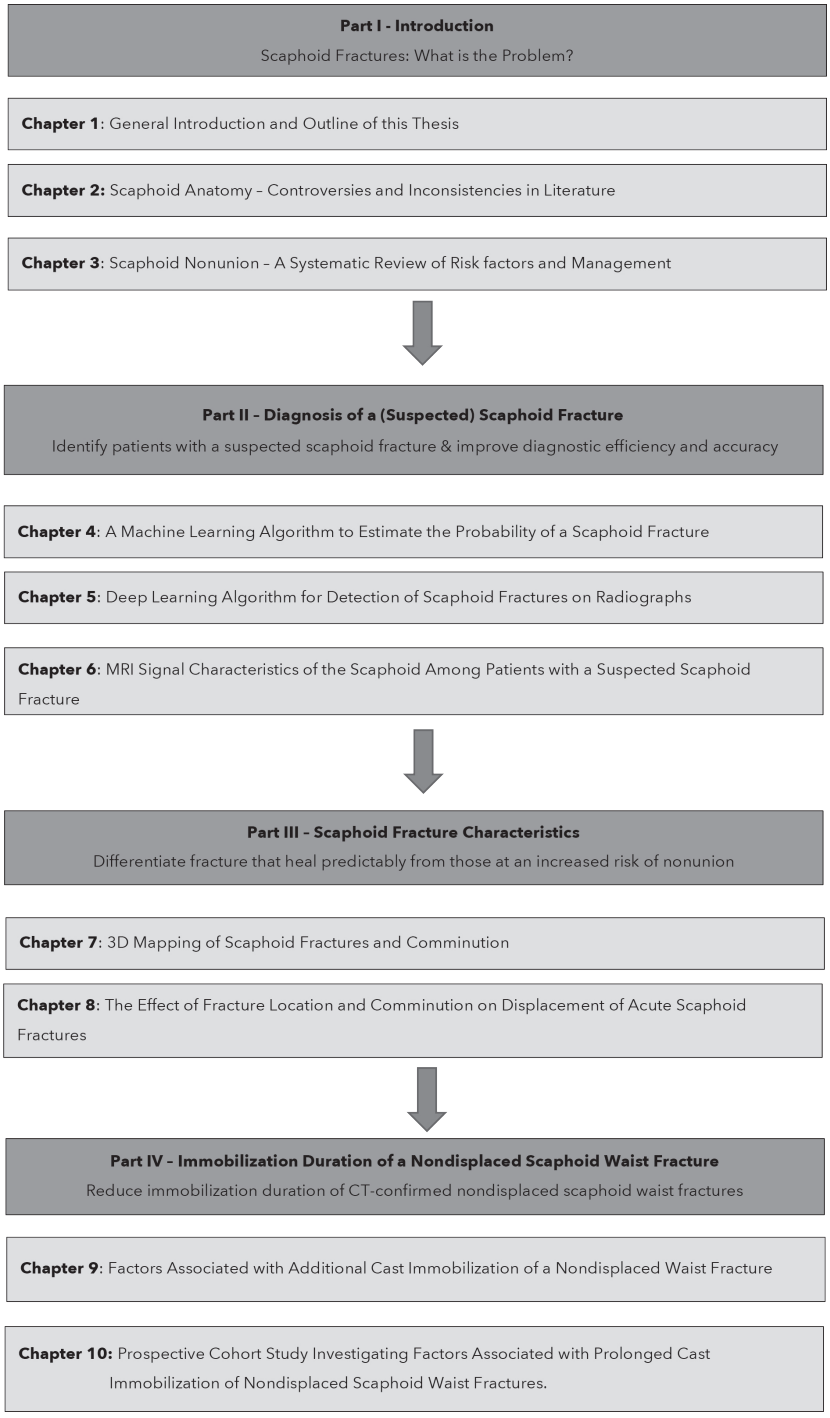

Figure 2. Thesis Outline and Aims

REFERENCES

1. Mallee WH, Wang J, Poolman RW, et al. Computed tomography versus magnetic resonance imaging versus bone scintigraphy for clinically suspected scaphoid fractures in patients with negative plain radiographs. *Cochrane Database Syst Rev.* 2015(6):CD010023.
2. Duckworth AD, Jenkins PJ, Aitken SA, Clement ND, Court-Brown CM, McQueen MM. Scaphoid fracture epidemiology. *J Trauma Acute Care Surg.* 2012;72(2):E41-45.
3. Garala K, Taub NA, Dias JJ. The epidemiology of fractures of the scaphoid: impact of age, gender, deprivation and seasonality. *Bone Joint J.* 2016;98-B(5):654-659.
4. Langhoff O, Andersen JL. Consequences of late immobilization of scaphoid fractures. *J Hand Surg Br.* 1988;13(1):77-79.
5. Reigstad O, Grimsgaard C, Thorkildsen R, Reigstad A, Rokkum M. Scaphoid non-unions, where do they come from? The epidemiology and initial presentation of 270 scaphoid non-unions. *Hand Surg.* 2012;17(3):331-335.
6. Dorsay TA, Major NM, Helms CA. Cost-effectiveness of immediate MR imaging versus traditional follow-up for revealing radiographically occult scaphoid fractures. *AJR Am J Roentgenol.* 2001;177(6):1257-1263.
7. Groves AM, Kayani I, Syed R, et al. An international survey of hospital practice in the imaging of acute scaphoid trauma. *AJR Am J Roentgenol.* 2006;187(6):1453-1456.
8. Jenkins PJ, Slade K, Huntley JS, Robinson CM. A comparative analysis of the accuracy, diagnostic uncertainty and cost of imaging modalities in suspected scaphoid fractures. *Injury.* 2008;39(7):768-774.
9. Mallee WH, Veltman ES, Doornberg JN, Blankevoort L, van Dijk CN, Goslings JC. [Variations in management of suspected scaphoid fractures]. *Ned Tijdschr Geneeskd.* 2012;156(28):A4514.
10. Jenkin M, Sitler MR, Kelly JD. Clinical usefulness of the Ottawa Ankle Rules for detecting fractures of the ankle and midfoot. *J Athl Train.* 2010;45(5):480-482.
11. Mallee W, Doornberg JN, Ring D, van Dijk CN, Maas M, Goslings JC. Comparison of CT and MRI for diagnosis of suspected scaphoid fractures. *J Bone Joint Surg Am.* 2011;93(1):20-28.
12. Clementson M, Jorgsholm P, Besjakov J, Bjorkman A, Thomsen N. Union of Scaphoid Waist Fractures Assessed by CT Scan. *J Wrist Surg.* 2015;4(1):49-55.
13. Dias JJ, Dhukaram V, Abhinav A, Bhowal B, Wildin CJ. Clinical and radiological outcome of cast immobilisation versus surgical treatment of acute scaphoid fractures at a mean follow-up of 93 months. *J Bone Joint Surg Br.* 2008;90(7):899-905.
14. McQueen MM, Gelbke MK, Wakefield A, Will EM, Gaebler C. Percutaneous screw fixation versus conservative treatment for fractures of the waist of the scaphoid: a prospective randomised study. *J Bone Joint Surg Br.* 2008;90(1):66-71.
15. Gellman H, Caputo RJ, Carter V, Aboulafia A, McKay M. Comparison of short and long thumb-spica casts for non-displaced fractures of the carpal scaphoid. *J Bone Joint Surg Am.* 1989;71(3):354-357.
16. Thomaidis VT. Elbow-wrist-thumb immobilisation in the treatment of fractures of the carpal scaphoid. *Acta Orthop Scand.* 1973;44(6):679-689.
17. Thompson JS. Comparison of short and long thumb-spica casts for non-displaced fractures of the carpal scaphoid. *J Bone Joint Surg Am.* 1990;72(2):309-310.
18. Brydie A, Raby N. Early MRI in the management of clinical scaphoid fracture. *Br J Radiol.* 2003;76(905):296-300.
19. Karl JW, Swart E, Strauch RJ. Diagnosis of Occult Scaphoid Fractures: A Cost-Effectiveness Analysis. *J Bone Joint Surg Am.* 2015;97(22):1860-1868.

20. De Zwart AD, Beeres FJ, Ring D, et al. MRI as a reference standard for suspected scaphoid fractures. *Br J Radiol.* 2012;85(1016):1098-1101.

21. Stirling PHC, Strelzow JA, Doornberg JN, White TO, McQueen MM, Duckworth AD. Diagnosis of Suspected Scaphoid Fractures. *JBJS Rev.* 2021;9(12).

22. Gholson JJ, Bae DS, Zurakowski D, Waters PM. Scaphoid fractures in children and adolescents: contemporary injury patterns and factors influencing time to union. *J Bone Joint Surg Am.* 2011;93(13):1210-1219.

23. Grewal R, Suh N, Macdermid JC. Use of computed tomography to predict union and time to union in acute scaphoid fractures treated nonoperatively. *J Hand Surg Am.* 2013;38(5):872-877.

24. Singh HP, Taub N, Dias JJ. Management of displaced fractures of the waist of the scaphoid: meta-analyses of comparative studies. *Injury.* 2012;43(6):933-939.

25. Suh N, Grewal R. Controversies and best practices for acute scaphoid fracture management. *J Hand Surg Eur Vol.* 2018;43(1):4-12.

26. Tait MA, Bracey JW, Gaston RG. Acute Scaphoid Fractures: A Critical Analysis Review. *JBJS Rev.* 2016;4(9).

27. Bhat M, McCarthy M, Davis TR, Oni JA, Dawson S. MRI and plain radiography in the assessment of displaced fractures of the waist of the carpal scaphoid. *J Bone Joint Surg Br.* 2004;86(5):705-713.

28. Buijze GA, Doornberg JN, Ham JS, Ring D, Bhandari M, Poolman RW. Surgical compared with conservative treatment for acute nondisplaced or minimally displaced scaphoid fractures: a systematic review and meta-analysis of randomized controlled trials. *J Bone Joint Surg Am.* 2010;92(6):1534-1544.

29. Buijze GA, Goslings JC, Rhemrev SJ, et al. Cast immobilization with and without immobilization of the thumb for nondisplaced and minimally displaced scaphoid waist fractures: a multicenter, randomized, controlled trial. *J Hand Surg Am.* 2014;39(4):621-627.

30. Clementson M, Jorgsholm P, Besjakov J, Thomsen N, Bjorkman A. Conservative Treatment Versus Arthroscopic-Assisted Screw Fixation of Scaphoid Waist Fractures--A Randomized Trial With Minimum 4-Year Follow-Up. *J Hand Surg Am.* 2015;40(7):1341-1348.

31. Geoghegan JM, Woodruff MJ, Bhatia R, et al. Undisplaced scaphoid waist fractures: is 4 weeks' immobilisation in a below-elbow cast sufficient if a week 4 CT scan suggests fracture union? *J Hand Surg Eur Vol.* 2009;34(5):631-637.

32. Grewal R, Suh N, MacDermid JC. Is Casting for Non-Displaced Simple Scaphoid Waist Fracture Effective? A CT Based Assessment of Union. *Open Orthop J.* 2016;10:431-438.

33. de Boer BNP DJ, Mallee WH, Buijze GA. Surgical treatment of non- and minimally-displaced acute scaphoid fractures favours over conservative treatment but only in the short term: an updates meta-analysis. *Journal of ISAKOS Joint Disorders & Orthopaedic Sports Medicine.* 2016.

34. Doornberg JN, Buijze GA, Ham SJ, Ring D, Bhandari M, Poolman RW. Nonoperative treatment for acute scaphoid fractures: a systematic review and meta-analysis of randomized controlled trials. *J Trauma.* 2011;71(4):1073-1081.

35. Rhemrev SJ, van Leerdam RH, Ootes D, Beeres FJ, Meylaerts SA. Non-operative treatment of non-displaced scaphoid fractures may be preferred. *Injury.* 2009;40(6):638-641.

36. Duckworth AD, Ring D, McQueen MM. Assessment of the suspected fracture of the scaphoid. *J Bone Joint Surg Br.* 2011;93(6):713-719.

37. Ring D, Lozano-Calderon S. Imaging for suspected scaphoid fracture. *J Hand Surg Am.* 2008;33(6):954-957.

38. Mallee WH, Henny EP, van Dijk CN, Kamminga SP, van Enst WA, Kloen P. Clinical diagnostic evaluation for scaphoid fractures: a systematic review and meta-analysis. *J Hand Surg Am.* 2014;39(9):1683-1691 e1682.

39. Pillai A, Jain M. Management of clinical fractures of the scaphoid: results of an audit and literature review. *Eur J Emerg Med.* 2005;12(2):47-51.

40. Buijze GA, Wijffels MM, Guitton TG, et al. Interobserver reliability of computed tomography to diagnose scaphoid waist fracture union. *J Hand Surg Am.* 2012;37(2):250-254.

41. Dias JJ, Taylor M, Thompson J, Brenkel IJ, Gregg PJ. Radiographic signs of union of scaphoid fractures. An analysis of inter-observer agreement and reproducibility. *J Bone Joint Surg Br.* 1988;70(2):299-301.

42. Hannemann PF, Brouwers L, Dullaert K, van der Linden ES, Poeze M, Brink PR. Determining scaphoid waist fracture union by conventional radiographic examination: an analysis of reliability and validity. *Arch Orthop Trauma Surg.* 2015;135(2):291-296.

43. Clementson M, Bjorkman A, Thomsen NOB. Acute scaphoid fractures: guidelines for diagnosis and treatment. *EFORT Open Rev.* 2020;5(2):96-103.

CHAPTER 2

Scaphoid Anatomy – Controversies and Inconsistencies in Literature

A.E.J. Bulstra

J.N. Doornberg

G.A. Buijze

G.I. Bain

In Buijze and Jupiter ed. *Scaphoid Fractures: Evidence-Based Management: Evidence-Based Management.* Elsevier; 2017; pp. 21-34.

ANATOMY OF THE SCAPHOID BONE AND LIGAMENTS

Key points

- The scaphoid articulates with five adjacent bones through a largely cartilaginous surface and features a complex network of ligamentous attachments, making it a unique and key component of the wrist.
- Variations in this anatomy, osseous and more importantly ligamentous, are likely to result in distinct kinematic patterns of the scaphoid, thus playing an important role in carpal (in)stability in both normal and injured wrists.
- In current literature no consensus has been reached on the description and classification of scaphoid anatomy and its variations.
- The inconsistency in ligament classification is due to the complexity of identifying and delineating complex soft tissue structures in cadaver dissections, as well as interindividual variability.

Case 1. A Patient with Ulnar Carpal Translocation

A 34-year-old man injured his right dominant hand during a bicycle accident, falling onto an outstretched hand. His wrist is painful and swollen. Radiographs show no fracture or dislocation and are interpreted as normal. One month later, the patient complains of persistent wrist pain. Careful revaluation of the radiographs reveals a subtle ulnar translocation of the radiocarpal joint (Figure 1). What pathoanatomic characteristic accounts for both the clinical presentation and radiologic findings in this patient?

IMPORTANCE OF THE PROBLEM

The scaphoid has characteristic anatomic features: it has a complex relation to surrounding structures through numerous ligamentous attachments and up to 80% of the scaphoid bony surface is covered with cartilage.[1-3] The interpretation and description of scaphoid anatomy has proven controversial in current literature. Consensus is specifically lacking on the anatomy and classification of the ligaments attaching to the scaphoid.[1] Variations in this anatomy result in distinct kinematic patterns of the scaphoid.[3] Clarification of the ligamentous anatomy will thus enhance our understanding of the role of the scaphoid in carpal stability, for example clarifying the different collapse patterns following scaphoid fractures. Furthermore, it will contribute to our radiographic diagnosis and interpretation of ligamentous injuries.

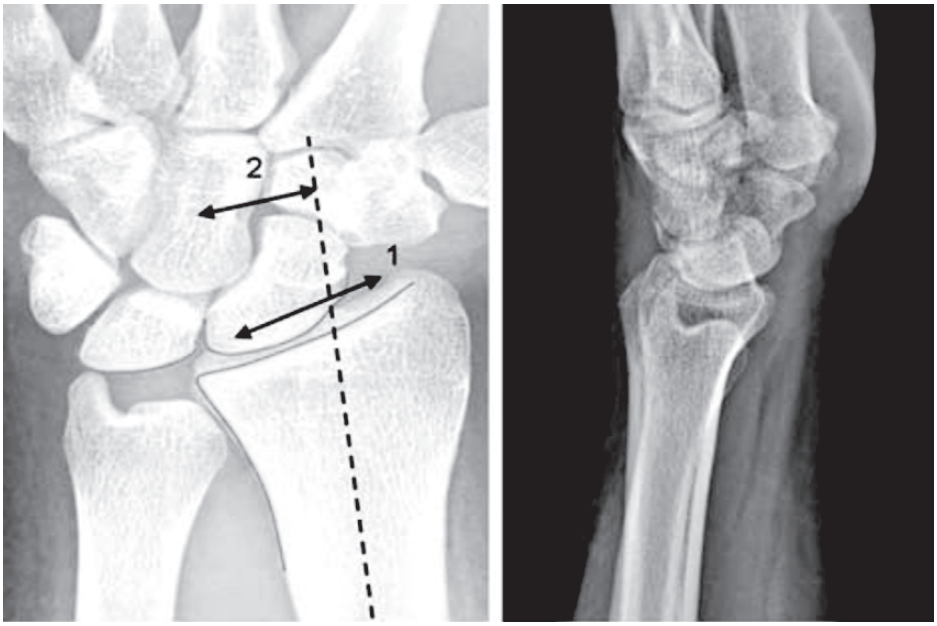

Figure 1. Posttraumatic Ulnar Translocation of the Radiocarpal Joint.

The interval designated by *line 1* demonstrates an increased distance between the radial styloid and scaphoid. Here, the scaphoid seems positioned in the lunate fossa. The interval designed by *line 2* indicates an increased distance between a line drawn centrally through the radius and through the centre of the capitate. The distance is more than the average 5.7 ± 1.4 mm, indicating ulnar translocation of the carpus. (From Rutgers M, Jupiter J, Ring D. Isolated posttraumatic ulnar translocation of the radiocarpal joint. *J Hand Microsurg*. 2009;1(2):108–112; with permission.)

Main question

What are current concepts on osseous and ligamentous scaphoid anatomy and what (in) consistencies exist in the anatomic description in current literature?

Current Opinion

The scaphoid and its ligamentous attachments play an important role in carpal stability.[1-4] Various classification systems exist to describe the anatomy of the scaphoid and the ligaments attached to it. To date, a universal description and classification system of the ligamentous anatomy has not been accepted.

Finding the Evidence

This chapter is an update of authors' previous systematic literature review on scaphoid osseous and ligamentous anatomy, using similar methodology[1]:

1. Online search
   - Medline: *ligament**[Title] AND (*carp** [Title] OR *scaph** [Title] OR *wrist* [Title]).
   - All original descriptions of the anatomy, morphology of the scaphoid, and/or ligaments available in full-text copy were included.
   - Articles that were not in English, French, Italian, Dutch, German, or Spanish were not included. Personal communications, letters, or meeting proceedings were excluded.

2. Manual search for book chapters
   - Screening of reference lists of all selected articles using the same inclusion and exclusion criteria was performed.

Quality of the Evidence

Current knowledge of scaphoid anatomy is based on both in vitro studies—cadaver dissections—and in vivo studies—imaging techniques. The evidence aggregated in this chapter is predominantly based on macroscopic dissections[2,5-19], combined with few arthroscopic[20] and magnetic resonance imaging studies.[17,21,22] No standardized criteria for evaluating the quality of such studies exist. The most important constraint in identifying ligamentous anatomy is the difficulty of delineating complex soft tissue structures in cadaver dissections, with risk of creating "iatrogenic" anatomy in complex fibrous structures. This may account for the variability in anatomy reported. In addition, interindividual variability in ligament insertion and morphology exists.[1] The variety in individual anatomy can only be explored through larger studies on cadaver specimens.

Findings

Osseous Anatomy

The scaphoid bone has a characteristic and irregular "boat-shaped" form (i.e., Latin *scaphoides* for bowl or boat shaped).[3,4,23] It is the largest bone of the proximal carpal row and is aligned on an oblique axis at 45 degrees to the long axis of the wrist, in both radial and volar directions.[3] Computed tomography (CT) reconstructions along this oblique axis are proven to be more accurate to detect an occult scaphoid fracture than standardized CT reconstructions in frontal, sagittal, and axial planes.[24,25] The scaphoid forms an important link between the proximal and distal carpalia, as it is the only bone to cross both carpal rows.[17,20]

Three-dimensional (3D) anatomic imaging of cadavers using CT and cryomicrotome imaging revealed a mean scaphoid surface of 1503 ± 17 mm^2.[2] Approximately 75% of this surface is covered with cartilage, articulating with five adjacent bones.[16] Traditionally four distinct anatomic regions of the scaphoid bone can be differentiated: (1) the proximal pole; (2) the distal pole; (3) the tubercle; and (4) the waist. A substantial variety of shapes has been described and classified (Box 1).[26,27]

BOX 1 Morphometric features and a variety in osseous anatomy

Although four distinct anatomic regions (proximal pole, distal pole, tubercle, and waist) can typically be differentiated, a substantial variety in shapes exists. An anatomic study on cadavers by Ceri et al. demonstrated the tubercle and a dorsal sulcus (Figure 2) to be present in all scaphoid specimens, whereas other features were often absent. A great variation in waist circumference, tubercle size, and sulcus width was also reported.[27]

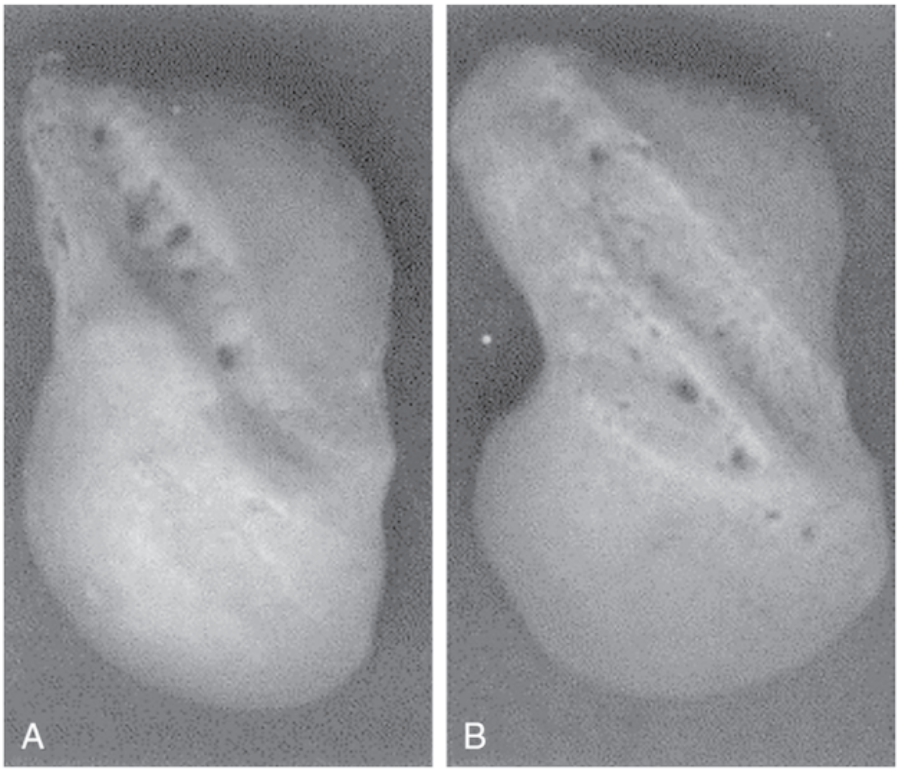

Figure 2. Variations in the Anatomy of the Dorsal Scaphoid Cortex.

Note the variation in the dorsal sulcus and its vascular foramina. **(A)** Main dorsal sulcus. **(B)** Two separate sulci. (From Ceri N, Korman E, Gunal I, et al. The morphological and morphometric features of the scaphoid. *J Hand Surg (Br.)*. 2004;29(4):396; with permission.

Proximal pole and articulations

Proximally, the biconvex dorsally sloped scaphoid surface articulates with the scaphoid fossa of the distal radius (Figure 3A–D). The orientation of the scaphoid fossa is 11° volar and 21° ulnar to the long axis of the radius, thus preventing dorsal and radial translation of the scaphoid.[28,29] This "dorsal lip" of the distal radius, covering the proximal pole of the scaphoid, makes a dorsal (percutaneous) approach for scaphoid fixation technically challenging.[30] On the proximal ulnar side, a flat and semilunate area of the scaphoid forms an articulation with the lunate bone (Fig. 3C).[28,29] The scapholunate articulation plays an important role in wrist kinematics, in which the lunate acts as a proximal anchor to the scaphoid, restrained by the scapholunate interosseous ligament (SLIO).[3]

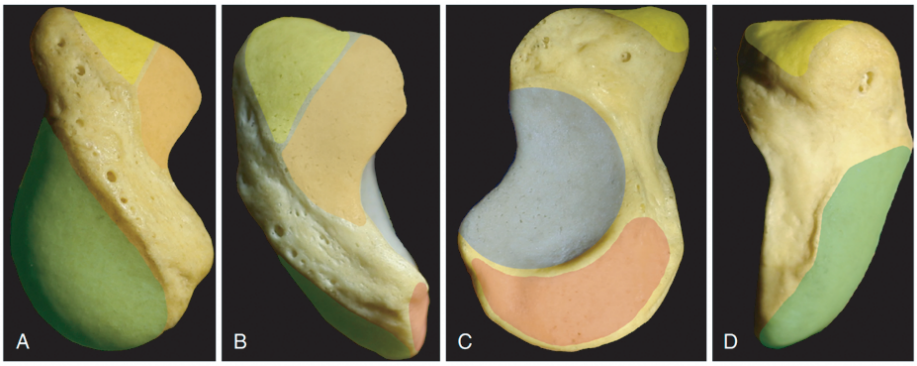

Figure 3. Osseous Anatomy and Articulations of the Scaphoid.

A) Radial, **(B)** dorsal, **(C)** ulnar, and **(D)** volar views of the scaphoid and its articular surfaces colour coded for contact with the distal radius (green), trapezium (yellow), trapezoid (orange), capitate (blue), and lunate (red). The bottom of each image represents the proximal and the top represents the distal end. Note the vascular foramina in the regions of the radiodorsal ridge and the tubercle. (From Buijze GA, Lozano-Calderon SA, Strackee SD, et al. Osseous and ligamentous scaphoid anatomy: Part I. A systematic literature review highlighting controversies. *J Hand Surg*. 2011;36(12):1929; with permission.)

Distal pole and articulations

Distally, the convex surface forms the scapho-trapezio-trapezoid (STT) joint, articulating with the trapezoid and the trapezium on the ulnodorsal and radiovolar sides, respectively (Fig. 3A–D).[28,29] The distal scaphoid surface has a cartilaginous ridge, dividing the articulation into the two facets of the STT joint.[26,28,29] Osteoarthrosis is commonly seen in this articulation, resulting in extension of the joint.[3] Anatomic variations in the shape of the distal articular surface, as described by Moritomo et al., may lead to divergent carpal kinematics contributing to degenerative changes.[14] Studies have suggested a direct association between scaphoid alignment, the extent to which the trapezium and trapezoid cover the scaphoid surface and the development of degenerative changes.[14]

BOX 2 Rotating (Type 1) and Flexing (Type 2) Scaphoids

Fogg et al. classified two subtypes of the scaphoid based on different kinematics resulting from alternative ligamentous insertions and articulations: a type 1 rotating scaphoid and a type 2 flexing scaphoid. A type 1 scaphoid has a single dorsal ridge oriented obliquely across the waist. A type 2 scaphoid has three similarly oriented ridges, which are located lower along the scaphoid waist. Each type is associated with specific alternative ligamentous attachments and articulations, resulting in distinct kinematic patterns. Table 1 summarizes the differences in ligamentous attachments. The ligament morphology of a type 1 or type 2 scaphoid allows the scaphoid to either rotate or flexion around its axis, respectively (Figure 4).[31]

On the ulnar distal side, the concave surface accommodates the proximal radial part of the capitate (Figure. 3C).[28,29] This concave facet may be elongated and shallow, when associated with a rotating scaphoid (type 1), or round and deep as seen in a flexing scaphoid (type 2) (Box 2, Figure 4).[31] Yazaki et al. described capitate morphology to vary from flat to V-shaped, articulating with type 1 and type 2 scaphoids, correspondingly.[32]

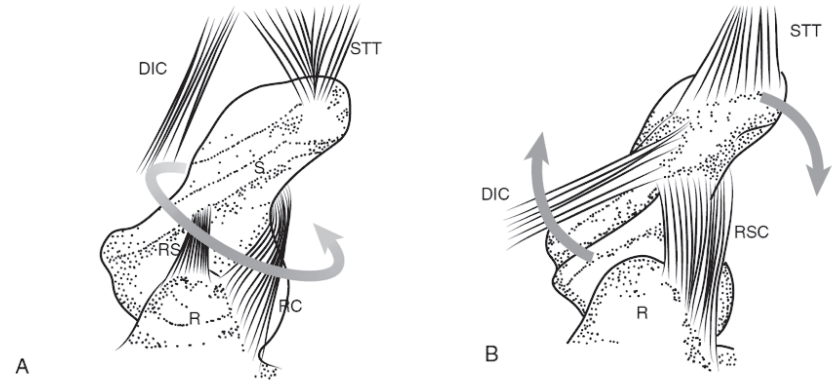

Figure 4. (A) Type 1 (Rotating) and (B) Type 2 (Flexing) Scaphoids.

DIC, dorsal intercarpal; *RC*, radiocapitate; *RS*, radioscaphoid; *RSC*, radioscaphocapitate; *STT*, scapho-trapezio-trapezoid; *R*, radius; *S,* scaphoid. (From Fogg QA. Scaphoid variation and an anatomical basis for variable carpal mechanics. Adelaide: University of Adelaide, Dept. of anatomical sciences; 2004:1:48; with permission.)

Table 1. Summary of Osseous and Ligamentous Variations in Wrists with Rotating (Type 1) and Flexing (Type 2) Scaphoids

		Rotating (Type 1)	Flexing (Type 2)
Distal pole	*Scaphotrapezial ligament*	Distally based "V" with narrow scaphoid attachment	Proximally based "V" with broad scaphoid attachment
	Scaphocapitate ligament	Long to allow rotation	Short (axis of flexion)
	Scaphocapitate articulation	Shallow capitate fossa, flat-type capitate	Deep capitate fossa, "V"- shaped capitate
Scaphoid waist	*Dorsal intercarpal ligament*	Attached to trapezium, not scaphoid	Attached to scaphoid
	Radioscaphocapitate ligament	Not attached to scaphoid	Scaphoid attachment
Proximal pole	*Scapholunate articulation*	To lunate with single distal facet	To lunate with distal double facet
Kinematics		Rotation around long axis of scaphoid	Flexion-extension around axis of scaphocapitate ligament
Radiology	*Lunate*	Single distal facet	Double distal facet
	CT-distance	<2 mm	>4 mm
	Scaphoid nonunion	DISI deformity	No carpal collapse

CT-distance, minimum distance between the capitate and triquetrum on an anteroposterior radiograph; *DISI*, dorsal intercalated segment instability. From Watts AC, McLean JM, Fogg Q, et al. Scaphoid anatomy. In: Slutsky DJ, Slade JF, editors. *The Scaphoid*. New York: Thieme; 2011; with permission.

Scaphoid tubercle

The volar side of the scaphoid is largely nonarticulate. It constitutes a depressed irregular zone on its proximal side and the tubercle, pointing radiovolarly, on its distal side. Various ligamentous attachments, including the flexor retinaculum, the flexor carpi radialis tendon sheath, the STT ligament, and a small portion of the origin of the abductor pollicis brevis attach to the distal tubercle.[12,26,33,34]

Scaphoid waist

The scaphoid waist acts as a point of attachment for the joint capsule and various ligaments.[12,26] Radial artery branches course into the scaphoid through dorsal foramina located on the scaphoid waist.[26,33] The ridges located obliquely across the scaphoid waist function as points of attachment of the dorsal joint capsule, dorsal intercarpal ligaments, and bundles of the radioscaphocapitate ligament (Figure 2).

Vascular Anatomy

Approximately 70%–80% of the intraosseous vascularity and the vascularity of the entire proximal pole is supplied by the radial artery branches entering through the dorsoradial ridge of the scaphoid.[35] There is substantial variation in the anatomy of the arteries entering the dorsal scaphoid cortex (Figure 2).[27,31] About 20%–30% of the scaphoid is vascularized by volar branches of the radial artery, entering through the vascular foramina located on the depressed volar side of the scaphoid.[35]

Ligament Anatomy

The ligaments attached to the scaphoid play a critical role in wrist kinematics and carpal stability, as exemplified by type 1 rotating and type 2 flexing scaphoid bones.[31,36] Buijze et al. demonstrated approximately 131±14mm^2 of the scaphoid surface to be covered by ligamentous attachments, accounting for 9±0.9% of the total surface.[2] Numerous classification systems for carpal ligaments have been described. To date, the most commonly used classification is the classification by Berger and Landsmeer. This nomenclature will therefore be used as a guideline in this chapter (Box 3).[5-7,20,26] Table 2 summarizes the variations in ligamentous anatomy described in this chapter.

BOX 3 Berger's Ligament Classification and Nomenclature

Berger's classification is based on the localization of the ligaments within the carpus and their organization within the joint capsule. The name of each ligament refers to the proximal (origin) and distal (insertion) attachment (Figure 5A and 6A).

Volar ligaments

Radioscaphocapitate ligament. The radioscaphocapitate (RSC) ligament originates from the volar side of the radial styloid and inserts on the volar central part of the capitate head[29,37] (Figure 5, 7, and 8). The RSC acts as a fulcrum around which the scaphoid rotates.[3] The presence of a large number of mechanoreceptors suggests a mechanical and proprioceptive role.[38] Separate bundles of the RSC have been described to insert on multiple locations on the scaphoid, such as the radial side of the scaphoid waist and tubercle. Fogg described the RSC ligament to attach to the waist of type 2 scaphoids only; whereas in type 1 scaphoids the RSC ligament is believed to "bypass" the scaphoid with attachments to the radial styloid and capitate only (Figure 4).[31] A study using cryomicrotome images of eight cadavers by Buijze et al. showed a small bundle of the RSC to attach onto the proximal edge of the scaphoid tubercle (Figure 8).[2] The RSC is commonly reported to form interdigitations with surrounding ligaments, including the ulnocapitate, triquetrocapitate, and volar scaphotriquetral ligament. This interdigitation forms the arcuate ligament, also known as the deltoid, palmar distal V, or Weitbrechts oblique ligament.[39-41] Many variations of this interdigitation have been reported.[17,21]

Long radiolunate ligament. According to general consensus, the long radiolunate (LRL) originates ulnar to the RSC ligament on the volar rim. It then courses over the anterior pole of the scaphoid and inserts on the lunate and triquetrum (Figure 5).[15,19,42] The LRL is sometimes referred to as radiolunotriquetral ligament.[12,39]

Volar scaphotriquetral ligament. The existence of the volar scaphotriquetral ligament (vScTq) remains controversial. Its presence has only been described by two studies.[17,21] Authors have inconsistently described the ligament as both a separate entity[21] and as part of other ligament attachments, such as the arcuate ligament.[17] In cadaver dissections, Buijze et al. recognized the vScTq as part of the arcuate ligament, rather than a separate ligament.[2]

Radioscapholunate ligament. The radioscapholunate (RSL) ligament originates on the volar rim of the distal radius and inserts on the proximal edge of the scaphoid and lunate (Figure 5).[1-3] It is one of the smallest extrinsic ligaments and lacks organized fascicular collagen bundles.[5,6,11] It is therefore considered a relatively weak structure. Some authors consider it a mesocapsular structure rather than a ligament.[6,11] Studies have revealed it to support abundant vascular and neural networks, including arterioles from the radial carpal arch and anterior interosseous nerve endings.[11,37] The RSL ligament courses along the interfossal ridge between the scaphoid and lunate fossa. During arthroscopy it will therefore cover the volar component of the SLIO.[3] Several authors regard the RSL ligament as a reinforcement of this volar component.[6,12,43] RSL ligament rupture is associated with SLIO ligament injury.[44]

Scaphocapitate ligament. The scaphocapitate (ScC) is a large capsular ligament originating from the distal pole of the scaphoid. It transverses obliquely to insert on the radial half of the volar capitate surface (Figure 5A and 7A). It is the thickest scaphoid ligament.[14,15] The ScC has the largest attachment surface area to the scaphoid bone — approximately 40% of the total surface area of scaphoid attachments— covering almost the entire ulnar part of the tubercle.[2] The ScC ligament is part of the scaphotrapezial ligament and is considered an important stabilizer of the midcarpal joint, restraining the distal pole of the scaphoid.[3,11] In individuals with a rotating scaphoid, the ScC ligament is typically longer, allowing for rotation of the bone.[3]

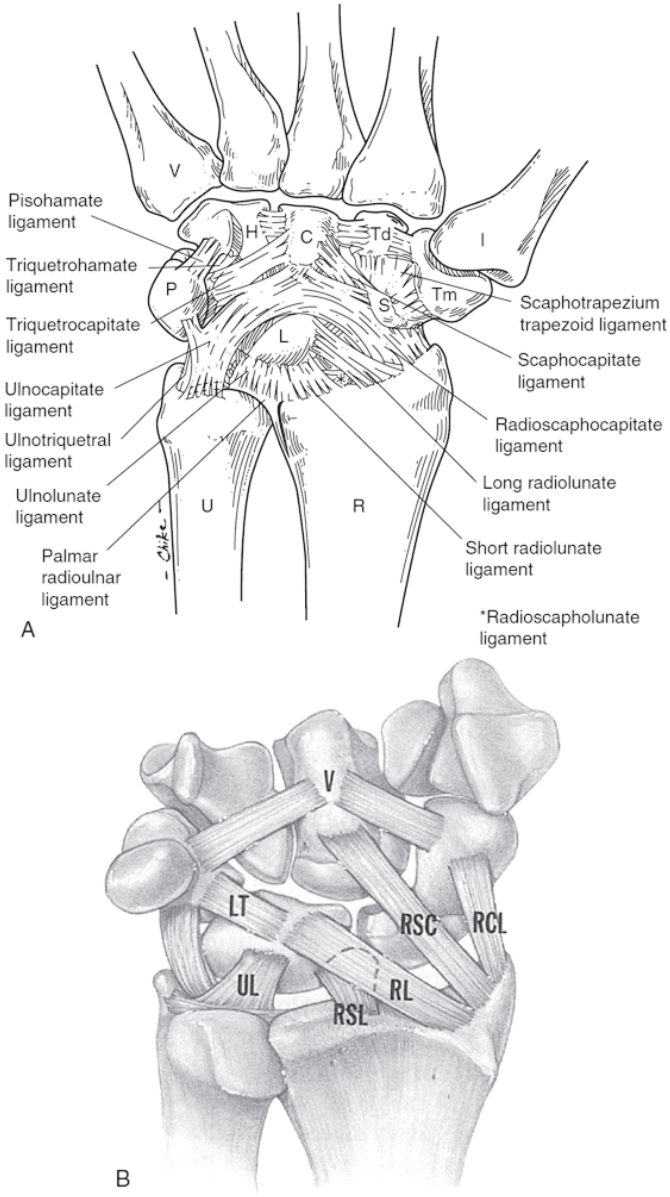

Figure 5. Volar Ligaments of the Scaphoid.

(A) Volar carpal ligaments according to Berger. *U*, ulna; *R,* radius; *P,* pisiforme; *L*, lunate; *S*, scaphoid; *Tm*, trapezium; *Td*, trapezoid; *C*, capitate; *H*, hamate. **(B)** Volar carpal ligaments according to Taleisnik. Note the presence of radial collateral ligament. *RCL*, radial collateral ligament; *RSC*, radioscaphocapitate; *RSL*, radioscapholunate; *RL*, radiolunate; *UL*, ulnolunate; *LT*, lunotriquetral. ((A) William P. Coomey, ed. The Wrist. Diagnosis and Operative Treatment. Ligament anatomy. St. Louis, MO: Elsevier Mosby-Year Book, 1998:79; vol. 1; with permission and (B) Courtesy of Elizabeth Martin/ Taleisnik J, ed. The Wrist. New York: Churchill Livingstone,1985; with permission.)

The scapho-trapezio-trapezoid ligament. The STT ligament comprises two or more bundles originating on the ulnar, volar, and radial edges of the distal pole of the scaphoid bone (distal to the RSC attachment).[15,26,39] Some studies describe two distinguishable bundles. Others report two separate ligaments inserting onto the trapezium and trapezoid: the scapotrapezium (ScTm) and scaphotrapezoid (ScTd) ligament, respectively.[15,26,39] (Figure 5A and 7A) The STT ligament, particularly the ScTm, functions as a stabilizer of the scaphoid and STT joint, inhibiting excessive flexion of the scaphoid.[45] In type 1 scaphoids, the ScTm attachment on the scaphoid apex is narrower than its insertion on the trapezium, rendering a V-shaped ligament allowing for rotation at the base of the V. In type 2 scaphoids a reversed V-shaped ScTm ligament is found, with a broad-based attachment to the scaphoid (Figure 4).[31] The presence of the ScTd ligament as a separate entity is controversial and has not been reported by all studies. In cadaver studies using three-dimensional imaging, it was identified as the narrowest and thinnest scaphoid ligament.[2]

Transverse carpal ligament. The transverse carpal ligament (TCL) is an extracapsular structure originating ulnarly on the hamate and pisiform. It inserts onto the entire volar trapezoidal ridge and the scaphoid (Figure 7A)[8,15,16,18] The TCL is described as the widest ligament attached to the scaphoid and forms the roof of the flexor carpi radialis tunnel. It is the middle part of the three portions (proximal, mid, and distal) comprising the flexor retinaculum.[9,16] Rupture of the TCL significantly disrupts scaphoid kinematics.[46,47]

Radial collateral ligament. The radial collateral ligament (RCL) is a controversial structure. Some studies report it as a separate ligament, connecting the scaphoid to the distal radius. [13,19,33,44] Others describe it as a bundle of the RSC or even deny its existence.[39,40] Buijze et al. did not identify any volar or dorsal radioscaphoid ligament. Instead, a capsular-like structure bypassing the scaphoid radiodorsally was found.[1]

Dorsal ligaments

Dorsal intercarpal ligament. The dorsal intercarpal (DIC) ligament originates from the dorsoradial part of the triquetrum.[1-3,48] Many variations on the insertion of the ligament have been described (Figs. 6 and 7B). In type 2 scaphoids the DIC ligament is described to insert onto the proximal crest of the waist.[3,31] Consistently, Buijze et al. reported its insertion on the dorsoradial ridge of the proximal and waist region.[2] In type 1 scaphoids, however, the DIC ligament reaches the margin STT complex, without attaching onto the scaphoid (Figure 4).[31] The DIC ligament forms a lateral configuration with the dorsal radiocarpal (DRC) ligament, formerly described at the dorsal V ligament. Together they restrain ulnar drift of the carpus.[14,33,37] Additional insertions on the lunate, trapezium, trapezoid, and/or capitate vary greatly.[2] Although the DIC ligament is a weak capsular structure, it functions as a stabilizer, restraining the dorsal proximal pole of the capitate. A proprioceptive role is suggested through the presence of numerous posterior interosseous nerve endings.[38] In type 2 scaphoids, the additional insertion of

the ligament onto the waist may provide additional stability, possibly reducing the risk of carpal collapse into a dorsal intercalated segment instability deformity.[14]

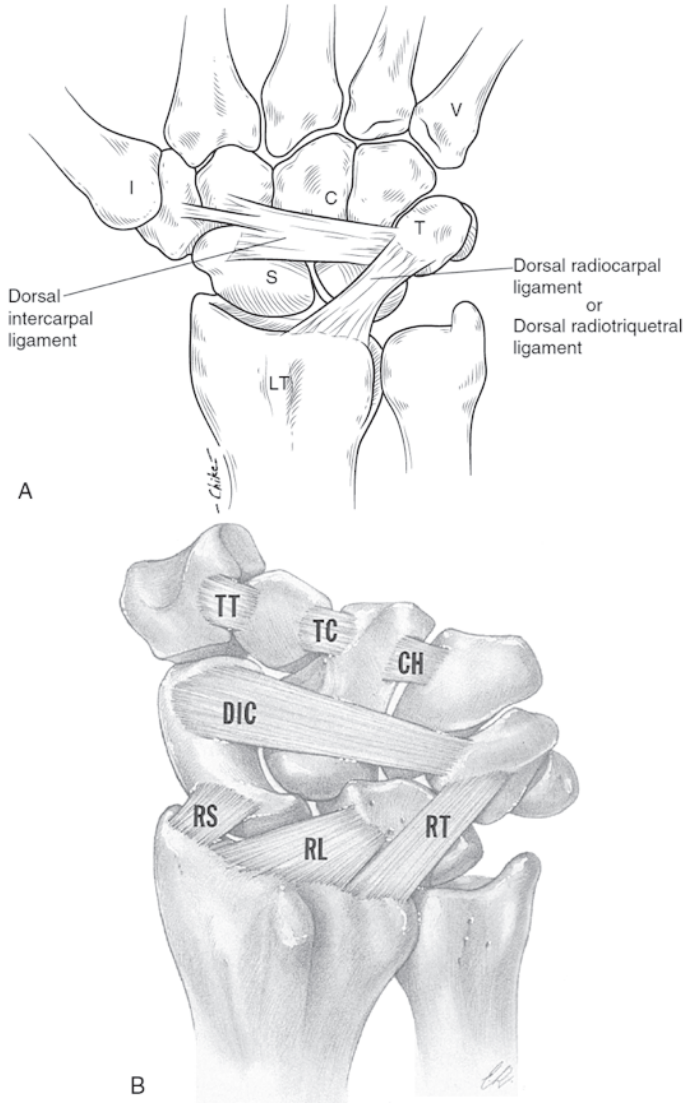

Figure 6. Dorsal Ligaments of the Scaphoid.

(A) Dorsal carpal ligaments according to Berger. *S*, scaphoid; *T*, triquetrum; *C*, capitate; *LT*, Lister's tubercle. **(B)** Dorsal carpal ligaments according to Taleisnik. Note the presence of the dorsal radioscaphoid ligament (see "RS"). *DIC*, dorsal intercarpal; *RS*, radioscaphoid; *RT*, radiotriquetral; *RL*, radiolunate; *TT*, trapeziotrapezoid; *TC*, trapeziocapitate; *CH*, capitohamate. ((A) From William P. Coomey, ed. The Wrist. Diagnosis and Operative Treatment. Ligament anatomy. St. Louis, MO: Elsevier Mosby-Year Book, 1998:79; vol. 1; with permission and (B) From Taleisnik J, ed. The Wrist. New York: Churchill Livingstone, 1985; with permission.)

Dorsal radiocarpal ligament. The DRC ligament is most commonly described to originate from the distal radius and to insert onto the lunate and triquetrum.[1] Controversy exists on its relation with the scaphoid. Some studies describe a thin ligamentous fibre coverage of the proximal scaphoid, providing dorsal stability without insertion.[13,49] Others describe no coverage or insertion of the ligament on the scaphoid bone at all.[12,13,15,22,44,49] Three-dimensional imaging of eight cadaver specimens showed no attachment to the scaphoid.[2]

Scapholunate interosseous ligaments

Scapholunate interosseous ligament. The SLIO ligament is a C-shaped ligament spanning the perimeter of the scapholunate joint (Figure 7B).[2] It divides the radiocarpal joint from the lunate facet. Along with the lunotriquetral ligament, it separates the radiocarpal from the midcarpal joints.[3] Tearing of the SLIO ligament will result in leakage of contrast into the mid- carpal joint, when injected into the radiocarpal joint. This does not confirm carpal instability, however.[3]

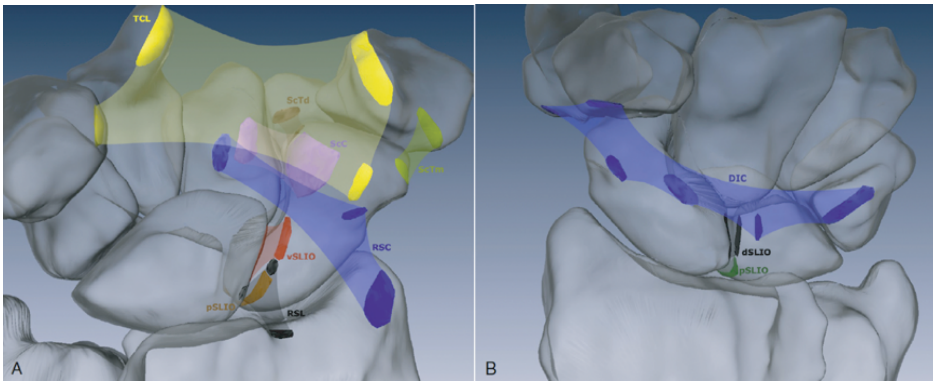

Figure. 7 (A) Volar and (B) Dorsal Views of the Three-Dimensional Representation of the Wrist, Showing the Scaphoid Ligaments and Its Attachments.

DIC, dorsal intercarpal; *pSLIO*, proximal portion of the scapholunate interosseous ligament; *dSLIO*, distal portion of the scapholunate interosseous ligament; *RSC*, radioscaphocapitate; *RSL*, radioscapholunate; *ScC*, scaphocapitate; *ScTd*, scaphotrapezoid; *ScTm*, scapotrapezium; *TCL*, transverse carpal ligament; *vSLIO*, volar portion of the scapholunate interosseous ligament. (From Buijze GA, Dvinskikh NA, Strackee SD, et al. Osseous and ligamentous scaphoid anatomy: Part II. Evaluation of ligament morphology using three-dimensional anatomical imaging. *J Hand Surg*. 2011;36(12):1942; with permission.)

The SLIO ligament is described to consist of three interconnecting bundles: a dorsal, proximal, and volar portion.[5,50] Minor inconsistencies consist regarding the dimensions of these bundles. The dorsal portion is generally considered the thickest and most crucial portion of the SLIO ligament.[51] It courses from the dorsal lunate horn to the ulnar-dorsal region of the proximal edge of the scaphoid. The most proximal portion of the SLIO ligament is considered the widest but weakest portion of the SLIO ligament. The volar portion courses obliquely between the proximal pole of the scaphoid and the

lunate. Along with the proximal bundle, it con- tributes to the rotational stability of the scapholunate joint.[51]

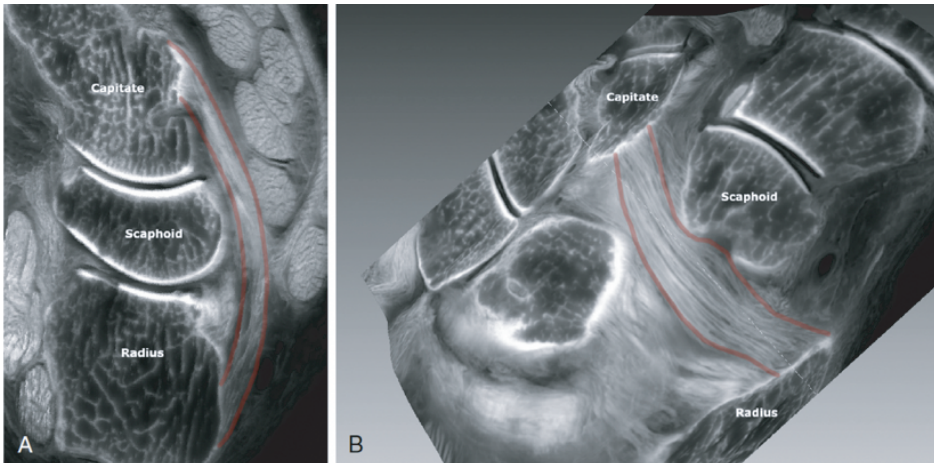

Figure. 8 Cryomicrotome Image of a Right Wrist.

(A) An oblique sagittal plane through the estimated centre of the radioscaphocapitate ligament and **(B)** a curved coronal surface fitted through this curved ligament, orthogonal to the oblique sagittal plane, to visualize its entire course from origin to insertion. The *red lines* indicate the margins of the ligament, used to indicate its thickness and width. Several ligament bundles deviate from the main ligament, directing radial to its attachment on the scaphoid. (From Buijze GA, Dvinskikh NA, Strackee SD, et al. Osseous and ligamentous scaphoid anatomy: Part II. Evaluation of ligament morphology using three-dimensional anatomical imaging. *J Hand Surg*. 2011;36(12):1938; with permission.

Table 2. Consistency and Controversies in Scaphoid Ligamentous Attachments in Literature

Ligament	Generally accepted	Controversial
RSC	Origin at the radial styloid Insertion on the volar capitate	Separate vScTq ligament[17,21] Separate vRSc ligament[21] Separate SC portion No insertion on the scaphoid[21]
RCL	Most radial carpal structure	Separate ligament[13,19,44] Part of RSC ligament[39,40] Radiodorsal origin[13] Radiovolar origin[19,44] Insertion(s)[13,19,44] RCL does not exist
LRL	No insertion on the scaphoid	LRL is also called RLTq[12,39,44]
RSL	All attachment areas	Histologically no true ligament[6,7,11,20]
SLIO	Dorsal, proximal and volar portions	Dimensions of the three portions[5,50]
DRC	Origin at the distal radius Insertions on lunate and triquetrum	Location of the origin on the distal radius[12,13,15,39,40,44,49] Dorsal radioscaphoid ligament[19,28] No insertion on the scaphoid[12,13,15,39,40,44,49]

Table 2. Consistency and Controversies in Scaphoid Ligamentous Attachments in Literature (continued)

Ligament	Generally accepted	Controversial
DIC	Origin at the dorsoradial triquetrum Insertion on the dorsoradial ridge of the scaphoid Varying additional insertion(s) on the lunate, trapezium, trapezoid and/or capitate	Insertion on the volar scaphoid[13] No insertion on the scaphoid[44] No insertion on the trapezium, lunate or capitate[37,39] No insertion on the trapezoid
STT	Two or more bundles originating at volar distal pole of scaphoid with an insertion on the trapezium	Additional insertion on trapezoid[15,26,39] No insertion on trapezoid[8,10,14,19]
ScC	Origin at the volar distal pole of the scaphoid Insertion on the radiovolar capitate	No controversies
TCL	Extra-articular structure Origin at the hook of hamate and pisiform and insertion on the volar trapezial ridge and scaphoid tubercle	Flexor retinaculum and TCL are different entities[9,16,18] TCL is the mid portion of the flexor retinaculum[9,16]

RECOMMENDATIONS

- A consistent description and classification of both osseous and ligamentous scaphoid anatomy is strongly advised to enhance our understanding of scaphoid kinematics.
- Berger's classification of scaphoid ligaments constitutes the most detailed subdivision of ligaments and the most independent ligaments of all classifications.[1,26,37,39]
- Classifying morphologic scaphoid subtypes and their correlated kinematic patterns—for instance, by classifying flexing and rotating scaphoids[3,31] — will allow these variations to be employed as a basis for carpal mechanics.
- Further cadaver studies are required to explore the variations in scaphoid anatomy and its clinical relevance in terms of carpal stability.

CONCLUSION

A substantial variety in both osseous and ligamentous scaphoid anatomy has been described in literature. Consensus is specifically lacking on scaphoid ligamentous attachments. Variations in anatomic features are known to result in distinct kinematic patterns. A thorough knowledge and consistent description of scaphoid anatomy—and more importantly its associated carpal mechanics—are therefore of crucial importance to understanding the role of the scaphoid in carpal stability in both normal and injured wrists.

REFERENCES

1. Buijze GA, Lozano-Calderon SA, Strackee SD, Blankevoort L, Jupiter JB. Osseous and ligamentous scaphoid anatomy: Part I. A systematic literature review highlighting controversies. *J Hand Surg Am.* 2011;36(12):1926-1935.
2. Buijze GA, Dvinskikh NA, Strackee SD, Streekstra GJ, Blankevoort L. Osseous and ligamentous scaphoid anatomy: Part II. Evaluation of ligament morphology using three-dimensional anatomical imaging. *J Hand Surg Am.* 2011;36(12):1936-1943.
3. Watts A.C. MJM, Fogg Q., Bain G.I.. . Scaphoid Anatomy. In: Slutsky D.J. SJF, ed. *The Scaphoid.* New York: Thieme; 2011:22-30.
4. Tueting J. Scaphoid Anatomy. In: Yao J, ed. *Scaphoid Fractures and Nonunions.* Switzerland: Springer International Publishing; 2015.
5. Berger RA. The gross and histologic anatomy of the scapholunate interosseous ligament. *J Hand Surg Am.* 1996;21(2):170-178.
6. Berger RA, Blair WF. The radioscapholunate ligament: a gross and histologic description. *Anat Rec.* 1984;210(2):393-405.
7. Berger RA, Kauer JM, Landsmeer JM. Radioscapholunate ligament: a gross anatomic and histologic study of fetal and adult wrists. *J Hand Surg Am.* 1991;16(2):350-355.
8. Bettinger PC, Linscheid RL, Berger RA, Cooney WP, 3rd, An KN. An anatomic study of the stabilizing ligaments of the trapezium and trapeziometacarpal joint. *J Hand Surg Am.* 1999;24(4):786-798.
9. Cobb TK, Dalley BK, Posteraro RH, Lewis RC. Anatomy of the flexor retinaculum. *J Hand Surg Am.* 1993;18(1):91-99.
10. Drewniany JJ, Palmer AK, Flatt AE. The scaphotrapezial ligament complex: an anatomic and biomechanical study. *J Hand Surg Am.* 1985;10(4):492-498.
11. Hixson ML, Stewart C. Microvascular anatomy of the radioscapholunate ligament of the wrist. *J Hand Surg Am.* 1990;15(2):279-282.
12. Mayfield JK, Johnson RP, Kilcoyne RF. The ligaments of the human wrist and their functional significance. *Anat Rec.* 1976;186(3):417-428.
13. Mizuseki T, Ikuta Y. The dorsal carpal ligaments: their anatomy and function. *J Hand Surg Br.* 1989;14(1):91-98.
14. Moritomo H, Viegas SF, Nakamura K, Dasilva MF, Patterson RM. The scaphotrapezio-trapezoidal joint. Part 1: An anatomic and radiographic study. *J Hand Surg Am.* 2000;25(5):899-910.
15. Nanno M, Patterson RM, Viegas SF. Three-dimensional imaging of the carpal ligaments. *Hand Clin.* 2006;22(4):399-412; abstract v.
16. Pacek CA, Chakan M, Goitz RJ, Kaufmann RA, Li ZM. Morphological analysis of the transverse carpal ligament. *Hand (N Y).* 2010;5(2):135-140.
17. Sennwald GR, Zdravkovic V, Oberlin C. The anatomy of the palmar scaphotriquetral ligament. *J Bone Joint Surg Br.* 1994;76(1):147-149.
18. Stecco C, Macchi V, Lancerotto L, Tiengo C, Porzionato A, De Caro R. Comparison of transverse carpal ligament and flexor retinaculum terminology for the wrist. *J Hand Surg Am.* 2010;35(5):746-753.
19. Taleisnik J. The ligaments of the wrist. *J Hand Surg Am.* 1976;1(2):110-118.
20. Berger RA. Arthroscopic anatomy of the wrist and distal radioulnar joint. *Hand Clin.* 1999;15(3):393-413, vii.
21. Smith DK. Volar carpal ligaments of the wrist: normal appearance on multiplanar reconstructions of three-dimensional Fourier transform MR imaging. *AJR Am J Roentgenol.* 1993;161(2):353-357.

22. Smith DK. Dorsal carpal ligaments of the wrist: normal appearance on multiplanar reconstructions of three-dimensional Fourier transform MR imaging. *AJR Am J Roentgenol.* 1993;161(1):119-125.

23. Wolfe P, Hotchkiss, Kozin. *Green's Operative Hand Surgery.* Vol 1. 6th ed: Churchill Livingstone; 2010.

24. Mallee W, Doornberg JN, Ring D, van Dijk CN, Maas M, Goslings JC. Comparison of CT and MRI for diagnosis of suspected scaphoid fractures. *J Bone Joint Surg Am.* 2011;93(1):20-28.

25. Mallee WH, Doornberg JN, Ring D, et al. Computed tomography for suspected scaphoid fractures: comparison of reformations in the plane of the wrist versus the long axis of the scaphoid. *Hand (N Y).* 2014;9(1):117-121.

26. Berger RA. The anatomy of the scaphoid. *Hand Clin.* 2001;17(4):525-532.

27. Ceri N, Korman E, Gunal I, Tetik S. The morphological and morphometric features of the scaphoid. *J Hand Surg Br.* 2004;29(4):393-398.

28. Taleisnik J. *The Bones of the Wrist.* New York: Churchill Livingstone; 1985.

29. Williams P.L. W, R. Osteology. In: *Gray's Anatomy.* 37th ed.1989:153-201.

30. Adamany DC, Mikola EA, Fraser BJ. Percutaneous fixation of the scaphoid through a dorsal approach: an anatomic study. *J Hand Surg Am.* 2008;33(3):327-331.

31. Fogg Q. *Scaphoid varation and an anatomical basis for variable carpal mechanics*. Adelaide: Department of anatomical sciences, University of Adelaide; 2004.

32. Yazaki N, Burns ST, Morris RP, Andersen CR, Patterson RM, Viegas SF. Variations of capitate morphology in the wrist. *J Hand Surg Am.* 2008;33(5):660-666.

33. Bogumill G. Anatomy of the Wrist. In: *The Wrist and its Disorders.* Philadelphia: WB Saunders; 1988:14-26.

34. Botte MJ. Skeletal anatomy. In: *Surgical Anatomy of the Hand and Upper Extremity.* Philadelphia: Lippincott Williams & Wilkins; 2003:3-91.

35. Gelberman RHM, J. The vascularity of the scaphoid bone. *J Hand Surg.* 1980:508-513.

36. McLean JM, Turner PC, Bain GI, Rezaian N, Field J, Fogg Q. An association between lunate morphology and scaphoid-trapezium-trapezoid arthritis. *J Hand Surg Eur Vol.* 2009;34(6):778-782.

37. Berger R.A. G-E, M. . General Anatomy of the Wrist. In: An K.N. BRA, Cooney W.P., ed. *Biomechanics of the wrist joint.* New York: Springer-Verlag; 1991:1-22.

38. Tomita K, Berger EJ, Berger RA, Kraisarin J, An KN. Distribution of nerve endings in the human dorsal radiocarpal ligament. *J Hand Surg Am.* 2007;32(4):466-473.

39. Berger RA. The ligaments of the wrist. A current overview of anatomy with considerations of their potential functions. *Hand Clin.* 1997;13(1):63-82.

40. Sennwald S. *The Wrist.* Berlin: Springer-Verlag; 1987.

41. Weitbrecht J. *Syndesmologia sive historia ligamentorum corporis humani, quam secundum observationes antaomicas concinnavit en figuris et objecta recetnia adumbratis illustravit.* Petropoli, Petersburg: Acadamy of Sciences; 1742.

42. Berger RA, Landsmeer JM. The palmar radiocarpal ligaments: a study of adult and fetal human wrist joints. *J Hand Surg Am.* 1990;15(6):847-854.

43. Lichtman DM. *The wrist and its disorders.* Philadelphia: WB Saunders; 1988.

44. Zancolli E. EP. The carpus. In: *Atlas of Surgical Anatomy of the Hand.* Singapore: Churchill Livingstone; 1992:416-430.

45. Boabighi A, Kuhlmann JN, Kenesi C. The distal ligamentous complex of the scaphoid and the scapho-lunate ligament. An anatomic, histological and biomechanical study. *J Hand Surg Br.* 1993;18(1):65-69.

46. Ishiko T, Puttlitz CM, Lotz JC, Diao E. Scaphoid kinematic behavior after division of the transverse carpal ligament. *J Hand Surg Am.* 2003;28(2):267-271.

47. Tengrootenhuysen M, van Riet R, Pimontel P, Bortier H, Van Glabbeek F. The role of the transverse carpal ligament in carpal stability: an in vitro study. *Acta Orthop Belg.* 2009;75(4):467-471.

48. Compson JP, Waterman JK, Heatley FW. The radiological anatomy of the scaphoid. Part 1: Osteology. *J Hand Surg Br.* 1994;19(2):183-187.

49. Viegas SF, Yamaguchi S, Boyd NL, Patterson RM. The dorsal ligaments of the wrist: anatomy, mechanical properties, and function. *J Hand Surg Am.* 1999;24(3):456-468.

50. Nagao S, Patterson RM, Buford WL, Jr., Andersen CR, Shah MA, Viegas SF. Three-dimensional description of ligamentous attachments around the lunate. *J Hand Surg Am.* 2005;30(4):685-692.

51. Berger RA, Imeada T, Berglund L, An KN. Constraint and material properties of the subregions of the scapholunate interosseous ligament. *J Hand Surg Am.* 1999;24(5):953-962.

CHAPTER 3

Scaphoid Nonunion

A.E.J. Bulstra

J.N. Doornberg

M.C. Obdeijn

G.A. Buijze

In Bhandari ed. Evidence Based Orthopedics, John Wiley and Sons; 2021; pp. 883-888.

Case Scenario

A 39-year old male presents with progressive wrist pain, possibly following a wrist sprain sustained 1.5 years ago, for which he did not seek medical attention. Physical examination reveals tenderness in the anatomic snuff box and a reduced range of motion. Computed tomography (CT) imaging confirms a nonunion of the scaphoid. (Figure 1)

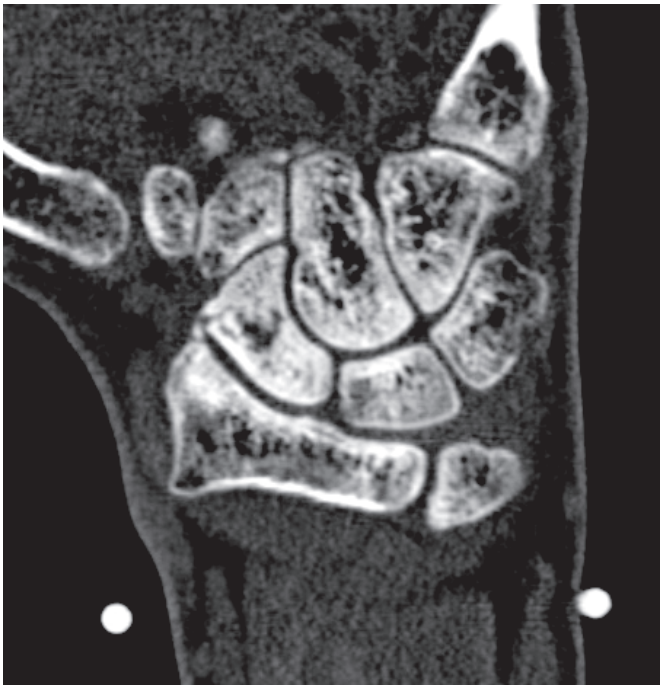

Figure 1. Computed Tomography (CT) Image of a Scaphoid Nonunion

Coronal CT image of the wrist displaying a non-acute fracture of the scaphoid waist extending to the distal pole, with a wide fracture cleft and sclerosis of the fracture surface, confirming scaphoid nonunion.

Key questions

- Which risk factors are associated with scaphoid nonunion?
- What is the preferred management of scaphoid nonunion?
- What is the preferred operative treatment of scaphoid nonunion advanced collapse (SNAC)?

QUESTION 1: WHICH RISK FACTORS ARE ASSOCIATED WITH SCAPHOID NONUNION?

Rationale

Identification of risk factors associated with scaphoid nonunion contributes to the prevention, diagnosis, and tailored treatment in patients at high risk of nonunion.

Clinical comment

Although the majority of scaphoid fractures heal when treated conservatively, nonunion rates of up to 34% are reported in the literature.[1,2] The relatively high rates of nonunion can be attributed to the scaphoid's tenuous vascular supply and the poor diagnostic reliability of radiographs to diagnose acute scaphoid fractures. Identifying risk factors for nonunion may optimize treatment strategies. Assuming that surgical intervention increases rates of union in specific cases, these patients may be offered early surgical intervention.

Available Literature and Quality of the evidence

Literature search, PubMed: ("fractures, ununited"[Mesh] OR "non-union" OR "nonunion") AND ("scaphoid"[Mesh] OR "scaphoid").

Level I

- 1 large inception cohort study[3]

Level II

- 1 retrospective case control study[4]

Level III

- 1 retrospective cohort study [5]
- 3 systematic reviews with methodological limitations [1,2,6]

Level IV

- 9 retrospective case series and reviews with methodological limitations.

Findings

Fracture location and displacement are considered important determinants for fracture union. Proximal pole fractures are at the highest risk for nonunion (10-34%) [1,7] compared to waist (0-33%) [8,9] and distal (0-2%)[10] pole fractures. The increased risk of nonunion in proximal pole fractures is typically attributed to the decreased arterial blood supply and associated risk of avascular necrosis.[1] In displaced fractures - generally defined as fractures with a gap of 1mm or greater between fragments - nonunion rates of up to 55% have been reported.[11] Computed tomography is the recommended diagnostic test to identify fracture displacement and bony configuration of scaphoid fractures.[4] An

exponential relationship exists between the amount of fracture diastasis on CT and the risk of nonunion.[4]

Delayed treatment, resulting from both patient delay and missed diagnosis, increases the risk of nonunion. Nonunion rates are higher in fractures diagnosed and immobilized after 4 weeks (40%) compared to those treated within four weeks (3%).[12] In a quantitative meta-analysis of 1827 patients with established scaphoid nonunion, Merrel et al. described union rates of 90% versus 80% when fractures were treated surgically within, or after 12 months, respectively ($p<0.0001$). [2]

A large inception cohort study by Zura et al. including 7149 scaphoid fractures, identified several risk factors for nonunion, including male sex, use of nonsteroidal anti-inflammatory drugs (NSAIDs) or opioids and osteoarthritis. [3] Other studies reported higher success rates in non-smokers undergoing corrective nonunion surgery than smokers.[5,6] (Table 1a-b)

Recommendations

- The risk of nonunion is increased in proximal pole, displaced and fractures with signs of avascular necrosis. (Overall quality: moderate)
- Adequate diagnosis and early treatment reduce the risk of nonunion. (Overall quality: moderate)
- Smoking decreases the chance of successful scaphoid reconstruction. (Overall quality: low)
- Excessive use of NSAIDs or opioids should be avoided where possible. (Overall quality: low)

Table 1a Fracture Location and Risk of Scaphoid Nonunion

	Study design	Patients (studies) F/U	Relative effect: risk of nonunion RR (95% CI)	Anticipated absolute effect (union rate, %)			Certainty GRADE
Fracture location			*Proximal versus non-proximal*	*Proximal*	*Waist*	*Distal*	
Eastley 2013	Systematic review	1147 (8) u	7.5 (95%CI 4.9-11.5)				⨁◯◯◯ VERY LOW[a,b]
Merrell 2002	Systematic review	676 (19) u		67% p<0.00001 (prox vs waist)	85% p=0.02 (waist vs distal)	100% p=0.02 (waist vs distal)	
Grewal 2013	Retrospective case control	219 (1)		86% p=underpowered	94% p=0.095 (waist vs prox)	100% p=0.065 (distal vs prox)	

F/U: follow up (years); u: unknown; prox: proximal; RR: risk ratio (relative risk) of proximal versus non-proximal acute fractures managed nonoperatively; CI: confidence interval

GRADE certainty assessment
No serious risk of bias, inconsistency, indirectness or imprecision unless otherwise stated.
[a] Serious indirectness: many studies did not assess fracture location with CT
[b] Serious imprecision: large confidence intervals

Table 1b. Other Risk Factors Associated with Scaphoid Nonunion

Risk factor	Study design	Patients (studies) F/U	Relative effect* OR (95% CI)	Anticipated absolute effects (Union rates)		Certainty GRADE
Time to surgery > 12 months				*>12months*	*<12months*	
Merrel 2002	Systematic review	1046 (28)	-	80%	90% p<0.0001	⨁⨁⨁◯ MODERATE
Fracture translation > 1mm				*>1mm*	*<1mm*	
Grewal 2013	Case controlled study	219 (1)	3.40 (1.02-11.29)	88%	96% p=0.040	⨁◯◯◯ VERY LOW[a]
Humpback deformity				*Humpback*	*No humpback*	
Grewal 2013	Case controlled study	219 (1)	6.89 (1.85-25.73)	78%	96% p=0.001	⨁◯◯◯ VERY LOW[a]
NSAID with opioids				*Use*	*No use*	
Zura 2016	Inception cohort study	7149 (1) ≥ 1	2.59 (2.09-3.22) p<0.001	-	-	⨁⨁◯◯ LOW
Opioids only				*Use*	*No use*	
Zura 2016	Inception cohort study	7149 (1) ≥ 1	3.14 (2.56-3.85) p<0.001	-	-	⨁⨁◯◯ LOW
Unknown energy vs. low energy				*Unknown*	*Low energy*	
Zura 2016	Inception cohort study	7149 (1) ≥ 1	2.37 (1.73-3.24) p<0.001	-	-	⨁⨁◯◯ LOW
Osteoarthritis				*Osteoarthritis*	*No osteoarthritis*	
Zura 2016	Inception cohort study	7149 (1) ≥ 1	2.20 (1.74-2.78) p<0.001	-	-	⨁⨁◯◯ LOW

Table 1b. Other Risk Factors Associated with Scaphoid Nonunion (continued)

Risk factor	Study design	Patients (studies) F/U	Relative effect* OR (95% CI)	Anticipated absolute effects (Union rates)		Certainty GRADE
Osteoporosis				*Osteoporosis*	*No osteoporosis*	
Zura 2016	Inception cohort study	7149 (1) ≥ 1	2.45 (1.31-4.58) p<0.005	-	-	⨁⨁◯◯ LOW
Male gender				*Male*	*Female*	
Zura 2016	Inception cohort study	7149 (1) ≥ 1	2.55 (2.09-3.11) p<0.001	-	-	⨁⨁◯◯ LOW
Patient age increase by 10 years						
Zura 2016	Inception cohort study	7149 (1) ≥ 1	0.80 (0.75-0.80) p<0.001	-	-	⨁⨁◯◯ LOW
Smoking [ϕ]				*Smoking*	*No smoking*	
Dinah and Vickers 2007	Retrospective cohort	34 (1) u	3.4	40.0%	82.4% p<0.01	⨁◯◯◯ VERY LOW[b]
Ditsios 2017	Meta-analysis	256 (5) u	10.06[α]	56.25%	92.71% p<0.01	

F/U: follow up (years); OR: odds ratio; CI: confidence interval; u: unknown
* Relative effect: Risk of nonunion in presence of risk factor
[ϕ] Studies report healing rate after surgery for established nonunion of the scaphoid bone
[α] OR for odds of healing i.e. non-smokers had a 10.06 higher chance of healing.

GRADE certainty assessment
No serious risk of bias, inconsistency, indirectness or imprecision unless otherwise stated.
[a] Serious imprecision: large confidence intervals.
[b] Serious inconsistency: inconsistent graft types

QUESTION 2: WHAT IS THE PREFERRED MANAGEMENT OF SCAPHOID NONUNIONS?

Rationale

The aim of treating scaphoid nonunion includes achieving fracture union, relief of symptoms and limiting degenerative wrist arthritis, known as the scaphoid nonunion advanced collapse (SNAC) wrist.[13]

Clinical comment

Persistence of unstable scaphoid nonunion leads to degenerative changes in the scaphoid, radial styloid and ultimately pancarpal arthritis of the scaphocapitate and capitolunate joints.[13] A 97% incidence rate of degenerative changes in untreated symptomatic nonunions older than 5 years has been described.[14] However, the actual correlation between symptoms and disease is poorly reported. It is not clear whether surgery significantly alters disease progression, even if union is attained.[15]

Available Literature and Quality of the evidence

Literature search, PubMed: ("fractures,ununited"[Mesh] OR "non-union"OR"nonunion") AND("scaphoid"[Mesh]OR"scaphoid").

Level II

- 3 randomized controlled trials (RCT) with methodological limitations[16-18]

Level III

- 1 RCT of limited methodological quality
- 4 retrospective comparative studies with methodological limitations[19-21]
- 7 systematic reviews of uncontrolled comparative studies and case series [2,6,22-26]

Level IV

- 159 retrospective case series

Findings

2.1 Operative treatment

The prevailing treatment of scaphoid nonunion constitutes the use of a bone graft and internal fixation.[25] Bone grafts may be vascularized (VBGs) or nonvascularized (NVBGs). VBGs include pedicled grafts from the distal radius or free vascularized grafts from the iliac crest and the medial femoral condyle (MFC). NVBGs include various types of (cortico) cancellous grafts, typically harvested from the iliac crest or distal radius.[15] (Figure 2)

In a meta-analysis of 1602 patients Pinder et al. reported comparable rates of union in VBGs (88%) and NVBGs (92%).[25] However, the vascular status as well as the bony

configuration should be taken into consideration when planning scaphoid reconstruction, using pre-operative MRI and CT, respectively.[4,27]

In case of unstable nonunions with a humpback deformity and dorsal intercalated segment instability (DISI), structural corticocancellous grafts allow for the restoration of scaphoid height and carpal alignment.[26] In a systematic review by Sayegh and Straugh, union rates of corticocancellous grafts were comparable to non-structural cancellous grafts (92% versus 95%, respectively, p=0.26) while functional outcomes were significantly higher.[26]

Regarding the scaphoid's vascular status, proximal pole viability should be assessed preoperatively. Gadolinium enhanced MRI has proven the most sensitive and specific diagnostic modality to assess the presence of avascular necrosis (AVN). [27] However, its correlation with rates of union after bone grafting remains inconclusive.[28] In the absence of AVN, NVBGs appear equivalent to VBGs in terms of union rate and functional outcome. [25,29] In case of AVN, VBGs are associated with higher rates of union than NVBGs. [2,23,25] Merrel et al. reported VBGs to yield significantly higher rates in patients with AVN (88% versus NVBGs 47%, p<0.01) and in patients who had previous surgery (94% versus 81%, p>0.05).[2] There is no consistent high quality evidence supporting the superiority of free VBGs versus pedicled VBGs.[6,30]

Regarding donor site morbidity, grafts from the distal radius (vascularized and nonvascularized) and free MFC are associated with the least donor site morbidity.[22,25] (Table 2a-b)

2.2 Adjunctive treatment

Treatment modalities such as pulsed electromagnetic field therapy (PEMF)[31], low-intensity pulsed ultra sound (LIPUS)[32] and the use of recombinant human bone morphogenetic proteins (rhBMP)[33] have been investigated as adjunctive therapy to increase union rates. Most studies reporting on the use of such modalities are subject to important methodological limitations affecting outcome reliability and should be interpreted with caution. Overall, there is insufficient evidence supporting the use of these adjunctive treatment modalities.

Recommendations

- In the absence of proximal pole AVN, NVBGs and VBGs yield equivalent union rates and functional outcomes. (Overall quality: moderate)
- In nonunions with DISI deformity, structural corticocancellous grafts can provide a better restoration of carpal geometry. (Overall quality: moderate)
- In case of AVN VBGs are associated with higher rates of union. (Overall quality: low-moderate)
- There is no consistent evidence supporting the superiority of free VBGs to pedicled VBGs in case of AVN. (Overall quality: low)
- There is insufficient evidence for the use of adjunctive treatments such as LIPUS, PEMF or rhBMP (Overall quality: low)

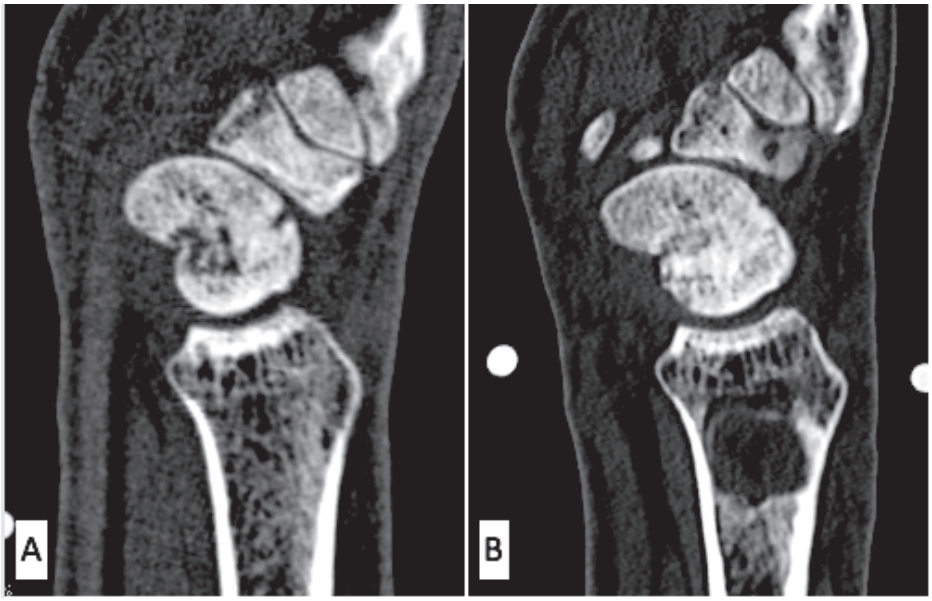

Figure 2. Resolution Clinical Scenario: Scaphoid Reconstruction with a Corticocancellous Bone graft

A. Pre-operative sagittal CT image of the wrist shows a tendency towards a humpback deformity.
B. Considering the presence of a mild humpback deformity the patient is treated with a nonvascularized corticocancellous graft of the distal radius. After thorough debridement of the fracture surfaces, the graft is placed between the proximal and distal fragment of the scaphoid, thereby restoring scaphoid height. The post-operative CT, 3 months after surgery, demonstrates improvement in scaphoid height and near complete consolidation.

QUESTION 3: WHAT IS THE PREFERRED OPERATIVE TREATMENT OF A SNAC WRIST?

Rationale

Proximal row carpectomy (PRC) and four-corner arthrodesis (4CA) are salvage procedures for stage II-III SNAC wrists. It is important to identify the relative advantages in terms of post-operative function, pain and risk of osteoarthritis associated with each procedure.

Clinical comment

In stage II and III SNAC wrists - or in case of unsuccessful nonunion surgery - salvage procedures aim to alleviate pain and preserve wrist function[15] Options include partial or complete wrist arthrodesis, PRC, radial denervation, radial styloidectomy, excision of the distal ununited scaphoid fragment or excision of the proximal pole and replacement with a pyrocarbon implant.[34,35] Management will largely be dictated by the stage of degenerative arthritis, as classified by Vender et al.[13] In stage II-III wrists PRC and scaphoid excision with 4CA are the most commonly described interventions.

Available Literature and Quality of the evidence

Literature search, PubMed: ("Fractures, Ununited"[Mesh] OR "non-union"OR "non-union") AND ("scaphoid"[Mesh] OR"scaphoid")

Level II

- 1 RCT with methodological limitations[36]

Level III

- 1 systematic review of comparative studies [37]
- 1 systematic review of non-comparative retrospective case series [38]
- 13 retrospective cohort studies.[37,39]

Level IV

- 78 retrospective case series

Findings

PRC and 4CA have proven equally effective in alleviating pain and comparable in terms of post-operative function.[37] A systematic review by Saltzman et al. reported no significant differences in the proportional change in grip strength (+17% 4CA; +19% PRC p=0.8), wrist extension (<+1% 4CA; (<+1% PRC), flexion (-13% 4CA; -14% PRC p=0.88) and ulnar deviation (+1% 4CA; -4.8% PRC p=0.28). [37] The change in radial deviation was significantly greater following 4CA (+55% versus -30% following PRC, p=0.02).[37] Studies report patient-rated wrist function to be better following PRC or similar following both procedures.[37,39] Brinkhorst et. al demonstrated patients in the PRC group to perform tasks significantly faster, except for activities requiring torque strength.[39] Importantly, Saltzman et al. reported the cumulative incidence of complications to be significantly higher in 4CA groups (29%, including 6.1% nonunion) than PRC (14%, p=0.01). [37] Long-term follow-up studies establishing the incidence of osteoarthritis are scarce. Some studies report a higher incidence of osteoarthritis in PRC groups, however without correlation to clinical symptoms.[38] In a 17 year follow-up by Berkhout et al, no differences in radiographic osteoarthritis or correlation with pain were described between PRC and 4CA.[40] (Table 3a-b)

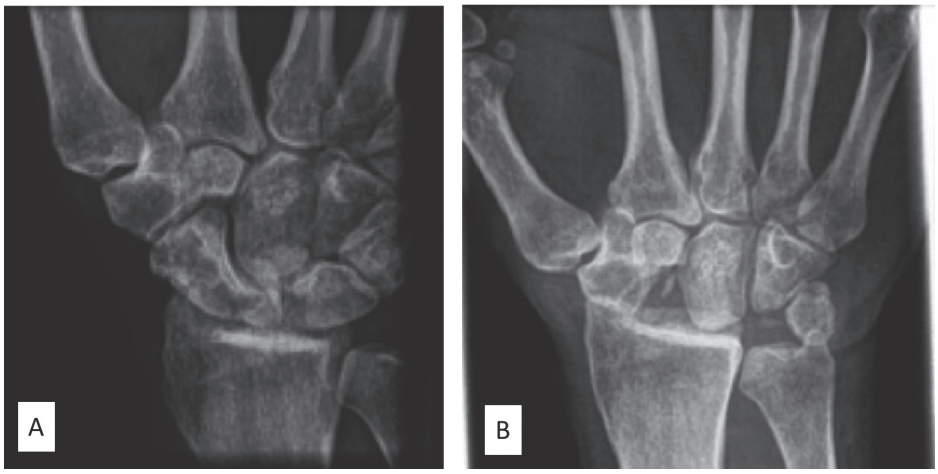

Figure 3. Resolution of Clinical Scenario: Salvage PRC for a stage II SNAC Wrist

Fifteen years after surgery, the patient returns with progressive complaints of wrist pain. Radiographs reveal degenerative changes conform SNAC stage III. Through shared-decision making the options for PRC and 4CA are discussed. In accordance with the patient's preference a PRC is planned.
A. Pre-operative plain radiograph illustrative of a patient with a SNAC stage III, demonstrating degenerative changes of the proximal scaphoid (in this case following a proximal pole fracture), the radial scaphoid fossa and scaphocapitate and lunocapitate joint.
B. Post-operative plain radiograph following a PRC.

Recommendations

- PRC and 4CA effectively alleviate pain and yield comparable results in terms of change in range of motion (overall quality: low)
- Patient-reported wrist function following PRC and 4CA is similar or better following PRC (overall quality: low)
- 4CA is associated with a higher overall complication rate. (overall quality: low)
- There is inconsistent evidence on the incidence of osteoarthritis following PRC and 4CA (overall quality: low)

Table 3a. Salvage procedures - PRC versus 4CA: range of motion, grip strength, function, pain

Outcome	Study design	Patients (studies) F/U		Absolute effect		Comments	Certainty GRADE
Range of Motion				*PRC*	*4CA*		
Aita* 2016	Non-blinded randomized trial	27 (1) 3.5-6		68.5%	58.01% p=0.593	Total ROM, relative to contralateral unaffected side.	⨁⨁◯◯[a,b] LOW
Saltzman* 2015	Systematic review	240 (7)	FE	75° (SD 10°)	62° (SD 14°) p<0.0001	No significant difference in post-operative change in FE arc between PRC and 4CA	⨁◯◯◯[c,d] VERY LOW
			UR	32° (SD 5)	30° (SD 9) p=0.0633	Change in radial deviation was significantly greater after 4CA (+55°) compared to PRC (-30°)	
Mulford* 2009	Systematic review	2143 (52)	FE	75°	64° p=u		
			UR	32°	41° p=u		
Grip strength (% relative to unaffected side)				*PRC*	*4CA*		
Aita 2016	Non-blinded randomized trial	27 (1) 3.5-6		78.7%	65.4% p=0.145		⨁⨁◯◯[a,b] LOW
Saltzman 2015	Systematic review	240 (7)		67% (SD 16)	74% (SD 13) p=0.0002	No significant difference in change in grip strength PRC: +19% and 4CA: +17%	⨁◯◯◯[c] VERY LOW
Mulford 2009	Systematic review	2143 (52)		70%	75% p=u		

Table 3a. Salvage procedures - PRC versus 4CA: range of motion, grip strength, function, pain (continued)

Outcome	Study design	Patients (studies) F/U	Absolute effect		Comments	Certainty GRADE
Function			*PRC*	*4CA*		
Aita 2016	Non-blinded randomized trial	27 (1) 3.5-6	11	13 p=0.697	Dash score	⨁⨁◯◯[a,b] LOW
Saltzman* 2009	Systematic review	u (2)	21 (SD 17)	28 (SD 31) p=1.102	Dash score	⨁◯◯◯[c] VERY LOW
Brinkhorst 2016	Retrospective cohort study	48 (1) 1.9 PRC 6.25 4CA	87 (range 61-100)	69 (range 18-99)	MHQ score	⨁◯◯◯[c] VERY LOW
			221 seconds	241 seconds p=0.0007	Sollerman hand function test: tests ADL Only activities requiring torque strength were faster in 4CA	
Pain			*PRC*	*4CA*		
Aita 2016	Non-blinded randomized trial	27 (1) 3.5-6	2.3	2.9 p=0.769	VAS score	⨁⨁◯◯[a,b] LOW
Brinkhorst 2016	Retrospective cohort study	48 (1) 1.9 PRC 6.25 4CA	10 median, (range: 0-40)	48 median (range: 0-85) p=u	MHQ scale	⨁◯◯◯ VERY LOW

Table 3a. Salvage procedures - PRC versus 4CA: range of motion, grip strength, function, pain (continued)

Outcome	Study design	Patients (studies) F/U	Absolute effect		Comments	Certainty GRADE
Mulford 2009	Systematic review	977 (27)	16%	15%	Percentage of patients reporting pain as "poor" versus "good"	⨁◯◯◯[b,c,d] VERY LOW

*Studies included patients with scaphoid nonunion advanced collapse and scapholunate advanced collapse.
Pts: patients; F/U: follow up in years; PRC: proximal row carpectomy; 4CA: 4 corner arthrodesis; SD: standard deviation; FE: flexion-extension arc; UR: ulnar-radial deviation arc; VAS: visual analogue scale; Dash score: lower score indicated better hand function; MHQ: Michigan Hand outcome Questionnaire (function: higher score indicates better hand function; pain: higher score indicates more pain)

GRADE certainty assessment
No serious risk of bias, inconsistency, indirectness or imprecision unless otherwise stated.
a. Serious risk of bias: lack of blinding
b. Serious imprecision: small number of patients
c Serious selection bias
d. Serious inconsistency: inconsistent results among studies

Table 3b. Proximal row carpectomy (PRC) versus 4 corner arthrodesis (4CA): Complications

Outcome	Study design	No of pts (studies) F/U	Absolute effect		Comments	Certainty GRADE
Overall complication rate			*PRC*	*4CA*		
Saltzman*	Systematic review	101 (6) u	14% 29%	p=0.01	Most commonly reported complications were synovitis and oedema (3.1%) in PRC group versus nonunion (6.9%) in 4CA group.	⨁◯◯◯ VERY LOW[a]
Risk of osteoarthritis			*PRC*	*4CA*		
Mulford*	Systematic review	2143 (52) u	3.7%	1.4% p<0.05		⨁◯◯◯ VERY LOW[a,b]
Risk of conversion to fusion			*PRC*	*4CA*		
Mulford	Systematic review	2143 (52) u	3.9%	2.9% p=0.22		⨁◯◯◯ VERY LOW[a,b,c]
Saltzman	Systematic review	101 (6) u	7.1%	10% p>0.05		

*Studies include patients with both scaphoid nonunion advanced collapse (SNAC) and scapholunate advanced collapse (SLAC)
Pts: patients; F/U: follow up in years; PRC: proximal row carpectomy; 4CA: 4 corner arthrodesis; SD: standard deviation; VAS: visual analogue scale; MHQ: Michigan Hand outcome Questionnaire.

GRADE certainty assessment
No serious risk of bias, inconsistency, indirectness or imprecision unless otherwise stated.
a. Serious selection bias
b. Serious imprecision due small number of patients
c Serious inconsistency in results among studies

SUMMARY OF RECOMMENDATIONS

- The risk of nonunion is increased in proximal pole fractures, fractures with AVN and displaced fractures.
- Delayed treatment, use of opioids or NSAIDs and smoking increase chances of nonunion and reduce chances of successful nonunion surgery.
- In the absence of AVN, scaphoid reconstructions with VBGs and NVBGs are equivalent in terms of union rates and functional outcome. Considering the technical difficulty of VBGs, NVBGs may be preferred.
- Structural bone grafts enable better restoration of carpal geometry in unstable scaphoid nonunions with DISI.
- In the context of AVN, VBGs yield superior union rates. There is no consistent evidence supporting the superiority of free VBGs compared to pedicled grafts.
- In SNAC stage II-III wrists, PRC and 4CA offer comparable results in terms of pain relief and range of motion.
- No evidence based recommendations can be made with regards to the risk of osteoarthritis following PRC or 4CA.

REFERENCES

1. Eastley N, Singh H, Dias JJ, Taub N. Union rates after proximal scaphoid fractures; meta-analyses and review of available evidence. *J Hand Surg Eur Vol.* 2013;38(8):888-897.
2. Merrell GA, Wolfe SW, Slade JF, 3rd. Treatment of scaphoid nonunions: quantitative meta-analysis of the literature. *J Hand Surg Am.* 2002;27(4):685-691.
3. Zura R, Xiong Z, Einhorn T, et al. Epidemiology of Fracture Nonunion in 18 Human Bones. *JAMA Surg.* 2016;151(11):e162775.
4. Grewal R, Suh N, Macdermid JC. Use of computed tomography to predict union and time to union in acute scaphoid fractures treated nonoperatively. *J Hand Surg Am.* 2013;38(5):872-877.
5. Dinah AF, Vickers RH. Smoking increases failure rate of operation for established non-union of the scaphoid bone. *Int Orthop.* 2007;31(4):503-505.
6. Ditsios K, Konstantinidis I, Agas K, Christodoulou A. Comparative meta-analysis on the various vascularized bone flaps used for the treatment of scaphoid nonunion. *J Orthop Res.* 2017;35(5):1076-1085.
7. Grewal R, Lutz K, MacDermid JC, Suh N. Proximal Pole Scaphoid Fractures: A Computed Tomographic Assessment of Outcomes. *J Hand Surg Am.* 2016;41(1):54-58.
8. Amirfeyz R, Bebbington A, Downing ND, Oni JA, Davis TR. Displaced scaphoid waist fractures: the use of a week 4 CT scan to predict the likelihood of union with nonoperative treatment. *J Hand Surg Eur Vol.* 2011;36(6):498-502.
9. Clementson M, Jorgsholm P, Besjakov J, Bjorkman A, Thomsen N. Union of Scaphoid Waist Fractures Assessed by CT Scan. *J Wrist Surg.* 2015;4(1):49-55.
10. Schuind F, Haentjens P, Van Innis F, Vander Maren C, Garcia-Elias M, Sennwald G. Prognostic factors in the treatment of carpal scaphoid nonunions. *J Hand Surg Am.* 1999;24(4):761-776.
11. Szabo RM, Manske D. Displaced fractures of the scaphoid. *Clin Orthop Relat Res.* 1988(230):30-38.
12. Langhoff O, Andersen JL. Consequences of late immobilization of scaphoid fractures. *J Hand Surg Br.* 1988;13(1):77-79.
13. Vender MI, Watson HK, Wiener BD, Black DM. Degenerative change in symptomatic scaphoid nonunion. *J Hand Surg Am.* 1987;12(4):514-519.
14. Ruby LK, Stinson J, Belsky MR. The natural history of scaphoid non-union. A review of fifty-five cases. *J Bone Joint Surg Am.* 1985;67(3):428-432.
15. Buijze GA, Ochtman L, Ring D. Management of scaphoid nonunion. *J Hand Surg Am.* 2012;37(5):1095-1100; quiz 1101.
16. Braga-Silva J, Peruchi FM, Moschen GM, Gehlen D, Padoin AV. A comparison of the use of distal radius vascularised bone graft and non-vascularised iliac crest bone graft in the treatment of non-union of scaphoid fractures. *J Hand Surg Eur Vol.* 2008;33(5):636-640.
17. Goyal T, Sankineani SR, Tripathy SK. Local distal radius bone graft versus iliac crest bone graft for scaphoid nonunion: a comparative study. *Musculoskelet Surg.* 2013;97(2):109-114.
18. Ribak S, Medina CE, Mattar R, Jr., Ulson HJ, Ulson HJ, Etchebehere M. Treatment of scaphoid nonunion with vascularised and nonvascularised dorsal bone grafting from the distal radius. *Int Orthop.* 2010;34(5):683-688.
19. Hirche C, Xiong L, Heffinger C, et al. Vascularized versus non-vascularized bone grafts in the treatment of scaphoid non-union. *J Orthop Surg (Hong Kong).* 2017;25(1):2309499016684291.
20. Jones DB, Jr., Burger H, Bishop AT, Shin AY. Treatment of scaphoid waist nonunions with an avascular proximal pole and carpal collapse. A comparison of two vascularized bone grafts. *J Bone Joint Surg Am.* 2008;90(12):2616-2625.

21. Tambe AD, Cutler L, Murali SR, Trail IA, Stanley JK. In scaphoid non-union, does the source of graft affect outcome? Iliac crest versus distal end of radius bone graft. *J Hand Surg Br.* 2006;31(1):47-51.

22. Al-Jabri T, Mannan A, Giannoudis P. The use of the free vascularised bone graft for nonunion of the scaphoid: a systematic review. *J Orthop Surg Res.* 2014;9:21.

23. Ferguson DO, Shanbhag V, Hedley H, Reichert I, Lipscombe S, Davis TR. Scaphoid fracture non-union: a systematic review of surgical treatment using bone graft. *J Hand Surg Eur Vol.* 2016;41(5):492-500.

24. Munk B, Larsen CF. Bone grafting the scaphoid nonunion: a systematic review of 147 publications including 5,246 cases of scaphoid nonunion. *Acta Orthop Scand.* 2004;75(5):618-629.

25. Pinder RM, Brkljac M, Rix L, Muir L, Brewster M. Treatment of Scaphoid Nonunion: A Systematic Review of the Existing Evidence. *J Hand Surg Am.* 2015;40(9):1797-1805 e1793.

26. Sayegh ET, Strauch RJ. Graft choice in the management of unstable scaphoid nonunion: a systematic review. *J Hand Surg Am.* 2014;39(8):1500-1506 e1507.

27. Cerezal L, Abascal F, Canga A, Garcia-Valtuille R, Bustamante M, del Pinal F. Usefulness of gadolinium-enhanced MR imaging in the evaluation of the vascularity of scaphoid nonunions. *AJR Am J Roentgenol.* 2000;174(1):141-149.

28. Megerle K, Worg H, Christopoulos G, Schmitt R, Krimmer H. Gadolinium-enhanced preoperative MRI scans as a prognostic parameter in scaphoid nonunion. *J Hand Surg Eur Vol.* 2011;36(1):23-28.

29. Caporrino FA, Dos Santos JB, Penteado FT, de Moraes VY, Belloti JC, Faloppa F. Dorsal vascularized grafting for scaphoid nonunion: a comparison of two surgical techniques. *J Orthop Trauma.* 2014;28(3):e44-48.

30. Chaudhry T, Uppal L, Power D, Craigen M, Tan S. Scaphoid Nonunion With Poor Prognostic Factors: The Role of the Free Medial Femoral Condyle Vascularized Bone Graft. *Hand (N Y).* 2017;12(2):135-139.

31. Pereira A, Hidalgo Diaz JJ, Saur M, Salazar Botero S, Facca S, Liverneaux P. Carpal scaphoid non-union treatment: a retrospective trial comparing simple retrograde percutaneous screw fixation versus percutaneous screw fixation plus pulsed electromagnetic fields (Physiostim(R)). *Eur J Orthop Surg Traumatol.* 2017;27(4):521-525.

32. Carlson EJ, Save AV, Slade JF, 3rd, Dodds SD. Low-intensity pulsed ultrasound treatment for scaphoid fracture nonunions in adolescents. *J Wrist Surg.* 2015;4(2):115-120.

33. Rice I, Lubahn JD. Use of bone morphogenetic protein-2 (rh-BMP-2) in treatment of wrist and hand nonunion with comparison to historical control groups. *J Surg Orthop Adv.* 2013;22(4):256-262.

34. Gras M, Wahegaonkar AL, Mathoulin C. Treatment of Avascular Necrosis of the Proximal Pole of the Scaphoid by Arthroscopic Resection and Prosthetic Semireplacement Arthroplasty Using the Pyrocarbon Adaptive Proximal Scaphoid Implant (APSI): Long-Term Functional Outcomes. *J Wrist Surg.* 2012;1(2):159-164.

35. Strauch RJ. Scapholunate advanced collapse and scaphoid nonunion advanced collapse arthritis--update on evaluation and treatment. *J Hand Surg Am.* 2011;36(4):729-735.

36. Aita MA, Nakano EK, Schaffhausser HL, Fukushima WY, Fujiki EN. Randomized clinical trial between proximal row carpectomy and the four-corner fusion for patients with stage II SNAC. *Rev Bras Ortop.* 2016;51(5):574-582.

37. Saltzman BM, Frank JM, Slikker W, Fernandez JJ, Cohen MS, Wysocki RW. Clinical outcomes of proximal row carpectomy versus four-corner arthrodesis for post-traumatic wrist arthropathy: a systematic review. *J Hand Surg Eur Vol.* 2015;40(5):450-457.

38. Mulford JS, Ceulemans LJ, Nam D, Axelrod TS. Proximal row carpectomy vs four corner fusion for scapholunate (Slac) or scaphoid nonunion advanced collapse (Snac) wrists: a systematic review of outcomes. *J Hand Surg Eur Vol.* 2009;34(2):256-263.

39. Brinkhorst ME, Singh HP, Dias JJ, Feitz R, Hovius SE. Comparison of activities of daily living after proximal row carpectomy or wrist four-corner fusion. *J Hand Surg Eur Vol.* 2016.

40. Berkhout MJ, Bachour Y, Zheng KH, Mullender MG, Strackee SD, Ritt MJ. Four-Corner Arthrodesis Versus Proximal Row Carpectomy: A Retrospective Study With a Mean Follow-Up of 17 Years. *J Hand Surg Am.* 2015;40(7):1349-1354.

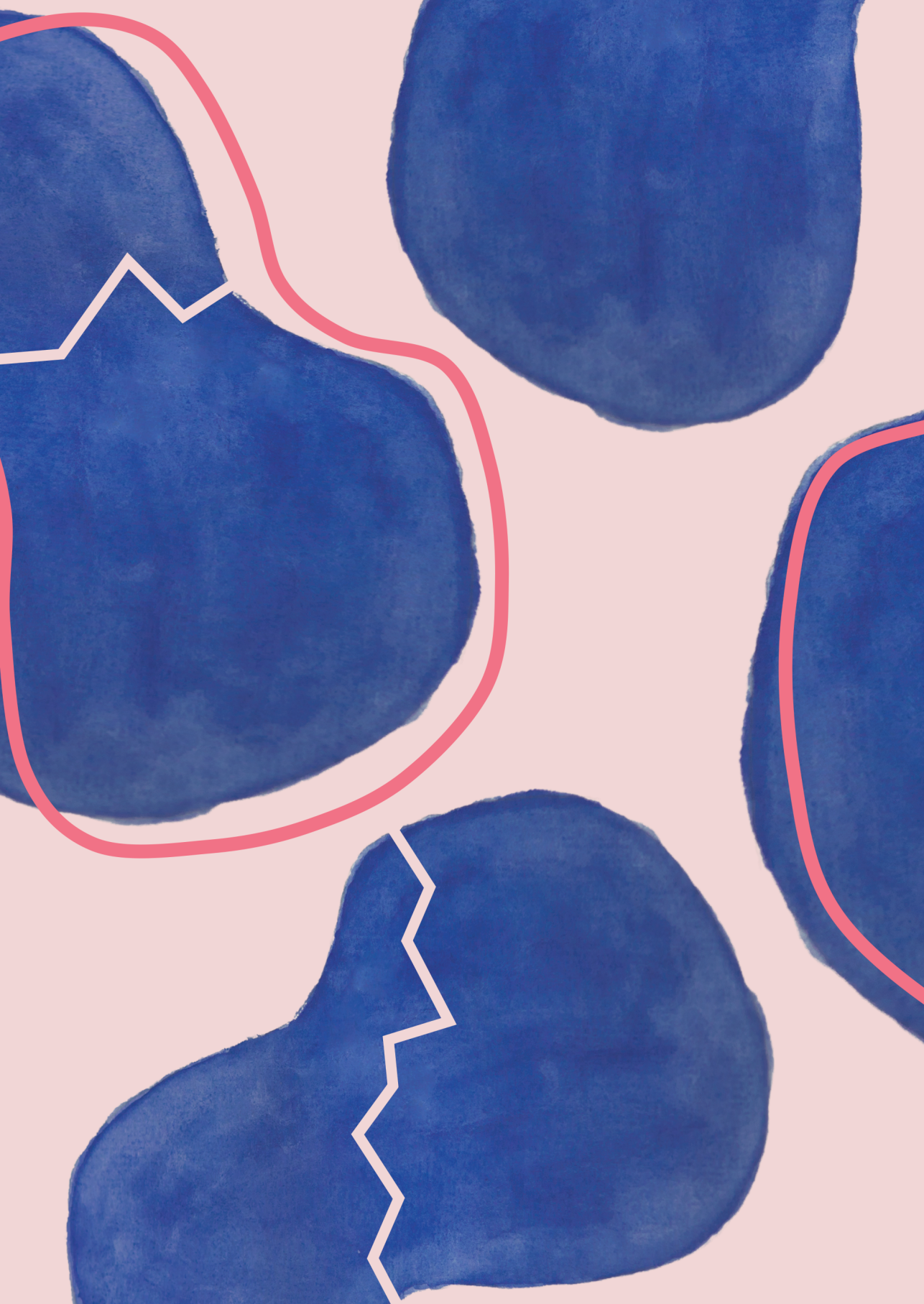

PART II

DIAGNOSIS OF THE (SUSPECTED) SCAPHOID FRACTURE

CHAPTER 4

Machine Learning Algorithm to Estimate the Probability of a True Scaphoid Fracture After Wrist Trauma Scaphoid

A.E.J. Bulstra on behalf of the Machine Learning Consortium*

* Alphabetical order: Geert A. Buijze, Anne Eva J. Bulstra, Abigail Cohen, Ruurd L. Jaarsma, Wouter H. Mallee, Marjolein A.M. Mulders, Margaret M. McQueen, Matthew Moran, Miryam C. Obdeijn, Gino M.M.J. Kerkhoffs, David Ring, Joost W. Colaris, Charles M. Court-Brown, Job N. Doornberg, Andrew D. Duckworth, J. Carel Goslings, Alasdair Gray, Laurent A.M. Hendrickx, Niels W.L. Schep, Monique M.J. Walenkamp

Journal of Hand Surgery America 2022 Aug; 47(8): 709-718 *(Selected as Journal's lead article of the month, featured in Journal of Hand Surgery Podcast.)*

ABSTRACT

Purpose

(1) Identify predictors of a true scaphoid fracture among patients with radial wrist pain following acute trauma; (2) train five machine learning (ML)-algorithms in predicting scaphoid fracture probability; (3) design a decision rule to initiate advanced imaging in high-risk patients.

Methods

Two prospective cohorts including 422 patients with radial wrist pain following wrist trauma were combined. There were 117 scaphoid fractures (28%) confirmed on CT, MRI or radiographs. Eighteen fractures (15%) were occult. Predictors of a scaphoid fracture were identified among demographics, mechanism of injury (MOI) and examination manoeuvres. Five ML-algorithms were trained in calculating scaphoid fracture probability. ML-algorithms were assessed on (1) ability to discriminate between patients with and without a fracture (area under the receiver operating characteristic curve [AUC]); (2) agreement between observed and predicted probabilities (calibration); (3) overall performance (Brier-score). The best performing ML-algorithm was incorporated in a probability calculator. A decision rule was proposed to initiate advanced imaging among patients with negative radiographs.

Results

Pain over scaphoid on ulnar deviation, sex, age and MOI were most strongly associated with a true scaphoid fracture. The best performing ML-algorithm yielded an AUC, calibration-slope, -intercept and Brier-score of 0.77, 0.84, -0.01 and 0.159, respectively. The ML-derived decision rule proposes to initiate advanced imaging in patients with radial sided wrist pain, negative radiographs, and a fracture probability of ≥10%. When applied to our cohort, this would yield 100% sensitivity, 38% specificity, and would have reduced the number of patients undergoing advanced imaging by 36% without missing a fracture.

Conclusion

The ML-algorithm accurately calculated scaphoid fracture probability based on scaphoid pain on ulnar deviation, sex, age and MOI. The ML-decision rule may reduce the number of patients undergoing advanced imaging by a third with a small risk of missing a fracture. External validation is required prior to implementation.

Level of Evidence

II

INTRODUCTION

It is estimated that between 6% to 25% of patients with scaphoid tenderness and normal initial radiographs after injury have a true scaphoid fracture.[1-4] Therefore, these patients are often immobilized until repeat examination or additional imaging lowers the probability of fracture to a more acceptable, albeit undefined, threshold.[4-6] Immediate MRI and CT in patients with a suspected scaphoid fracture are used to identify patients that can safely return to work or sports without immobilization. They are considered the best available modalities for acute scaphoid fracture diagnosis.[7,8] However, a low prevalence of true fractures among patients with a suspected scaphoid fracture can make even MRI and CT less accurate and useful. This is because under these low-probability circumstances – and in the absence of a perfect agreed reference standard – a false positive diagnosis may occur almost as frequently as a true positive diagnosis.[9] The result is the potential for unnecessary immobilization.[10,11]

A clinical decision rule to selectively identify high risk patients that benefit from advanced imaging might increase the pre-test probability of a fracture. This may reduce the number of patients that undergo additional imaging and improve the utility of advanced imaging in patients with a suspected scaphoid fracture.[9] Duckworth et al. and Mallee et al. designed clinical prediction rules incorporating clinical and demographic predictors of both radiographically visible and occult fractures confirmed on repeat radiographs, CT or MRI.[12,13] Duckworth et al. reported a fracture probability of 39% and 74%, respectively, among patients with three or four predictive signs (male sex, sports injury, anatomic snuffbox [ASB] pain on ulnar deviation of the wrist and pain on thumb index pinch at initial presentation).[12] Among patients with none, one or only two of the predictive signs, the fracture probability was 0%, 2% and 20%, respectively. Mallee et al. calculated the probability of a fracture based on patient sex, ASB swelling, ASB tenderness, pain over the scaphoid on ulnar deviation and painful longitudinal thumb compression at presentation.[13] Their prediction rule correctly identified 97% of the true fractures, while reducing the number of patients undergoing radiographs by 15%.[13] Thus far it has been challenging to develop a decision rule that is both specific and sensitive using conventional statistical methods.

In some settings, Machine Learning (ML) models yield more accurate predictions than traditional prediction models based on classic regression or latent class analysis.[14-16] ML and Artificial Intelligence (AI) cover a variety of computer applications varying from computer vision to detect fractures[17-19], to risk stratification models used in clinical prediction rules.[15,20-26] ML-derived models offer the potential advantage of processing complex nonlinear relationships and interactions.[14] ML-algorithms can adapt and improve when they are retrained over time once more data is available to add to the dataset.[27]

In this preliminary study we aimed to (1) identify predictors of a true scaphoid fracture among patients with radial sided wrist pain presenting within 72 hours after acute wrist trauma; (2) train and evaluate five ML-algorithms in predicting the probability of a scaphoid fracture among patients with radial sided wrist pain within 72 hours after wrist trauma; and

(3) deploy the best performing ML-algorithm as a probability calculator and propose a decision rule to initiate advanced imaging in selected patients with negative radiographs.

PATIENTS AND METHODS

Study design and setting

Databases of two prospective studies that previously developed a clinical decision rule for a true scaphoid fracture were combined for analysis.[12,13] Both studies included patients with radial sided wrist pain after a fall or other wrist trauma presenting within 72 hours after injury. Both studies were approved by local ethics committees. Data was shared following the WHO data sharing agreement.

This study was conducted according to the Guidelines for Developing and Reporting Machine Learning Predictive Models in Biomedical Research and the Transparent Reporting of Multivariable Prediction Models for Individual Prognosis or Diagnosis (TRIPOD) guideline.[28,29]

Participants

Patients enrolled at the Royal Infirmary of Edinburgh included 223 patients (≥13 years) with clinical symptoms of a scaphoid fracture and a radiologically visible or occult scaphoid fracture presenting within 72 hours after injury. Patients with major concomitant ipsilateral injury were excluded.[12] As there is no evidence that predictors or presentation of a radiographically visible fracture differ from those of occult fractures, all 223 patients were included for training the algorithm.

The study cohort from Amsterdam University Medical Centre included 235 adult patients (≥18) enrolled at five different institutions.[13] Patients with a suspicion for a scaphoid fracture, as assessed by the treating Emergency Department (ED) physician, presenting within 72 hours after injury were included prior to radiographic examination. For the current study, patients with 1) a concomitant ipsilateral distal radius, carpal or metacarpal fracture (n=33) and 2) patients who had three or more (out of five) missing values for clinical scaphoid tests (n=3) were excluded. A total of 199 patients were included.

The combined cohorts included a total of 422 patients. A scaphoid fracture was present in 117 (28%) patients. Ninety-nine (84%) of the fractures were diagnosed on initial radiographs. Eighteen fractures (15%) were occult fractures, not visible on initial radiographs: Nine (7%) were diagnosed on repeat 2-week radiographs and nine (8%) on MRI or CT. (Table 1) There were another 37 patients that had MRI or CT that did not show a scaphoid fracture. Patients without scaphoid tenderness on repeat examination manoeuvres and negative radiographs at two-week review were defined as no scaphoid fracture. [12,13]

TABLE 1. Patient Demographics and Clinical Variables

Variable		
Sex, n (%)		
Male	210	(49.8)
Female	212	(50.2)
Age, median (IQR)	35	(24-53)[†]
Affected side is dominant side, n (%)		
Yes	225	(53.3)
No	197	(46.7)
Mechanism of injury, n (%)		
Fall from standing	226	(53.6)
Sports injury	89	(21.1)
Road traffic accident	43	(10.2)
Fight / assault	19	(4.5)
Fall from height	13	(3.1)
Other	32	(7.6)
Examination manoeuvre, n (%)		
ASB tenderness on palpation	361	(86)
Tubercle tenderness on palpation	279	(66)
Tenderness on axial thumb compression	261	(62)
Painful OK-sign (thumb-index pinch)	271	(64)
Pain over scaphoid on ulnar deviation	289	(68)
Scaphoid fracture, n (%)		
No	305	(72.3)
Yes	117	(27.7)
Visible on initial radiographs	99	(85.0)
Occult	18	(15.0)

n=number of patients; IQR = first quartile – third quartile
[†] Age range: 13-99 years.

Variables and predictor variable selection

We extracted all patient and clinical variables that were recorded in both databases as potential predictor variables (Table 1). Missing variables (<1%) were imputed using the 'missForest' algorithm.[30]

An algorithm for variable selection ("Boruta Algorithm") identified the combination of variables that yielded the greatest accuracy in predicting the probability of a scaphoid fracture.[31] This Random Forest based algorithm identifies variables that are statistically more relevant to predicting a scaphoid fracture than artificially created 'noise variables'.[31] These so-called 'important' variables were incorporated in the ML prediction models.

Algorithm development

In machine learning, multiple algorithms are typically trained as performance varies per dataset. Following previous studies developing ML-algorithms to predict a binary outcome, we trained five supervised ML-algorithms in estimating the probability of a true scaphoid fracture based on the selected input variables: 1) Bayes Point Machine 2) Boosted Decision Tree 3) Penalized Logistics Regression 4) Neural Network 5) Support Vector Machine.[22,23,25,26,32] (See Supplementary Material Table 1). 'Supervised' ML implies that algorithms are trained on a labelled dataset and validated on 'unseen' data. [27] Split sample approaches - in which data is split into a training and validation set - are prone to bias when sample size is limited.[33] Therefore, a method called 10-fold cross-validation was used. [23,25,26,34,35] Ten-fold cross-validation allows the use of the entire dataset for both training and validation by dividing the dataset in 10 subsets or "folds".[33] The model is subsequently trained using 9 out of the 10 folds, using the 10th 'unseen' fold as a validation dataset. This is repeated 10 times until each fold has been used as a validation set. Cross-validation was repeated three times. (Supplementary Material, Figure 1)

Algorithm performance

The performance of the ML-algorithms was assessed and compared based on 1) its ability to discriminate between patients with and without a fracture (discrimination); 2) the agreement between predicted and observed probabilities (calibration) and 3) overall model performance (Brier Score) according to Steyerberg's structured 'ABCD-methodology' for clinical prediction rules.[36,37]

Model discrimination was expressed as the area under the receiver operating characteristics (ROC)-Curve (AUC).[36] Perfect discrimination is reflected by an AUC of 1, while an AUC of 0.5 corresponds to a non-informative model.[36]

Model calibration, plotted on a calibration curve, describes the agreement between the predicted (x-axis) and observed (y-axis) probabilities. The calibration curve of a perfect model has a slope of 1 and an intercept of 0.[36]

The Brier score represents the squared differences between the actual outcome and the predicted outcome. The score can range from 0 for a perfect model to 0.25 for a non-informative model with a 50% incidence of the outcome. The score should be interpreted relative to the upper-limit Brier score.[36] When the prevalence of the outcome of interest is lower, the upper-limit Brier score is lower. Based on the 28% prevalence of scaphoid fractures in this cohort, the upper-limit Brier score was calculated to be 0.202. A lower score relative to this upper-limit represents a better performance relative to a non-informative model.[36]

Development decision rule

The best performing algorithm was deployed as a probability calculator (see Supplementary Material Figure 5) and incorporated in a clinical decision rule to initiate advanced imaging in selected patients. To simulate the clinical scenario to which a decision rule would be most applicable, it was applied to patients with clinical symptoms

of a fracture and initial negative or equivocal (scaphoid) radiographs only (n=323). Patients with a radiographically visible fracture (n=99) were excluded for this part of this study. To minimize the occurrence of a false negative diagnosis, we selected a fracture probability threshold to initiate advanced imaging at which sensitivity was optimized.[13]

RESULTS

Predictors of a true scaphoid fracture

The Boruta algorithm identified pain over the scaphoid with ulnar deviation of the wrist within 72 hours after injury, patient sex, age, and mechanism of injury as the only relevant predictor variables for a true scaphoid fracture. These four variables were used for algorithm training. (Figure 1)

We observed an interaction effect between patient age and sex as predictors. Among patients with scaphoid pain on ulnar deviation of the wrist after a fall from standing the ML-estimated probability of a scaphoid fracture increased with age among women aged 23 years and older, but decreased among men aged 23 and older. Relative youth was thus a risk factor among male patients, while older age was a risk factor for female patients in this group. (Figure 2)

Algorithm Performance

Model performance was comparable across the algorithms (Table 2, see Supplementary Figure 3 and 4 for AUC and calibration curves). However, the Boosted Decision Tree demonstrated the best agreement between predicted probabilities and those observed in the sample over the entire range of probabilities based on visual assessment of the calibration curve. This model was therefore selected as the algorithm of choice (Figure 3A, 3B).

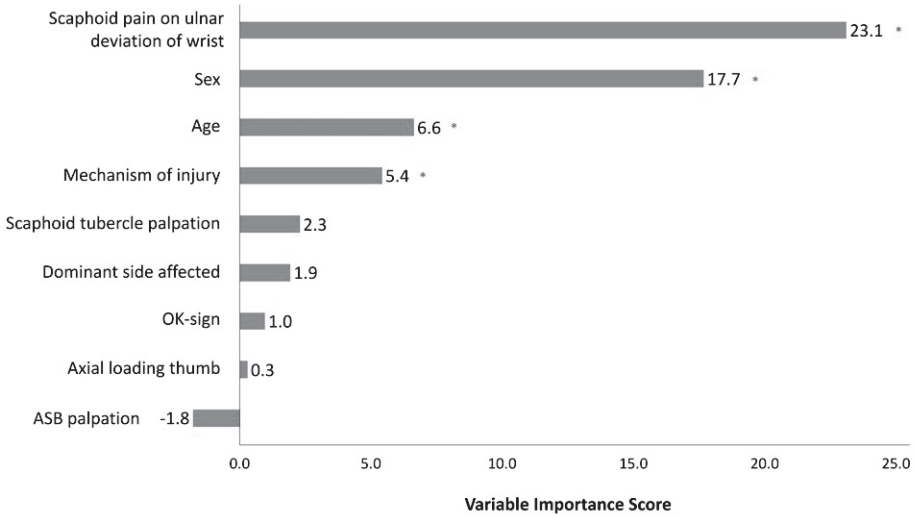

Figure 1. Variable Importance for Prediction of a True Scaphoid Fracture

Variable importance score: a higher score indicates greater importance of the variable in predicting the outcome of interest. * Variables identified as relevant to predicting a scaphoid fracture included in the prediction model.

Table 2. ML Algorithm Performance in Estimating the Probability of a True Scaphoid Fracture

	AUC (95% CI)	Calibration Slope (95%CI)	Calibration Intercept (95%CI)	Brier-Score*
Bayes Point Machine	0.72 (0.69-0.75)	0.92 (0.77-1.07)	-0.03 (-0.16-0.11)	0.168
Boosted Decision Tree	0.77 (0.74-0.80)	0.84 (0.73-0.96)	-0.01 (-0.15-0.13)	0.159
Penalized Logistic Regression	0.74 (0.71-0.77)	0.99 (0.84-1.14)	0.00 (-0.13-0.14)	0.165
Neural Network	0.76 (0.73-0.79)	0.88 (0.75-1.00)	-0.05 (-0.19-0.09)	0.163
Support Vector Machine	0.73 (0.70-0.76)	0.86 (0.72-1.00)	-0.01 (-0.14-0.13)	0.172

* Upper-limit Brier Score: 0.220; AUC: Area Under the Receiver Operating Characteristic Curve; 95%CI: 95% Confidence Interval

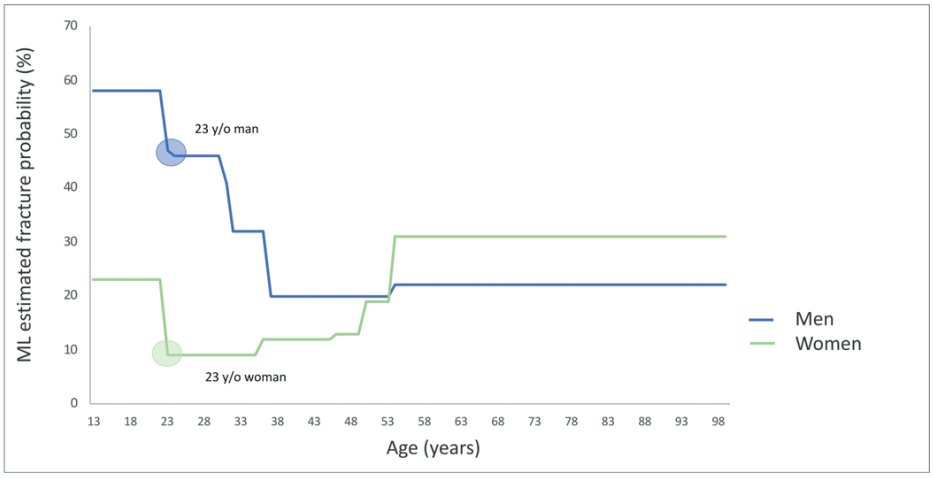

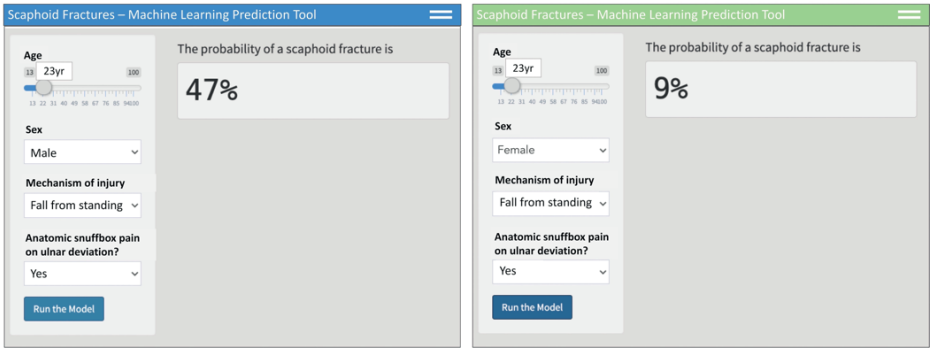

Figure 2. Interaction Between Patient Age and Sex as Predictor Variables After a Fall from Standing

Top row: Graph demonstrating the effect of age on the probability of a scaphoid fracture among men and women presenting with scaphoid pain on ulnar deviation of the wrist after a fall from standing. *Bottom row:* The probability of a scaphoid fracture is calculated for a 23 year old man and a 23 year old woman presenting with pain over the scaphoid on ulnar deviation of the wrist after a fall from standing. ML = Machine Learning.

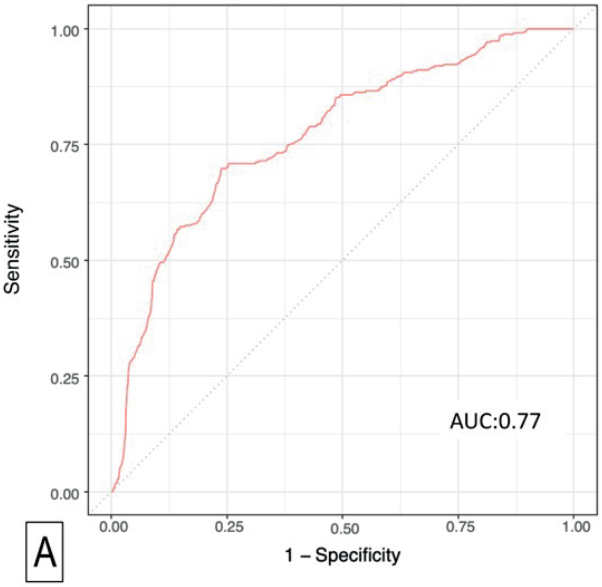

Figure 3A. Area under the ROC curve Boosted Decision Tree

ROC: Receiver Operating Characteristic; AUC: Area under the Receiver Operating Characteristic Curve

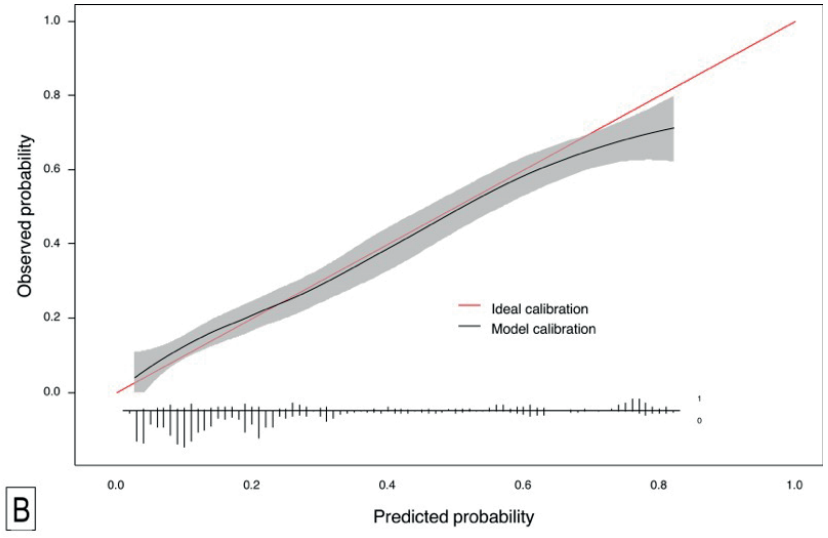

Figure 3B. Calibration curve Boosted Decision Tree

Calibration curve of the Boosted Decision tree showing good correspondence between predicted and actual probabilities of a scaphoid fracture

Decision rule

Studying the ML-calculated fracture probabilities yielded by the probability calculator in our current dataset (Figure 4), we selected a fracture probability threshold at which sensitivity was optimized.[13] The highest sensitivity was seen at an ML-calculated fracture probability of ≥10%. Sensitivity and specificity were 100% and 38% respectively. Based on the preliminary findings of this study we would propose a decision rule in which patients with negative radiographs and an ML-calculated fracture probability of ≥10% are referred for advanced imaging.

If a ≥10% fracture probability had been implemented to initiate advanced imaging in the current cohort, 18 out of 18 patients with a fracture (100%) and 190 out of 305 patients (62%) without a fracture would be referred for advanced imaging. Of the 305 patients without a fracture, 115 (38%) would have been discharged without further imaging. As such, in this cohort the number of patients undergoing advanced imaging would have been reduced by 36% without missing a fracture (Figure 4). Among the 208 patients with radial sided wrist pain, negative radiographs and a fracture probability of ≥10%, 18 patients had a true scaphoid fracture. This amounts to a pre-test probability of 8.7%. This is a slight increase compared to a pre-test probability of 5.6% in the setting in which all 323 patients with radial sided wrist pain, negative radiographs would have undergone MRI or CT at our institution. (Figure 5)

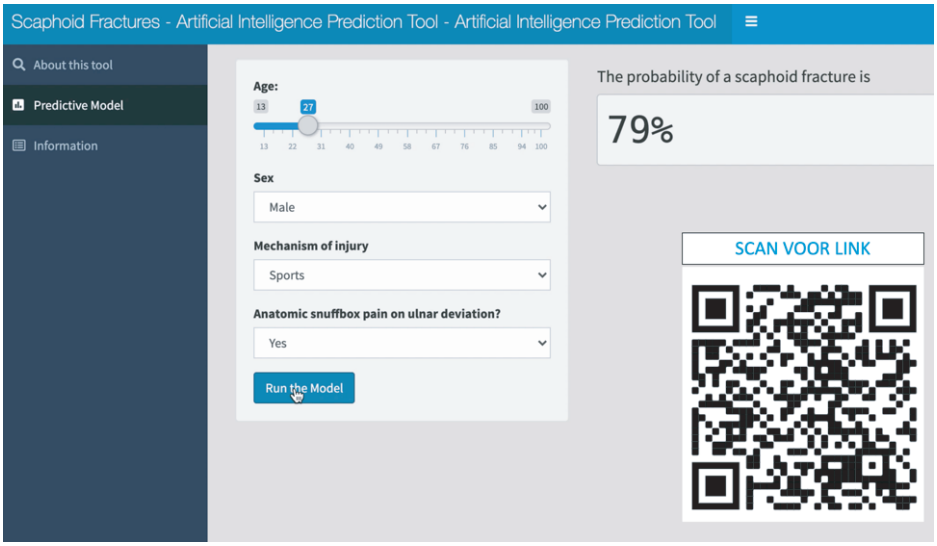

Figure 4. Boosted Decision Tree Algorithm Deployed as an Open Access Probability Calculator

Please note: at this stage the tool is intended for research and educational purposes only and not yet to be implemented for clinical use. Source: https://traumaplatform-ai-prediction-tools.shinyapps.io/Scaphoid-fractures/

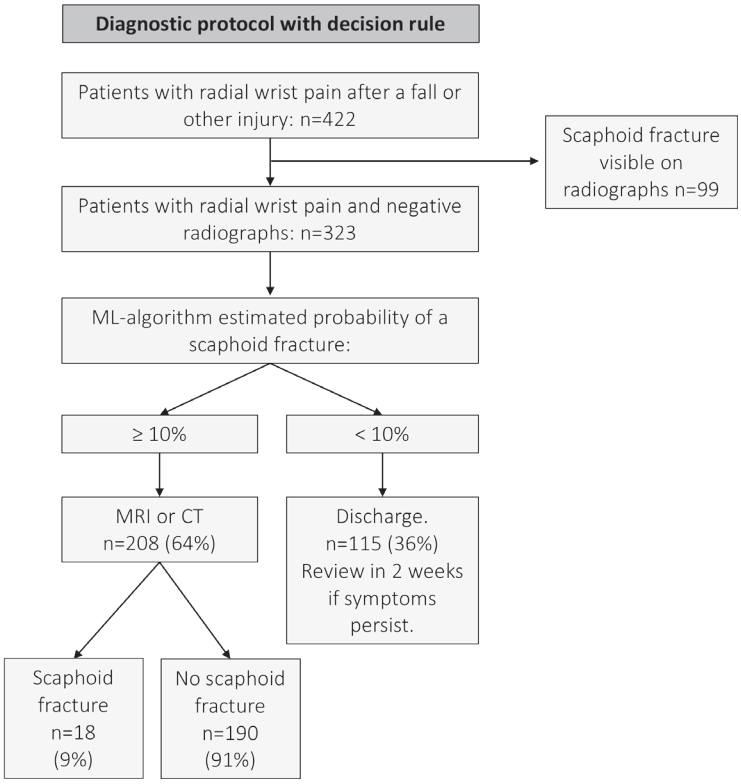

Figure 5 Diagnostic Workflow with and without Decision Rule at our Institution

Diagnostic workflow when implementing the decision rule on our current dataset. At our institution advanced imaging (MRI) is initiated in all patients with radial sided wrist pain and negative radiographs following wrist trauma.

The pre-test probability of a fracture when all patients with radial sided wrist pain and negative radiographs (n=323) undergo MRI or CT among patients undergoing MRI or CT is 18/323 or 5.6%.

The pre-test probability of a fracture among patients with radial sided wrist pain, negative radiographs and a ML-estimated fracture probability of equal to or greater than 10% (n=208) undergoing MRI or CT is 18/208 or 8.7%.

DISCUSSION

More accurate estimations of the probability of a true scaphoid fracture among patients with scaphoid tenderness after an acute wrist injury can help identify patients that benefit most from advanced imaging. In this preliminary study we developed an ML-algorithm that calculates the probability of a true scaphoid fracture based on scaphoid pain on ulnar

deviation of the wrist within 72 hours after injury, patient sex, age and mechanism of injury. Furthermore, we designed a decision rule to initiate advanced imaging in patients with negative radiographs and an ML-estimated fracture probability of ≥10%. Based on our current study sample, we estimate that the ML-decision rule has the potential to reduce the number of patients undergoing advanced imaging by more than a third (36%). In the current dataset no fractures were missed at this fracture probability threshold.

Strengths of this study include the use of multicentre prospective data, which may contribute to external validity.[37] Additionally, the ML-algorithm identified interactions between risk factors that were not previously identified. Limitations include the lack of a consistent reference standard for a true fracture in all patients. There is a small chance that some scaphoid fractures were missed among the patients with negative repeat radiographs and no pain on clinical exam two weeks after initial presentation. These patients were discharged and not followed up. Secondly, the sample is not large for ML-standards. This implies that interactions observed may not be generalizable to other populations. Importantly, the number of confirmed occult fractures (n=18) to which the decision rule was applied was limited. Furthermore, although the algorithm was trained and tested on 'unseen' data using 10-fold cross validation, the decision rule was applied to the same cohort of patients upon which the algorithm was trained. Applying the decision rule to an external cohort may yield different sensitivities and specificities. In a different setting more fractures may be missed at the 10% fracture probability threshold. We therefore consider this preliminary work to be built on using larger datasets. Fourthly, only variables included in both study cohorts were considered. Also, the current cohort included patients presenting within 72 hours after injury only. As diagnostic performance characteristics of examination manoeuvres vary over time, the algorithm may not apply to patients presenting after 72 hours.[12] Lastly, these findings may best apply to our institution's diagnostic protocol. The efficacy and implications may differ for institutions that repeat radiographs prior to performing advanced imaging.

Compared to previous scaphoid fracture prediction rules including up to five variables, we identified a combination of four variables relevant to predicting the presence of a true scaphoid fracture. Contrary to previous studies, combining clinical tests did not improve the diagnostic performance when used in conjunction to patient age, sex and the mechanism of injury.[38] Using one examination manoeuvre simplifies clinical assessment and may remove variation associated with non-specific and potentially unreliable clinical scaphoid tests.[38,39] Additionally, we identified an interaction effect between age and sex that has previously not been reported. Duckworth et al. and Mallee et al. identified male sex as a risk factor and included patient sex in each of their decision rules.[12,13] Duckworth et al. identified relative youth as a predictor of a true scaphoid fracture.[12] We found that the ML-estimated probability of a scaphoid fracture increased above the age of 23 for women, but decreased among men aged 23 and older, when presenting with pain over the scaphoid on ulnar deviation of the wrist after a fall from standing. As such, the ML-algorithm might provide more patient specific probabilities across the entire spectrum of patients.

Algorithm performance was comparable across the five ML-algorithms. The limited discrimination (AUC: 0.72-0.77; 95% CI 0.69-0.80) emphasizes that the diagnosis of a scaphoid fracture at initial assessment (<72 hours) remains a probability rather than a certainty.[13] It also means that when selecting a probability threshold to initiate advanced imaging, one must choose between optimizing either sensitivity or specificity. To minimize the risk of a missed diagnosis, we chose to optimize sensitivity by selecting an ML-estimated fracture probability of ≥10% to initiate advanced imaging in patients with negative radiographs. The performance characteristics reported by Mallee et al. were comparable to the current study, with an AUC of 0.72 (95%CI: 0.65-0.78) and a calibration slope of 1.0 (95% CI: 0.59-1.40). Importantly however, they implemented their rule among all patients presenting with radial wrist pain prior to radiographs. In contrast, we designed our rule to be implemented among patients with negative radiographs only to initiate advanced imaging (MRI/CT) in selected patients.

Two previous studies employing ML among a cohort of comparable sizes reported higher AUC values than 0.72. Hendrickx et al. reported an AUC of 0.89 for an ML-algorithm developed to predict the risk of a posterior malleolar fracture among 263 patients with a tibial shaft fracture.[32] Staartjes et al. reported AUC's of 0.84-0.98 for machine learning algorithms predicting mean leg and back pain scores after diskectomy among 422 patients with lumbar disk hernia.[15] These differences highlight the lack of strong predictor variables for scaphoid fracture diagnosis.

The observation that, with our data, a fracture probability threshold of ≥10% to initiate advanced imaging would reduce the number of patients undergoing advanced imaging by 36%, suggests that accepting a small risk of missing a fracture may be a useful strategy for a decision rule. Importantly, external validation in an external prospective cohort is essential to validate this threshold prior to implementation. At this stage, we therefore recommend patients to be reviewed within two weeks if clinical symptoms persist, even with a fracture probability <10%. Further training the algorithm using larger datasets including more variables may result in more accurate prediction models. If future research confirms the ML-derived decision rule to be a safe and effective diagnostic pathway, the algorithm may be deployed as an online probability calculator (https://traumaplatform-ai-prediction-tools.shinyapps.io/Scaphoid-fractures/). This would not only allow for open access use, but also for the model to be further trained and adapted when new data is entered into the model.

In conclusion, in this preliminary study we have developed an ML-algorithm that predicts the probability of a scaphoid fracture, based on pain over the scaphoid on ulnar deviation of the wrist, sex, age and mechanism of injury. Our decision rule proposes to initiate advanced imaging in patients with negative initial radiographs and an ML-estimated fracture probability of ≥10%. This can reduce the number of patients undergoing advanced imaging with a small possibility of missing a scaphoid fracture. Further training using larger datasets and external validation is essential prior to implementing the decision rule in clinical practice.

REFERENCES

1. Mallee W, Doornberg JN, Ring D, van Dijk CN, Maas M, Goslings JC. Comparison of CT and MRI for diagnosis of suspected scaphoid fractures. *J Bone Joint Surg Am.* 2011;93(1):20-28.
2. Bergh TH, Lindau T, Soldal LA, et al. Clinical scaphoid score (CSS) to identify scaphoid fracture with MRI in patients with normal x-ray after a wrist trauma. *Emerg Med J.* 2014;31(8):659-664.
3. Daniels AM, Bevers M, Sassen S, et al. Improved Detection of Scaphoid Fractures with High-Resolution Peripheral Quantitative CT Compared with Conventional CT. *J Bone Joint Surg Am.* 2020;102(24):2138-2145.
4. Rua T, Gidwani S, Malhotra B, et al. Cost-Effectiveness of Immediate Magnetic Resonance Imaging In the Management of Patients With Suspected Scaphoid Fracture: Results From a Randomized Clinical Trial. *Value Health.* 2020;23(11):1444-1452.
5. Suh N, Grewal R. Controversies and best practices for acute scaphoid fracture management. *J Hand Surg Eur Vol.* 2018;43(1):4-12.
6. Jenkins PJ, Slade K, Huntley JS, Robinson CM. A comparative analysis of the accuracy, diagnostic uncertainty and cost of imaging modalities in suspected scaphoid fractures. *Injury.* 2008;39(7):768-774.
7. Karl JW, Swart E, Strauch RJ. Diagnosis of Occult Scaphoid Fractures: A Cost-Effectiveness Analysis. *J Bone Joint Surg Am.* 2015;97(22):1860-1868.
8. Mallee WH, Wang J, Poolman RW, et al. Computed tomography versus magnetic resonance imaging versus bone scintigraphy for clinically suspected scaphoid fractures in patients with negative plain radiographs. *Cochrane Database Syst Rev.* 2015(6):CD010023.
9. Ring D, Lozano-Calderon S. Imaging for suspected scaphoid fracture. *J Hand Surg Am.* 2008;33(6):954-957.
10. Pillai A, Jain M. Management of clinical fractures of the scaphoid: results of an audit and literature review. *Eur J Emerg Med.* 2005;12(2):47-51.
11. DaCruz DJ, Bodiwala GG, Finlay DB. The suspected fracture of the scaphoid: a rational approach to diagnosis. *Injury.* 1988;19(3):149-152.
12. Duckworth AD, Buijze GA, Moran M, et al. Predictors of fracture following suspected injury to the scaphoid. *J Bone Joint Surg Br.* 2012;94(7):961-968.
13. Mallee WH, Walenkamp MMJ, Mulders MAM, Goslings JC, Schep NWL. Detecting scaphoid fractures in wrist injury: a clinical decision rule. *Arch Orthop Trauma Surg.* 2020;140(4):575-581.
14. Bertsimas D, Dunn J, Velmahos GC, Kaafarani HMA. Surgical Risk Is Not Linear: Derivation and Validation of a Novel, User-friendly, and Machine-learning-based Predictive OpTimal Trees in Emergency Surgery Risk (POTTER) Calculator. *Ann Surg.* 2018;268(4):574-583.
15. Staartjes VE, de Wispelaere MP, Vandertop WP, Schroder ML. Deep learning-based preoperative predictive analytics for patient-reported outcomes following lumbar diskectomy: feasibility of center-specific modeling. *Spine J.* 2018.
16. Christodoulou E, Ma J, Collins GS, Steyerberg EW, Verbakel JY, Van Calster B. A systematic review shows no performance benefit of machine learning over logistic regression for clinical prediction models. *J Clin Epidemiol.* 2019;110:12-22.
17. Kim DH, MacKinnon T. Artificial intelligence in fracture detection: transfer learning from deep convolutional neural networks. *Clin Radiol.* 2018;73(5):439-445.
18. Langerhuizen DWG, Bulstra AEJ, Janssen SJ, et al. Is Deep Learning On Par with Human Observers for Detection of Radiographically Visible and Occult Fractures of the Scaphoid? *Clin Orthop Relat Res.* 2020;478(11):2653-2659.
19. Langerhuizen DWG, Janssen SJ, Mallee WH, et al. What Are the Applications and Limitations of Artificial Intelligence for Fracture Detection and Classification in Orthopaedic Trauma Imaging? A Systematic Review. *Clin Orthop Relat Res.* 2019;477(11):2482-2491.

20. Goto T, Camargo CA, Jr., Faridi MK, Freishtat RJ, Hasegawa K. Machine Learning-Based Prediction of Clinical Outcomes for Children During Emergency Department Triage. *JAMA Netw Open.* 2019;2(1):e186937.

21. Oosterhoff JHF, Doornberg JN, Machine Learning C. Artificial intelligence in orthopaedics: false hope or not? A narrative review along the line of Gartner's hype cycle. *EFORT Open Rev.* 2020;5(10):593-603.

22. Karhade AV, Ogink P, Thio Q, et al. Development of machine learning algorithms for prediction of discharge disposition after elective inpatient surgery for lumbar degenerative disc disorders. *Neurosurg Focus.* 2018;45(5):E6.

23. Karhade AV, Thio Q, Ogink PT, et al. Development of Machine Learning Algorithms for Prediction of 30-Day Mortality After Surgery for Spinal Metastasis. *Neurosurgery.* 2018.

24. Levin S, Toerper M, Hamrock E, et al. Machine-Learning-Based Electronic Triage More Accurately Differentiates Patients With Respect to Clinical Outcomes Compared With the Emergency Severity Index. *Ann Emerg Med.* 2018;71(5):565-574 e562.

25. Thio Q, Karhade AV, Ogink PT, et al. Can Machine-learning Techniques Be Used for 5-year Survival Prediction of Patients With Chondrosarcoma? *Clin Orthop Relat Res.* 2018;476(10):2040-2048.

26. Machine Learning Consortium obotS, Investigators F. A Machine Learning Algorithm to Identify Patients with Tibial Shaft Fractures at Risk for Infection After Operative Treatment. *J Bone Joint Surg Am.* 2021;103(6):532-540.

27. Bayliss L, Jones LD. The role of artificial intelligence and machine learning in predicting orthopaedic outcomes. *Bone Joint J.* 2019;101-B(12):1476-1478.

28. Luo W, Phung D, Tran T, et al. Guidelines for Developing and Reporting Machine Learning Predictive Models in Biomedical Research: A Multidisciplinary View. *J Med Internet Res.* 2016;18(12):e323.

29. Moons KG, Altman DG, Reitsma JB, et al. Transparent Reporting of a multivariable prediction model for Individual Prognosis or Diagnosis (TRIPOD): explanation and elaboration. *Ann Intern Med.* 2015;162(1):W1-73.

30. Stekhoven DJ, Buhlmann P. MissForest--non-parametric missing value imputation for mixed-type data. *Bioinformatics.* 2012;28(1):112-118.

31. Kursa MB, Rudnkicki WR. Feature Selection with the Boruta Package. *Journal of Statistical Software.* 2010;36(11).

32. Hendrickx LAM, Sobol GL, Langerhuizen D, et al. A Machine Learning Algorithm to Predict the Probability of (Occult) Posterior Malleolar Fractures Associated with Tibial Shaft Fractures to Guide "Malleolus First" Fixation. *Journal of Orthopaedic Trauma.* 2019. doi:10.1097/BOT.0000000000001663. Published Oct 10, 2019. Accessed Dec 12, 2019.

33. Steyerberg EW. Validation in prediction research: the waste by data splitting. *J Clin Epidemiol.* 2018;103:131-133.

34. Esteva A, Kuprel B, Novoa RA, et al. Dermatologist-level classification of skin cancer with deep neural networks. *Nature.* 2017;542(7639):115-118.

35. Maroco J, Silva D, Rodrigues A, Guerreiro M, Santana I, de Mendonca A. Data mining methods in the prediction of Dementia: A real-data comparison of the accuracy, sensitivity and specificity of linear discriminant analysis, logistic regression, neural networks, support vector machines, classification trees and random forests. *BMC Res Notes.* 2011;4:299.

36. Steyerberg EW, Vickers AJ, Cook NR, et al. Assessing the performance of prediction models: a framework for traditional and novel measures. *Epidemiology.* 2010;21(1):128-138.

37. Steyerberg EW, Vergouwe Y. Towards better clinical prediction models: seven steps for development and an ABCD for validation. *Eur Heart J.* 2014;35(29):1925-1931.

38. Mallee WH, Henny EP, van Dijk CN, Kamminga SP, van Enst WA, Kloen P. Clinical diagnostic evaluation for scaphoid fractures: a systematic review and meta-analysis. *J Hand Surg Am.* 2014;39(9):1683-1691 e1682.

39. Walker-Bone K, Byng P, Linaker C, et al. Reliability of the Southampton examination schedule for the diagnosis of upper limb disorders in the general population. *Ann Rheum Dis.* 2002;61(12):1103-1106

SUPPLEMENTARY MATERIAL

Supplementary Table 1. Machine Learning Algorithms

Machine Learning Algorithm	Working Mechanism	Visual representation (simplified)
Boosted Decision Tree[1]	Classification model in the form of a decision tree. The data is split into smaller subgroups along the tree's structure based on the data features. Data is split into groups to achieve maximum homogeneity between datapoints *within* each group, and maximum heterogeneity *between* each group.	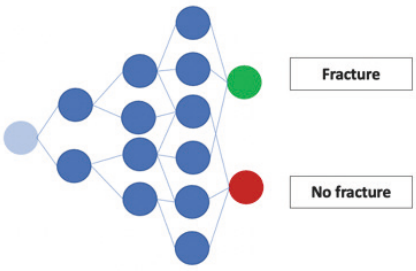
Penalized Logistic Regression[2]	This model is similar to standard logistic regression, apart from the fact that these models impose a penalty to a model for having too many variables.	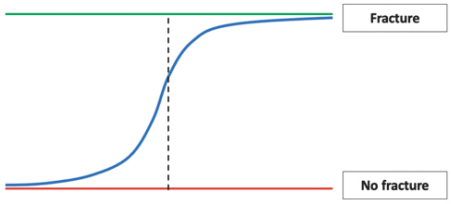
Neural Network[3]	Computational model designed to mimic the human brain. The model contains a layer of input nodes (variables) and an output layer. A network of connected nodes (like interconnected neurons) connects the input and output layers. The weight of each connecting node is altered to compute an outcome that predicts the outcome variable.	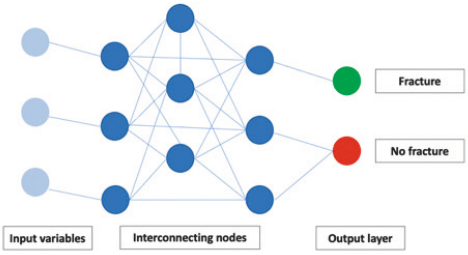

Supplementary Table 1. Machine Learning Algorithms (continued)

Machine Learning Algorithm	Working Mechanism	Visual representation (simplified)
Support Vector Machine[4]	Kernel-based algorithm that seeks to divide a dataset into two classes by creating a hyperplane. Datapoints are plotted in a multi-dimensional space. A divisional hyperplane is subsequently created at which the distance between all points of the two classes is at its maximum.	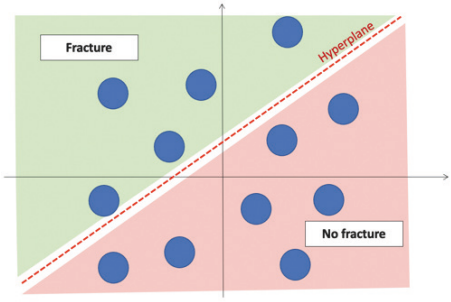
Bayes Point Machine[5]	Kernel-based algorithm (*see support vector machine)* based on a Bayesian approach to linear classification. It is designed to approximate the theoretical optimal Bayesian average of various linear classifiers by identifying an average classifier	-

REFERENCES

1. Kingsford C, Salzberg SL. What are decision trees? *Nat Biotechnol*. 2008;26(9):1011-1013.
2. Doerken S, Avalos M, Lagarde E, Schumacher M. Penalized logistic regression with low prevalence exposures beyond high dimensional settings. *PLoS One.* 2019;14(5):e0217057.
3. Cross SS, Harrison RF, Kennedy RL. Introduction to neural networks. *Lancet.* 1995;346(8982):1075-1079.
4. Noble WS. What is a support vector machine? *Nat Biotechnol.* 2006;24(12):1565-1567.
5. Herbrich R, Graepel T, Campbell C, Bayes Point Machine. *J Mach Learn Res.* 2001;1(Aug):245-279.

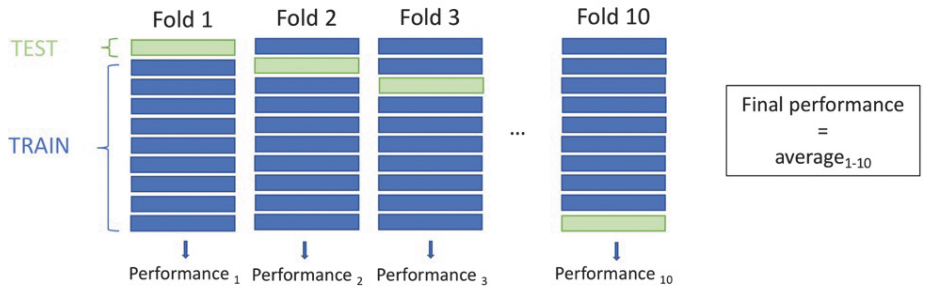

Supplementary Figure 1 - Schematic display of 10-fold cross validation

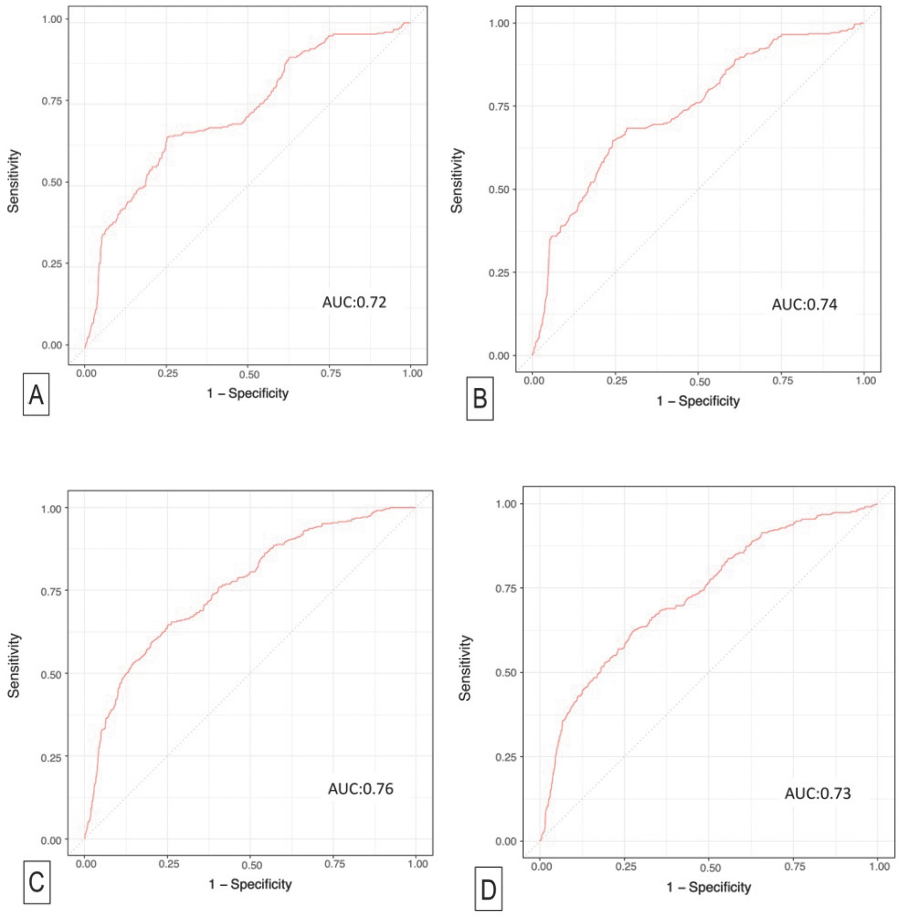

Supplementary Figure 2– ROC Curves

Receiver Operating Characteristic (ROC) curves for **A.** Bayes Point Machine **B.** Penalized Logistic Regression **C.** Neural Network **D**. Support Vector Machine

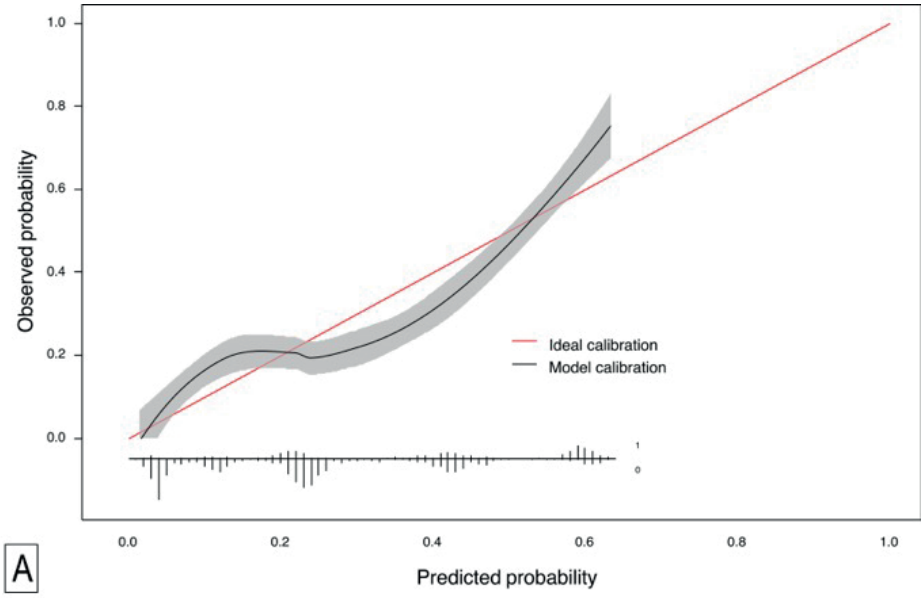

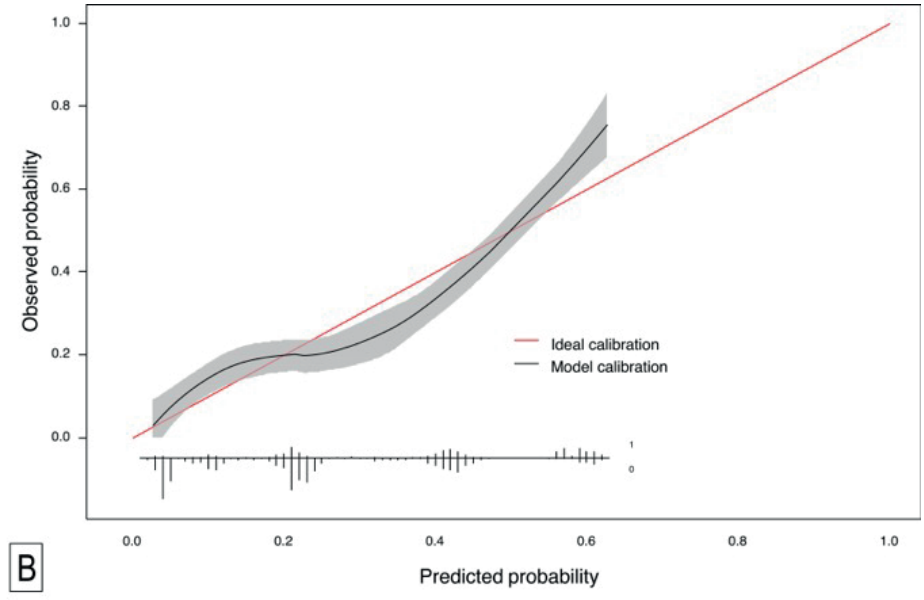

Supplementary Figure 3 – Calibration curves

Calibration curves for predicted and actual probabilities for a scaphoid fracture for **A.** Bayes Point Machine **B**. Penalized Logistic Regression

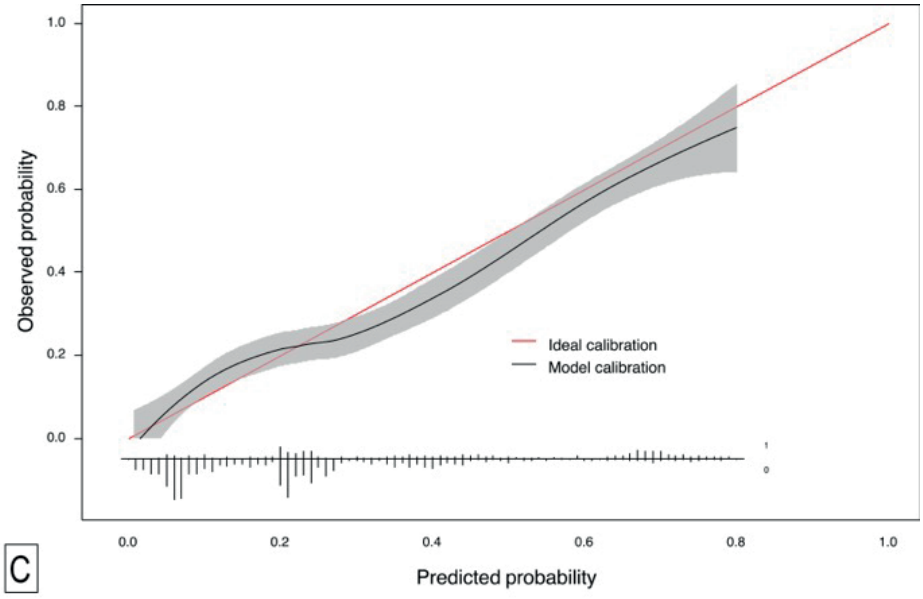

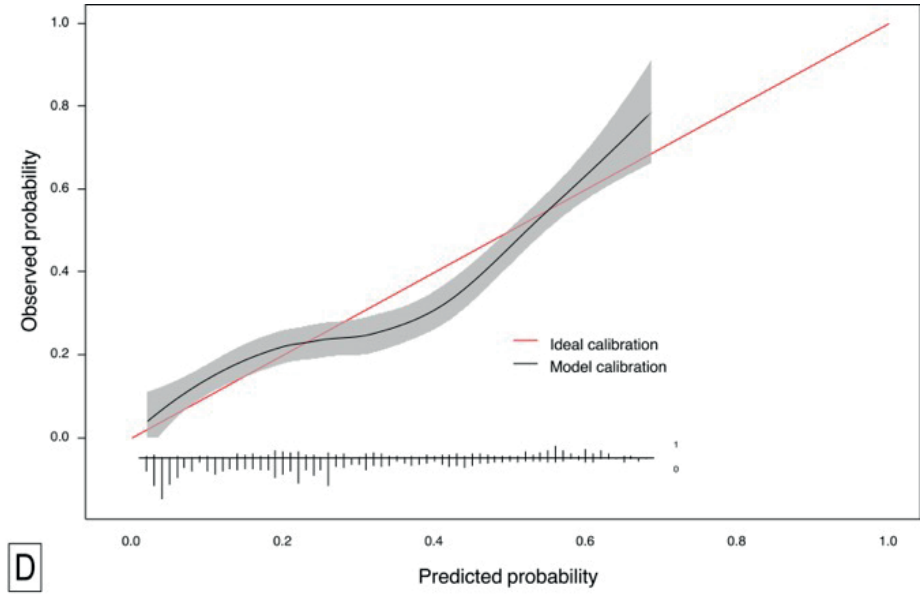

Supplementary Figure 3 – Calibration curves (continued)

Calibration curves for predicted and actual probabilities for a scaphoid fracture for **C.** Neural Network **D**. Support Vector Machine

CHAPTER 5

Is Deep Learning On Par with Human Observers for Detection of Radiographically Visible and Occult Fractures of the Scaphoid?

D. W. G. Langerhuizen
A.E.J. Bulstra
S. J. Janssen
D. Ring
G.M.M.J. Kerkhoffs
R.L. Jaarsma
J.N. Doornberg

In Clinical Orthopaedics and Related Research 2020 Nov; 478(11): 2653-2659

ABSTRACT

Background

Preliminary experience suggests that deep learning algorithms are nearly as good as humans in detecting common, displaced, and relatively obvious fractures (such as, distal radius or hip fractures). However, it is not known whether this also is true for subtle or relatively nondisplaced fractures that are often difficult to see on radiographs, such as scaphoid fractures.

Questions/purposes

(1) What is the diagnostic accuracy, sensitivity, and specificity of a deep learning algorithm in detecting radiographically visible and occult scaphoid fractures using four radiographic imaging views? (2) Does adding patient demographic (age and sex) information improve the diagnostic performance of the deep learning algorithm? (3) Are orthopaedic surgeons better at diagnostic accuracy, sensitivity, and specificity compared with deep learning? (4) What is the interobserver reliability among five human observers and between human consensus and deep learning algorithm?

Methods

We retrospectively searched the picture archiving and communication system (PACS) to identify 300 patients with a radiographic scaphoid series, until we had 150 fractures (127 visible on radiographs and 23 only visible on MRI) and 150 non-fractures with a corresponding CT or MRI as the reference standard for fracture diagnosis. At our institution, MRIs are usually ordered for patients with scaphoid tenderness and normal radiographs, and a CT for patients with a radiographically visible scaphoid fracture. We used a deep learning algorithm (a convolutional neural network [CNN]) for automated fracture detection on radiographs. Deep learning, an advanced subset of artificial intelligence, combines artificial neuronal layers to resemble a neuron cell. CNNs—essentially deep learning algorithms resembling interconnected neurons in the human brain—are most commonly used for image analysis. Area under the receiver operating characteristic curve (AUC) was used to evaluate the algorithm's diagnostic performance. An AUC of 1.0 would indicate perfect prediction, whereas 0.5 would indicate that a prediction is no better than a flip of a coin. The probability of a scaphoid fracture generated by the CNN, sex, and age were included in a multivariable logistic regression to determine whether this would improve the algorithm's diagnostic performance. Diagnostic performance characteristics (accuracy, sensitivity, and specificity) and reliability (kappa statistic) were calculated for the CNN and for the five orthopaedic surgeon observers in our study.

Results

The algorithm had an AUC of 0.77 (95% CI 0.66 to 0.85), 72% accuracy (95% CI 60% to 84%), 84% sensitivity (95% CI 0.74 to 0.94), and 60% specificity (95% CI 0.46 to 0.74).

Adding age and sex did not improve diagnostic performance (AUC 0.81 [95% CI 0.73 to 0.89]). Orthopaedic surgeons had better specificity (0.93 [95% CI 0.93 to 0.99]; $p < 0.01$), while accuracy (84% [95% CI 81% to 88%]) and sensitivity (0.76 [95% CI 0.70 to 0.82]; $p = 0.29$) did not differ between the algorithm and human observers. Although the CNN was less specific in diagnosing relatively obvious fractures, it detected five of six occult scaphoid fractures that were missed by all human observers. The interobserver reliability among the five surgeons was substantial (Fleiss' kappa = 0.74 [95% CI 0.66 to 0.83]), but the reliability between the algorithm and human observers was only fair (Cohen's kappa = 0.34 [95% CI 0.17 to 0.50]).

Conclusions

Initial experience with our deep learning algorithm suggests that it has trouble identifying scaphoid fractures that are obvious to human observers. Thirteen false positive suggestions were made by the CNN, which were correctly detected by the five surgeons. Research with larger datasets—preferably also including information from physical examination—or further algorithm refinement is merited.

Level of Evidence

Level III: diagnostic study.

INTRODUCTION

Deep learning gained great appeal when Google's DeepMind computer defeated the world's number one Go player.[1] Deep learning, an advanced subset of artificial intelligence, combines artificial neuronal layers to resemble a neuron cell. Essentially, these algorithms highly complex mathematical models—derive rules and patterns from data to estimate the probability of a diagnosis or outcome without human intervention. These algorithms can be applied to imaging tasks such as skin cancer detection on photographs or detection of critical findings in head CT scans.[2,3]

Using different data set sizes, initial experience with fracture detection on radiographs suggests that deep learning algorithms are (nearly) as good as humans at detecting certain common fractures such as distal radius, proximal humerus, and hip fractures.[4] However, many of those fractures are displaced and relatively obvious on radiographs.

It is known that scaphoid fractures can have long-term consequences if not properly diagnosed. A previous study applied five deep learning algorithms to detect wrist, hand (including scaphoid), and ankle fractures; however, they did not report their algorithm's performance for scaphoid fractures specifically.[5] As such, it is not yet clear whether deep learning algorithms will be useful for the detection of relatively subtle and often radiographically invisible nondisplaced femoral neck or scaphoid fractures that are often overlooked by humans, particularly nonspecialists.[6]

Therefore, we asked: (1) What is the diagnostic accuracy, sensitivity, and specificity of a deep learning algorithm in detecting radiographically visible and occult scaphoid fractures using four radiographic imaging views? (2) Does adding patient demographic (age and sex) information improve the diagnostic performance of the deep learning algorithm? (3) Are orthopaedic surgeons better at diagnostic accuracy, sensitivity, and specificity compared with deep learning? (4) What is the interobserver reliability among five human observers and between human consensus and deep learning algorithm?

PATIENTS AND METHODS

Data Set and Pre-processing

Our institutional review board approved this retrospective study. Our institution still uses a paper medical record, which makes it difficult to search for patients with specific diagnoses and tests. The picture archiving and communication system (PACS) is electronic and easier to search. We used two strategies to identify at least 300 scaphoid series of radiographs.

The first strategy was based on the fact that clinicians in our institution usually order an MRI in patients with suspected scaphoid fractures and normal radiographs and a CT with radiographically visible scaphoid fracture. This strategy identified MRI and CT of the scaphoid and then sought corresponding radiographs of scaphoid fractures. We searched the PACS database using the terms "MR scaph", "CT hand", "CT wrist", and "CT

extr" and identified 326 patients: 150 that were excluded because the radiographs were incomplete or distorted by cast or splint materials and 176 with adequate radiographic scaphoid series including 13 MRI confirmed fractures, 59 CT-confirmed fractures, and 104 MRI-confirmed nonfractures.

In the second strategy, we searched PACS for "Xr scaph" and searched them one by one for a corresponding MRI or CT image and an adequate series of radiographs not distorted by plaster. We found 124 additional patients including 10 with MRI-confirmed fractures, 68 with CT-confirmed fractures, 46 MRI-confirmed nonfractures, and 17 CT-confirmed nonfractures. Two observers (DWGL, AEJB) used this strategy to identify patients until we had 150 radiographs of scaphoids with a fracture (127 visible on radiographs and 23 only visible on MRI) and 150 without a fracture, numbers chosen before starting the search and based on typical training strategies. Age and sex demographics were provided by PACS. The mean age at diagnosis was 36 years (Standard Deviation (SD) 16), and 62% (185 of 300) of patients were male. We randomly divided the dataset into a train, a validation, and a test group (180:20:100), each divided 50:50 by presence of a fracture. The radiographically invisible fractures were randomly and evenly distributed between the three groups. To match the predefined image size of the deep learning framework (Figure 1), we manually cropped and resized all Digital Imaging and Communications in Medicine (DICOM) files into a 350 x 300 pixels rectangle capturing the scaphoid (see Supplementary Material 1). By automatically rotating, zooming, changing height and width, and horizontal or vertical flipping, all preformatted images were 10-fold augmented with the intent to increase robustness of the algorithm.

Algorithm: Convolutional Neural Network

Convolutional neural networks (CNNs) are complex algorithms resembling interconnected neurons in the human brain. CNNs are a form of deep learning commonly used to analyse images. In deep learning, the computer analyses both features that are recognizable to humans (for example, the eyes or the nose) and features that are not recognizable to humans (such as edges or transitions). A CNN learns by developing and testing algorithms again and again (in iterations) until it has optimized its ability to identify the feature assigned: in this case, fracture of the scaphoid. When approaching a new image recognition task, it can be helpful to start with a CNN that is already trained to identify features in images. We used an opensource pretrained CNN (Visual Geometry Group, Oxford, United Kingdom[7] trained on more than 1 million nonmedical images with 1000 object categories (see Supplementary Material 2). [8]

A test group of 100 images was randomly selected for use in the tests to determine the algorithm performance. We evaluated the model using the following performance metrics: area under the receiving operating characteristic (AUC) curve, accuracy, sensitivity, and specificity. We set the diagnostic cut-off point at a value that maximized sensitivity, at the cost of a slightly decreased specificity.[6,9,10]

Codes were written in Python Version 3.6.8 (Python Software Foundation, Wilmington, DE, USA) with the packages scikit-learn (0.20.3) and TensorFlow (1.13.1).

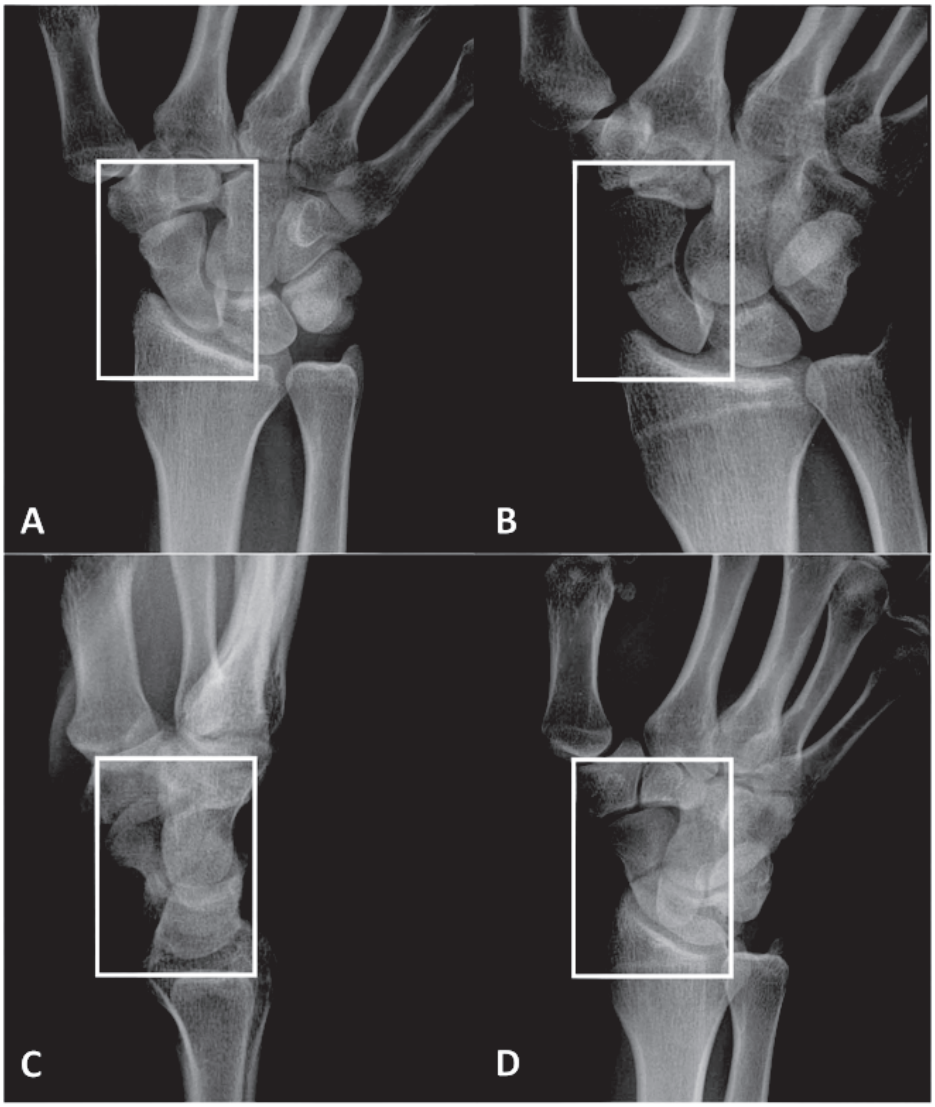

Figure 1. A radiographic scaphoid fracture series for patients with a clinical suspicion for scaphoid fracture at our hospital.

The following four projections were fed into the deep learning framework: **(A)** posterior-anterior ulnar deviation; **(B)** uptilt (that is, an elongated view with tube angle adjusted over 30°); **(C)** lateral; and **(D)** 45° oblique projections. The white boxes illustrate the cropped and resized radiographs (350 x 300 pixels) that are fed into the deep learning framework (VGG 16).

Human Observers

We compared the performance metrics of the model with five surgeons (RLJ, JND, MMAJ, NK, JWW). Three orthopaedic trauma surgeons (16, 3, and 2 years after completion of residency training) and two upper limb surgeons (25 and 2 years after completion residency training) each reviewed the same 100 patients as the model. In our hospital, upper limb surgeons deliver care for the entire upper extremity. The surgeons were not aware of the total number of fracture and nonfracture patients in the test set. All fractures were presented as uncropped

Digital Imaging and Communications in Medicine (DICOM) files, which we loaded into Horos (version 3.3.4, Annapolis, MD, USA). Surgeons were asked to identify the presence or absence of a scaphoid fracture on four radiographic views. Again, we calculated the accuracy, sensitivity, and specificity for each surgeon as well as the mean among surgeons for each measure to compare with the CNN.

Statistical Analysis

Continuous variables were presented with mean and SD and categorical variables with frequencies and percentages.

Accuracy is defined as the proportion of correctly detected cases among all cases. The AUC reflects the probability that a binary classifier will rank a randomly chosen positive instance higher than a randomly chosen negative one.[11] An AUC of 1.0 corresponds to perfect classification, whereas 0.5 indicates a prediction equal to chance. Sensitivity corresponds to the proportion of correctly identified fractures among all actual fractures, while specificity refers to the proportion of correctly identified nonfractures among all nonfractures. We calculated 95% confidence intervals using a Z-score of 1.96. Overlapping 95%CIs indicate no significant difference. A McNemar's test was used to compare sensitivity and specificity between the algorithm and human observers. The probability of a scaphoid fracture generated by the CNN, sex, and age were included in a multivariable logistic regression to determine whether this would improve the algorithm's diagnostic performance

Kappa, which is a chance-corrected measure, corresponds to the agreement among observers. We used Fleiss' kappa to determine interobserver reliability among surgeons for evaluating the presence or absence of scaphoid fractures. We used Cohen's kappa to calculate reliability between the CNN and majority vote of human observers. According to Landis and Koch[12], a kappa between 0.21 and 0.40 reflects fair agreement, a kappa between 0.41 and 0.60 indicates moderate agreement, a kappa between 0.61 and 0.80 reflects substantial agreement, while a kappa above 0.80 indicates almost perfect agreement

We performed statistical analyses using Stata 15.0 (StataCorp LP, College Station, TX, USA) and RStudio (Boston, MA, USA) with the packages CalibrationCurves, ggplot2, grid, and precrec. There were no missing data.

RESULTS

Performance of CNN

For detection of scaphoid fractures among suspected scaphoid fractures, the CNN reported an AUC of 0.77 (95% CI 0.66 to 0.85) (Figure 2). The CNN correctly detected 72 of 100 patients (accuracy 72% [95% CI 60% to 84%]). Eight of 50 confirmed scaphoid fractures were not identified (sensitivity 0.84 [95% CI 0.74 to 0.94]), while 20 of 50 patients without a fracture were incorrectly diagnosed as having a fracture of the scaphoid (specificity 0.60 [95% CI 0.46 to 0.74]).

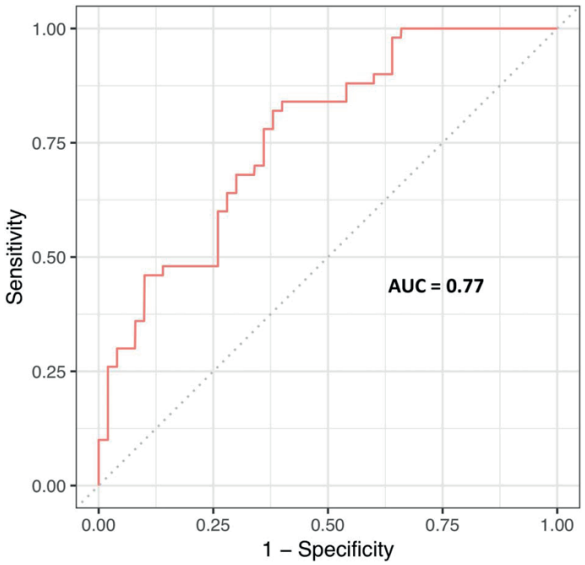

Figure 2. Receiver Operating Characteristic Curve for the CNN

This figure depicts the receiver operating curve for the CNN at the optimal diagnostic cutoff point (0.37).

Performance of CNN Combined with Patient Demographics

Combining age and sex with the generated probabilities of the CNN did not improve the AUC (0.81; 95% CI 0.73 to 0.89). The output of this model was converted into a formula for calculating the probability of a fracture (see Supplementary Material 3).

Performance of CNN Compared with Human Observers

Specificity favoured the human observers (five orthopaedic surgeons 0.93 [95% CI 0.87 to 0.99] versus CNN 0.60 [95% CI 0.46 to 0.74]; $p < 0.01$). Accuracy for distinguishing between scaphoid fractures and nonfractures was comparable between human observers and the CNN (five orthopaedic surgeons 84% [95% CI 81% to 88%] versus CNN 72% [95% CI 60 to 84]) (Table 1). Sensitivity was also comparable between the CNN and

human observers (five orthopaedic surgeons: 0.76 [95% CI 0.70 to 0.82]) versus CNN: 0.84 [95% CI 0.74 to 0.94]; p = 0.29). Six scaphoid fractures were missed by all surgeons and therefore considered occult fractures. The CNN detected five of six occult scaphoid fractures. In addition, five human observers detected three fractures that were missed by the CNN. Two fractures, diagnosed by four of five human observers, were also missed by the CNN. In contrast, thirteen false positive suggestion of the CNN, were correctly detected by the surgeons.

Table 1. A comparison of performance metrics between the CNN and the mean of five orthopaedic surgeons

Diagnostic performance characteristic	CNN[a]	Orthopaedic surgeons	p-value
Accuracy (95% CI)	72% (63-81%)	85% (82-88%)	
Sensitivity (95% CI)	0.84 (0.74-0.94)	0.78 (0.71-0.85)	0.29
Specificity (95% CI)	0.60 (0.46-0.74)	0.92 (0.87-0.97)	<0.01*

[a] CNN = convolutional neural network at cut-off point 0.37
[b] We did not calculate a p value, since McNemar's test is sensitive to the proportion of fractures as well as nonfractures.
* Statistical significance (p < 0.05).

The Interobserver Reliability of Human Observers

Interobserver agreement between five surgeons was higher than between human consensus and the algorithm (0.74 [95% CI 0.66 to 0.83] versus 0.34 [95% CI 0.17 to 0.50]) (Table 2).

Table 2. Contingency table comparing prediction of CNN to human consensus

		Fracture (n=50)	Non-fracture (n=50)
Fracture (predicted)	CNN	42	20
	Human consensus	38	1
Non-fracture (predicted)	CNN	8	30
	Human consensus	12	49

CNN = convolutional neural network

DISCUSSION

In medicine, deep learning has primarily been applied to image analysis. In a research setting, use of deep transfer learning showed promising performance for fracture detection and classification for relatively straightforward clinical scenarios.[4] It is not yet

clear that deep learning will be useful for radiographic fracture detection in scenarios where fractures are often overlooked by human observers. Using a relatively small data set of 300 patients, our deep learning algorithm demonstrated a moderate better overall performance for detection of radiographically visible and occult fractures (AUC 0.77 [95% CI 0.66 to 0.85]) and human observers had notably better specificity. The algorithm might have performed better if provided with more data.

This study has several limitations. First, we selected our patients from readily available and searchable radiology reports and intentionally introduced a spectrum bias by collecting 150 MRI- or CT-confirmed fractures and 150 confirmed nonfractures. Although this was needed to sufficiently train the algorithm, readers should keep in mind that our data set does not represent the true prevalence of radiographic scaphoid fracture appearance. Second, we were only able to include 300 patients because we could only search a 9-year period starting in January 2010. Three hundred radiographs is a relatively small sample size for deep learning, but more than adequate for logistic regression. A larger data set might improve the diagnostic performance of the CNN. We cannot be certain because, to this point, there is no consensus on a priori sample size in deep learning. It depends on the specific image analysis task, the quality of the data set, the programming techniques used, and type of deep learning algorithm applied.[13] Third, the ground truth labels (that is, the reference standard diagnosis of scaphoid fracture or not) are based on radiologist interpretations of CT or MRI images, which have limited reliability and untestable accuracy. Given the small number of MRIs with diagnosed fracture and CT with diagnosed nonfractures, we believe any misdiagnoses would have little influence on the model. Fourth, radiographs were manually cropped and resized by one investigator (DWGL), which might introduce bias. However, given that cropping was assisted by an easy-to-use program scripted in Python, we feel it is very likely that another investigator would resize the images similarly. But, one should keep in mind that cropped radiographs may not reflect a clinical scenario, as other potentially relevant findings in a real-size radiograph were not assessable (such as, concomitant fractures or scapholunate dissociation). Furthermore, irrelevant regions in a radiograph were removed and therefore not evaluated by the model. A more in-depth deep learning framework, accounting for the entire wrist radiograph, merits further study. For now, the memory capacity of graphics processing units limits the usable image size. Fifth, among the five human observers, two surgeon raters treated some of the patients in the study, which might have influenced their diagnoses. We feel this would have negligible influence on our findings. Sixth, although incorporating injury details, signs, and symptoms would have been of interest to incorporate in a logistic regression model as it typical for a clinical prediction rule, they were not commonly reported in a patient's medical record. CNNs only evaluate images, but the probabilities generated can be included in clinical prediction rules.

The AUC of the CNN for detection of scaphoid fractures is not good enough to replace human observers or more sophisticated imaging, but it does suggest the potential to be used as a pre-screen or clinical prediction rule for triage of suspected scaphoid fractures

that might benefit additional imaging. Displaced proximal humerus, distal radius, and intertrochanteric hip fractures are relatively easy to detect and not a good test of the potential utility of artificial intelligence.[6,9,14] Subtle and invisible fractures may be more of a challenge. Prior studies using deep learning algorithms to detect radiographically subtle hip and distal radius fractures had better performance than our model.[6,14-16] Larger data sets, use of other pretrained CNNs, varying degrees of algorithm refinement and hyper-parameter tuning, as well as other anatomical fracture locations may explain why these studies differ with our findings. Also, we might not have had sufficient images to train the upper layers of the pretrained CNN.

Adding sex and age did not improve diagnostic performance. Future research might investigate whether incorporating computer analysis of images improves performance of clinical prediction rules that include demographics, injury details, symptoms, and signs to better triage the use of MRI as well as increase its diagnostic performance by increasing the pretest odds of a fracture.[17,18] The pretest odds could be increased with CNNs, clinical prediction rules, or a combination of both.

Our deep learning algorithm was less specific than human observers but detected five of six occult fractures in the test dataset. On the other hand, caution is warranted because the CNN missed some radiographically visible fractures.

The finding that reliability of fracture diagnosis was substantial (0.74) for the five orthopaedic surgeons and only fair (0.34) between the surgeons and the CNN we interpret as a reflection of the difficulty the deep learning algorithm has with detecting radiographically visible fractures. At the diagnostic cut-off point—chosen to maximize sensitivity— the algorithm's specificity was considerably lower compared with human observers. A different cut-off point may have resulted in more or less the same reliability for detecting scaphoid fractures. It may go without saying that CNNs are known for being highly complex and, to date, not intuitive for the end-user. It is therefore not possible to understand how a CNN reaches its suggestion.

In conclusion, using a relatively small dataset, a deep learning algorithm was inferior to human observers at identifying scaphoid fractures on radiographs. Further study may help evaluate whether a larger dataset and algorithm refinement can increase the performance of deep learning for the diagnosis of scaphoid fractures, some of which are radiographically invisible. In addition, incorporating predictions from a deep-learning algorithm into clinical prediction rules that also account for demographics, injury details, symptoms, and signs merits further study.

Acknowledgments

We thank the following orthopaedic surgeons for their participation: M. M. A. Janssen MD, PhD, N. Kruger MD, and J. W. White MBBS, PhD.

REFERENCES

1. British Broadcasting Corporation. Artificial intelligence: Go master Lee Se-dol wins against AlphaGo program. Available at: https://www.bbc.com/news/technology-35797102. Accessed March 13, 2016.
2. Chilamkurthy S, Ghosh R, Tanamala S, Biviji M, Campeau NG, Venugopal VK, Mahajan V, Rao P, Warier P. Deep learning algorithms for detection of critical findings in head CT scans: a retrospective study. Lancet (London, England). 2018;392: 2388-2396.
3. Chung SW, Han SS, Lee JW, Oh KS, Kim NR, Yoon JP, Kim JY, Moon SH, Kwon J, Lee HJ, Noh YM, Kim Y. Automated detection and classification of the proximal humerus fracture by using deep learning algorithm. Acta Orthop. 2018;89:468-473.
4. Duckworth AD, Buijze GA, Moran M, Gray A, Court-Brown CM, Ring D, McQueen MM. Predictors of fracture following suspected injury to the scaphoid. J Bone Joint Surg Br. 2012;94: 961-968.
5. Esteva A, Kuprel B, Novoa RA, Ko J, Swetter SM, Blau HM, Thrun S. Dermatologist-level classification of skin cancer with deep neural networks. Nature. 2017;542:115-118.
6. Fawcett T. An introduction to ROC analysis. Pattern Recognition Letters. 2006;27:861-874.
7. Gale W, Oakden-Rayner L, Carneiro G, Bradley AP, Palmer LJ. Detecting Hip Fractures with Radiologist-Level Performance Using Deep Neural Networks. 2017; Available at: https://arxiv.org/abs/1711.06504. Accessed November 17, 2017.
8. Gan K, Xu D, Lin Y, Shen Y, Zhang T, Hu K, Zhou K, Bi M, Pan L, Wu W, Liu Y. Artificial intelligence detection of distal radius fractures: a comparison between the convolutional neural network and professional assessments. Acta Orthop. 2019;90: 394-400.
9. Kim DH, MacKinnon T. Artificial intelligence in fracture detection: transfer learning from deep convolutional neural networks. Clin Radiol. 2018;73:439-445.
10. Landis JR, Koch GG. The measurement of observer agreement for categorical data. Biometrics. 1977;33:159-174.
11. Langerhuizen DWG, Janssen SJ, Mallee WH, van den Bekerom MPJ, Ring D, Kerkhoffs G, Jaarsma RL, Doornberg JN. What Are the Applications and Limitations of Artificial Intelligence for Fracture Detection and Classification in Orthopaedic Trauma Imaging? A Systematic Review. Clin Orthop Relat Res. 2019.
12. Lindsey R, Daluiski A, Chopra S, Lachapelle A, Mozer M, Sicular S, Hanel D, Gardner M, Gupta A, Hotchkiss R, Potter H. Deep neural network improves fracture detection by clinicians. Proc Natl Acad Sci U S A. 2018;45:11591-11596.
13. Olczak J, Fahlberg N, Maki A, Razavian AS, Jilert A, Stark A, Skoldenberg O, Gordon M. Artificial intelligence for analyzing orthopedic trauma radiographs. Acta Orthop. 2017;88:581-586.
14. Ranschaert ER. Artificial Intelligence in Medical Imaging. eBook. Switzerland, AG: Springer. 2019.
15. Rhemrev SJ, Beeres FJ, van Leerdam RH, Hogervorst M, Ring D. Clinical prediction rule for suspected scaphoid fractures: A prospective cohort study. Injury. 2010;41:1026-1030.
16. Russakovsky O, Olga R, Jia D, Hao S, Jonathan K, Sanjeev S,115. ImageNet large scale visual recognition challenge. Int J Comput Vis. 2015:211–252.
17. Urakawa T, Tanaka Y, Goto S, Matsuzawa H, Watanabe K, Endo N. Detecting intertrochanteric hip fractures with orthopedistl evel accuracy using a deep convolutional neural network. Skeletal Radiol. 2018;48:239-244.
18. Zhong S, Li K, Feng R. Deep Convolutional Hamming Ranking Network for Large Scale Image Retrieval. Available at: https:// ieeexplore.ieee.org/document/7052856. Accessed August 19, 2016.

SUPPLEMENTARY MATERIAL

Supplementary Material 1. Code for capturing radiographs into 350 x 300 pixels rectangle

```
#load libraries and packages
import numpy as np
import pandas as pd
import matplotlib.pyplot as plt
import pydicom
import os
import sys
import pickle
from scipy import ndimage

savefile = directory

#load file
df = pd.read_pickle(savefile) #load savefile
df

# create dictionary to lookup images
ext=directory
pt_list=os.listdir(ext)
#enter second nested file
print(ext)
print(pt_list)

d= for f in pt_list:
 if f==‘.DS_Store‘:
 continue
 pt_list2 = ext + ‘/‘ + f
 dir2 = os.listdir(pt_list2)
 extlist = []
 for dcmfile in dir2:
 if dcmfile==‘.DS_Store‘:
 continue
 dcm_ext = pt_list2 + ‘/‘ + dcmfile
 extlist.append(dcm_ext)

 d[f] = extlist

#find radiograph to crop and resize
pydicom.dcmread(d[‘xx‘][x])

#ptn
p=‘xx‘
#projection
x=#
ext=d[p][x]
print(ext)
#print(‘study exists of:‘, len(d[list(d.keys())[p]]), ‘images‘)
dcm=pydicom.dcmread(ext)
date=dcm.StudyDate
time=dcm.StudyTime[:6]
image = dcm.pixel_array
print(‘date_time_stamp:‘,date, time)
print(dcm.pixel_array.shape)
plt.imshow(image, cmap=plt.cm.bone)

print(df.iloc[-5:,:])
```

```
def rotate_img(img, angl):
 rotated_img = ndimage.rotate(img, angle = angl, reshape=False)
 return rotated_img

#dcm=pydicom.dcmread(ext).pixel_array
angl = x
image = rotate_img(image, angl)
plt.imshow(image, cmap=plt.cm.bone)
plt.show()

def crop_dicom(img, y_start, x_start, len_y, len_x):
 #pix_array=pydicom.dcmread(extension).pixel_array
 pix_array = img
 print(pix_array.shape)

 pix_crop=pix_array[y_start:y_start+len_y,x_start:x_start+len_x]

 return pix_crop

imt='pa'

if imt=='pa':
 ly=350
 lx=300
elif imt=='lat':
 ly= 350
 lx = 300
elif imt=='obl':
 ly=350
 lx=300
elif imt=='up':
 ly=350
 lx=250

crop_img=crop_dicom(image, y_start= 50, x_start=0, len_y=ly,len_x=lx)
plt.imshow(crop_img, cmap=plt.cm.bone)
shape=crop_img.shape
print('date_time_stamp:',date, time)
print(shape)

#save cropped radiographs
def append_data(img_array, ptno, shape, df, type_):
 newrow=[ptno, shape, img_array, type_]
 df.loc[len(df)]=newrow
 return df
df=append_data(crop_img, p, shape, df, imt)
df.iloc[-5:,:]

#write to disk
df.to_pickle(savefile)
```

SUPPLEMENTARY MATERIAL 2

Pre-processing of Data

The algorithm was optimized according to the following train, validation, and test split: 180-20-100. All radiographs were manually cropped and resized to match the predefined image size of the deep learning framework (that is, a 200 x 300 pixels rectangle). We downscaled the pixel intensity by averaging each pixel based on minimum and maximum intensity of the radiograph. To increase robustness of the algorithm, we 10-fold augmented the training and validation set by using rotation (-15° and +15°), shifting of height and width (10%), zooming (between 0.8 and 1.1), and horizon flipping. The test set only composed of original radiographs.

Training of Deep Learning Framework

We used keras API (https://keras.io) to run on top of the open-source Imagenet pre-trained Visual Geometry Group (VGG) 16-layer convolutional neural network (CNN) [7]. We ran Intel(R) Xeon(R) W-2175 (clock speed 2.50GHz, 64 GB RAM) with NVIDIA TITAN V (boostclock 1455 MHz, 12 GB HBM2). The outputs of the last CNN-layer were fine-tuned to our scaphoid fracture dataset with a concatenation operation followed by the fully connected top network. End-to-end fine-tuning of the last convolutional layers was performed, while earlier layers—containing more generic features—were kept fixed. We decided not to further fine-tune the convolution layers because it resulted in more overfitting.

SUPPLEMENTARY MATERIAL 3

Odds ratios for age and sex and equation formula of the prediction model

Odds Ratios
Age: 0.97 (95% confidence interval 0.94 to 1.01)
Sex: 2.55 (95% CI 0.76 to 8.55)

Linear Predictor
-1.816599 + (probability CNN) * 4.680619 + (age) * -0.0265213 + (sex) * 0.9346456

Equation Formula to Calculate Probability of a Scaphoid Fracture
EXP(Linear Predictor) / (EXP(Linear Predictor) + 1

CHAPTER 6

MRI Signal Characteristics of the Scaphoid in Patients with a Suspected Scaphoid Fracture

A.E.J. Bulstra
M.F. van Boxel
T.J. Crijns
J. Kelly
M.C. Obdeijn
G.M.M.J. Kerkhoffs
J.N. Doornberg
D. Ring
R.L. Jaarsma

This is an original version of an article published in revised and final form in Clinical Orthopaedics and Related Research 2020 Nov; 478(11): 2653-2659 (Featured in CORR Editor's Spotlight section)

ABSTRACT

Purpose

This study aimed to 1) identify patterns of MRI signal change present among patients with a suspected scaphoid waist fracture; 2) measure the reliability of identifying those patterns and 3) identify factors associated with signal changes that represent likely scaphoid waist fractures.

Methods

Two-hundred-and-sixty-seven (267) consecutive MRI scans of patients 16 years or older evaluated for a clinically suspected scaphoid fracture within 3 weeks of injury were included. MRI scans were grouped into categories of common patterns of signal change. Two observers categorized a consecutive sample of 45 scans using these categories to measure interobserver reliability. Logistic regression analysis identified factors associated with signal changes categorized as "looks like a scaphoid waist fracture."

Results

Signal variations were present in 92 of 267 scans (34%): 15 (5.6%) were categorized as "looks like a scaphoid waist fracture" (4 of these [4/267 or 1.5%] were categorized as "clearly a scaphoid waist fracture"); 36 (14%) were categorized as "might be confused with a waist fracture"; and 41 (15%) were categorized as "clearly not a scaphoid waist fracture." The interobserver reliability in distinguishing between patterns of signal change was substantial (kappa: 0.62 [95% confidence interval (CI) 0.43-0.80]) for the four main categories and moderate when including subcategories (kappa: 0.55 [95% CI 0.39-0.72]). Men were more likely to have signal changes that look like a scaphoid waist fracture.

Conclusions

The high prevalence of signal changes that may be confused with a scaphoid waist fracture, the low prevalence of signal changes that clearly represent a scaphoid waist fracture, the moderate to substantial interobserver reliability in distinguishing between categories of signal changes, and the low pretest odds of true fracture among suspected scaphoid fracture indicate that MRI carries a notable risk of overdiagnosis and overtreatment in the evaluation of the suspected scaphoid fracture.

Level of Evidence

Diagnostic, III

INTRODUCTION

Patients with scaphoid tenderness and normal radiographs after a fall onto the outstretched hand have a suspected scaphoid fracture.[1,2] MRI (Magnetic Resonance Imaging) is increasingly being used to attempt to identify true scaphoid waist fractures among suspected fractures.[3-7] Among patients with a suspected scaphoid waist fracture MRI has a good negative predictive value. [8-10] This is in part due to the low the prevalence of true fractures among suspected fractures, and in part due to the fact that MRI is very sensitive for small anatomical and physiological variations. As such, there is growing consensus that MRI is a useful way to assess whether the scaphoid is safe to return to heavy labour or sport.[3,10-12]

On the other hand, MRI's ability to depict variations in anatomy and pathology that may not represent a fracture contribute to a low positive predictive value. A study of uninjured scaphoids identified variations in signal intensity at risk of being interpreted as a fracture.[8] It is possible that some people have a bone bruise without fracture.[8,9] In others, anatomical structures such as a vascular channel or pre-existing signal variation might simulate a fracture.[8,9] The low prevalence of true fractures among suspected fractures, combined with the low positive predictive value of MRI results in the potential for harm via overdiagnosis, overprotection, and overtreatment.

To reduce the risk of overdiagnosis we first need better insight into patterns of signal change present among patients with a suspected scaphoid fracture. This may aid in recognizing signal change associated with a true scaphoid fracture and ultimately contribute to establishing consensus definitions of what constitutes a scaphoid fracture on MRI.

This primary aim of this exploratory study was to identify the patterns of MRI signal change present among patients with a clinically suspected scaphoid waist fracture and to measure their frequency. Secondary aims were to measure the reliability of identifying those patterns and to identify factors associated with signal changes that represent likely scaphoid waist fractures.

METHODS

Study design and setting

This study was approved by the Southern Adelaide Clinical Human Research Ethics Committee (SAC HREC EC00188I; reference number 257.19). At our institution (level I trauma centre), patients with scaphoid tenderness after acute wrist trauma and negative radiographs usually receive an immediate MRI scan to diagnose a fracture or lower the probability of a scaphoid fracture to an acceptable threshold to return to work or sports in consultation with the patient. A retrospective search of the medical imaging archiving system was performed to identify all patients (>15 years) with a clinically suspected scaphoid waist fracture who had an MRI between 1st of January 2012 and 1st of September

2019. Exclusion criteria included 1) a scaphoid fracture visible on radiographs prior to MRI as reported by the radiologist 2) no available radiographs prior to MRI; 3) MRI more than 3 weeks after injury and 4) unknown date of injury.

A total of 310 MRI scans were identified retrospectively. Four MRI scans (1.3%) were excluded because a scaphoid fracture was present on radiographs prior to MRI as reported by the radiologist. Two patients (0.65%) were excluded as there were no radiographs available prior to MRI. Twenty-eight patients (9.0%) who had an MRI scan more than three weeks after injury and nine (2.9%) patients whose date of injury was unknown were also excluded. This resulted in 267 MRI scans in 257 patients available for analysis (Table 1).

Table 1. Patient demographics and clinical variables

Variable	N (%) or median (IQR)
Sex	
Men	107 (40)
Women	160 (60)
Age, years	34 (21-50)
Affected side	
Left	123 (46)
Right	144 (54)
Mechanism of injury	
FOOSH	126 (47)
Sports	66 (25)
Motor vehicle accident	28 (10)
Fall from height	11 (4.1)
Fight or assault	7 (2.6)
Other or unknown	29 (11)
Days to MRI since injury	8 (2-13)

Continuous variables are presented as median (interquartile range)
Discrete variables as number (percentage); N=number, IQR = interquartile range.

MRI protocol

MRI scans were performed using a dedicated wrist coil on a 3T scanner. The standard scaphoid protocol had a slice thickness of 2.0 to 2.5mm and constituted the following sequences 1) coronal T1-weighted turbo spin-echo (T1); 2) coronal proton density (PD) fat suppressed (FS) turbo-spin echo; 3) sagittal PD turbo-spin echo.

Two out of 267 MRI scans (0.7%) were lacking a sagittal sequence. The PDFS coronal and T1 sequences of these scans were included and assessed for signal change. These two scans had minimal signal changes and did not look like scaphoid waist fractures.

MRI signal characteristics

MRI scans were screened by two observers (AEB, JK) for the presence of scaphoid signal change. Any disagreement was resolved through discussion by one of the senior authors (JD, RJ). MRI scans with signal change were screened for common characteristics of signal change by two observers with (research) experience in hand- and wrist surgery (AEB, DR). The presence of these characteristics was assessed on each of the available MRI sequences (PDFS coronal, T1 coronal, PD sagittal). The pattern of signal change was scored to be present on none, one or more than one of the cuts per sequence (Table 2, Figure 1). Based on qualitative analysis of the above characteristics (Table 2), MRI scans were clustered into categories of common patterns of signal change as assessed by two observers (AEB, DR).

Interobserver reliability

A consecutive sample of 42 MRI scans was selected. To ensure a sample of each of the patterns, an MRI scan was randomly selected from any group of patterns that was not represented in the consecutive sample. This resulted in the random selection of 3 additional scans amounting to a series of 45 MRI scans. Two observers (AEB, MvB) independently assessed the 45 MRI scans and assigned each scan to one of the pre-defined patterns. Observers were blinded to each other's assessment. Clinical and demographic variables were not considered when categorizing the MRI scans. The interobserver reliability of patterns of MRI signal change was assessed.

Table 2. Characteristics of MRI signal change

MRI signal change characteristics	Signal change scored to be present on N° of cuts per MRI sequence		
Focal bicortical linear signal change in waist area			
PDFS coronal sequence	0	1	>1
T1 coronal sequence	0	1	>1
PD sagittal sequence	0	1	>1
Bicortical oedema in waist area			
PDFS coronal sequence	0	1	>1
T1 coronal sequence	0	1	>1
PD sagittal sequence	0	1	>1
Near transverse orientation of linear signal abnormality		Yes	No
Oedema adjacent to linear bicortical signal		Yes	No

PD proton density; FS fat suppressed; T1 weighted turbo spin echo

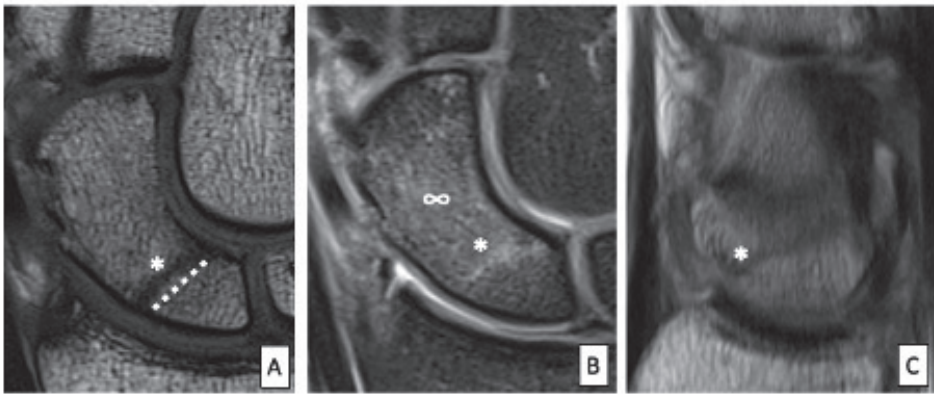

Figure 1. MRI signal change characteristics

Example of A) T1 coronal B) PDFS coronal and C) PD sagittal cut of an MRI in a patient with a suspected waist fracture demonstrating:
* Focal bicortical linear signal change in waist area
∞ Bicortical oedema in waist area (and adjacent to fracture site)
(Near) transverse orientation of linear signal change relative to scaphoid long axis

Statistical analysis

Fleiss' kappa was calculated as a measure of the interobserver reliability, and bootstrapping was used (1000 resamples) to determine the standard error, z statistic and 95% Confidence Intervals. The kappa values were interpreted according to the Landis and Koch classification for categorical data: 0.01-0.20 represented 'slight' agreement; 0.21-0.40 represented 'fair' agreement; 0.41-0.60 represented 'moderate' agreement; 0.61-0.80 represented 'substantial' agreement; and 0.81-0.99 represented 'near perfect' agreement[13]

To identify factors associated with MRI signal changes that look like a scaphoid waist fracture (vs. all other signal changes), we conducted logistic regression analysis, accounting for patient sex, age, days since injury to MRI, laterality, and mechanism of injury. Backwards elimination was used to create parsimonious regression models, with alpha set at 0.05. Because of heterogeneity in the mechanism of injury, groups with fewer than 10 patients were pooled with 'unknown.' Odds Ratios (OR), standard errors, 95% Confidence Intervals (95%CI) and *p*-values were reported. All *p*-values below 0.05 were considered statistically significant.

RESULTS

There were 92/267 MRI scans (34%) with signal change in the scaphoid. Three distinct patterns were identified: signal changes that 1) look like a scaphoid waist fracture; 2) may be confused for a scaphoid waist fracture; and 3) are clearly not a scaphoid waist fracture.

In 15 scans (5.6%) there were signal changes that "look like a scaphoid waist fracture"; 4 of these (1.5%) were categorized as "clearly a scaphoid waist fracture." Thirty-six scans (14%) showed signal changes categorized as "might be confused for a waist fracture." The remaining MRI scans showed signal changes categorized as "clearly not a scaphoid waist fracture" (n=41, 15%) and no scaphoid signal changes (n=175, 66%) (Table 3).

MRI signal changes that "look like a scaphoid waist fracture"

Scans in the first category ("looks like a scaphoid waist fracture") showed a linear, focal and bicortical signal abnormality, usually with adjacent oedema. (Figure 2a) The linear signal had a relatively transverse orientation relative to the scaphoid long axis. When the transverse linear signal was visible on more than one cut on both the T1 coronal, PDFS coronal and PD sagittal sequence, and there was adjacent oedema, the signal was described as "clearly a scaphoid waist fracture". If the linear bicortical transverse signal was present on more than one cut in at least one plane – or at least one cut in both sagittal and coronal planes - with adjacent oedema, the signal changes were described as "likely a scaphoid waist fracture". A linear bicortical and transverse signal on multiple cuts on multiple sequences without adjacent oedema, was described as "possibly a scaphoid waist fracture".

MRI signal changes that "may be confused for a scaphoid waist fracture"

MRI signal changes of the scaphoid waist without a transverse and linear signal were described as "may be confused for a scaphoid waist fracture". Two patterns were identified. The first pattern constituted diffuse unicortical signal emerging from the distal radial end of the scaphoid without reaching the ulnar cortex. The second group showed diffuse bicortical signal emerging from the distal radial end of the scaphoid reaching the ulnar cortex in the scaphoid waist (Figure 2b).

MRI signal change interpreted as "clearly not a scaphoid waist fracture"

Signal change categorized as "clearly not a scaphoid waist fracture" included for example proximal pole fractures, scapholunate (SL) ligament injuries and degenerative changes. These were described as "organized signal changes clearly not a scaphoid waist fracture" We also identified "disorganized signal changes clearly not a scaphoid waist fracture". In this group no specific pattern could be identified. Finally, "signal changes that look like a vessel" were frequently identified as a linear signal with an oblique orientation emerging from the radial distal end of the scaphoid. (Figure 2c, Supplemental data Table S1)

Table 3. Categories of MRI signal change

Category	N (%)
I. MRI signal changes that look like a scaphoid waist fracture	15 (5.6)
a. Signal changes that clearly represent a scaphoid waist fracture	4 (1.5)
b. Signal changes that likely represent a scaphoid waist fracture	9 (3.4)
c. Signal changes that possibly represent a scaphoid waist fracture	2 (0.75)
II. MRI signal changes that might be confused for a scaphoid waist fracture	36 (14)
Diffuse unicortical signal abnormality of waist area without fracture line	17 (6.4)
Diffuse bicortical signal abnormality of waist area without fracture line	19 (7.1)
III. MRI signal changes that clearly do not represent a scaphoid waist fracture	41 (15)
Organized signal changes clearly not representing a scaphoid waist fracture	14 (5.2)
Disorganized (nonspecific) signal changes that do not look like a scaphoid waist fracture	8 (3.0)
Vessel	19 (7.1)
IV: no scaphoid signal change	175 (66)

Discrete variables are presented as number (percentage); N = number
See Figure 2 and Supplementary Material Table S1 for details on the classification.

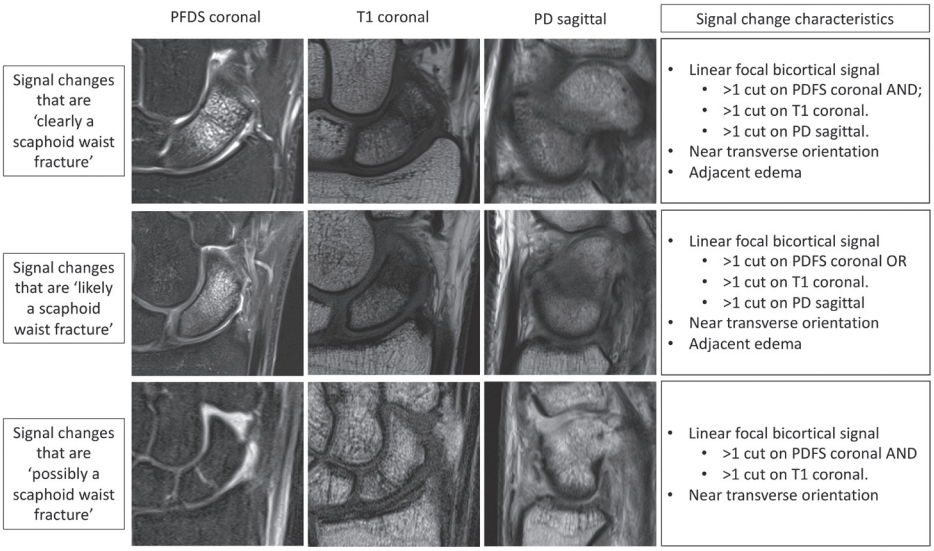

Figure 2a MRI patterns of signal change that "look like a scaphoid waist fracture"

PDFS coronal, T1 coronal and PD sagittal sequences of MRIs demonstrating signal changes that "look like a scaphoid waist fracture".
Top row: signal changes that "are clearly a scaphoid waist fracture"
Middle row: signal changes that "are likely a scaphoid waist fracture"
Bottom row: signal changes that "are possibly a scaphoid waist fracture"

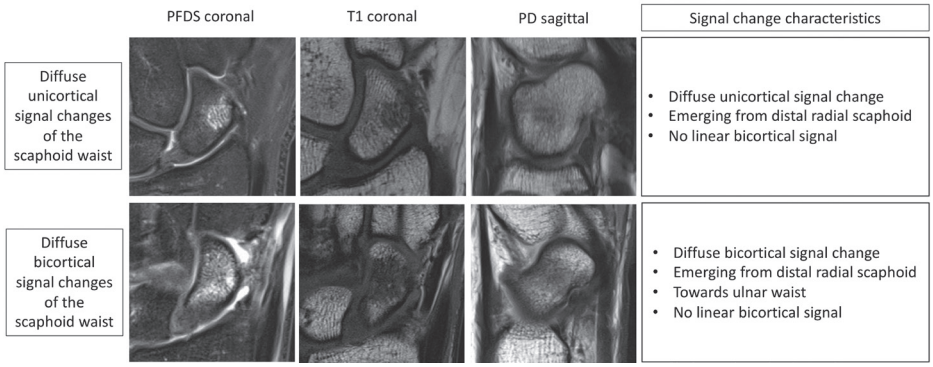

Figure 2b MRI patterns of signal change that "may be confused for a scaphoid waist fracture"

PDFS coronal, T1 coronal and PD sagittal sequences of MRIs demonstrating signal changes that "may be confused for a scaphoid waist fracture"
Top row: diffuse unicortical signal changes of the scaphoid waist
Bottom row: diffuse bicortical signal changes of the scaphoid waist

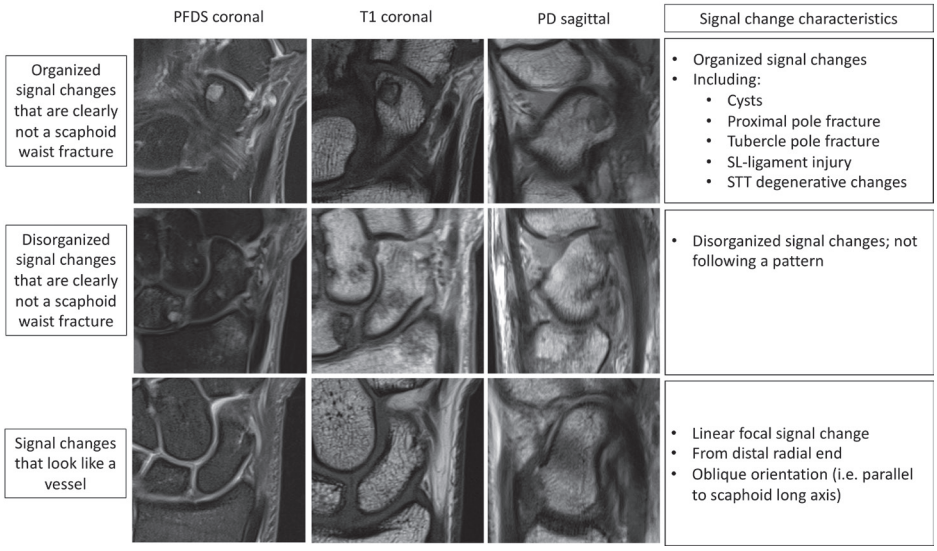

Figure 2c MRI patterns of signal change that are "clearly not a scaphoid waist fracture"

PDFS coronal, T1 coronal and PD sagittal sequences of MRIs demonstrating signal changes that "are clearly not a scaphoid waist fracture".
Top row: organized signal changes
Middle row: disorganized signal changes

Bottom row: signal changes that look like vessels

Interobserver reliability

The interobserver reliability of identifying the four main categories of MRI signal change was substantial (Fleiss' kappa value: 0.62; 95% Confidence Interval (CI): 0.43-0.8). Interobserver reliability was moderate (Fleiss' kappa value 0.55, 95% CI 0.0.39-0.72) for the four main categories including subcategories (Table 3).

Factors associated with MRI signal changes that "look like a scaphoid waist fracture"

After backward elimination, male sex was the only factor associated with signal changes that "look like a scaphoid waist fracture" (OR= 3.3; 95% CI= 1.1-10; p<0.05). Age and mechanism of injury were not (Table 4).

Table 4. Final model of multivariable regression analysis of factors associated with MRI signal changes categorized as "looks like a scaphoid waist fracture"

	OR (95% CI)	p-value
Men	3.4 (1.1-10.3)	<0.05*
Days since injury to MRI	0.92 (0.84-1.0)	<0.05*

OR: Odds Ratio; CI: Confidence Interval; * p-value statistically significant at p<0.05

DISCUSSION

MRI is frequently used to assess whether patients with a clinically suspected scaphoid fracture can safely return to work or sports without further immobilization. However, its ability to detect small anatomical and physiological variations in signal makes it prone to overdiagnosis and potentially overtreatment. Better insight into the patterns of signal change present among patients with a suspected scaphoid may aid in reducing overdiagnosis and overtreatment. In this study we identified MRI signal changes in over a third of the patients evaluated for a suspected scaphoid fracture. In only 1.5% of the MRI's, signal change was assessed as "clearly a scaphoid waist fracture"; while in 14% of the MRI's there were signal changes that "may be confused for a scaphoid waist fracture". The interobserver agreement of distinguishing between the categories was moderate. These findings contribute to the line of evidence suggesting that MRI risks a false positive diagnosis of scaphoid waist fracture on MRI.

There are several factors to keep in mind when interpreting these data. First, the rates may be somewhat specific to our patient population and our institution's imaging protocols, including MRI settings such as slide thickness and sequence. The types of signal change however, are likely to be observed by other institutions and protocols, while the relative rates may vary. We did not study accuracy of the observed patterns because there is no consensus reference standard for the presence of a scaphoid waist fracture.

The finding that signal changes were present in over one third of the MRI scans, and that signal changes that "may be confused for a scaphoid waist fracture" (14%) were more common than signal changes that "look like a scaphoid fracture" (5.6%), emphasizes the potential for misdiagnosis of scaphoid fracture when using MRI to diagnose true fractures among suspected fractures. These findings are in line with a study performed by de Zwart et al.[8] that asked musculoskeletal radiologists to assess 124 MRI scans including 64 scans of healthy volunteers and 60 MRI scans of patients with a clinically suspected scaphoid fracture. Among the 64 MRI scans of healthy volunteers without history of hand- or wrist injury 13 scans were rated as "scaphoid fracture" (20%). The high likelihood of a false positive diagnosis of a scaphoid fracture is consistent with the current study, in which many signal changes likely reflect anatomical and physiologic variations. The low prevalence of signal changes that look like a scaphoid waist fracture (5.6%) is at the low range of the 5-20% prevalence rate of true scaphoid fractures among suspected scaphoid fractures reported in previous studies. This is consistent with the increasingly observed strategy of having a low threshold to order MRI for suspected scaphoid fracture out of fear of missing a scaphoid fracture.[1,14-16] Clinicians should be aware that, in the assessment of a suspected scaphoid fracture, the prevalence of a true scaphoid fractures is low, and a false positive diagnosis may occur as frequently as a true positive diagnosis, contributing to a very low positive predictive value.[1,10]

The interobserver reliability of categorizing MRI signal change to the four different categories (k=0.62) is comparable to the interobserver reliability of diagnosing a scaphoid fracture on MRI reported by de Zwart et al (k=0.44)[8] and Beeres et al (0.67).[17] Importantly however, latter studies had broader inclusions and included also fractures of the proximal, middle and distal third of the scaphoid. Furthermore, the sample assessed by de Zwart et al. included patients with a suspected scaphoid fracture as well as healthy individuals. It has previously been reported that the definition of a scaphoid waist fracture on MRI is known to vary from "an extensive zone of oedema"[9] to a "cortical or trabecular fracture line".[7] The patterns established in this study can aid in defining a consensus definition on what constitutes a scaphoid waist fracture on MRI. In order to do so, future research should assess the accuracy and reliability of patterns of scaphoid signal abnormality.

The finding that male sex was associated with signal changes that look like a scaphoid waist fracture is in line with previous studies.[18,19] It is unclear why age and mechanism of injury were not associated with signal changes that look like a scaphoid waist fracture in our study. This is in contrast with previous studies that have identified age and mechanism of injury as predictors of a scaphoid fracture.[18,19]

Based on the findings in this study, MRI obtained to diagnose true scaphoid waist fractures among suspected fractures is associated with a high prevalence of signal changes that may be confused with a scaphoid waist fracture; a low prevalence of signal changes that clearly represent a scaphoid waist fracture; and moderate to substantial interobserver reliability in distinguishing between categories of signal changes. This suggests that MRI carries a risk of overdiagnosis and overtreatment. The patterns established in this study provide a stepping stone for future research to establish

definitions and measurements of signal changes that constitute a scaphoid waist fracture on MRI, aiming to reach a consensus definition that is as reliable and accurate as possible. Given the shortcomings of imaging, clinicians should be aware of the variety of patterns of signal change present among patients with a suspected scaphoid fracture, and their risk of being misinterpreted as a fracture. More importantly, more restrictive strategies – for instance clinical decision rules - that increase the prevalence of true fractures among suspected fractures can be investigated to improve the positive predictive value. This should still allow the vast majority of people with a suspected scaphoid fracture to have the problem treated as a wrist sprain or contusion and safely return to work or sport, perhaps with some small but acceptable risk of a true fracture, likely well under 1%.

CONTRIBUTORS

We thank Joshua Kelly for his contributions to data acquisition.

REFERENCES

1. Duckworth AD, Ring D, McQueen MM. Assessment of the suspected fracture of the scaphoid. *J Bone Joint Surg Br.* 2011;93(6):713-719.
2. Mallee WH, Henny EP, van Dijk CN, Kamminga SP, van Enst WA, Kloen P. Clinical diagnostic evaluation for scaphoid fractures: a systematic review and meta-analysis. *J Hand Surg Am.* 2014;39(9):1683-1691 e1682.
3. Brydie A, Raby N. Early MRI in the management of clinical scaphoid fracture. *Br J Radiol.* 2003;76(905):296-300.
4. Dorsay TA, Major NM, Helms CA. Cost-effectiveness of immediate MR imaging versus traditional follow-up for revealing radiographically occult scaphoid fractures. *AJR Am J Roentgenol.* 2001;177(6):1257-1263.
5. Jenkin M, Sitler MR, Kelly JD. Clinical usefulness of the Ottawa Ankle Rules for detecting fractures of the ankle and midfoot. *J Athl Train.* 2010;45(5):480-482.
6. Karl JW, Swart E, Strauch RJ. Diagnosis of Occult Scaphoid Fractures: A Cost-Effectiveness Analysis. *J Bone Joint Surg Am.* 2015;97(22):1860-1868.
7. Memarsadeghi M, Breitenseher MJ, Schaefer-Prokop C, et al. Occult scaphoid fractures: comparison of multidetector CT and MR imaging--initial experience. *Radiology.* 2006;240(1):169-176.
8. De Zwart AD, Beeres FJ, Ring D, et al. MRI as a reference standard for suspected scaphoid fractures. *Br J Radiol.* 2012;85(1016):1098-1101.
9. Mallee W, Doornberg JN, Ring D, van Dijk CN, Maas M, Goslings JC. Comparison of CT and MRI for diagnosis of suspected scaphoid fractures. *J Bone Joint Surg Am.* 2011;93(1):20-28.
10. Ring D, Lozano-Calderon S. Imaging for suspected scaphoid fracture. *J Hand Surg Am.* 2008;33(6):954-957.
11. Hunter JC, Escobedo EM, Wilson AJ, Hanel DP, Zink-Brody GC, Mann FA. MR imaging of clinically suspected scaphoid fractures. *AJR Am J Roentgenol.* 1997;168(5):1287-1293.
12. Khalid M, Jummani ZR, Kanagaraj K, Hussain A, Robinson D, Walker R. Role of MRI in the diagnosis of clinically suspected scaphoid fracture: analysis of 611 consecutive cases and literature review. *Emerg Med J.* 2010;27(4):266-269.
13. Landis JR, Koch GG. The measurement of observer agreement for categorical data. *Biometrics.* 1977;33(1):159-174.
14. Mallee WH, Wang J, Poolman RW, et al. Computed tomography versus magnetic resonance imaging versus bone scintigraphy for clinically suspected scaphoid fractures in patients with negative plain radiographs. *Cochrane Database Syst Rev.* 2015(6):CD010023.
15. Pillai A, Jain M. Management of clinical fractures of the scaphoid: results of an audit and literature review. *Eur J Emerg Med.* 2005;12(2):47-51.
16. DaCruz DJ, Bodiwala GG, Finlay DB. The suspected fracture of the scaphoid: a rational approach to diagnosis. *Injury.* 1988;19(3):149-152.
17. Beeres FJ, Hogervorst M, Kingma LM, Le Cessie S, Coerkamp EG, Rhemrev SJ. Observer variation in MRI for suspected scaphoid fractures. *Br J Radiol.* 2008;81(972):950-954.
18. Duckworth AD, Buijze GA, Moran M, et al. Predictors of fracture following suspected injury to the scaphoid. *J Bone Joint Surg Br.* 2012;94(7):961-968.
19. Mallee WH, Walenkamp MMJ, Mulders MAM, Goslings JC, Schep NWL. Detecting scaphoid fractures in wrist injury: a clinical decision rule. *Arch Orthop Trauma Surg.* 2020;140(4):575-581.

SUPPLEMENTARY MATERIAL

Table S1. MRI categories and definitions

Category I. MRI signal changes that look like a scaphoid waist fracture
a. Signal changes that clearly represent a scaphoid waist fracture • Linear and focal bicortical signal change visible on ≥1 cut in the waist area on T1 coronal, PDFS coronal and PD sagittal sequence. • Near transverse orientation of linear signal change relative to scaphoid long axis • Oedema adjacent to linear bicortical signal change
b. Signal changes that likely represent a scaphoid waist fracture • Linear and focal bicortical signal change visible on ≥1 cut in the waist area on either T1 or PDFS coronal sequence • Linear and focal bicortical signal change on ≥ 1 cut on the PD sagittal sequence • Near transverse orientation of linear signal change relative to scaphoid long axis • Oedema adjacent to linear bicortical signal change
c. Signal changes that possibly represent a scaphoid waist fracture • Linear and focal bicortical signal change visible on ≥1 cut in the waist area on both T1 and PDFS coronal sequence • Near transverse orientation of linear signal change relative to scaphoid long axis
Category II. MRI signal changes that might be confused for a scaphoid waist fracture
c. Diffuse unicortical signal change *of waist area without fracture line* • Diffuse unicortical signal change emerging from distal radial end of scaphoid • Extending from volar-radial-distal towards proximal ulnar side of scaphoid without reaching ulnar cortex
d. Diffuse bicortical signal change of waist area without fracture line • Diffuse bicortical signal change extending from distal radial end of scaphoid to proximal ulnar side of scaphoid.
Category III. MRI signal changes that clearly do not represent a scaphoid waist fracture
d. Organized signal changes clearly not representing a scaphoid waist fracture • Including, but not limited to: proximal pole fractures, tubercle fractures, cysts, SL ligament injury, degenerative changes.
e. Disorganized (nonspecific) signal changes that do not look like a scaphoid waist fracture
f. Vessel • Linear focal signal change • Frequently entering from radial distal end of scaphoid • Oblique orientation, parallel to scaphoid longitudinal axis

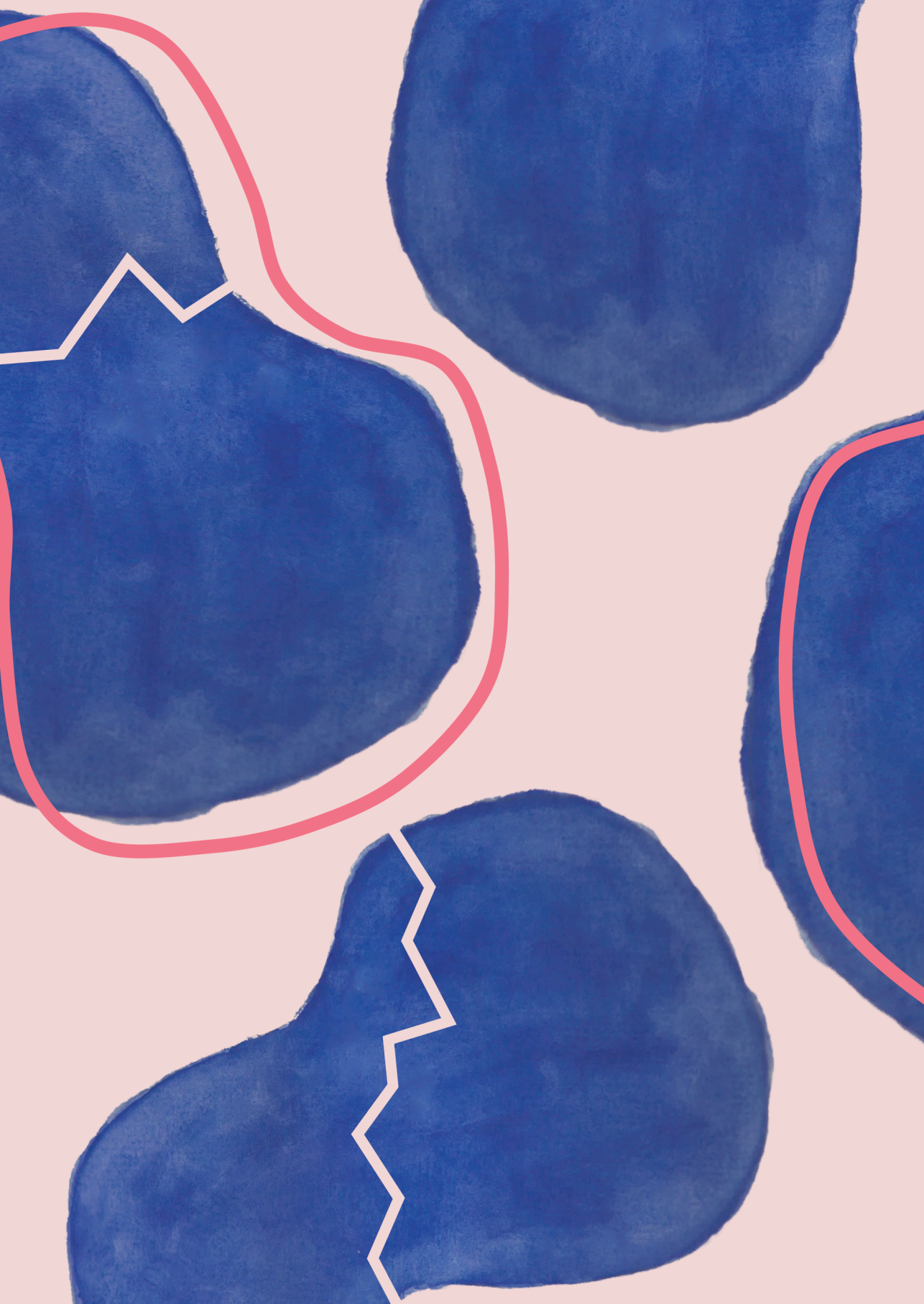

PART III

SCAPHOID FRACTURE CHARACTERISTICS

CHAPTER 7

Three-Dimensional Mapping of Scaphoid Fractures and Comminution

A.E.J. Bulstra and A. Turow
M.G.E. Oldhoff
B. Hayat
J.N. Doornberg
J. White
R.L. Jaarsma
G.I. Bain

In Skeletal Radiology, 2020 October; 49(10):1633-1647.

ABSTRACT

Objective

Acute and subacute scaphoid fractures were assessed using 3D computed tomography (CT). The aims were to describe fracture morphology, to map fractures onto a 3D scaphoid model and to correlate this to scaphoid anatomy.

Materials and methods

A retrospective, multicentre database search was performed to identify CT studies of acute and subacute scaphoid fractures. CT scans of scaphoid fractures less than 6 weeks from time of injury were included in this retrospective, multicentre study. CTs were segmented and converted into three-dimensional models. Following virtual fracture reduction, fractures were mapped onto a three-dimensional scaphoid model.

Results

Seventy-five CT scans were included. The median time from injury to CT was 29 days. Most studies were in male patients (89%). Most fractures were comminuted (52%) or displaced (64%). A total of 73% of displaced fractures had concomitant comminution. Waist fractures had higher rates of comminution and displacement compared to all other fractures. Comminution was located along the dorsal ridge and the volar scaphoid waist.

Conclusion

Our study is the first to describe acute fracture morphology using 3D CT and to correlate comminution and displacement to fracture types. The dorsal ridge and volar waist need prudent assessment, especially in waist fractures.

INTRODUCTION

Scaphoid fractures have traditionally been described based on radiographs. From the first description of the scaphoid fracture in 1905 by Destot[1], various classification systems have been developed.[2] The most commonly used classification systems are Herbert[3], Mayo[4] and Russe.[5] They take fracture location, stability and chronicity into consideration; however, given the heterogenicity of fracture patterns, accurate fracture description remains challenging.

The scaphoid shows considerable size and shape variation[6] and has complex kinematics.[7,8] Consequently, despite being the preferred initial imaging modality in suspected scaphoid fractures,[9] radiographs have limitations in fracture description and diagnosis.[10,11] The correlation between fracture characteristics and clinical outcomes has been well established.[12-14] Accurate fracture description is, therefore, paramount in management choice and operative planning. There has been a paucity of studies investigating acute scaphoid fracture morphology. A recent computerised 3-dimentional analysis examined acute scaphoid fractures and found that most waist fractures were horizontal oblique, rather than transverse[15], which is contrary to previous reports that this fracture pattern is uncommon.[16,17] Scaphoid fracture comminution has been shown to exist in certain fracture types.[18] Comminution has been associated with fracture instability, longer time to union and higher rates of nonunion.[19-21] However, literature about comminution patterns in various fracture types has been lacking. Furthermore, despite 3D CT being known for increased reliability in fracture evaluation[22], only a limited number of studies has investigated the scaphoid fracture in 3D. The aims of this study were to describe acute fracture morphology, to map these fractures onto a 3D scaphoid model and to correlate this to scaphoid anatomy.

MATERIAL AND METHODS

In this multicentre, retrospective study, scaphoid fractures investigated with a CT scan between 2008 and 2018 were examined. CT scans underwent initial assessment for fracture morphology, comminution and displacement. Subsequently, CTs were segmented, 3D models prepared and virtually reduced. Fractures were mapped onto an intact scaphoid model and fracture patterns and comminution were assessed.

Subjects

CT scans of 75 adult patients (≥18 years) presenting with a scaphoid fracture were reviewed. CT scans within six weeks of the index injury were included. Patients that had pre-existing scaphoid pathology, such as previously documented scaphoid trauma, were excluded. Only CT scans of adequate quality were considered for further 3D analysis. The parameters included slice thickness of at most 1mm on axial imaging, no motion artefact and complete visualization of the scaphoid and all its articulations. A previously published

grading system for high resolution peripheral computed tomography was utilised.[23] Only grade one (no motion artefact) or grade two scans (minor motion artefact) were included for analysis. Initial CT assessment

Axial imaging was reviewed together with multiplanar reconstructions (MPR) in the coronal and sagittal planes. The following criteria for bone fracture on CT were used: (1) a step in the cortex, (2) cortical discontinuity, (3) any displacement or comminution of bone fragments. Comminution was defined as more than two fracture fragments or two fracture fragments with signs of impaction. A fracture was considered displaced if it was translated ≥1mm in any plane.[24,25] MPR in the plane of the wrist and along central, longitudinal axis of the scaphoid[26] were assessed for displacement using the Radiant DICOM Viewer™(Version 4.6.9; Poznań, Poland)

Three-dimensional model preparation

De-identified scans were exported in the Digital Imaging and Communication in Medicine (DICOM) format, loaded into 3D Slicer (Version 4.8.1; Boston, MA, USA) and segmented. (Figure 1) Segmentation data was exported into Rhinoceros™ (Version 5.4.2; McNeel, Seattle,WA, USA), and fracture fragments were virtually reduced. A reduction was deemed anatomical when the following anatomical aspects of the scaphoid were restored: (1) concavity of the capitate fossa; (2) concavity of the radial and ulnar aspects of the scaphoid waist; (3) convexity of the radial and ulnar aspects of the proximal and distal poles; (4) alignment of the dorsal ridge. Comminuted fragments were measured and assessed by three separate authors (A.T, A.B. & J.W.). Fragments less than 2 mm were excluded from further assessment.

Model alignment

All left-sided scaphoid models were mirrored using Meshmixer™ (version 3.5, Autodesk, Inc) The reduced scaphoid fragments were aligned to a standard scaphoid 3D template using Artec Studio™ (version 3.5, Autodesk, Inc) in two sequential steps. First, six anatomical landmarks, as described by Schwarcz and colleagues[27], were marked on both the template and the fractured model. Second, the non-rigid Mesh Alignment Tool was used to calculate the best fit of the fractured scaphoid mesh and the template scaphoid mesh. Correct alignment was verified by two authors (A.T and A.B.). Any discrepancies were re-assessed, and alignment re-adjusted to ensure best fit. (Figure 2) Only correctly reduced 3D models would allow for the six anatomical landmarks to align correctly. Hence, correct alignment was also used as a secondary checkpoint for the virtual fracture reduction performed earlier.

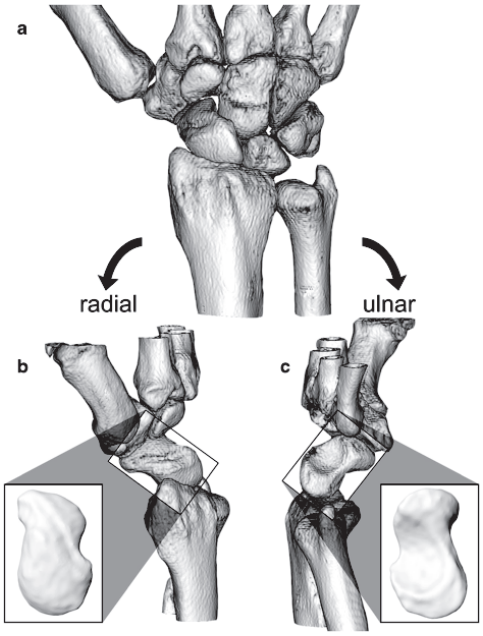

Figure 1. 3D model preparation

(a) 3D reconstruction of fine axial slices of an uninjured wrist with subsequent **(b)** radial and **(c)** ulnar views of the scaphoid. With the exception of the trapezium and trapezoid, the carpus is subtracted for better visualization of the scaphoid in **(b)** and **(c)**

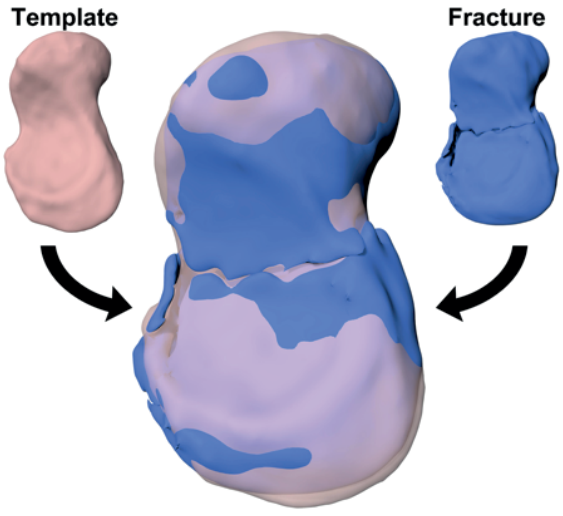

Figure 2. Ulnar views of a comminuted waist fracture aligned onto the template

Pink scaphoid model: scaphoid template of uninjured scaphoid. *Blue scaphoid model*: comminuted waist fracture. The two 3D models were superimposed onto each other to allow for fracture mapping onto the common template (pink scaphoid).

Fracture mapping

After successful model alignment, assessment was continued in Rhinoceros™. The template was rotated 45° along its longitudinal axis, creating eight standardised viewpoints to allow for reproducible and accurate fracture line mapping across all fractured scaphoids. Fracture lines were then transposed from the fractured scaphoid onto the scaphoid template. Where there was any opening of the fracture, the lines were drawn at the halfway point between the fracture fragments. Any impaction or comminution was marked separately.

The main fracture patterns were defined based on the dorsal ridge as viewed from the radial aspect of the scaphoid (Figure 3 and 4). The dorsal ridge was chosen for fracture description from preliminary mapping analysis. This demonstrated fracture grouping based on differences in fracture angle relative to the dorsal ridge. Fracture lines that followed the dorsal ridge closely were near parallel to the ridge. Angles measured between the ridge axis and the fracture lines were less than 30˚. In contrast, fractures with a short path through the dorsal ridge were more obtuse with angles measuring 50˚ and more.

Fractures passing proximal to the dorsal ridge, were defined as proximal pole fractures. Fractures crossing the dorsal ridge were defined as waist fractures. Waist fractures were sub-classified further based on their angular morphology. For each fracture line, a line of best fit between the most radial and ulnar extents was drawn. Angles between this line and the longitudinal axis of the dorsal ridge were measured. Transverse waist types were defined as those that subtended angles of more than 30˚ and oblique fractures less than or equal to 30˚ (Figure 5). Involvement of the most dorsal and ulnar non-articulating part of the scaphoid, the scaphoid apex[28], was noted. Fractures distal to the transverse ridge were defined as distal pole and tubercle fractures. These distal fractures were divided further into intra- and extra-articular based on the classification by Prosser et al.[29] Incomplete fractures showed cortical discontinuity only on one aspect of the scaphoid with the fracture line fading within the trabecular bone. In cases with three or more dominant fracture fragments, the fracture was classified as segmental.

Statistical Analysis

Categorical variables were examined using Fisher's exact test and continuous variables were compared by analysis of variance (ANOVA). To determine predictors of fracture type, univariate analysis was performed on comminution, fracture displacement and presence of concurrent wrist injuries. Waist fractures were examined separately to compare their obliquity with reference to the dorsal ridge axis. Angles subtended were assessed using the independent sample t-test. A p-value of <0.05 was considered statistically significant.

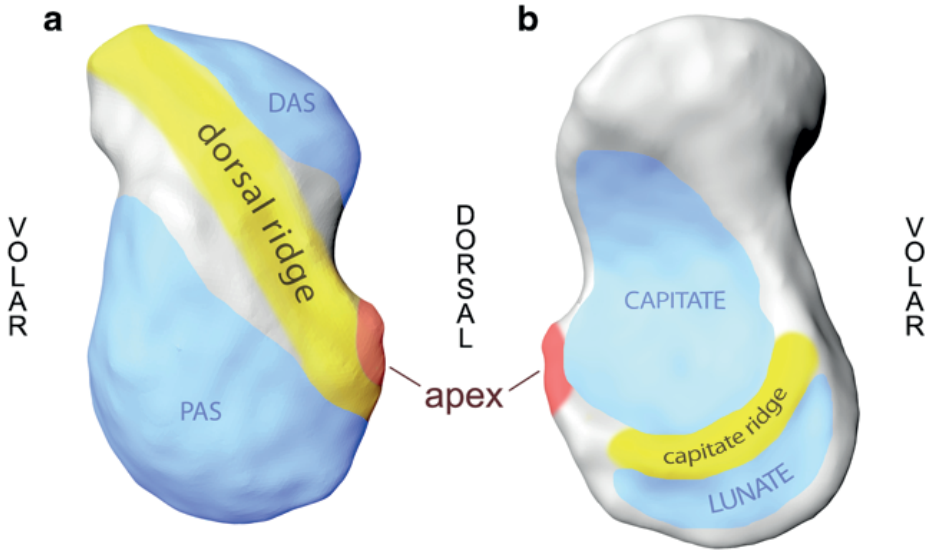

Figure 3. Anatomical landmarks on scaphoid template

(a) radial and **(b)** ulnar view of anatomical landmarks on scaphoid template. Articular surfaces were adapted from Fogg and are marked blue. DAS distal articular surface, PAS proximal articular surface.

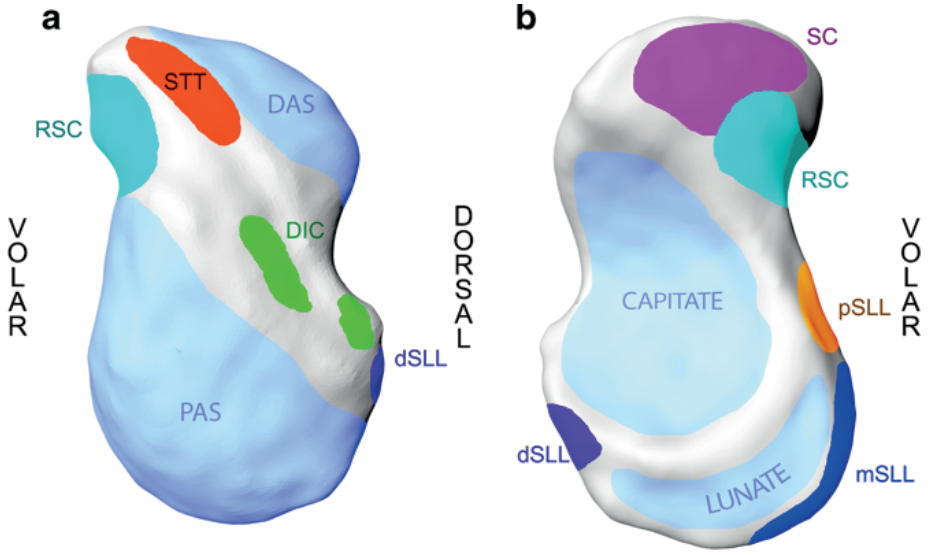

Figure 4. Ligament attachments on scaphoid template

(a) radial and **(b)** ulnar of scaphoid template with ligamentous attachments. Adapted from Fogg[30] and Kijima et al.[31] Articular surfaces are marked blue. DAS distal articular surface, PAS proximal articular surface, STT scaphotrapeziotrapezoid ligament complex, RSC radioscaphocapitate ligament, DIC dorsal intercarpal ligament, SC scaphocapitate ligament; dSLL, mSLL and pSLL are dorsal, membranous and palmar scapholunate ligaments

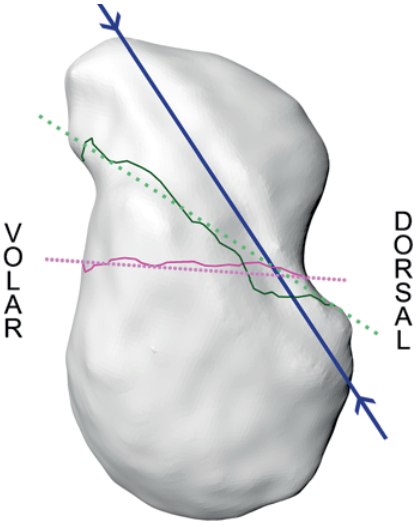

Figure 5. Assessment of fracture angle of scaphoid waist fractures

Radial view of a right scaphoid model (template). A typical transverse waist fracture is shown (pink) and its line of best fit (dotted pink). The green line shown a typical oblique waist fracture, with its line of best fit (dotted green). Measurements of fracture angles were made relative to the dorsal ridge axis (blue)

RESULTS

Seventy-five CT scans fulfilled the inclusion criteria (Table 1; Figure 6 and 7). The mean age was 36 years (range 18-84). The majority of fractures were seen in males (n=66, 88%). The fractures involved the left (n=39, 52%) and right (n=36, 48%) wrists. The mean delay from injury to CT was 12 days (range 0-42).

Table 1. Fracture types and fracture characteristics.

Fracture Type	Number		Displacement		Comminution		Concurrent #		Perilunate	
Proximal Pole	6	(8)	2	(33)	1	(17)	4	(67)	2	(33)
Waist Transverse	28	(37)	22*	(79)	15	(54)	10	(36)	3	(11)
Waist Oblique	24	(32)	15	(63)	16*	(67)	13	(54)	3	(13)
Distal Pole	1	(1)	1	(100)	1*	(100)	0	(0)	0	(0)
Tubercle	8	(11)	3	(38)	1*	(13)	3	(38)	0	(0)
Incomplete	3	(4)	0	(0)	0	(0)	1	(33)	0	(0)
Segmental	5	(7)	5	(100)	5*	(100)	3	(60)	2	(40)
Total	**75**		**64%**		**52%**		**45%**		**13%**	

Absolute numbers are reported, with percentages of each shown in (). *statistically significant

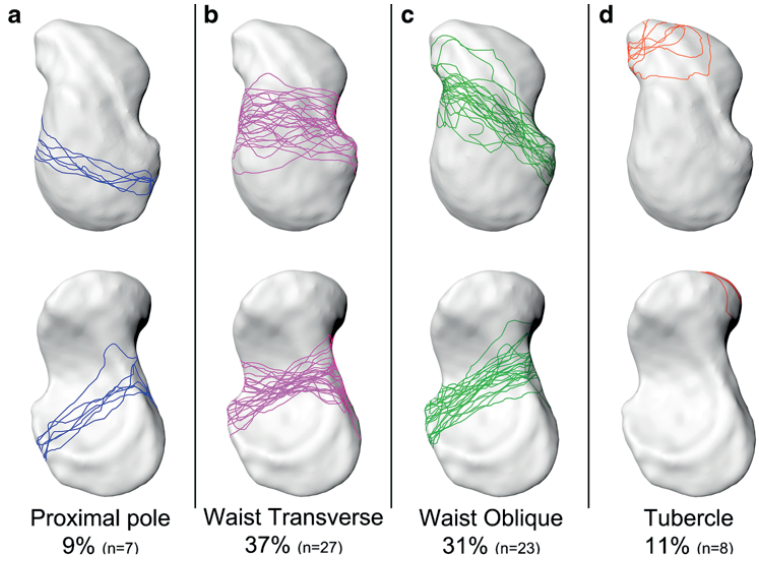

Figure 6. Fracture maps of the four main fracture types

Top row: template shown from radial view. *Bottom row:* ulnar view.
(a) proximal pole fractures. **(b)** transverse waist fractures **(c)** oblique waist fractures **(d)** tubercle fractures

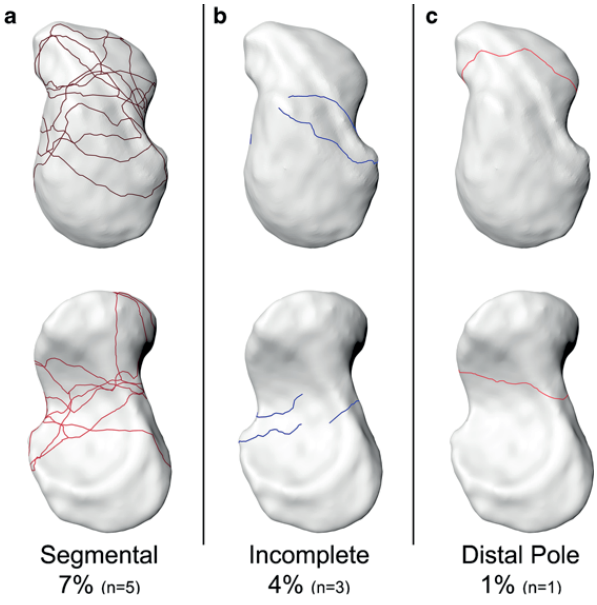

Figure 7. Fracture maps of uncommon fractures

Top row: template shown from radial view. *Bottom row:* ulnar view.
(a) segmental fractures. **(b)** incomplete fractures **(c)** distal pole fractures

Proximal pole

There were seven proximal pole fractures (9%; Figures 7-9). One fracture was displaced, and one had comminution. All fractures showed similar patterns. Radially, the fractures passed obliquely from the proximal/dorsal to the distal/volar border. The scaphoid apex was spared in all cases (Figure 8). At the dorsal border, fractures appeared to either be proximal to the dorsal scapholunate ligament (dSLL) footprint or to be extending directly into its attachment. The only case with comminution had a small fragment just proximal to the scaphoid apex, likely representing an avulsion of the dSLL. On the volar aspect, the fractures continued a more distal path, approaching the scaphoid waist. Proximal pole fractures ran obliquely across the capitate fossa between the palmar scapholunate ligament (pSLL) and the dSLL. On the volar aspect, most fractures (n=5, 71%) involved the pSLL, with the remainder exiting through an area between then RSC and the pSLL. With the exception of this dSLL and pSLL involvement, proximal pole fractures were purely intra-articular. None of the fractures involved the proximal capitate ridge.

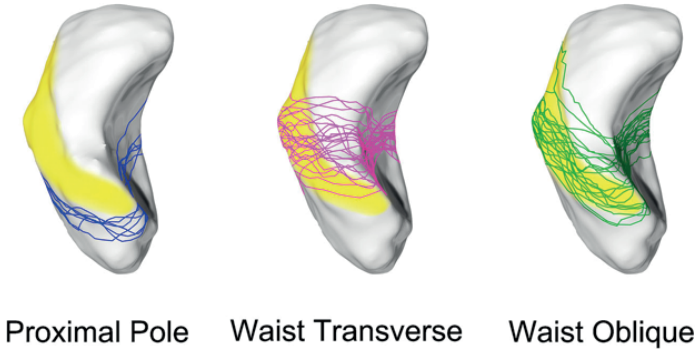

Figure 8. Fracture types relative to the dorsal ridge

Dorsal ridge involvement in proximal pole, transverse waist and oblique waist fractures. Dorsal ridge is outlined in yellow

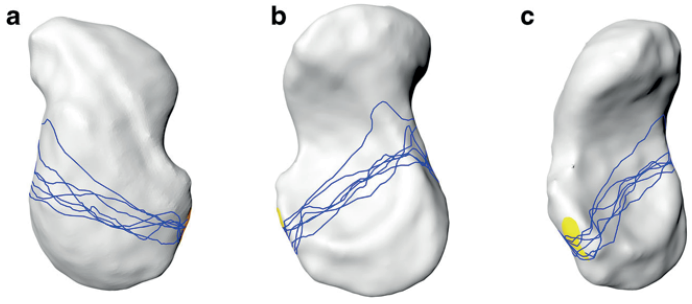

Figure 9. Proximal pole fractures

(a) radial; **(b)** ulnar and **(c)** apex view of scaphoid template with map of proximal pole fractures. One comminuted fragment was observed in only one case, and this is marked in yellow

Waist Fractures

Most scaphoid fractures had their dominant fracture line at the waist (n=51, 69.3%). With respect to the dorsal ridge axis, oblique waist fractures (n=24; 32%) subtended an average angle of 15.4° (range 6-28°) and transverse fractures (n=28; 37%) an average angle of 51.1° (range 30-77°).

Transverse

Dorsally, transverse fractures were confined to the proximal half of the dorsal ridge (Figure 8). They were aggregated around the dorsal concavity, with 29% (n=8) involving the scaphoid apex. This was mirrored on the volar side, with fractures exiting between the widest part of the proximal scaphoid and the most concave waist. Fractures were uniformly distributed around the waist of the scaphoid. The capitate fossa was fractured at its middle with sparing of the proximal capitate ridge. Comminution was present in 54% (n=15) of cases. The capitate fossa showed comminution in a transverse direction, similar to the overall fracture morphology (Figure 10).

Oblique

Oblique waist fractures involved almost the entire dorsal ridge (Figure 8). Most oblique waist fractures involved the scaphoid apex (n=18, 78%). Dorsally, oblique waist fractures showed to be more distal than their transverse counterparts, extending into the distal pole. Fracture morphology was similar across the capitate fossa when compared to transverse waist fractures. It was not possible to make clear distinctions between the two waist types in this region. Comminution was present in 70% (n=16) of cases and this was largely located dorsally. Comminuted fragments tended to be large at 6-10mm and spanned most of the dorsal ridge. Comminution across the capitate fossa followed a more oblique pattern and was more frequent than in transverse types (Figure 11).

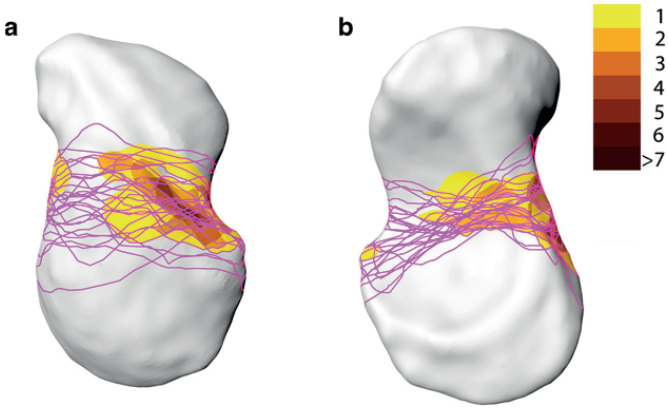

Figure 10. Comminution in transverse waist fractures

(a) radial and **(b)** ulnar view scaphoid template with fracture map of transverse waist fractures. Comminution is marked in yellow, with overlapping cases allocated darker colour

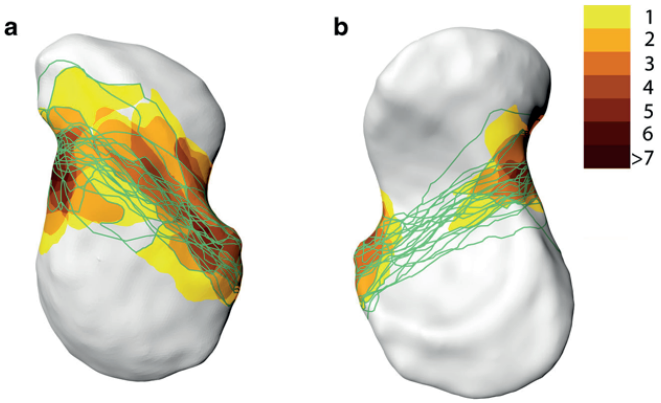

Figure 11. Comminution in oblique waist fractures

(a) radial and **(b)** ulnar view scaphoid template with fracture map of oblique waist fractures. Comminution is marked in yellow, with overlapping cases allocated darker colour

Distal Pole

Nine distal pole fractures were identified (12%). Only one fracture ran transversely across the widest portion of the distal pole. In this case, dorsal and ulnar comminution was present. The remainder of fractures involved the tubercle. Of those, 25% (n=2) were extra-articular and 75% (n=6) were intra-articular. All intra-articular fractures involved the radial half of the scaphotrapeziotrapezoid joint (STT). Larger articular fragments were associated with comminution and fracture displacement (Figure 12). Distal fragment size was on average 3.5mm for extra-articular and 8.2mm for intra-articular tubercle fractures.

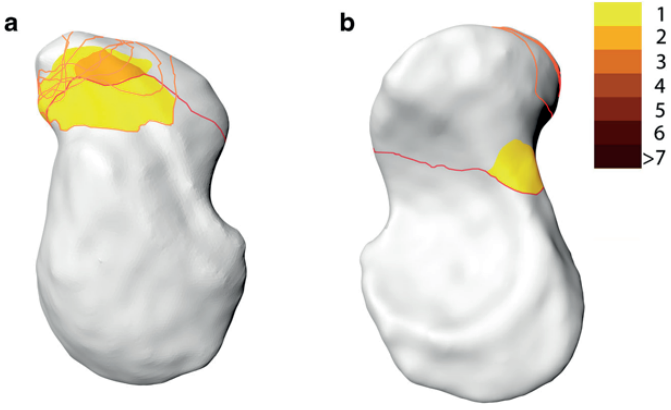

Figure 12. Comminution in distal pole and tubercle fractures

(a) radial and **(b)** ulnar view scaphoid template with fracture map of distal pole and tubercle fractures. Comminution is marked in yellow, with overlapping cases allocated darker colour

Incomplete

Three incomplete fractures were included. Two were traversing across the narrowest part of the scaphoid waist. Their dorsal and volar morphology approximated that of transverse waist fractures. One incomplete fracture followed the dorsal ridge as was seen in oblique waist fractures. No comminution or displacement was present.

Segmental

Segmental fractures represented 7% of all examined fractures (n=5). (Figure 13) All were displaced. Comminution spanned the entire dorsal ridge across the waist and distal pole of the scaphoid. The capitate fossa demonstrated fracture morphology similar to waist fractures. None of the segmental fractures involved the proximal pole. The proximal capitate ridge and the lunate articular surface that articulated with the lunate remained spared, just like in waist and proximal pole fractures.

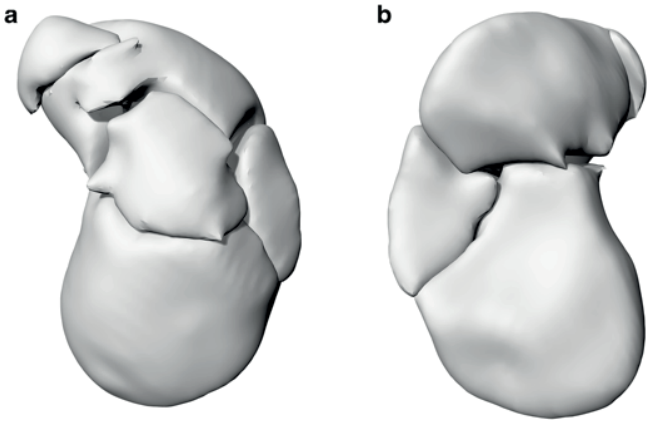

Figure 13. Comminuted fracture

(a) radial and **(b)** ulnar view of the scaphoid of a communited fracture

Displacement

More than half of fractures were displaced (n=48, 64%). All segmental fractures were displaced; however, due to small numbers in this subgroup, this did not reach statistical significance when comparing to all other fracture types (p=0.153). There was a strong correlation between displacement and comminution (p<0.001; Figures 14 and 15), with 90% of comminuted fractures being displaced. Transverse waist fractures were more frequently displaced (n=22, 79%) than were oblique waist fractures (n=15, 65%). Transverse waist fractures showed the highest rate of displacement amongst any fracture type (p=0.042). In comparison, proximal pole fractures were less likely to be displaced when comparing to other fracture types (29%, p=0.040). Three displaced tubercle fractures (38%) were identified. Their comparative displacement rates were similar to other fracture types (p=0.128).

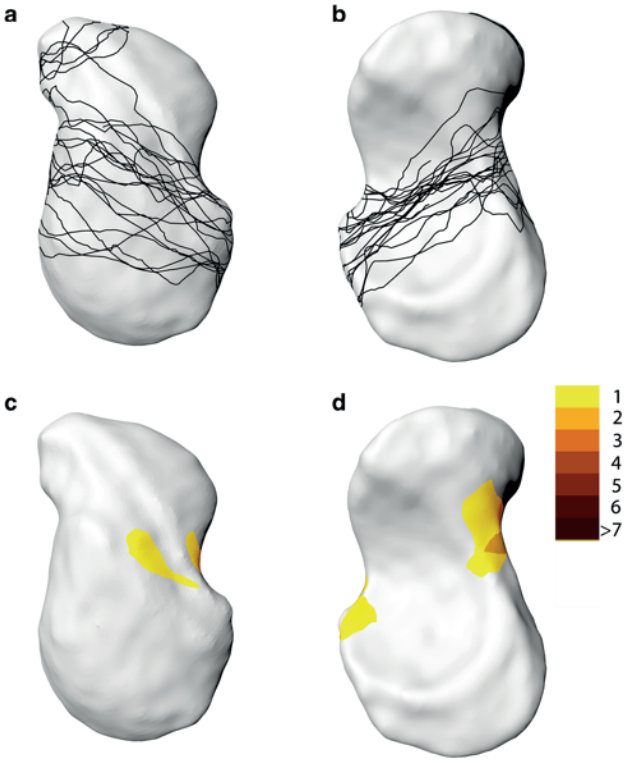

Figure 14. Fracture map of nondisplaced fractures and comminution

(a) radial and **(b)** ulnar view of all nondisplaced fractures on scaphoid template
(c) radial and **(d)** ulnar view of communition (in yellow) in nondisplaced fractures. Comminution was only present in 4 of the 27 nondisplaced scaphoid fractures.

Comminution

Fifty-two percent of fractures were comminuted. Transverse and oblique waist fractures showed comparable comminution rates (39% and 41%, respectively). However, oblique waist fractures demonstrated higher rates of comminution (70%) when comparing to other fracture types (44%, p=0.043). Higher rates of comminution were also observed when grouping all waist fractures together (61%, p=0.026). In contrast, proximal pole fractures were less often comminuted (14%, p=0.042). Similarly, the rate of comminution in tubercle fractures (13%) was significantly lower when comparing to other fracture types (57%, p=0.025). Scaphoid comminution did not appear to be random but was localised to specific anatomical areas of the scaphoid (Figure 16). Radially, comminution was highest along the proximal half of the dorsal ridge. This was in-line with the axis of the ridge and extended into the scaphoid apex. The dorsal intercarpal ligament (DIC) finds attachment to the proximal ridge and, in part, to the scaphoid apex. On the ulnar aspect, comminution was aggregated between the attachments of the radioscaphocapitate (RSC) ligament and the pSLL. Comminution was distributed at near right angles to the longitudinal axis of

the scaphoid. The highest rate of comminution was seen at the isthmus of the scaphoid waist. The narrowest part of the scaphoid corresponds to an area of inflection. At this point, the relatively shallow concavity of the waist tapers into a sharp convexity as the waist transitions into the distal pole.

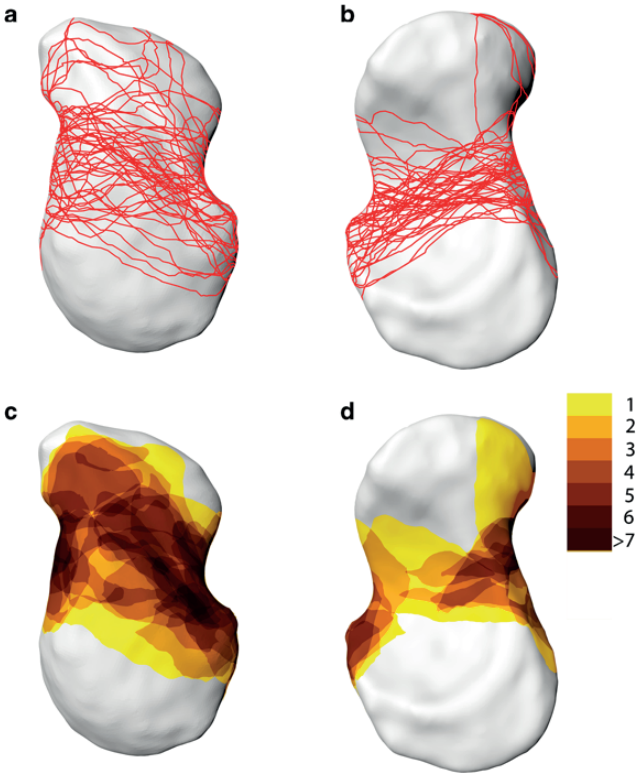

Figure 15. Fracture map of displaced fractures and comminution

(a) radial and **(b)** ulnar view of all displaced fractures on scaphoid template
(c) radial and **(d)** ulnar view of communition (in yellow) in displaced fractures.

Concurrent Fractures

Almost half of all scaphoid fractures had an associated wrist injury (45%). In ten cases, a scaphoid fracture was present as part of a greater arc, perilunate dislocation. Subgroup analysis showed that a greater percentage of segmental fractures (40%) were associated with a perilunate dislocation than proximal pole (33%), oblique waist (13%) or transverse (11%) fractures; however, concurrent fractures were not significantly associated with a particular fracture type (p=0.613).

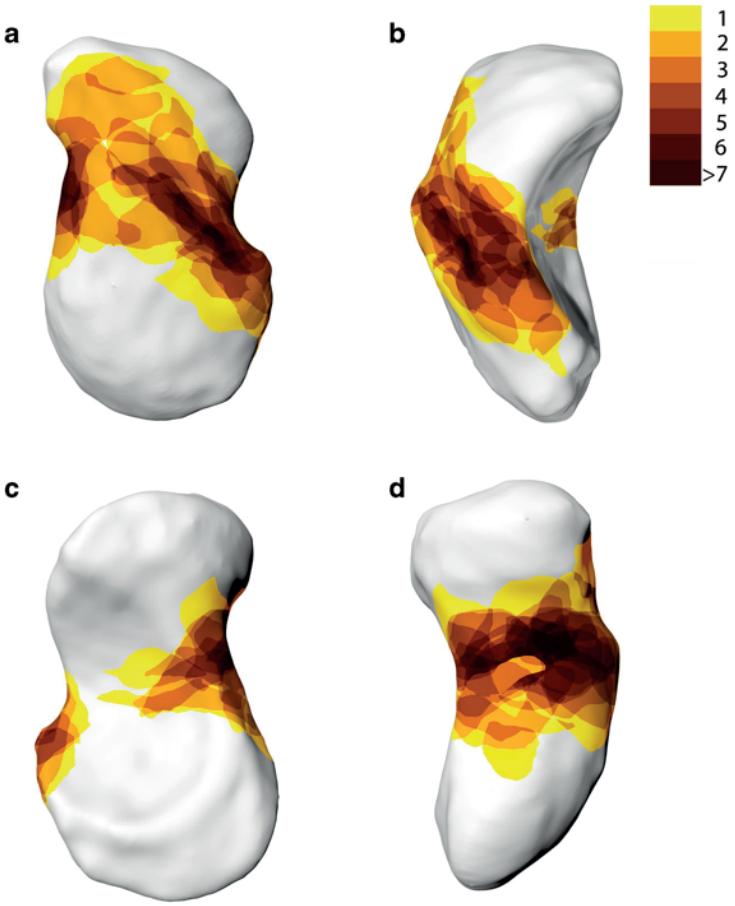

Figure 16. Fracture map of comminution

(a) radial; **(b)** dorsal **(c)** ulnar and **(d)** volar view of all comminuted areas on scaphoid template Comminution was only present in 4 of the 27 nondisplaced scaphoid fractures.

DISCUSSION

One of the first scaphoid studies to look at 3D fracture morphology came from Compson who combined plain radiography with anatomical landmarks.[18] He found three main fracture types: dorsal sulcus, surgical waist and proximal pole. He made attempts at including comminution in his study but noted that to be challenging. There has been a paucity of studies investigating acute fracture morphology with CT. Luria and colleagues examined 124 acute scaphoid fractures.[15] The authors found waist fractures to be horizontal oblique rather than transverse. Garala and Dias[34] utilised CT in a study adapted from the early work done by Compson.[18] The authors superimposed radiographs of 379

acute scaphoid fractures onto a 3D model. They confirmed the obliquity of waist fractures. Our study confirmed a spectrum of waist fractures ranging from transverse and oblique types. Furthermore, it is the first study to correlate 3D morphology of acute scaphoid fractures to displacement and comminution.

Proximal pole fractures are traditionally regarded as challenging to treat, unstable and with a high risk of non-union.[35] In the current study, acute proximal pole fractures were undisplaced and had low rates of comminution. The only comminution was seen proximal to the scaphoid apex, likely representing a dorsal scapholunate ligament (dSLL) avulsion. Low rates of displacement could be explained by fractures running between the attachments of the dSLL and pSLL. Fibres of the corresponding SLL would lie on either side of the fracture and could aid in preventing proximal pole extension relative to the distal fragment. The proximal pole is mostly articular and is known to have the thickest trabeculae of the entire scaphoid.[36] As a fracture would propagate through the proximal pole, a single fracture line is created. The bordering thick trabeculae would prevent secondary fracture propagation.

In contrast to proximal pole fractures, waist fractures had the highest rates of comminution and displacement of any fracture type. This is consistent with the pathomechanisms resulting in scaphoid waist fractures. Most commonly, the scaphoid fractures with wrist extension and concurrent axial loading.[37] Axial loading of a neutral wrist or forced hyperextension of an unloaded wrist can also result in a scaphoid waist fracture.[38,39] As the scaphoid is locked between the capitate and the distal radius, the degree of ulnar or radial wrist deviation can determine the resultant fracture morphology.[40]. The ensuing forces on the scaphoid create a volar tension and a dorsal compression side. Dorsal compression results in comminution. With wrist mobility, extension of the lunate and the proximal scaphoid fragment occurs.[27] This can result in volar collapse and further comminution, producing a humpback deformity in the chronic setting. The sequelae of volar collapse, in particular volar bone loss, have been confirmed by quantitative and qualitative 3D CT.[41] Our study confirms these initial observations and aids in identification of areas with high rates of comminution. These zones of comminution should be carefully examined to determine fracture stability and to guide treatment.

In our study, comminution was predominantly localised to dorsal ridge. The dorsal intercarpal ligament (DIC) and the dorsal capsule attach at the proximal dorsal ridge.[16] The DIC can have different insertion patterns depending on the dorsal ridge morphology.[32] In a rotating scaphoid (type 1), the DIC bypasses the dorsal ridge and finds attachment near the scaphotrapeziotrapezoid joint. During an injury of a type 1 scaphoid, the DIC can act a fulcrum over which the dorsal scaphoid extends, causing depression and comminution of the entire dorsal ridge. In a flexing scaphoid (type 2), the DIC inserts directly onto the proximal crest. As a type 2 scaphoid fractures, the DIC acts as the dorsal check for the capitate.[16] During injury, hyperextension is followed by scaphoid flexion resulting in tensioning of the DIC. This causes avulsion of its attachment at proximal dorsal ridge only (Figure 17).

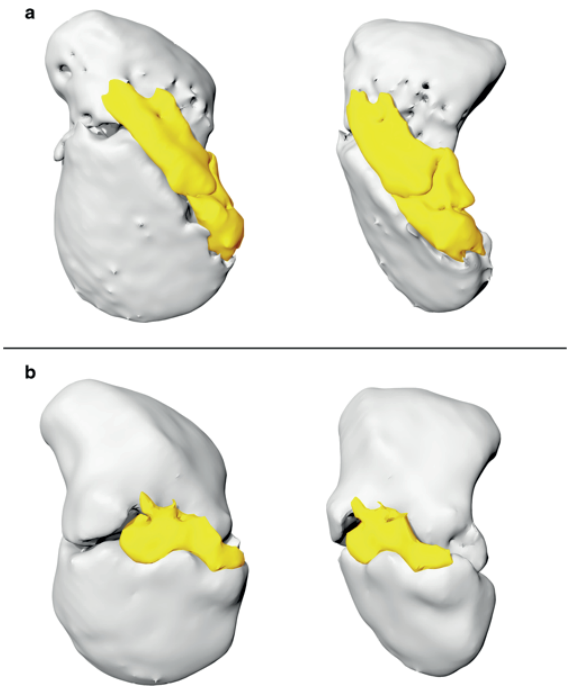

Figure 17. Dorsal comminution in an oblique and transverse waist fracture

Examples of dorsal comminution, marked in yellow.
(a) Type 1 scaphoid with a single high crest and comminution of the entire dorsal non-articulating area.
(b) Type 2 scaphoid with several lower crests and comminution at the DIC insertion only

Volarly, comminution was localised between the radioscaphocapitate ligament (RSC) and the pSLL. The RSC lies on the volar concavity of the scaphoid waist, acting as a fulcrum around which the scaphoid rotates[16]. Volar comminution was aggregated at this concavity, representing the scaphoid isthmus (Figure 18). Comminution was at near right angles to the longitudinal axis of the scaphoid. Most fractures were located either at the attachment of the pSLL or just distal to it. The RSC was spared in the majority of fractures. Only a few fractures extended more proximally into the membranous SLL or more distally into the attachment of the RSC. Comminution and its orientation in this area can be explained by (1) the direction of the RSC in this area, (2) the scaphoid pivoting over the RSC during flexion and (3) by an abrupt change in cortical thickness at the waist.[36]

Some areas of the scaphoid were observed to be either protected against fracturing or experienced low rates of displacement and comminution. The distal pole was one of those areas. The distal scaphoid is stabilised by strong volar ligaments: two limbs of the scapho-trapezium-trapezoid ligament, the scaphocapitate ligament and the capitate-trapezium ligament. This anchors the distal pole between the trapezium-trapezoid complex and the capitate, shielding it from the forces experienced during an injury. This is reflected by the low frequency of distal pole fractures (12%), a finding that has been observed by previous

epidemiological work.[5] There were no fractures that involved the proximal ridge of the capitate fossa. The osseous microarchitecture in this area is likely the reason for this finding. The proximal pole is widest in this part of the scaphoid. Su-Bum and colleagues examined the trabecular structure and bone density of the scaphoid using micro-CT.[36] The authors found the proximal capitate fossa to have the highest bone mineral density and the largest number of trabeculae of the entire scaphoid.

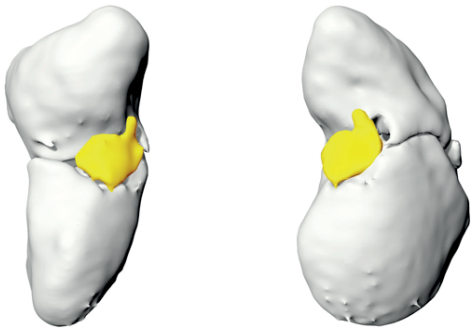

Figure 18. Volar comminution in a waist fracture

Example of volar comminution, marked in yellow. Comminution is located at the isthmus of the scaphoid, likely caused by flexion of the distal pole relative to the proximal pole.

Scaphoid fractures are known to have concurrent injuries of the carpus as well as the distal radius and ulna. Leslie and colleagues reported that 12.5% of the 247 patients with a scaphoid fracture had an associated injury.[42] We observed associated fractures in 45% (n=34) of cases. Our cohort is likely corresponding to patient presenting with higher energy injuries, resulting in a higher rate of concurrent fractures. The cohort may also be subjected to selection bias of patients that undergo CT.

The limitations of this study include sampling bias and the retrospective nature of this review. Most of the CT exams obtained for this cohort came from a level one trauma centre. Consequently, fracture types associated with high energy injuries are likely overrepresented. Transcription of fracture lines onto a representative scaphoid model is another limitation of this study. However, throughout this laborious aspect of the study, great care was taken to ensure accuracy of transcription. This was performed by two assessors, any differences were re-assessed and, hence, imprecisions avoided.

Our study is the first of its kind to investigate acute scaphoid fracture morphology using 3D CT. It is also the first study to examine scaphoid fracture comminution and to correlate this to displacement and fracture type. We have shown waist fractures to have high rates of comminution and displacement. Hence, waist fractures, should be carefully examined for dorsal ridge volar waist comminution. Finally, with modern CT scanners and imaging software, automated 3D reconstruction has become increasingly accessible. Inspection of the 3D anatomy of the fracture plane, concurrent comminution and direction of displacement can be a valuable tool in scaphoid fracture management.

REFERENCES

1. Destot E. The classic: injuries of the wrist: a radiological study. New York, NY: Paul B. Hoeber; 1926. *Clin Orthop Relat Res.* 2006;445:8-14.
2. Ten Berg PW, Drijkoningen T, Strackee SD, Buijze GA. Classifications of Acute Scaphoid Fractures: A Systematic Literature Review. *J Wrist Surg.* 2016;5(2):152-159.
3. Herbert TJ, Fisher WE. Management of the fractured scaphoid using a new bone screw. *The Journal of bone and joint surgery British volume.* 1984;66(1):114-123.
4. Cooney WP, Dobyns JH, Linscheid RL. Fractures of the scaphoid: a rational approach to management. *Clin Orthop Relat Res.* 1980(149):90-97.
5. Russe O. Fracture of the carpal navicular: diagnosis, non-operative treatment, and operative treatment. *JBJS.* 1960;42(5):759-768.
6. Ceri N, Korman E, Gunal I, Tetik S. The morphological and morphometric features of the scaphoid. *J Hand Surg Br.* 2004;29(4):393-398.
7. Craigen M, Stanley J. Wrist kinematics: row, column or both? *J Hand Surg Am.* 1995;20(2):165-170.
8. Garcia-Elias M, Ribe M, Rodriguez J, Cots M, Casas J. Influence of joint laxity on scaphoid kinematics. *J Hand Surg Am.* 1995;20(3):379-382.
9. Shenoy R, Pillai A, Hadidi M. Scaphoid fractures: variation in radiographic views - a survey of current practice in the West of Scotland region. *Eur J Emerg Med.* 2007;14(1):2-5.
10. Tiel-van Buul MM, van Beek EJ, Broekhuizen AH, Nooitgedacht EA, Davids PH, Bakker AJ. Diagnosing scaphoid fractures: radiographs cannot be used as a gold standard! *Injury.* 1992;23(2):77-79.
11. Hunter JC, Escobedo EM, Wilson AJ, Hanel DP, Zink-Brody GC, Mann FA. MR imaging of clinically suspected scaphoid fractures. *AJR Am J Roentgenol.* 1997;168(5):1287-1293.
12. Amirfeyz R, Bebbington A, Downing ND, Oni JA, Davis TR. Displaced scaphoid waist fractures: the use of a week 4 CT scan to predict the likelihood of union with nonoperative treatment. *J Hand Surg Eur Vol.* 2011;36(6):498-502.
13. Eastley N, Singh H, Dias JJ, Taub N. Union rates after proximal scaphoid fractures; meta-analyses and review of available evidence. *J Hand Surg Eur Vol.* 2013;38(8):888-897.
14. Grewal R, Suh N, Macdermid JC. Use of computed tomography to predict union and time to union in acute scaphoid fractures treated nonoperatively. *J Hand Surg Am.* 2013;38(5):872-877.
15. Luria S, Schwarcz Y, Wollstein R, Emelife P, Zinger G, Peleg E. 3-dimensional analysis of scaphoid fracture angle morphology. *J Hand Surg Am.* 2015;40(3):508-514.
16. Green DP, Wolfe SW. *Green's operative hand surgery.* 6th ed. Philadelphia: Saunders/Elsevier; 2011.
17. Slutsky DJ, Slade JF. *Scaphoid.* New York: Thieme; 2011.
18. Compson J. The anatomy of acute scaphoid fractures: a three-dimensional analysis of patterns. *The Journal of bone and joint surgery British volume.* 1998;80(2):218-224.
19. Clementson M, Jørgsholm P, Besjakov J, Björkman A, Thomsen N. Union of scaphoid waist fractures assessed by CT scan. *Journal of wrist surgery.* 2015;4(01):049-055.
20. Buijze GA, Jørgsholm P, Thomsen NO, Björkman A, Besjakov J, Ring D. Factors associated with arthroscopically determined scaphoid fracture displacement and instability. *The Journal of hand surgery.* 2012;37(7):1405-1410.
21. Grewal R, Lutz K, MacDermid JC, Suh N. Proximal pole scaphoid fractures: a computed tomographic assessment of outcomes. *The Journal of hand surgery.* 2016;41(1):54-58.

22. Hu Y-L, Ye F-G, Ji A-Y, Qiao G-X, Liu H-F. Three-dimensional computed tomography imaging increases the reliability of classification systems for tibial plateau fractures. *Injury.* 2009;40(12):1282-1285.

23. Pialat J, Burghardt A, Sode M, Link T, Majumdar S. Visual grading of motion induced image degradation in high resolution peripheral computed tomography: impact of image quality on measures of bone density and micro-architecture. *Bone.* 2012;50(1):111-118.

24. Cooney WP, Linscheid RL, Dobyns JH, Wood MB. Scaphoid nonunion: role of anterior interpositional bone grafts. *J Hand Surg Am.* 1988;13(5):635-650.

25. Temple CL, Ross DC, Bennett JD, Garvin GJ, King GJ, Faber KJ. Comparison of sagittal computed tomography and plain film radiography in a scaphoid fracture model. *J Hand Surg Am.* 2005;30(3):534-542.

26. Sanders WE. Evaluation of the humpback scaphoid by computed tomography in the longitudinal axial plane of the scaphoid. *J Hand Surg Am.* 1988;13(2):182-187.

27. Schwarcz Y, Schwarcz Y, Peleg E, Joskowicz L, Wollstein R, Luria S. Three-dimensional analysis of acute scaphoid fracture displacement: proximal extension deformity of the scaphoid. *JBJS.* 2017;99(2):141-149.

28. Moritomo H, Murase T, Oka K, Tanaka H, Yoshikawa H, Sugamoto K. Relationship between the fracture location and the kinematic pattern in scaphoid nonunion. *The Journal of hand surgery.* 2008;33(9):1459-1468.

29. Prosser A, Brenkel I, Irvine G. Articular fractures of the distal scaphoid. *J Hand Surg Am.* 1988;13(1):87-91.

30. Fogg Q. *Scaphoid varation and an anatomical basis for variable carpal mechanics*. Adelaide: Department of anatomical sciences, University of Adelaide; 2004.

31. Kijima Y, Viegas SF. Wrist anatomy and biomechanics. *J Hand Surg Am.* 2009;34(8):1555-1563.

32. Fogg QA. *Scaphoid variation and an anatomical basis for variable carpal mechanics* 2004.

33. Kijima Y, Viegas SF. Wrist anatomy and biomechanics. *The Journal of hand surgery.* 2009;34(8):1555-1563.

34. Garala K, Dias J. Scaphoid fracture geometrics: an assessment of location and orientation. *J Plast Surg Hand Surg.* 2019:1-8.

35. Trumble TE, Vo D. Proximal pole scaphoid fractures and nonunion. *Journal of the American Society for Surgery of the Hand.* 2001;1(3):155-171.

36. Su-Bum AL, Hyo-Jin BK, Jae-Myeung CC, et al. Osseous microarchitecture of the scaphoid: Cadaveric study of regional variations and clinical implications. *Clin Anat.* 2012;25(2):203-211.

37. Weber E, Chao E. An experimental approach to the mechanism of scaphoid waist fractures. *The Journal of hand surgery.* 1978;3(2):142-148.

38. Green JJ, Rayan G. Scaphoid fractures in soccer goalkeepers. *The Journal of the Oklahoma State Medical Association.* 1997;90(2):45-47.

39. Horii E, Nakamura R, Watanabe K, Tsunoda K. Scaphoid fracture as a" puncher's fracture". *J Orthop Trauma.* 1994;8(2):107-110.

40. Apergis E. *Fracture-dislocations of the Wrist.* Springer; 2013.

41. Oka K, Murase T, Moritomo H, Goto A, Sugamoto K, Yoshikawa H. Patterns of bone defect in scaphoid nonunion: a 3-dimensional and quantitative analysis. *The Journal of hand surgery.* 2005;30(2):359-365.

42. Leslie I, Dickson R. The fractured carpal scaphoid. Natural history and factors influencing outcome. *The Journal of bone and joint surgery British volume.* 1981;63(2):225-230.

CHAPTER 8

The Influence of Fracture Location and Comminution on Acute Scaphoid Fracture Displacement: Three-Dimensional CT Analysis

A.E.J. Bulstra
R.M.A. Al-Dirini
A. Turow
M.G.E. Oldhoff
K. Bryant
M.C. Obdeijn
J.N. Doornberg
R.L. Jaarsma
G.I. Bain

In Journal of Hand Surgery European volume; December 2021; 46(10):1072-1080

ABSTRACT

We aimed to assess the influence of fracture location and comminution on acute scaphoid fracture displacement using three-dimensional CT. CT-scans of 51 adults with an acute scaphoid fracture were included. Three-dimensional CT was used to assess fracture location, comminution and displacement. Fracture location was expressed as the height of the cortical breach on the volar and dorsal side of the scaphoid relative to total scaphoid length (%), corresponding to the fracture's entry and exit point, respectively. We found a near linear relation between dorsal fracture location and displacement. As dorsal fracture location became more distal, translation (ulnar, proximal, volar) and angulation (flexion, pronation) of the distal fragment relative to the proximal fragment increased. Comminuted fractures had more displacement. Dorsal fracture location predictably dictates the direction of translation and angulation in displaced scaphoid fractures. Surgeon attention to dorsal fracture location can help identify displacement patterns and provide guidance in adequately reducing a displaced scaphoid fracture.

Level of evidence

III

INTRODUCTION

Scaphoid fracture displacement is associated with a higher risk of nonunion[1] and may be an indication for operative fixation.[2,3] However, diagnosing scaphoid fracture displacement is challenging. Plain radiography and even computed tomography (CT) have limited interobserver reliability and accuracy for diagnosing displacement.[4,5] Identifying fracture characteristics associated with displacement, may aid surgeons in recognizing fractures at risk of displacement and select patients that will benefit from advanced imaging.

Studies using 3D-CT to analyse fracture and displacement patterns in acute scaphoid fractures are scarce. Among 14 subacute and 11 chronic scaphoid fractures Nakamura et al. (1991) identified a volar and dorsal displacement pattern in fractures proximal and distal to the scaphoid apex, respectively.[6] Schwarcz et al. reported displacement to be characterized by extension of the proximal pole along with the lunate, rather than by flexion of the distal fragment.[7]

These previous studies applied binary classifications of displaced *versus* nondisplaced fractures; or fractures located proximal *versus* distal to the apex. The aim of this study was to investigate the influence of (1) fracture location and (2) comminution on acute scaphoid fracture displacement, using continuous measures of fracture location and displacement through 3D-CT analysis.

METHODS

A search of the medical imaging archiving systems was performed to retrospectively identify patients diagnosed with an acute scaphoid fracture treated at three different institutions between 2008 and 2018. Adult (>17 years) patients with a scaphoid fracture who had a CT-scan within 6 weeks of injury were included. At these institutions CT-scans of the scaphoid are performed when patients present with a clinically suspected scaphoid fracture (typically nondisplaced fractures) or when there may be an indication for surgery (e.g. proximal pole or displaced fractures). Scans were obtained with the wrist in neutral position. The minimal CT-slice thickness was 1mm. Exclusion criteria were: (1) unicortical, segmental or tubercle fractures; (2) fractures associated with perilunate dislocation or scapholunate (SL) ligament injury; (3) concomitant displaced distal radius fracture; (4) a history of scaphoid pathology; 5) CT-scans on which the fracture line could not clearly be delineated on CT, as assessed by two independent observers (AB, AT).

This study was approved by the Southern Adelaide Clinical Human Research Ethics Committee (SAC HREC EC00188; reference number: 207.18).

Three-dimensional model reconstruction

Segmentation

CT-scans were imported into 3D slicer (Version 4.8.1; Boston, MA, USA) in Digital Imaging and Communication in Medicine (DICOM) format. The distal radius and scaphoid fragments were manually segmented to create surface rendered models. Segmentation was performed by one author (AB or MO) and reviewed by a second author (AB, AT). Stereolithography files (STL) of the segmented models were imported into Rhinoceros™ (Version 5.4.2; McNeel, Seattle, WA, USA). Left sided models were mirrored.

Reduction

Scaphoid fragments were virtually reduced in Rhinoceros™ by one author (AB) and assessed by a second observer (AT). The distal fragment was reduced towards the proximal fragment. To ensure correct reduction, anatomic alignment of the (1) capitate fossa, (2) dorsal and (3) volar curvature of the scaphoid waist and (4) dorsal ridge was assessed (Figure S1). Scaphoid fragments (pre- and post-reduction) and the distal radius were exported as STL files.

Fracture characteristics

To standardize fracture location among all models, reduced scaphoid models were aligned with a 3D template of an intact scaphoid using a closest iterative point algorithm (Artec Studio™, version 3.5, Autodesk Inc). Correct alignment was verified by examining six anatomical landmarks (AB, AT).[7] Fracture lines were then superimposed onto the common template in Rhinoceros™. On a standardized radial view of the template, we determined the location of the cortical breach on the volar and dorsal side of the scaphoid, corresponding to the fracture's entry and exit point, respectively (Figure 1). The corresponding (1) volar and (2) dorsal fracture location were quantified separately as percentages, by determining the height of the cortical breaches on the volar and dorsal sides of the scaphoid, relative to total scaphoid length. Comminution was defined as fractures with more than two fragments.

Three-dimensional analysis of displacement

Definition coordinate system

Displacement was defined as the change in position of the distal scaphoid fragment relative to the proximal fragment, pre- and post-virtual reduction. This was expressed as the translation along (mm) and angulation around (degrees) the axes of a common coordinate system of the distal radius (adapted from the International Society of Biomechanics recommendations for joint coordinate systems) [8]. Translation along x, y, or z-axis of the distal radius produced ulnar (-) to radial (+), distal (-) to proximal (+) and volar (-) to dorsal (+) translations, respectively. Rotation around the x, y, z-axis resulted in

flexion (+) or extension (-); pronation (+) or supination (-) and radial (+) or ulnar (-) deviation of the distal fragment, respectively (Figure S2).

Registration of displacement

The STL models of the distal radius and scaphoid fragments (pre- and post-reduction) were imported into Matlab® (version 2017b, The MathWorks, Natick, USA). A custom code implementing a rigid interactive closest point algorithm calculated the spatial transformations required for fragment reduction by comparing the position of the fragments pre- and post-reduction relative to the distal radius. [9] Translation reflected the change in position of the centroid of the distal fragment. Angulation described the rotations required for aligning the pre- and post-reduction local coordinate systems.

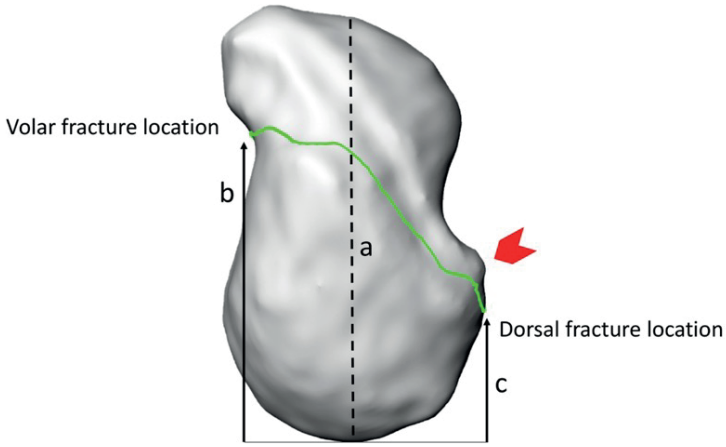

Figure 1. Standardized radial view of the 3D scaphoid template illustrating the volar and dorsal fracture location.

a) total scaphoid length; **b)** volar fracture location **c)** dorsal fracture location. Volar fracture location (%): (b/a)*100. Dorsal fracture location (%): (c/a)*100. The red arrow corresponds to the location of the scaphoid apex

Statistics

Bivariable linear regression analysis was performed to identify which variables among dorsal, volar fracture location and comminution were associated with translation and/or angulation. Variables with a p-value less than 0.10 in bivariable linear regression analysis were included for multivariable linear regression analysis. Bootstrapping was used to estimate the 95% confidence intervals (95% CI). [10]

RESULTS

Fracture characteristics

Fifty-one scaphoid fractures were included (Table 1). On the volar side of the scaphoid, fractures breached the cortex distal to the volar SL-ligament and proximal to scaphoid tubercle. The height of the cortical breach on the volar side of the scaphoid - i.e. the fracture's entry point or "volar fracture location" – was expressed as a percentage relative to the total scaphoid length and varied from 28 to 78% (mean 58%). (Figure 1) Dorsally, fractures exited diffusely along the concavity of the dorsal waist, with the most proximal fractures exiting proximal to the dorsal SL-ligament. The height of the cortical breach on the dorsal side of the scaphoid relative to the total scaphoid length expressed as a percentage – i.e. the fracture's exit point or "dorsal fracture location" - ranged from 21 to 64% (mean 43%) Figure 1).

Comminution was present in 28 (55%) of the fractures. Comminution was predominantly localized along the dorsal ridge of the scaphoid along the dorsal intercarpal (DIC) ligament attachments.

Table 1. Patient demographics and fracture characteristics

Variable	N (%)
Sex	
Male	45 (88)
Female	6 (12)
Age	35 (18-84)
Affected side	
Right	25 (49)
Left	26 (51)
Fracture location (%)	
Dorsal	43 (21-64)
Volar	58 (28 -78)
Fracture type	
Proximal	5 (9.8)
Transverse waist	25 (49)
Oblique waist	20 (39)
Distal	1 (2.0)
Comminution	
Yes	28 (55)
No	23 (45)

Continuous variables are represented as mean (range)
Discrete variables as number (percentage)

Fracture location and displacement

In bivariable analysis, dorsal fracture location correlated with all components of displacement (p<0.01), except radial deviation. On the contrary, volar fracture location did not correlate with displacement (Supplementary Material, Table S1, S2).

As dorsal fracture location became more distal, total translation of the distal fragment increased (Figure 2a, Figure 3). Along the ulnar-radial axis, translation progressed from radial in proximal fractures to increasingly ulnar in distal fractures (Figure 2b). Along the dorsal-volar axis, translation of the distal fragment changed from dorsal to increasingly volar in more distal fractures (Figure 2c). The degree of proximal translation also increased in distal fractures (Figure 2d). Correcting for comminution in multivariable regression analysis, a 1% increase in dorsal fracture location in the distal direction corresponded to 0.07mm increase in volar translation (95% CI 0.04-0.1, p<0.01); 0.04mm increase in proximal translation (95% CI 0.01-0.07, p<0.01) and 0.03mm increase in ulnar translation (95% CI 0.02-0.06, p<0.01) of the distal fragment relative to the proximal fragment. In total, translation of the distal fragment increased with 0.07mm (95% CI 0.04-0.1, p<0.01), per 1% increase in dorsal fracture location, corrected for comminution (Table 2).

Flexion of the distal fragment increased as dorsal fracture location became more distal (Figure 3, Figure 4a). Angulation furthermore progressed from supination in proximal fractures to increased pronation in distal fractures (Figure 4b). There was no significant correlation between dorsal fracture location and ulnar deviation in bivariable analysis (Supplementary Material, Table S1, S2). Correcting for comminution in multivariable analysis, there was 0.2 degree increase in flexion (95% CI 0.05-0.4, p<0.01) and 0.2 degree increase in pronation (95% CI 0.07- 0.4, p<0.01) of the distal fragment relative to the proximal fragment per 1% increase in dorsal fracture location (Table 3).

In displaced fractures with a dorsal fracture location distal to the apex, the distal fragment most commonly translated in the ulnar, volar and proximal direction, relative to the proximal fragment. The distal fragment predominantly flexed and pronated (Figure 5, Supplementary Material, Figure S3). Fractures with a dorsal fracture location proximal to the apex did not displace or displaced in the opposite direction, by dorsal or radial translation and/or supination of the distal fragment (Figure 5, Figure S4). Some fractures did not show translation (<0.5mm) or rotation (<1 degree). All but two of these fractures were located proximal to the apex (Figure 5, Supplementary Material Figure S5).

Presence of comminution and displacement

In bivariable analysis, comminuted fractures had more translation (ulnar, volar, proximal) and angulation (flexion, pronation and ulnar deviation) than simple scaphoid fractures (Supplementary Material, Tables S1, S2). Following multivariable analysis, comminution was associated with greater proximal and total translation, flexion and pronation of the distal fragment relative to the proximal fragment (p<0.03, Table 2 and 3). Correcting for fracture location, comminuted fractures had on average 0.8 mm (95% CI 0.4-1 p=0.02) more proximal translation and 1.5 mm (95% CI 0.7-2, p<0.01) more total translation than simple scaphoid fractures (Table 2). There was on average 8 degrees (95% CI 4-12,

p<0.01) more flexion and 4 degrees more pronation (95% CI 1-8, p=0.02), in comminuted fractures than in simple fractures (Table 3).

Overall, comminution and dorsal fracture location explained 40% of the variation (R^2) in total translation measured. For pronation and flexion, the presence of comminution and dorsal fracture location explained 31% of the observed variation in angulation (Table 3).

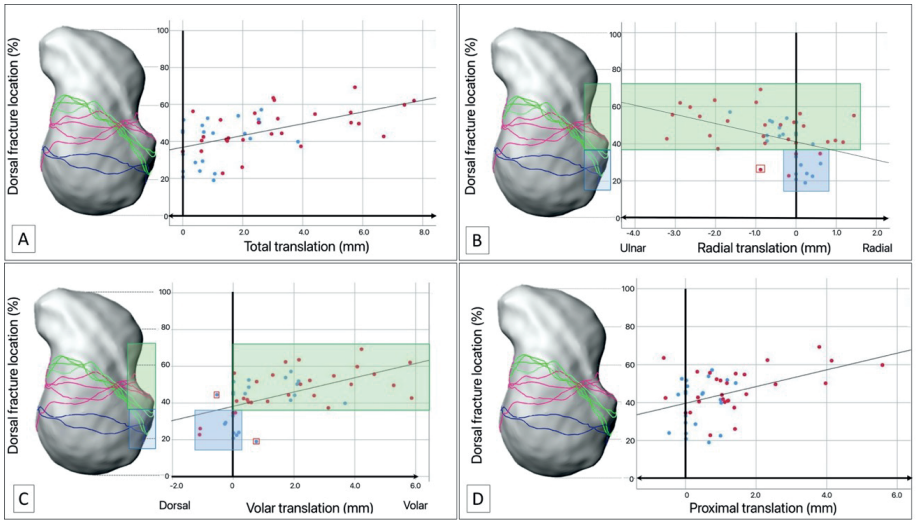

Figure 2. Correlation between dorsal fracture location (y-axis) and translation of the distal fragment relative to the proximal fragment (x-axis)

The radial view of the standardized scaphoid template demonstrates common fracture types and their dorsal fracture location corresponding to the y-axis.
Red dots, Comminuted fractures; *Blue dots,* Simple fractures; *Green box:* the majority of the fractures distal to the scaphoid apex translated in an ulnar **(B)** and volar **(C)** direction; *Blue box,* fractures proximal to the apex translated minimally or in a radial **(B)** and mostly in a dorsal direction **(C);** *Red box,* outliers.

Table 2. Multivariable linear regression analysis of fracture characteristics associated with translation

	Translation (mm)											
	Radial			Volar			Proximal			Total		
Variable	*B coefficient (95% CI)*	*p*	R^2	*B coefficient (95% CI)*	*p*	R^2	*B coefficient (95% CI)*	*p*	R^2	*B coefficient (95% CI)*	*p*	R^2
Dorsal fracture location	-0.03 (-0.06 to -0.02)[v]	<0.01*		0.07 (0.04 to 0.1)00	<0.01*		0.04 (0.01 to 0.07)	0.01*		0.07 (0.04 to 0.1)0	<0.01*	
Comminution	-0.4 (-0.9 to 0.1)[v]	0.17		0.70 (0.07 to 1.6)	0.10		0.8 (0.4 to 1.3)	0.02*		1.5 (0.7 to 2.3)	<0.01*	
			0.22			0.36			0.29			0.40

B coefficient: regression coefficient; 95%CI: bootstrapped 95% Confidence Interval; p: p-value;
[v] negative regression coefficient corresponds to ulnar translation; *significant at p<0.05; R^2: variance

Table 3. Multivariable linear regression analysis of fracture characteristics associated with angulation

	Angulation (degrees)								
	Flexion			Ulnar deviation			Pronation		
Variable	*B coefficient (95% CI)*	*p*	R^2	*B coefficient (95% CI)*	*p*	R^2	*B coefficient (95% CI)*	*p*	R^2
Dorsal fracture location	0.2 (0.05-0.4)	<0.01*		-	-	-	0.2 (0.07-0.4)	<0.01*	
Comminution	8 (3-12)	<0.01*		-	-	-	4 (1-8)	0.02	
			0.31	-	-	-			0.31

95%CI: bootstrapped 95% Confidence Interval; p: p-value; * significant at p<0.05; there were no fracture characteristics associated with ulnar deviation; R^2: variance

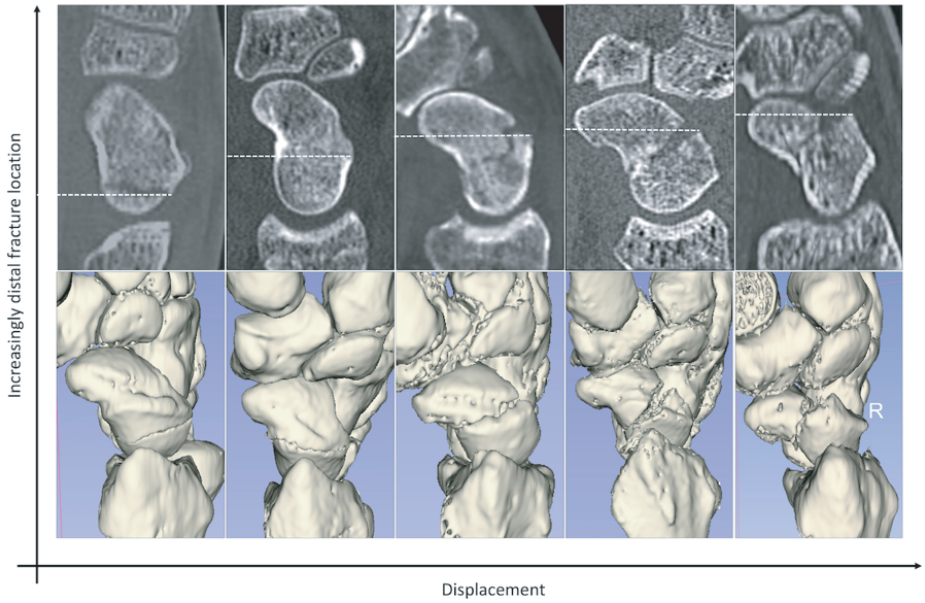

Figure 3. Correlation between dorsal fracture location and displacement

Illustration showing 2D CT and corresponding 3D reconstructions of increasingly distal fractures. The amount of displacement increases as dorsal fracture location becomes more distal.

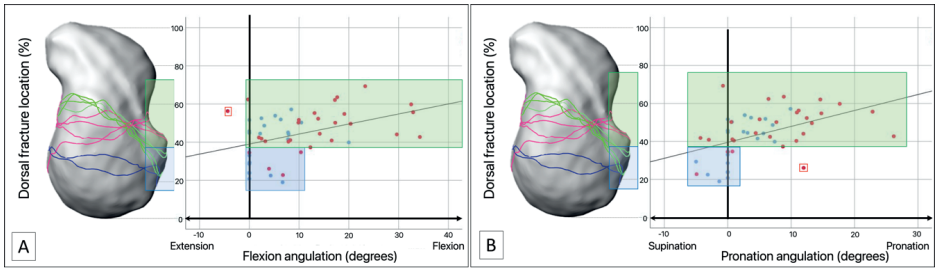

Figure 4. Correlation between dorsal fracture location (y-axis) and angulation of the distal fragment relative to the proximal fragment (x-axis)

Red dots, Comminuted fractures; *Blue dots,* Simple fractures; *Green box,* demonstrating greater flexion **(A)** and pronation **(B)** in fractures distal to the scaphoid apex; *Blue box,* demonstrating fractures proximal to apex showing little flexion (**A)** and more likely supination **(B)** ; *Red box,* outliers; including the only fracture showing extension of the distal fragment relative to the proximal fragment **(A).**

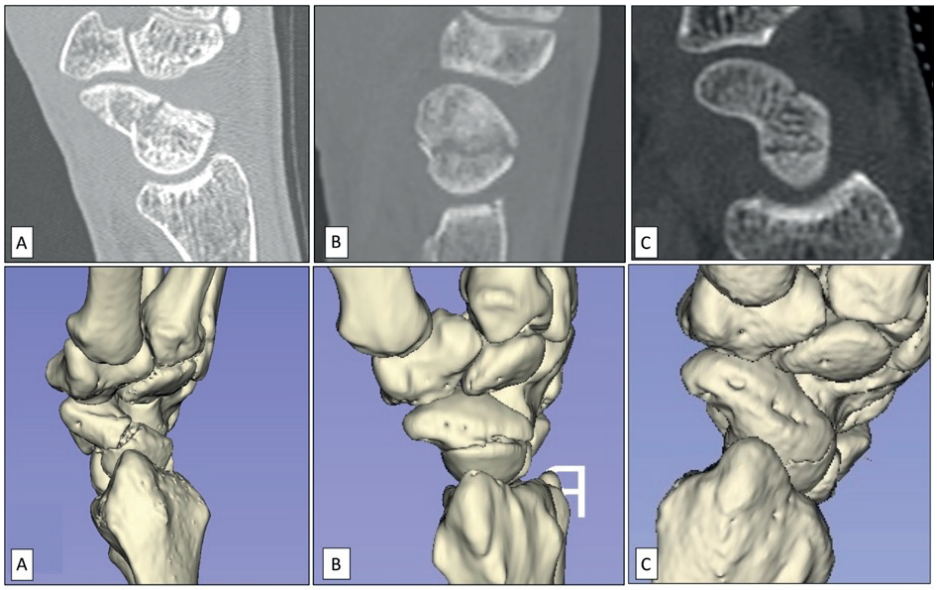

Figure 5. Typical displacement pattern of a scaphoid waist fracture in relation to scaphoid apex

Upper row, Sagittal 2D CT; *Lower row,* 3D reconstruction CT ;
A. Fractures distal to scaphoid apex showing flexion and pronation of distal fragment relative to the proximal fragment. There is also ulnar, volar and proximal translation.
B. Fractures proximal to the scaphoid apex showing dorsal translation and minimal supination and mild flexion of the distal fragment.
C. Majority of scaphoid fractures without translation or rotation were located proximal to the scaphoid apex and many were proximal to the scaphoid dorsal ridge.

DISCUSSION

This study investigated the influence of fracture location on the dorsal and volar side of the scaphoid and comminution on displacement of acute scaphoid fractures using 3D-CT analysis. We established a near linear relation between dorsal fracture location and interfragmentary translation and angulation. Comminuted fractures showed more translation and angulation than simple fractures.

Strengths of this study include the large consecutive series of fractures including a wide spectrum of fracture types. Furthermore, we evaluated fracture location and displacement as a continuous, rather than binary, spectrum. Limitations include manual segmentation and virtual reduction of fractures, which may be subject to human error. Secondly, to compare scaphoids of variable morphology, fracture characteristics were assessed on a template which may alter fracture location. Alignment was performed based on anatomical landmarks including the apex. As such, relative fracture location is unlikely to be affected. Thirdly, there might be spectrum bias of fractures that had CT performed. Lastly, mechanism of injury was not evaluated as a factor affecting displacement.

Angulation (flexion, pronation) and translation (ulnar, volar, proximal) of the distal fragment relative to the proximal fragment increased as dorsal fracture location became more distal. Using the distal fragment as a stable reference, this corresponds to the relative extension and supination of the proximal fragment reported by Schwarz et al. [7] We found a spectrum of displacement patterns correlating closely to fracture location. Fractures with a dorsal fracture location proximal to the apex did not displace or displaced predominantly in the opposite direction (dorsal, radial translation and supination of the distal fragment). Buijze et al. did not find a correlation between displacement and fracture location relative to the apex.[11] This may be due to their binary measure of displacement. The observation that volar fracture location did not correlate with displacement may be explained by the dorsal localization of most important stabilizing ligaments. [12]

Moritomo et al. described the importance of the dorsal SL-ligament (dSL) and proximal DIC attachments onto the scaphoid apex in volar and dorsal deformity patterns in scaphoid nonunions.[13] The apex has since often been used as a reference when evaluating displacement or deformity.[11,14] The binary analysis of displacement (volar versus dorsal) and fracture location (proximal versus distal to the apex) runs counter to the fact that (1) scaphoid fractures, especially waist fractures, include a continuous range of fracture locations[15]; (2) the DIC does not only attach onto the apex, but has multiple attachments along the scaphoid radiodorsal ridge.[12] The DIC is important in maintaining scaphoid and lunate alignment.[16] As demonstrated in this study, it may be more plausible to consider scaphoid fracture displacement as a continuous spectrum, correlating closely to fracture location and comminution.

In increasingly distal fractures, the dSL and most of the DIC will attach onto the proximal, rather than distal fragment. While the distal fragment is stabilized by tight ligaments of the immobile distal carpal row and flat scaphotrapeziotrapezoid joint, the proximal fragment will extend and supinate with the lunate.[7] This corresponds to relative flexion and pronation of the distal fragment. This pattern was seen in transverse waist fractures with a dorsal fracture location distal to the apex, likely crossing the dorsal ridge distal to the DIC attachments. In increasingly proximal fractures, more of the DIC will attach onto the stable distal fragment. This may balance the extension and flexion forces on the scaphoid resulting in less displacement. When extension forces from the ulnar column prevail, the intact DIC attachments may cause the distal fragment to displace minimally along with the lunate. This could account for the opposite displacement pattern observed in proximal and oblique waist fractures characterized by limited supination and dorsal translation of the distal fragment.

The finding that comminuted fractures showed more displacement confirms previous studies.[11] We found comminution to be frequently located along the scaphoid dorsal ridge, corresponding to the site of the DIC attachment. Comminution may therefore disrupt the stability offered by the DIC.

Our findings demonstrate that dorsal fracture location predictably dictates the direction of translation and angulation. These aspects of displacement should be considered, defined and addressed when reducing a displaced scaphoid fracture. The

current study also provides insights into possible mechanisms of fracture instability in nondisplaced fractures. Future research, preferably dynamic CT assessment[17,18] should investigate whether dorsal fracture location also correlates with fracture instability. If evidence confirms a relation between dorsal fracture location and stability, dorsal fracture location could form a relative indication for surgery.

While 3D-CT analysis allows for accurate visualization of dorsal fracture location, comminution and direction displacement, 3D-CT may not be widely accessible as a routine modality. Whether dorsal fracture location can be reliably assessed on (oblique) radiographs or two-dimensional CT merits further investigation. If so, a distal dorsal fracture location on radiographs or two-dimensional CT may form an indication for advanced imaging.

To conclude, dorsal fracture location and comminution correlate closely to acute scaphoid fracture displacement. This can be attributed to the dorsal localization of the DIC and dSL ligaments as important stabilizers. As dorsal fracture location predictably dictates the direction of translation and angulation, surgeon attention to dorsal fracture location can help identify patterns of displacement and provide guidance in adequately reducing a displaced scaphoid fracture.

REFERENCES

1. Grewal R, Suh N, Macdermid JC. Use of computed tomography to predict union and time to union in acute scaphoid fractures treated nonoperatively. *J Hand Surg Am.* 2013;38(5):872-877.
2. Singh HP, Taub N, Dias JJ. Management of displaced fractures of the waist of the scaphoid: meta-analyses of comparative studies. *Injury.* 2012;43(6):933-939.
3. Suh N, Grewal R. Controversies and best practices for acute scaphoid fracture management. *J Hand Surg Eur Vol.* 2018;43(1):4-12.
4. Buijze GA, Jorgsholm P, Thomsen NO, Bjorkman A, Besjakov J, Ring D. Diagnostic performance of radiographs and computed tomography for displacement and instability of acute scaphoid waist fractures. *J Bone Joint Surg Am.* 2012;94(21):1967-1974.
5. Lozano-Calderon S, Blazar P, Zurakowski D, Lee SG, Ring D. Diagnosis of scaphoid fracture displacement with radiography and computed tomography. *J Bone Joint Surg Am.* 2006;88(12):2695-2703.
6. Nakamura R, Imaeda T, Horii E, Miura T, Hayakawa N. Analysis of scaphoid fracture displacement by three-dimensional computed tomography. *J Hand Surg Am.* 1991;16(3):485-492.
7. Schwarcz Y, Schwarcz Y, Peleg E, Joskowicz L, Wollstein R, Luria S. Three-Dimensional Analysis of Acute Scaphoid Fracture Displacement: Proximal Extension Deformity of the Scaphoid. *J Bone Joint Surg Am.* 2017;99(2):141-149.
8. Wu G, van der Helm FC, Veeger HE, et al. ISB recommendation on definitions of joint coordinate systems of various joints for the reporting of human joint motion--Part II: shoulder, elbow, wrist and hand. *J Biomech.* 2005;38(5):981-992.
9. Manu. Rigid ICP registration. https://www.mathworks.com/matlabcentral/fileexchange/40888-rigid-icp-registration. Published 2020. Accessed October 23, 2020.
10. Haukoos JS, Lewis RJ. Advanced statistics: bootstrapping confidence intervals for statistics with "difficult" distributions. *Acad Emerg Med.* 2005;12(4):360-365.
11. Buijze GA, Jorgsholm P, Thomsen NO, Bjorkman A, Besjakov J, Ring D. Factors associated with arthroscopically determined scaphoid fracture displacement and instability. *J Hand Surg Am.* 2012;37(7):1405-1410.
12. Kijima Y, Viegas SF. Wrist anatomy and biomechanics. *J Hand Surg Am.* 2009;34(8):1555-1563.
13. Moritomo H, Viegas SF, Elder KW, et al. Scaphoid nonunions: a 3-dimensional analysis of patterns of deformity. *J Hand Surg Am.* 2000;25(3):520-528.
14. de Roo MGA, Dobbe JGG, van der Horst C, Streekstra GJ, Strackee SD. Carpal kinematic changes after scaphoid nonunion: an in vivo study with four-dimensional CT imaging. *J Hand Surg Eur Vol.* 2019;44(10):1056-1064.
15. Luria S, Schwarcz Y, Wollstein R, Emelife P, Zinger G, Peleg E. 3-dimensional analysis of scaphoid fracture angle morphology. *J Hand Surg Am.* 2015;40(3):508-514.
16. Mitsuyasu H, Patterson RM, Shah MA, Buford WL, Iwamoto Y, Viegas SF. The role of the dorsal intercarpal ligament in dynamic and static scapholunate instability. *J Hand Surg Am.* 2004;29(2):279-288.
17. Carr R, MacLean S, Slavotinek J, Bain GI. Four-Dimensional Computed Tomography Scanning for Dynamic Wrist Disorders: Prospective Analysis and Recommendations for Clinical Utility. *J Wrist Surg.* 2019;8(2):161-167.
18. de Roo MGA, Dobbe JGG, Ridderikhof ML, et al. Analysis of instability patterns in acute scaphoid fractures by 4-dimensional computed tomographic imaging - A prospective cohort pilot study protocol. *Int J Surg Protoc.* 2018;9:1-5.

Table S1. Bivariable linear regression analysis of fracture characteristics associated with translation

	Translation (mm)							
	Radial		Volar		Proximal		Total	
	B coefficient (95% CI)	*p*	*B coefficient (95% CI)*	*p*	*B coefficient (95% CI)*	*p*	*B coefficient (95% CI)*	*p*
Dorsal fracture location	-0.04[v] (-0.06 to -0.02)	<0.01*	0.08 (0.06 to 0.1)	<0.01*	0.05 (0.01 to 0.08)	0.01*	0.09 (0.05 to 0.1)	<0.01*
Volar fracture location	0.00 (-0.02 to 0.03)	0.84	-0.02[λ] (-0.06 to 0.03)	0.43	-0.01[λ] (-0.04 to 0.02)	0.67	-0.01 (-0.06 to 0.04)	0.76
Comminution	-0.6[v] (-1 to -0.05)	0.04*	1 (0.4 to 2)	<0.01*	1 (0.4 to 2)	<0.01*	2 (1 to 3)	<0.01*

B coefficient: regression coefficient; 95% CI: bootstrapped 95% Confidence Interval; [v] negative regression coefficient corresponds to ulnar translation; [λ] negative regression coefficient corresponds to dorsal translation; * variables with p<0.1 were included in the multivariable regression analysis.

Table S2. Bivariable linear regression analysis of fracture characteristics associated with angulation

	Angulation (degrees)					
	Flexion		Ulnar deviation		Pronation	
	B coefficient (95% CI)	*p*	*B coefficient (95% CI)*	*p*	*B coefficient (95% CI)*	*p*
Dorsal fracture location	0.3 (0.1 to 0.5)	<0.01*	0.4 (-0.06 to 0.2)	0.41	0.3 (0.1 to 0.4)	<0.01*
Volar fracture location	0.1 (-0.1 to 0.4)	0.33	-0.05 (-0.1 to 0.05)[v]	0.29	0.01 (-0.2 to 0.2)	0.91
Comminution	9 (5 to 14)	<0.01*	0.8 (-1 to 3)	0.47	6 (2 to 9)	<0.01*

95% CI: bootstrapped 95% Confidence Interval; p: p-value; [v]negative regression coefficient corresponds to radial deviation; * variables with p<0.1 were included in multivariable regression analysis.

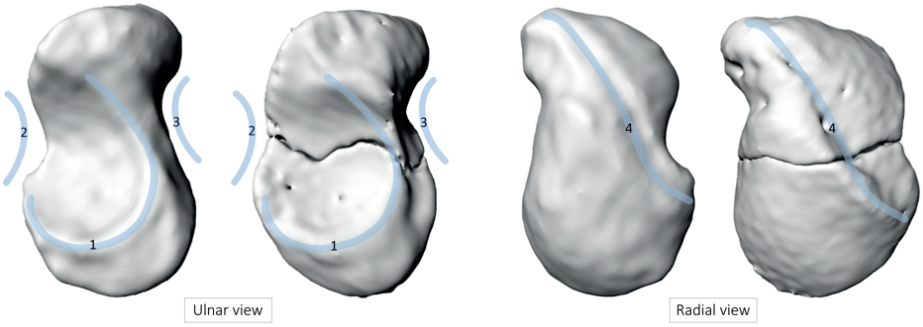

Figure S1. Anatomic landmarks for reduction

Ulnar and radial view of scaphoid template and fractured scaphoid after reduction showing anatomic landmarks. 1) Capitate fossa; 2) Dorsal curvature; 3) Volar curvature; 4) Dorsal ridge.

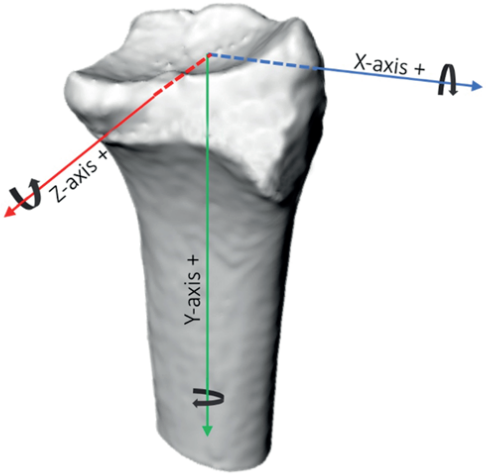

Figure S2. Common coordinate system distal radius and directions of displacement

Displacement was measured as translation along and rotation around the three radial axes. Blue x-axis: ulnar (-) to radial (+) axis. The ulnar-radial axis was defined on axial views as the line intersecting the most radial prominence of the distal radius and the midpoint of the line between the volar and dorsal lips of the sigmoid notch. Rotation around the x-axis produces flexion (+) or extension (-); Green y-axis: distal (-) to proximal (+) axis. The longitudinal y-axis runs parallel to the radial shaft. It was designed to intersect the centre of the radial circumference determined at 1/4th and 3/4th of the length of the distal radius model.* Rotation around the axis produces pronation (+) or supination (-); Red axis z-axis: dorsal (-) to volar (+) axis. The z-axis was designed to run orthogonally to the defined y- and x-axes. Rotation around this axis yields radial (-) or ulnar (+) deviation. *In 10 distal radius models the longitudinal y-axis could not be accurately established as the length of the radial shaft was shorter than the width of the distal articular surface. For these models, the longitudinal orientation of the radial shaft was corrected by adjusting the orientation of the model to correspond to the radial inclination and volar tilt of the distal radius measured on plain radiographs.

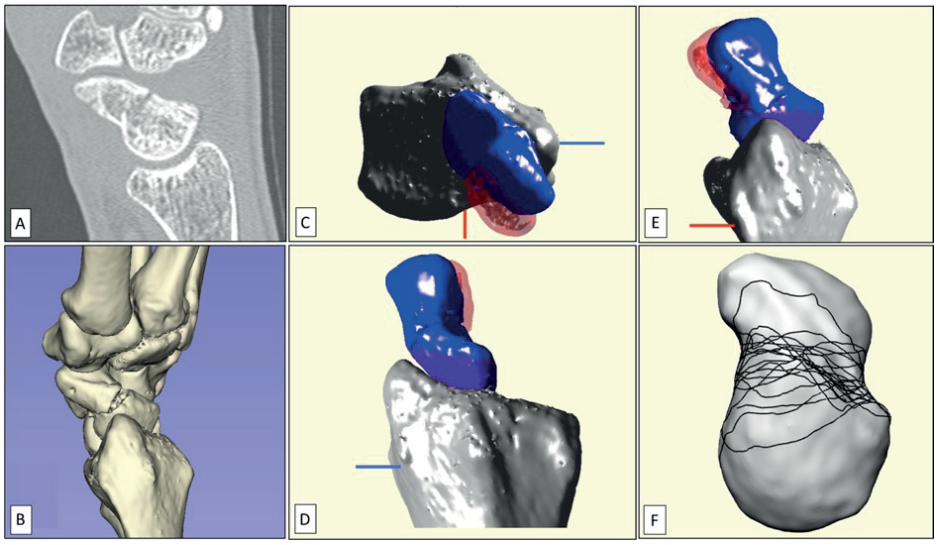

Figure S3. Typical displacement pattern of a scaphoid waist fracture distal to the apex.

A. Sagittal 2D CT and **B.** 3D reconstruction of displaced scaphoid fracture; **C.** Axial; **D.** Radial; **E.** Dorsal view of the scaphoid fracture pre- and post-reduction relative to the distal radius.
Red scaphoid: fragments pre-reduction. **Blue scaphoid:** fragments post-reduction.
The distal fragment has flexed and pronated relative to the proximal fragment. There is also ulnar, volar and proximal translation. This displacement pattern was typically seen in fractures distal to the scaphoid apex.
F. Radial view of all fractures with an equivalent displacement pattern (volar, proximal, ulnar translation, flexion and pronation) depicted on a standardized template of the scaphoid. All but one of these fractures were located distal the scaphoid apex and crossed the dorsal ridge. One fracture passed through the scaphoid apex.

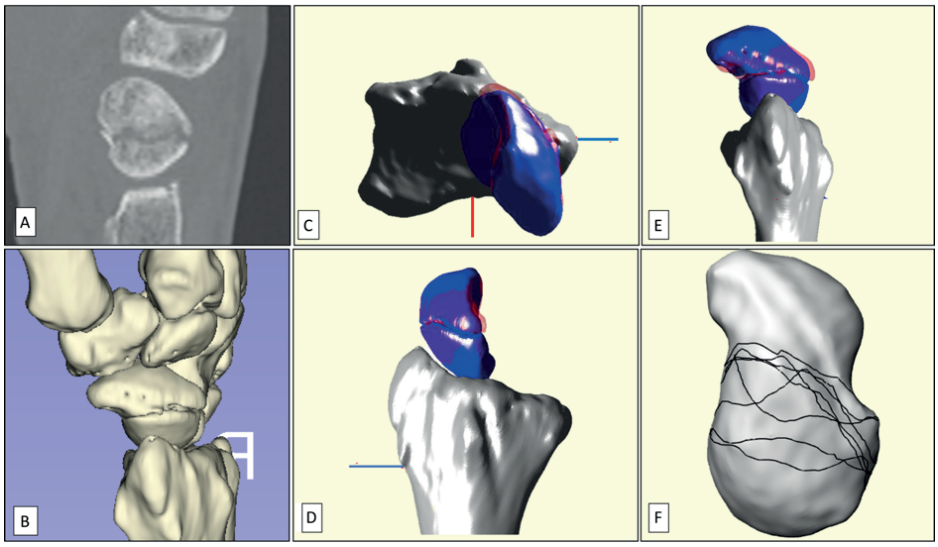

Figure S4. Typical displacement pattern of fractures proximal to the scaphoid apex.

A. Sagittal 2D CT and **B.** 3D reconstruction of displaced scaphoid fracture; **C.** Axial; **D.** Radial; **E.** Dorsal view of the scaphoid fracture pre- and post-reduction relative to the distal radius.
Red scaphoid: fragments pre-reduction. **Blue scaphoid:** fragments post-reduction.
The distal fragment has translated dorsally and supinated minimally.
F. Radial view of all fractures in which the distal fragment extended (>1 degree), supinated (> 1 degree), or translated dorsally (>0.5mm). The majority of these fractures were located proximal to the scaphoid apex. Many were proximal to the scaphoid dorsal ridge.

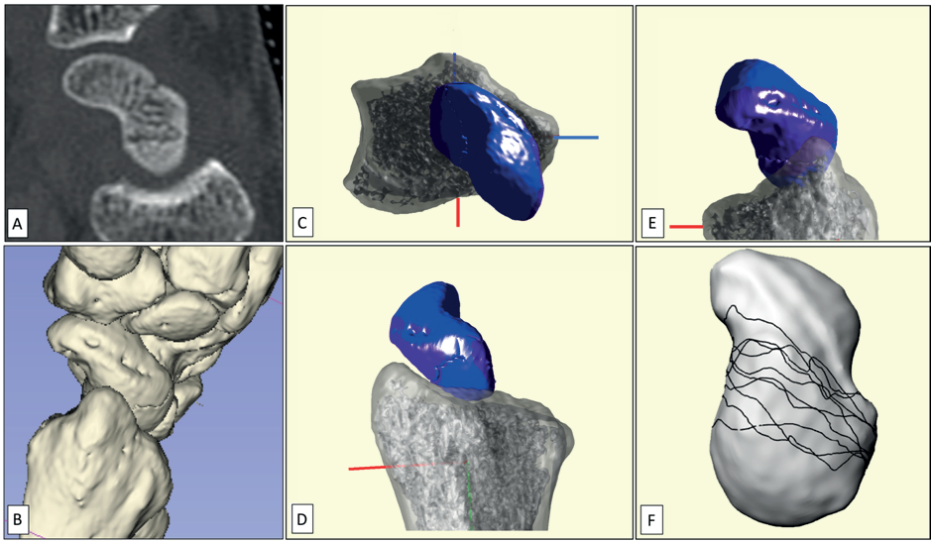

Figure S5. Scaphoid fracture without translation or rotation

A. Sagittal 2D CT and **B.** 3D reconstruction of displaced scaphoid fracture; **C.** Axial; **D.** Radial; **E**. Dorsal view of the scaphoid fracture pre- and post-reduction relative to the distal radius.
Red scaphoid: fragments pre-reduction. **Blue scaphoid:** fragments post-reduction.
F. Radial view of all fractures that had no or minimal translation (<0.5mm) and angulation (<1 degrees), depicted on a standardized template of the scaphoid. The majority of these fractures were located proximal to the scaphoid apex. Many were proximal to the scaphoid dorsal ridge.

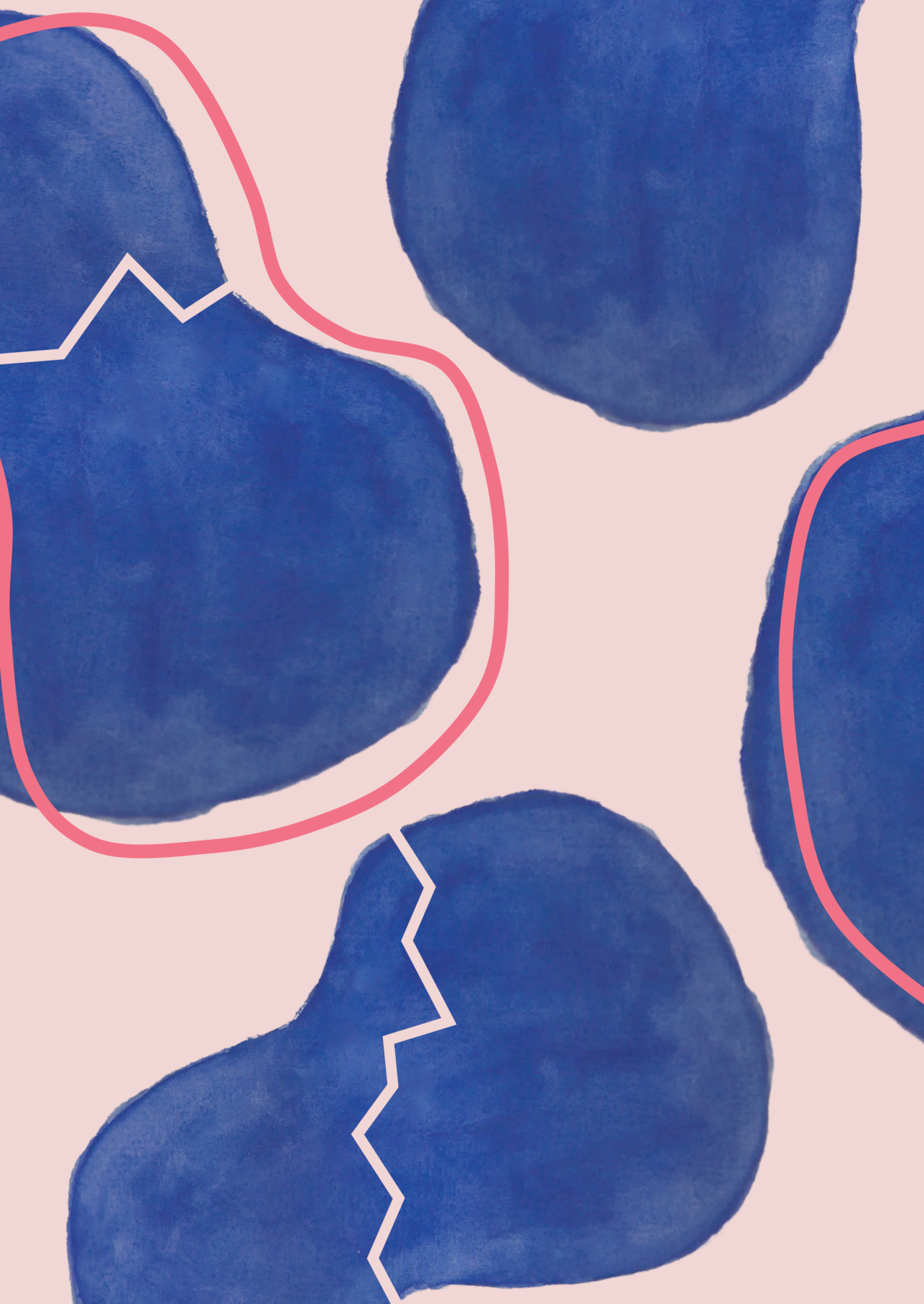

PART IV

IMMOBILIZATION DURATION OF A NONDISPLACED SCAPHOID WAIST FRACTURE

CHAPTER 9

Factors Associated with Surgeon Recommendation for Additional Cast Immobilization of a CT-Verified Nondisplaced Scaphoid Waist Fracture

A.E.J. Bulstra
T.J. Crijns
S.J. Janssen
G.A. Buijze
D. Ring
R.L. Jaarsma
G.M.M.J. Kerkhoffs
M.C. Obdeijn
J.N. Doornberg

The Science Of Variation Group*

In Archives of Orthopaedic and Trauma Surgery. November 2021 Nov;141(11): 2011-2018

*__Group authorship:__ The Science of Variation Group: A. Peters, A.B. Spoor, Abhay Shrivastava, Aakash Chauhan, Adam Shafritz, Asif M. Ilyas, Anne J.H. Vochteloo, Andrew John Powell, Alberto Pérez Castillo, Alexandre Leme Godoy-Santos, Amparo Gomez Gelvez, Andrea Bauer, Antonio Barquet, Anze Kristan, Ante Prkic, Axel Jubel, Boj Mirck, B.E. Kreis, H. Brent Bamberger, William Dias Belangero, Bernard F. Hearon, Bradley Palmer, Brad Hyatt, Brian P.D. Wills, Henry Broekhuyse, Richard Buckley, Burak Altintas, Sean T. Campbell, Carl Ekholm, Carlos Henrique Fernandes, C.H. Fernandes, Carl Weiss, Christos Garnavos, Charles Metzger, Christopher J. Wilson, Chris Bainbridge, Christian Deml, Jesus Moreta, Conor Kleweno, Constanza L. Moreno-Serrano, Craig B. Ordway, Cyrus Klostermann, David Zeltser, David G. Dennison, Diederik O. Verbeek, Dan Polatsch, Camilo Jose Romero Barreto, Koroush Kabir, Mohamed Shafi, Juan M Patiño, Roger van Riet, Samir Sodha, Scott Duncan, Daniel C. Wascher, Edward F Ibrahim, Efstathios G. Ballas, Edward Harvey, Edward K Rodriguez, Emilia Stojkovska Pemovska, E. Walbeehm, Peter J. Evans, Ezequiel E. Zaidenberg, Fred O'Brien, Franz Josef Seibert, Frank W. Bloemers, Gladys Cecilia Zambrano Caro, Gregory DeSilva, George Babis, George Pianka, Michael Githens, Giselly Miranda Veríssimo, Grant E. Garrigues, Guido Fierro, Holger Durchholz, Jeremy Hall, Hal McCutchan, Michael Nancollas, Colby Young, Greg P. Watchmaker, Gary M. Pess, Lewis B. Lane, Harold Alonso Villamizar, Ippokratis Pountos, Hervey L. Kimball, Eric P. Hofmeister, Iain McGraw, Konul Erol, J.F. Di Giovanni, Jacob W Brubacher, Jan Biert, Jason C. Fanuele, Jason D Tavakolian, Jack Choueka, Jose Eduardo Grandi Ribeiro, Jose Eduardo Grandi Ribeiro Filho, Joseph M. Conflitti, J.M.R Roiz, John Munyak, James F. Nappi, Job N. Doornberg, John M. Erickson, Jorge G. Boretto, Joel M. Post, Jorge Rubio, John A. Scolaro, John Taras, Julio Domenech, Julio Sandoval, Jeffrey Wint, Katherine Celeste Faust, Ken Butters, Kyle Jeray, Karl-Josef Prommersberger, Kagan Ozer, GA Kraan, Kyle J Chepla, L.M.S.J. Poelhekke, Ladislav Mica, Lawrence Weiss, Lars Adolfsson, Lars C. Borris, Louis Christopher Grandizio, Leon Elmans, Naquira Escobar Luis Felipe, L.W. van der Plaat, M. Verhofstad, Marcos Sanmartin-Fernandez, Mario Di Micoli, Matej Kastelec, Maurizio Calcagni, Max Talbot, Maarten W.G.A. Bronkhorst, John A. McAuliffe, Michael Behrman, M. Quell, Michael Nakashian, Minoo Patel, Matthew Bengard, M. Jason Palmer, Michael Prayson, Matthias Knobe, Marinis Pirpiris, Minos Tyllianakis, Michael W. Grafe, Neal Chen, Nelson Elias, Ngozi M. Akabudike, Nathan A Hoekzema, Nicholas L. Shortt, Nikolaos Kanakaris, Nikolas H. Kazmers, Nina Lightdale-Miric, Jim Calandruccio, Ole Brink, Martin Richardson, Jose A. Ortiz Jr, Pascal F.W. Hannemann, P.V. van Eerten, Prashanth Inna, Peter Althausen, Panagiotis Lygdas, Nata Parnes, Paul A. Martineau, Prosper Benhaim, Philip Forno, Pradeep Choudhari, Peter Hahn, Peter Fedele Townsend, Peter Giannoudis, Paul Guidera, Philipp Muhl, Philipp Streubel, Peter Jebson, Patrick W. Owens, Tamir Pritsch. Paul J. Scibetta Jr., Rob Nelissen, Robert Haverlag, R.H. van Leerdam, Ramon de Bedout, Sergio Rowinski, Reid W. Draeger,R. Fricker, Richard Wallensten, Richard S. Gilbert, Marco Rizzo, Richard Jenkinson, Robert E. Van Demark Jr, Craig Rodner, Rachel S. Rohde M.D., Richard S. Page, David Ruch, Vani J. Sabesan, Stephen A Kennedy. Niels W.L. Schep, Scott Mitchell, Sebastian Farr, Paul A. Sibley D.O., Scott G Kaar, S.A. Meylaerts, Steven L. Henry, Steven Meletiou, Steven J Morgan, Marc Swiontkowski, T. Schepers, Thomas DeCoster, Taizoon Baxamusa, F. Thomas D. Kaplan, Thierry Begue, Thomas Mittlmeier, Thomas Rebele, T Apard, Tim Chesser, Tomo Havlifçek, T. Rozental, Theodoros Tosounidis, H. Utkan Aydin, Vincenzo Giordano, Varun Kashyap Gajendran, Vasileios S. Nikolaou, Vincent Ruggiero, Warren C. Hammert, Yoram Weil, Wojciech Satora, Zsolt Balogh.

ABSTRACT

Introduction

Data from clinical trials suggest that CT-confirmed nondisplaced scaphoid waist fractures heal with less than the conventional 8-12 weeks of immobilization. Barriers to adopting shorter immobilization times in clinical practice may include a strong influence of fracture tenderness and radiographic appearance on decision-making. This study aimed to investigate 1) the degree to which surgeons use fracture tenderness and radiographic appearance of union, among other factors, to decide whether or not to recommend additional cast immobilization after 8 or 12 weeks of immobilization; 2) identify surgeon factors associated with the decision to continue cast immobilization after 8 or 12 weeks.

Materials and methods

In a survey-based study, 218 surgeons reviewed 16 patient scenarios of CT-confirmed nondisplaced waist fractures treated with cast immobilization for 8 or 12 weeks and recommended for or against additional cast immobilization. Clinical variables included patient sex, age, a description of radiographic fracture consolidation, fracture tenderness and duration of cast immobilization completed (8 versus 12 weeks). To assess the impact of clinical factors on recommendation to continue immobilization we calculated posterior probabilities and determined variable importance using a random forest algorithm. Multilevel logistic mixed regression analysis was used to identify surgeon characteristics associated with recommendation for additional cast immobilization.

Results

Unclear fracture healing on radiographs, fracture tenderness and 8 (versus 12) weeks of completed cast immobilization were the most important factors influencing surgeons' decision to recommend continued cast immobilization. Women surgeons (OR 2.96; 95%CI 1.28-6.81, p=0.011), surgeons not specialized in orthopaedic trauma, hand and wrist or shoulder and elbow surgery (categorized as 'other') (OR 2.64; 95%CI 1.31-5.33, p=0.007) and surgeons practicing in the United States (OR 6.53, 95%CI 2.18-19.52, p=0.01 versus Europe) were more likely to recommend continued immobilization.

Conclusion

Adoption of shorter immobilization times for CT-confirmed nondisplaced scaphoid waist fractures may be hindered by surgeon attention to fracture tenderness and radiographic appearance.

INTRODUCTION

Evidence from clinical trials suggests that a scaphoid waist fracture that is nondisplaced on computed tomography (CT) will heal with adequate immobilization. [1-5] Screw fixation helps people with a nondisplaced waist fracture avoid cast wear, but it does not improve long-term outcomes. [6-8] A shorter period of immobilization may reduce the perceived benefits of operative treatment. [6] In the absence of a second injury, the probability of nonunion for a CT-or MRI-confirmed nondisplaced scaphoid waist fracture is below 1%.[1-5,9] Among five clinical prospective and one retrospective series that used CT or MRI to diagnose displacement, only two in 362 (0.6%) of the nondisplaced waist fractures treated with cast immobilization did not heal. [1-5,9] It is not clear whether the diagnosis of nonunion in these two fractures was based on imaging 4 to 12 weeks after injury, or also confirmed radiologically 6 months or more after injury. [3,4] Radiological diagnosis of union is unreliable on radiographs and is of questionable reliability on CT within 3 to 4 months after injury. [10-12] It is also possible that at least one of these fractures was displaced as it demonstrated moderate translation on the 4 week CT scan and there was no CT scan at the time of injury. [4]

The improved understanding of the link between displacement and nonunion has led some to consider shorter (less than the conventional 8-12 weeks) and less rigid (e.g. thumb free) types of immobilization for CT-confirmed nondisplaced scaphoid waist fractures. [1,3-5,13] Some have tested immobilization of CT- or MRI-confirmed nondisplaced fractures with as few as 4 to 6 weeks of immobilization with good results in preliminary trials.[4]

In our experience, the concepts leading some to consider a shorter immobilization duration for nondisplaced scaphoid waist fractures conflict with the fact that 1) radiographic appearance of union, and 2) tenderness at the fracture site upon physical examination (fracture tenderness) are often used to decide whether to continue cast immobilization. These traditional concepts run counter to lines of evidence that 1) diagnosis of scaphoid fracture union on radiographs is unreliable [11,12] and 2) patient reported pain intensity, including fracture tenderness[14], is strongly related to patient psychosocial factors including cognitive biases about pain and coping strategies in patients with upper extremity injury. [15-17]

Based on studies reporting near 100% of the CT-confirmed nondisplaced waist fractures heal and that radiographs and examination are unreliable and inaccurate for diagnosis of union, one can argue that using fracture tenderness and radiographic appearance to recommend additional cast wear after 8 weeks of immobilization may lead to unhelpful and potentially harmful overtreatment in a substantial proportion of patients. To reduce immobilization time, surgeon decision making would need to evolve to match the existing evidence. One can therefore argue that surgeons may need to accept the uncertainty about radiographic appearance and fracture tenderness.

This study aimed to identify 1) what proportion of surgeons recommends additional cast immobilization of a CT-verified nondisplaced scaphoid waist fracture after

8 and 12 weeks of cast wear; 2) what clinical variables (patient sex, age, healing on radiographs, fracture tenderness, duration of cast wear completed) are associated with surgeon recommendation to continue immobilization of a nondisplaced scaphoid waist fracture after 8 and 12 weeks and 3) what surgeon variables (sex, location of practice, subspeciality, years in practice) are associated with surgeon recommendation to continue immobilization of a nondisplaced scaphoid waist fracture after 8 and 12 weeks.

METHODS

Patient scenarios

Sixteen scenarios of patients with a nondisplaced scaphoid waist fracture were presented to orthopaedic surgeons, (European) trauma surgeons that treat scaphoid fractures, and (plastic) hand- and wrist surgeons. Scenarios contained brief descriptions of patients with a CT-confirmed nondisplaced scaphoid waist fracture, treated nonoperatively with 8 or 12 weeks of cast immobilization. Surgeons were asked whether they would recommend to continue cast immobilization. For each case scenario, the following five clinical (patient) variables varied: 1) sex, 2) description of fracture healing on radiographs (clear *versus* unclear healing), 3) presence of fracture tenderness (minimal to none *versus* notable), 4) duration of completed cast immobilization (8 *versus* 12 weeks) and patient age, randomly generated between 18-32 years and 43-57 years. SurveyMonkey (Palo Alto, CA, USA) was used to create an online survey. The vignettes were presented in random order.

Participants (surgeons)

We invited members of the 'Science of Variation Group' (SOVG) to participate in this web-based study. The SOVG is an international web-based collaboration of orthopaedic, trauma and hand and wrist surgeons, set out to investigate the variation in interpretation, classification, and treatment of illness among surgeons through web-based experiments. [18] The SOVG provides no other incentive for participation than group authorship or acknowledgement, depending on the publishing Journal.

A total of 225 surgeons participated. Seven respondents that were residents (physicians in training) were excluded, leaving 218 participants for analysis. Participating surgeon demographics are summarized in Table 1.

Statistical methods

Descriptive analysis was performed, reporting the number of recommendations for continued cast immobilization per patient scenario. We pooled surgeon practice location as 'Other' for surgeons practicing outside the United States or Europe.

To assess the impact of clinical (patient) factors on surgeon recommendation to continue cast immobilization we used two approaches: (1) posterior probabilities were calculated [19] and (2) variable importance was determined using a random forest algorithm.[20]

Posterior probabilities were calculated using Bayes' theorem. First, the case scenario data were pooled to calculate the unadjusted probabilities for recommending continued cast immobilization for each included patient variable: age, sex, radiographic fracture healing, fracture tenderness and duration of cast immobilization completed. The unadjusted probability was calculated as the percentage of cases in which surgeons recommended continued immobilization in the presence of each variable. Posterior probability describes the conditional probability of an event occurring, in the presence of a combination of variables, by incorporating the associated probabilities of each of the variables.[19] The resulting posterior probability represents the probability of continuing cast immobilization given the combination of factors and is represented as a percentage. A posterior probability of 100% indicates that participants uniformly agree to continue cast immobilization, a posterior probability of 0% indicates that participants uniformly agree to discontinue immobilization.[19] (See Supplementary Material for additional information.)

A random forest algorithm was applied to rank the "importance" of each patient variable. [20] Random forest is a supervised machine learning algorithm that is mostly used for prediction. It is a decision tree-based model that involves repetitive partitioning of a given dataset into two groups until optimized. The variable importance indicates the improvement in functioning of the model based on the included variable; the variable importance score is normalized to the most important variable having an importance score of one. [20]

To identify surgeon variables associated with surgeon recommendation for continued cast immobilization, multilevel logistic mixed regression models were constructed. Random intercepts were chosen at the surgeon level. Odds ratio, 95% confidence interval, standard error, random-effects estimate, and p-values are reported. All two-tailed p values <0.05 were considered statistically significant. Reference values were chosen so that odds ratios were greater than one.

An ante-hoc sample size calculation demonstrated a minimum sample size of 90 participants to provide 80% statistical power (beta = 0.20; two-tailed alpha = 0.05) to detect a medium effect size of 0.3, using a paired t-test.

Compliance with Ethical Standards

Ethical approval was not sought for the present study because it was based on fictional case scenarios and did not make use of patient data. Written informed consent to be approached for questionnaires was obtained from all participants of the survey (surgeons part of the Science of Variation Group, SOVG) upon joining the SOVG. Participation in the SOVG and this survey was voluntary.

Table 1. Participating Surgeon Characteristics

	n	%
Sex		
Male	205	94
Female	13	6
Location of practice		
United States	102	47
Europe	75	34
Other	41	19
Subspecialty		
Hand and wrist	93	43
Orthopaedic trauma	67	31
Shoulder and elbow	30	14
Other	28	13
Years in practice		
0-5	61	28
6-10	50	23
11-20	66	30
21-30	41	19
Supervising trainees		
Yes	175	80
No	43	20

n=number of participating surgeons

RESULTS

Proportion of surgeons recommending additional cast immobilization

The proportion of surgeons recommending continued cast immobilization after 8 weeks of cast wear averaged 47% (range: 10% to 84%) depending on patient characteristics. After 12 weeks of immobilization the proportion of surgeons recommending additional cast wear averaged 21% (range: 2% to 49%) (Table 2).

Table 2. Patient Scenario Characteristics and Surgeon Recommendation to Continue Cast Immobilization

Patient scenario number	Age (years)	Sex	Fracture healing on radiograph	Fracture tenderness	Cast duration (weeks)	Surgeons recommending to continue cast immobilization	
						n	%
2	22	Female	Unclear	Yes	8	178	84
10	48	Male	Unclear	Yes	8	169	80
4	20	Female	Unclear	No	8	131	62
12	56	Male	Unclear	No	8	115	54
1	23	Female	Unclear	Yes	12	103	49
9	52	Male	Unclear	Yes	12	92	43
6	57	Female	Clear	Yes	8	84	39
14	23	Male	Clear	Yes	8	83	39
11	31	Male	Unclear	No	12	51	24
3	51	Female	Unclear	No	12	46	22
13	49	Male	Clear	Yes	12	31	15
5	18	Female	Clear	Yes	12	27	13
8	57	Female	Clear	No	8	23	11
16	23	Male	Clear	No	8	21	9.9
7	46	Female	Clear	No	12	5	2.3
15	19	Male	Clear	No	12	5	2.3

n= number of surgeons

Clinical (patient) variables associated with surgeon recommendation for additional immobilization

Appearance of fracture healing on radiographs, fracture tenderness, and duration of cast immobilization were the most important factors when recommending additional cast immobilization or not. Based on posterior probabilities, we found that a combination of unclear fracture healing on radiographs, the presence of notable fracture tenderness, and 8 weeks (vs. 12 weeks) of cast immobilization yielded the highest posterior probability of surgeon recommendation to continue cast immobilization (range: 73% to 76%). The lowest posterior probability was yielded in cases with clear radiographic fracture healing, no fracture tenderness, and 12 weeks of immobilization completed (6%) (Table 3). Random forest analysis demonstrated that the most predictive factors for recommending to continue cast immobilization or not were in order of importance: radiographic fracture healing, duration of cast immobilization, and fracture tenderness; followed by age and sex which were of equal importance (Figure 1).

Table 3. Patient variables: Posterior Probability of Surgeon Recommendation to Continue Cast Immobilization

Age (years)	Sex	Fracture healing on radiograph	Fracture tenderness	Cast duration (weeks)	Posterior probability[a] (%)
<35	Female	Unclear	Yes	8	76
>35	Male	Unclear	Yes	8	73
<35	Female	Unclear	No	8	54
<35	Male	Clear	Yes	8	51
>35	Male	Unclear	No	8	50
<35	Female	Unclear	Yes	12	49
>35	Male	Unclear	Yes	12	45
>35	Female	Clear	Yes	8	35
<35	Male	Unclear	No	12	25
>35	Female	Unclear	No	12	25
<35	Male	Clear	No	8	17
>35	Female	Clear	No	8	16
<35	Female	Clear	Yes	12	15
>35	Male	Clear	Yes	12	13
<35	Male	Clear	No	12	5.6
>35	Female	Clear	No	12	5.6

[a] The posterior probability of surgeons recommending to continue cast immobilization is defined as the probability of a surgeon recommending to continue cast immobilization in the presence of five defined variables, taking into account the unadjusted probability to continue cast immobilization of each variable. See Supplementary Material for details.

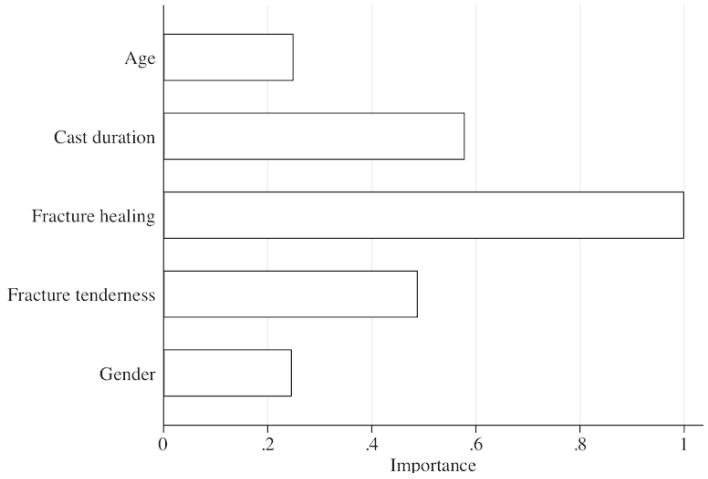

Figure 1. Random Forest Variable Importance Score of Predictor Patient Variables for Surgeon Recommendation to Continue or not Continue Cast Immobilization

Ranked importance score of each patient variable as a predictor for surgeon recommendation to continue cast immobilization. The variable importance score is normalized to the most important variable having an importance score of one.

Surgeon variables associated with surgeon recommendation for additional immobilization

Multilevel logistic mixed regression analysis identified that surgeons not specialized in hand and wrist surgery, shoulder and elbow or orthopaedic trauma (categorized as 'other') were more likely to recommend longer cast wear compared to hand and wrist surgeons. Surgeons practicing outside of Europe (i.e. United States or 'Other') were significantly more likely to continue cast wear compared to surgeons practicing in Europe. Female surgeons were more likely to continue cast immobilization compared to male surgeons. Years of practice or whether surgeons supervised trainees, were not associated with surgeon recommendation to continue cast immobilization (Table 4).

Table 4. Multilevel Logistic Regression Analysis of Surgeon Variables Associated with Surgeon Recommendation to Continue Cast Immobilization

	Odds ratio	95% CI	Standard error	p-value
Sex				
Male		*reference value*		
Female	2.96	1.28-6.81	1.26	0.011*
Years in practice				
0-5	1.61	0.97-2.66	0.41	0.064
6-10		*reference value*		
11-20	1.09	0.72-1.66	0.23	0.668
21-30	1.49	0.90-2.46	0.38	0.119
Location of practice				
Europe		*reference value*		
United States	6.53	2.18-19.52	3.65	0.001*
Other	4.22	1.71- 10.38	1.94	0.002*
Supervising trainees				
Yes		*reference value*		
No	1.11	0.76-1.60	0.21	0.593
Subspecialty				
Hand and wrist		*reference value*		
Orthopedic trauma	1.05	0.73-1.52	0.20	0.785
Shoulder and elbow	1.31	0.81-2.10	0.32	0.266
Other	2.64	1.31-5.33	0.95	0.007*

*Significant at $p < 0.05$; 95% CI= 95% Confidence Interval
Random-effects estimate (95% CI): 2.1 (0.82 to 5.38); standard error: 1.0

DISCUSSION

An increasing number of studies is considering immobilization times less than the conventional 8 to 12 weeks for the treatment of CT-confirmed nondisplaced scaphoid waist fractures. [1,2,4] The decision to continue immobilization is often based on radiographs and fracture tenderness. This conflicts with evidence that radiographs are unreliable to diagnose scaphoid union[10-12] and that pain intensity is strongly correlated to coping strategies in response to nociception in patients with upper extremity injury. [14-17] The discrepancy between current evidence and surgeon-decision making may result in unhelpful additional immobilization. This study investigated clinical (patient) and surgeon variables associated with surgeon decision to continue cast immobilization after 8 or 12 weeks.

This study has several limitations. It is possible that some surgeons interpreted the decision against additional immobilization as representing the option to perform surgery instead. We introduced the scenario as a patient with a nearly 100% likelihood of union with nonoperative treatment. It is notable that at least one surgeon considered surgery an option when choosing not to continue immobilization and contacted us. Based on comments and observed trends in recommendations most surgeons appear to have understood that the survey was not positing surgery as an option. Secondly, case descriptions can only approximate clinical encounters. To allow for statistical analysis, we studied five patient factors. We did not study presentation delay, mechanism of injury, or profession. Also, surgeons were given the option to continue cast immobilization. Options such as removable splints were not included. Furthermore, surgeons were presented with a description of a radiograph, rather than an actual radiograph. Since we were interested in the effect of radiographic union on decision-making –and not surgeons' individual radiographic interpretations– this was done deliberately to avoid noise from the unreliability of radiographic interpretation of union. Only 13 out of 218 surgeons were women and our findings may not be representative of all female surgeons. The finding that women were more likely to continue immobilization is contradictory to findings by Paulus et al. and may be spurious. [21]

On average, 47% and 21% of the surgeons recommended continued immobilization of a nondisplaced scaphoid waist fracture after 8 and 12 weeks of completed cast wear, respectively. Traditionally, cast immobilization has been prescribed for 8-12 weeks. [22-24] More recent studies have investigated immobilization as short as 4-6 weeks for CT-verified nondisplaced waist fractures.[2,4] Geoghegan et al. allowed patients with scaphoid waist fractures to mobilize if their fracture appeared united and nondisplaced on a 4-week CT scan. All such fractures united.[4] All but one of the remaining nondisplaced waist fractures healed with 5-8 weeks of immobilization. The one fracture that was reported as ununited showed moderate translation on the 4-week CT and may have been displaced.[4] Studies implementing shorter cast duration regardless of radiographic appearance at 4 to 12 weeks, or randomized controlled trials comparing less than or more than 8 weeks of immobilization are lacking. This and the limited reliability of radiographs [11,12] or CT [10] to diagnose nonunion within 4 months after injury create a situation of uncertainty and room for patients to express their preferences regarding the various treatment approaches. A return appointment to document union after 6 months could be considered.

Radiographic appearance of union, fracture tenderness and the duration of cast immobilization were the most important clinical factors affecting surgeon recommendation for additional immobilization. Nearly half the patients immobilized for 8 weeks and a fifth of patients immobilized for 12 weeks were recommended to continue immobilization if radiographic union was "unclear". This runs counter to good evidence that radiographs have poor to moderate reliability in assessing scaphoid union and are inaccurate at diagnosing nonunion.[11,12] CT scans are considered more reliable and accurate than radiographs to assess union by some.[25] Caution is warranted however, even when relying on CT to assess union. The low prevalence of nonunion in

CT-confirmed nondisplaced waist fractures, makes the diagnosis of non- or delayed union more likely to be inaccurate within 4 months after injury, even with CT.[10] Importantly, Buijze et al. confirmed union on 24-week radiographs, in all patients with a CT-confirmed nondisplaced waist fracture, whose immobilization was discontinued after 10 weeks despite 'incomplete' (<25% trabecular bridging) or no signs of healing on a 10-week CT scan.[5] As such, it is not clear whether the appearance of a scaphoid fracture on CT 6 to 12 weeks after injury is associated with a benefit from additional immobilization. This suggests that a shorter duration of immobilization will only be possible if surgeons are influenced less by radiographic appearance and rely more on the evidence that a CT-confirmed nondisplaced scaphoid waist fracture is very likely to heal no matter the radiographic appearance 12 weeks after injury.

Fracture tenderness also led to additional immobilization. There is considerable evidence that pain intensity is strongly associated with symptoms of depression, anxiety and less effective coping strategies in response to nociception.[15-17] Gonzalez et al reported a correlation between greater pain on examination and less adaptive responses to pain among 117 people with a healing upper extremity function with no risk of nonunion. This suggests that fracture tenderness may not be a helpful measure of fracture union.[14]

We identified variation in surgeon recommendation to continue immobilization among surgeons of different specialties, regions and sex. This reflects the lack of evidence-based decision-making and may be due to disagreement about optimal cast duration. Differences in medicolegal systems may also play part in this variation. Surgeons practicing in the United States may be more likely to recommend additional immobilization due to the more litigious medicolegal climate compared to Europe. A survey study of 494 international surgeons documented 30%, 33% and 27% of the surgeons recommending 6, 8 or 12 week of cast immobilization respectively, with no variation by specialty. [21]

In conclusion, fracture tenderness and radiographic appearance of union have a substantial influence on surgeon recommendation for additional immobilization of a CT-confirmed nondisplaced scaphoid waist fracture, even after 12 weeks of immobilization. Because fractures are likely to have some residual tenderness and equivocal radiological appearance after 8 to 12 weeks, the continued influence of these factors may result in unhelpful immobilization. To adopt shorter immobilization times, surgeons may need to accept uncertainty regarding fracture tenderness and radiographic fracture appearance and rely more on the evidence suggesting these fractures are very likely to heal, even with relatively brief protection.

REFERENCES

1. Clementson M, Jorgsholm P, Besjakov J, Bjorkman A, Thomsen N. Union of Scaphoid Waist Fractures Assessed by CT Scan. *J Wrist Surg.* 2015;4(1):49-55.
2. Clementson M, Jorgsholm P, Besjakov J, Thomsen N, Bjorkman A. Conservative Treatment Versus Arthroscopic-Assisted Screw Fixation of Scaphoid Waist Fractures--A Randomized Trial With Minimum 4-Year Follow-Up. *J Hand Surg Am.* 2015;40(7):1341-1348.
3. Grewal R, Suh N, MacDermid JC. Is Casting for Non-Displaced Simple Scaphoid Waist Fracture Effective? A CT Based Assessment of Union. *Open Orthop J.* 2016;10:431-438.
4. Geoghegan JM, Woodruff MJ, Bhatia R, et al. Undisplaced scaphoid waist fractures: is 4 weeks' immobilisation in a below-elbow cast sufficient if a week 4 CT scan suggests fracture union? *J Hand Surg Eur Vol.* 2009;34(5):631-637.
5. Buijze GA, Goslings JC, Rhemrev SJ, et al. Cast immobilization with and without immobilization of the thumb for nondisplaced and minimally displaced scaphoid waist fractures: a multicenter, randomized, controlled trial. *J Hand Surg Am.* 2014;39(4):621-627.
6. Buijze GA, Doornberg JN, Ham JS, Ring D, Bhandari M, Poolman RW. Surgical compared with conservative treatment for acute nondisplaced or minimally displaced scaphoid fractures: a systematic review and meta-analysis of randomized controlled trials. *J Bone Joint Surg Am.* 2010;92(6):1534-1544.
7. de Boer BNP DJ, Mallee WH, Buijze GA. Surgical treatment of non- and minimally-displaced acute scaphoid fractures favours over conservative treatment but only in the short term: an updates meta-analysis. *Journal of ISAKOS Joint Disorders & Orthopaedic Sports Medicine.* 2016.
8. Dias JJ, Brealey S, Cook L, et al. Scaphoid Waist Internal FIxation for Fractures Trial (SWIFFT): a randomised controlled trial, economic evaluation and nested qualitative study of cast versus surgical fixation for the treatment of adult patients with a bi-cortical fracture of the scaphoid waist. *Health Technology Assessment; http://nrlnorthumbriaacuk/38659/* 2019.
9. Bhat M, McCarthy M, Davis TR, Oni JA, Dawson S. MRI and plain radiography in the assessment of displaced fractures of the waist of the carpal scaphoid. *J Bone Joint Surg Br.* 2004;86(5):705-713.
10. Buijze GA, Wijffels MM, Guitton TG, et al. Interobserver reliability of computed tomography to diagnose scaphoid waist fracture union. *J Hand Surg Am.* 2012;37(2):250-254.
11. Dias JJ, Taylor M, Thompson J, Brenkel IJ, Gregg PJ. Radiographic signs of union of scaphoid fractures. An analysis of inter-observer agreement and reproducibility. *J Bone Joint Surg Br.* 1988;70(2):299-301.
12. Hannemann PF, Brouwers L, Dullaert K, van der Linden ES, Poeze M, Brink PR. Determining scaphoid waist fracture union by conventional radiographic examination: an analysis of reliability and validity. *Arch Orthop Trauma Surg.* 2015;135(2):291-296.
13. Clementson M, Bjorkman A, Thomsen NOB. Acute scaphoid fractures: guidelines for diagnosis and treatment. *EFORT Open Rev.* 2020;5(2):96-103.
14. Gonzalez AI, Kortlever JTP, Crijns TJ, Ring D, Reichel LM, Vagner GA. Pain during physical examination of a healing upper extremity fracture. *J Hand Surg Eur Vol.* 2020:1753193420952010.
15. Vranceanu AM, Bachoura A, Weening A, Vrahas M, Smith RM, Ring D. Psychological factors predict disability and pain intensity after skeletal trauma. *J Bone Joint Surg Am.* 2014;96(3):e20.
16. Moradi A, Mellema JJ, Oflazoglu K, Isakov A, Ring D, Vranceanu AM. The Relationship Between Catastrophic Thinking and Hand Diagram Areas. *J Hand Surg Am.* 2015;40(12):2440-2446 e2445.
17. Oh Y, Drijkoningen T, Menendez ME, Claessen FM, Ring D. The Influence of Psychological Factors on the Michigan Hand Questionnaire. *Hand (N Y).* 2017;12(2):197-201.
18. Neuhaus V, Bot AG, Guitton TG, Ring DC. Influence of surgeon, patient and radiographic factors on distal radius fracture treatment. *J Hand Surg Eur Vol.* 2015;40(8):796-804.

19. Lyman S, Oh LS, Reinhardt KR, et al. Surgical decision making for arthroscopic partial meniscectomy in patients aged over 40 years. *Arthroscopy.* 2012;28(4):492-501 e491.

20. Zou RY, Schonlau M. The Random Forest Algorithm for Statistical Learning with Applications in Stata. *The Stata Journal.* 2018.

21. Paulus MC, Braunstein J, Merenstein D, et al. Variability in orthopedic surgeon treatment preferences for nondisplaced scaphoid fractures: A cross-sectional survey. *J Orthop.* 2016;13(4):337-342.

22. Adolfsson L, Lindau T, Arner M. Acutrak screw fixation versus cast immobilisation for undisplaced scaphoid waist fractures. *J Hand Surg Br.* 2001;26(3):192-195.

23. Dias JJ, Dhukaram V, Abhinav A, Bhowal B, Wildin CJ. Clinical and radiological outcome of cast immobilisation versus surgical treatment of acute scaphoid fractures at a mean follow-up of 93 months. *J Bone Joint Surg Br.* 2008;90(7):899-905.

24. McQueen MM, Gelbke MK, Wakefield A, Will EM, Gaebler C. Percutaneous screw fixation versus conservative treatment for fractures of the waist of the scaphoid: a prospective randomised study. *J Bone Joint Surg Br.* 2008;90(1):66-71.

25. Hannemann PF, Brouwers L, van der Zee D, et al. Multiplanar reconstruction computed tomography for diagnosis of scaphoid waist fracture union: a prospective cohort analysis of accuracy and precision. *Skeletal Radiol.* 2013;42(10):1377-1382.

SUPPLEMENTARY MATERIAL

Posterior Probabilities Patient Variables

Posterior probabilities were calculated using the formulas detailed below.[19] First, the unadjusted probabilities of surgeons recommending to continue cast (Pcc) or not continue cast (Pnc) immobilization were calculated for the conditional presence of each variable. For example, for patient sex, the probabilities of continuing cast (Pcc) and not continuing cast (Pnc) were calculated for the variable male (Pcc|male, Pnc|male) and female (Pcc|female, Pnc|female).

Subsequently, the probability of continuing cast immobilization (Pcc) for each case scenario was calculated by combining the conditional probabilities associated with each variable, as well as the overall probability of continuing cast immobilization regardless of any variables (Pcc|overall) as follows:

Pcc = [(Pcc|age)*(Pcc|sex)*(Pcc|fracture healing)*(Pcc|fracture tenderness)*(Pcc|cast duration)]* (Pcc|overall)

The probability of not continuing cast immobilization was calculated as follows:

Pnc= (Pnc|age)*(Pnc|sex)*(Pnc|fracture healing)*(Pnc|fracture tenderness)*(Pnc|cast duration)*(Pnc|overall)

Finally, the posterior probability of recommending continued cast immobilization for each case scenario is calculated as follows:

PPcc = Pcc / (Pcc + Pnc)

The unadjusted probabilities for each variable are summarized in Table S1.

Using these values, the highest posterior probability of surgeons recommending to continue cast immobilization was in female patients, under 35 years of age, with unclear fracture healing on radiographs, fracture tenderness and 8 weeks of cast immobilization completed:

PPcc = (0.515*0.513*0.760*0.659*0.691*0.342) / (0.492*0.493*0.364*0.417*0.402*0.658)

PPcc = 0.76, or 76%

Table S1. Unadjusted Probabilities of Surgeon Recommendation to Continue or not Continue Cast Immobilization Associated with Patient Variables

	P (continue cast immobilization)	P (not continue cast immobilization)
Overall probability	0.342	0.658
<35 years of age	0.515	0.492
>35 years of age	0.485	0.508
Male sex	0.487	0.507
Female sex	0.513	0.493
Clear fracture healing	0.240	0.636
Unclear fracture healing	0.760	0.364
No fracture tenderness	0.341	0.583
Fracture tenderness	0.659	0.417
12 weeks cast duration	0.309	0.598
8 weeks cast duration	0.691	0.402

P: unadjusted probability. The unadjusted probability is calculated as the proportion of cases in which surgeons recommended for or against continued cast immobilization in the presence of each variable.

CHAPTER 10

Prospective Cohort Study to Investigate Factors Associated with Continued Immobilization of a Nondisplaced Scaphoid Waist Fracture

A.E.J. Bulstra
L.A.M. Hendrickx
I. N. Sierevelt
G. A. Buijze
G.M.M.J. Kerkhoffs
D. Ring
R. L. Jaarsma
J.N. Doornberg

In Journal of Hand Surgery America. August 2021;46(8):685-694. (Editor's Choice)

ABSTRACT

Purpose

The decision to continue immobilization of a nondisplaced scaphoid waist fracture is often based on radiographic appearance (despite evidence that radiographs are unreliable and inaccurate for diagnosis of scaphoid union 6-12 weeks after fracture) and fracture tenderness (even though it is influenced by cognitive biases about pain). This may result in unhelpful additional immobilization. We studied nondisplaced scaphoid waist fractures to determine factors associated with: 1) surgeon decision to continue cast or splint immobilization at the first visit where cast removal was being considered; 2) greater pain on examination; 3) surgeon concern about radiographic consolidation.

Methods

We prospectively included 46 patients with a nondisplaced scaphoid waist fracture treated nonoperatively. At the first visit where cast removal was considered- after an average of 6 weeks of immobilization - patients rated pain during 4 examination manoeuvres. The treating surgeon assessed union on radiographs. The surgeon decided to continue or discontinue immobilization. Patients completed measures of a) the degree to which pain limits activities (PROMIS Pain Interference Computer Adaptive Test [CAT], Pain Self-Efficacy Questionnaire [PSEQ-2]) 2); b) symptoms of depression (PROMIS Depression CAT); c) upper extremity function (PROMIS Upper Extremity Function CAT). We used multivariable regression analysis to investigate factors associated with each outcome.

Results

Perceived inadequate radiographic healing and greater symptoms of depression were independently associated with continued immobilization. Pain during examination was not associated with continued immobilization. Patient age was associated with pain on examination. Shorter immobilization duration was the only factor associated with surgeon perception of inadequate radiographic consolidation.

Conclusions

Inadequate radiographic healing and greater symptoms of depression are associated with surgeon decision to continue cast or splint immobilization of a nondisplaced scaphoid waist fracture.

Clinical relevance

Overreliance on radiographs and inadequate accounting for psychological distress may hinder the adoption of shorter immobilization times for nondisplaced waist fractures.

INTRODUCTION

Nondisplaced scaphoid waist fractures nearly always heal with adequate cast immobilization.[1-5] An increasing number of studies support the use of less rigid and shorter types of immobilization (4-6 weeks) for the treatment of CT-confirmed nondisplaced scaphoid waist fractures.[2-6] In clinical practice the decision to continue immobilization of a nondisplaced waist fracture is often based on 1) radiographic fracture appearance and 2) fracture tenderness to assess fracture healing after 6-12 weeks of immobilization. This runs counter to good evidence that radiographic assessment of scaphoid union within 6-12 weeks after fracture is unreliable and inaccurate.[7-9] In addition, pain intensity[10-12], including fracture tenderness[13,14], in patients with (traumatic) upper-extremity illness is also influenced to some degree by a person's mindset, unhealthy thoughts in response to nociception and symptoms of depression in particular.

If additional evidence supports shorter immobilization times for nondisplaced scaphoid waist fractures, this option will only be viable if surgeons are comfortable with uncertainty about radiographs and continued tenderness. The implementation of strategies for shorter duration of immobilization can be informed by a better understanding of the variables affecting surgeon decision-making and the recommendation for additional immobilization of a nondisplaced scaphoid waist fracture.

This study tested the primary null hypothesis that 1) there are no factors (demographic, examination, radiological, psychological, surgeon experience level) associated with surgeon decision to continue cast or splint immobilization at the first visit where cast removal was being considered. We also tested the secondary null hypotheses that at this visit there are no factors associated with: 2) pain during examination manoeuvres including palpation; 3) surgeon perception of inadequate fracture consolidation on radiographs; and 4) upper extremity activity intolerance as measured by the PROMIS Upper Extremity Function CAT.

PATIENTS AND METHODS

This study was approved by the institutional review board. We obtained written consent from each patient prior to inclusion. This report was written following the Strengthening the Reporting of Observational Studies in Epidemiology (STROBE) guidelines. This was a pragmatic design to study surgeon decision making, that anticipated typical variations in care—no attempt was made to standardize the diagnostic or treatment protocol.[15,16]

Patients

Between May 2018 and September 2019, all patients (>17 years) presenting to the Orthopaedic Trauma Clinic diagnosed with a nondisplaced scaphoid waist fracture treated nonoperatively, were prospectively identified and considered for inclusion. Scaphoid fractures were diagnosed on radiographs or MRI. All patients with radial sided

wrist tenderness and normal or equivocal radiographs had an MRI. Displacement was defined as more than 1mm translation or gap on radiographs, MRI, or CT. When in doubt, a CT was obtained at the treating surgeon's discretion.

In total, seventeen patients had MRI or CT that confirmed the absence of displacement Exclusion criteria were as follows: patients presenting more than 3 weeks after injury; patients with a previous scaphoid fracture or concomitant ipsilateral upper extremity injury; and patients unable to provide informed consent.

We screened seventy-five patients with a nondisplaced scaphoid waist fracture. Twenty-nine patients were not eligible for inclusion. Sixteen patients had concomitant ipsilateral upper extremity injury; 2 had a previous scaphoid fracture, 4 patients presented more than 3 weeks after injury; 2 patients having surgery for a lower limb injury opted for operative treatment of the scaphoid fracture. Two patients chose not to participate and 3 were unable to provide informed consent. One patient did not have radiographs at the first visit where cast removal was being considered. The missing value was imputed using a random Forest Algorithm.[17] We included forty-six patients meeting the inclusion criteria (Table 1).

Treatment protocol

At our institution, patients with a nondisplaced waist fracture are immobilized in a below-elbow thumb-spica cast and considered for cast removal 6 weeks later, no matter the interval between injury and initial cast immobilization. Patients advised to continue with cast immobilization are re-evaluated in 3 weeks.

Measurements

The primary outcome measure was the decision to continue cast or splint immobilization at the first visit where cast removal was being considered**.** An independent observer not involved in patient care recorded the surgeons' decision. Type of immobilization prescribed was also recorded: below-elbow thumb-spica cast or removable splint.

Patients rated the pain experienced with each of four examination manoeuvres performed by the treating surgeon on an 11-point ordinal scale ranging from 0 (no pain) to 10 (worst pain): 1) palpation of the anatomic snuffbox with the wrist in ulnar deviation; 2) palpation of scaphoid tubercle; 3) longitudinal thumb compression; and 4) thumb-index pinch. An independent observer recorded scores for each test. The four test scores were summed for a total score between 0 and 40. This was done based on previous studies demonstrating improved accuracy for diagnosis of a scaphoid fracture when combining physical examination maneuvers.[18,19] Studies on the accuracy of examination manoeuvres to assess scaphoid union are lacking.

Surgeons rated fracture healing on radiographs as adequate or inadequate prior to seeing the patient. Surgeons were aware of the date of injury and days of immobilization completed when reviewing the radiographs. Radiographic scaphoid series included posterior-anterior views in ulnar deviation, lateral, 45° oblique, and one elongated scaphoid view with the wrist in ulnar deviation.

At the first visit where cast removal was being considered patients completed the following questionnaires: 1) a 2-question measure of Pain Self-Efficacy (PSEQ-2)[20], 2) Patient Reported Outcome Measure Interactive System (PROMIS) Pain Interference (PI) Computer Adaptive Test (CAT) v1.1[21], 3) PROMIS Depression CAT v1.0.[22] Patients were instructed by an independent researcher, the treating surgeon had no insight in the results of the questionnaire.

The PSEQ-2 measures the ability to perform daily tasks despite the pain. A higher score reflects greater ability to do one's normal activities in spite of pain (i.e. greater self-efficacy).[20] The PROMIS PI CAT assesses the degree to which pain interferes with daily activities.[23-25] Pain interference was designed as an outcome measure, but correlates highly with measures of cognitive coping strategies, and may be measuring a similar underlying construct.[25] PROMIS measurements are standardized based on the general population having a mean t-score of 50. Higher scores indicate a greater degree of the variable measured. Higher pain interference scores and lower pain self-efficacy scores correlate with unhealthy thoughts such as worst-case (catastrophic) thinking and fear of painful movement (kinesiophobia).[24-26]

Patients completed measures of upper extremity activity intolerance (PROMIS Upper Extremity CAT v1.2).[23]

A total of 18 different surgeons reviewed the patients included in this study cohort: 8 residents and 10 attendings.

Statistical analysis

To identify factors associated with 1) continued cast or splint immobilization; 2) pain intensity during clinical examination; 3) surgeon perception of inadequate radiographic consolidation and 4) upper extremity specific activity intolerance (PROMIS Upper Extremity Function CAT) at the first visit where cast removal was being considered, we conducted bivariable analysis using chi-square, independent t-tests and Pearson correlation.

Factors with a p-value < 0.10 in bivariable analysis were entered into multivariable regression analysis with backward stepwise selection to identify factors associated with each of the four separate outcome measures. The significance level for multivariable analysis was set at $p<0.05$.

An a priori power analysis showed that 43 participants would provide 80% power, with a 0.05 significance, for a logistic regression in which a judgement of inadequate consolidation made on the basis of radiographs was associated with an odds ratio of 5 for additional immobilization and the complete model would account for 25% of the variability in surgeon recommendation for additional immobilization.

Table 1. Patient demographics, questionnaire scores and clinical variables

Variables	Value
Patient variables	
Sex	
Men	30 (65)
Women	16 (35)
Age (years)	28 (21-50)[v]
BMI	26 (19-48)
Smoker	8 (17)
Affected side is dominant side	22 (48)
Work status	
Sedentary	25 (54)
Non sedentary	21 (46)
Questionnaire scores	
PROMIS Depression CAT	50 (34-68)
PROMIS Pain Interference CAT	54 (39-74)
PROMIS Physical Function Upper Extremity CAT	34 (20-56)
PSEQ-2	9.0 (4.0-12)
Days since injury at first follow up	46 (36-71)
Days of immobilization completed at first follow up	43 (28-65)
Continued Immobilization	
None	22 (48)
Splint	16 (35)
Cast	8 (17)
Pain intensity during clinical examination	3 (1-6)[v]
Surgeon assessment of radiograph	
Adequate healing	28 (61)
Inadequate healing	18 (39)
Surgeon level*	
Resident	23 (50)
Attending	23 (50)

Continuous variables are represented as mean (range),[v] or as median (lower – upper quartile); discrete variables as number (percentage); PROMIS: Patient-Reported Outcome Measurement Information System; CAT: computer adaptive test; PSEQ: pain self-efficacy questionnaire; * number of patients reviewed by junior or senior surgeon.

RESULTS

Factors associated with continued cast or splint immobilization

After an average of forty-six days after injury (range 36-71) – after 6 weeks of cast wear (mean: 43 days, range: 28-65 days) - immobilization was discontinued in 22 (48%) patients. Sixteen (35%) patients were changed to splint immobilization and 8 patients (17%) continued immobilization in a cast.

In bivariable analysis, continued immobilization was associated with smoking, inadequate radiographic healing, and greater symptoms of depression. Pain during examination and hindrance of daily activities by pain were not associated with continued immobilization (Table 2). In multivariable analysis, continued immobilization was independently associated with perceived inadequate radiographic healing and more symptoms of depression. Patients with perceived inadequate radiographic healing were more likely to receive continued immobilization (OR 8.4; 95%CI 1.9-37)). For every single point increase in PROMIS Depression CAT score, the odds that immobilization was continued, increased by 1.1 or 10% (Table 3).

Factors associated with pain intensity during clinical examination manoeuvres

In bivariable analysis, pain intensity during clinical examination was associated with patient age and the degree to which pain interfered with daily activities as measured with PROMIS CAT PI (Table 4). In multivariable analysis, only older age was associated with greater pain intensity during examination (regression coefficient 0.11; 95%CI 0.027-0.20; $p<0.05$).

Factors associated with surgeon perception of inadequate radiographic consolidation

Surgeon concern about radiographic healing was associated with a shorter duration of immobilization completed. Days since injury was not associated with surgeon interpretation of radiographic healing (Table 5).

Factors associated with upper extremity activity tolerance

In bivariable analysis better upper extremity function at the first visit where cast removal was being considered was associated with younger age, male sex, lower BMI and greater ability to continue activities in spite of pain measured by lower PROMIS PI CAT scores. The ability to perform daily tasks despite the pain as measured by PSEQ scores and whether the dominant hand was affected were also included in multivariable analysis ($p<0.10$) (Table 6). In multivariable analysis, male sex, lower BMI and greater ability to continue activities in spite of pain measured with PROMIS PI CAT were independently associated with better patient reported upper extremity function at the first visit where cast removal was being considered. (Table 7).

Table 2. Bivariable analysis of factors associated with continued cast or splint immobilization

	Continued cast or splint immobilization (n=24)	Discontinued immobilization (n=22)	p-value
Patient variables			
Age	36 (22-51)ᵛ	26 (20-48)ᵛ	0.37
Sex			0.40
Women	7 (44)	9 (56)	
Men	17 (57)	13 (43)	
BMI	27 (19-48)	25 (19-42)	0.29
Smoker			<0.05*
No	17 (45)	21 (55)	
Yes	7 (88)	1 (13)	
Dominant side affected			0.37
No	11 (46)	13 (54)	
Yes	13 (59)	9 (41)	
Sedentary work			0.57
No	12 (57)	9 (43)	
Yes	12 (48)	13 (52)	
Questionnaire scores			
PROMIS Depression CAT	53 (34-68)	47 (34-68)	<0.05*
PROMIS Pain Interference CAT	55 (39-64)	53 (39-74)	0.26
PSEQ-2	8.8 (4-12)	9.7 (5-12)	0.16
Days since injury at first follow up	45 (36-71)	47 (38-66)	0.26
Days of immobilization completed at first follow up	43 (35-53)	45 (28-65)	0.38
Pain intensity during clinical examination	4.5 (2.0-6.8)ᵛ	2.0 (1-5)ᵛ	0.30
Surgeon assessment of radiograph			<0.05*
Adequate healing	10 (36)	18 (64)	
Inadequate healing	14 (78)	4 (22)	
Surgeon level			0.38
Resident	10 (43)	13 (57)	
Attending	14 (61)	9 (39)	

Continuous variables are represented as mean (range), ᵛ or as median (lower – upper quartile); discrete variables as number (percentage); * variables with p<0.1 included in multivariable regression analysis

Table 3. Final model of multivariable regression analysis of factors associated with continued cast or splint immobilization

	OR (95% CI)	p-value
Questionnaire scores		
PROMIS Depression CAT	1.1 (1.0-1.2)	<0.05*
Surgeon assessment of radiograph		
Inadequate healing	8.4 (1.9-37)	<0.05*

OR: odds ratio; 95% CI: 95% confidence interval; * statistically significant at p<0.05

Table 4. Bivariable analysis of factors associated with pain at clinical examination maneuvers

	Correlation coefficient or mean pain intensity score	p-value
Patient variables		
Age	0.37	<0.05*
Sex		0.25
Men	4.4 (0-18)	
Women	6.6 (0-22)	
BMI	0.17	0.27
Smoking		0.12
Yes	8.1 (0-21)	
No	4.5 (0-22)	
Dominant side affected		0.75
Yes	5.5 (0-18)	
No	4.9 (0-22)	
Sedentary work		0.14
Yes	6.4 (0-22)	
No	3.7 (0-17)	
Questionnaire Scores		
PROMIS Depression CAT	0.14	0.36
PROMIS Pain Interference CAT	0.34	<0.05*
PSEQ-2	-0.90	0.55
Days since injury at first follow up	0.092	0.54
Days of immobilization completed at first follow up	0.066	0.66
Surgeon assessment of radiograph		0.97
Adequate healing	5.2 (0-22)	
Inadequate healing	5.1 (0-21)	

Table 4. Bivariable analysis of factors associated with pain at clinical examination maneuvers (continued)

	Correlation coefficient or mean pain intensity score	p-value
Surgeon level		0.25
Resident	6.2 (0-22)	
Attending	4.1 (0-21)	

Correlation coefficients are reported for linear explanatory variables, mean (range) pain intensity scores for dichotomous variables; 95% CI: 95% Confidence Interval; * variables with p<0.1 included in multivariable regression analysis

Table 5. Bivariable analysis of factors associated with surgeon interpretation of healing on radiographs

	Adequate healing	Inadequate healing	p-value
Patient variables			
Age	27 (19-49)[ᵞ]	42 (23-55)[ᵞ]	0.15
Sex			
Men	18 (60)	12 (40)	0.87
Women	10 (63)	6 (38)	
BMI	27 (19-48)	26 (19-42)	0.79
Smoking			0.49
Yes	4 (50)	4 (50)	
No	24 (63)	14 (37)	
Dominant side affected			0.71
Yes	14 (64)	8 (36)	
No	14 (58)	10 (42)	
Sedentary work			0.43
Yes	16 (57)	9 (50)	
No	12 (43)	9 (50)	
Questionnaire Scores			
PROMIS Depression CAT	50 (34-67)	50 (34-64)	0.94
PROMIS Pain Interference CAT	55 (39-74)	53 (39-64)	0.50
PSEQ-2	9.3 (4-12)	9.1 (4-12)	0.78
Days since injury at first follow up	47 (38-66)	45 (36-71)	0.32
Days of immobilization completed at first follow up	45 (37-65)	42 (28-53)	0.05*
Surgeon level			1.00
Resident	14 (50)	9 (50)	
Attending	14 (50)	9 (50)	

Continuous variables are represented as mean (range), [ᵞ]or as median (lower – upper quartile); discrete variables as number (percentage); OR: odds ratio; 95% CI: 95% Confidence Interval; * statistically significant at p<0.05

Table 6. Bivariable analysis factors associated with upper extremity function as measured with the PROMIS Upper Extremity CAT

	Correlation coefficient or mean upper extremity score	p-value
Patient variables		
Age	-0.44 (-0.65 to -0.24)	<0.05*
Sex		<0.05*
Men	36 (21-56)	
Women	31 (21-45)	
BMI	-0.51 (-0.68 to -0.30)	<0.05*
Smoking		0.68
Yes	33 (26-42)	
No	35 (20-56)	
Dominant side affected		0.08*
Yes	32 (21-45)	
No	36 (20-56)	
Sedentary work		0.38
Yes	32 (21-45)	
No	36 (21-56)	
Questionnaire Scores		
PROMIS Depression CAT	-0.17 (-0.42 to 0.10)	0.26
PROMIS Pain Interference CAT	-0.39 (-0.61 to -0.11)	<0.05*
PSEQ-2	0.82 (-0.13 to 1.8)	0.09*
Days since injury at first follow up	-0.20 (-0.53 to 0.12)	0.21
Days of immobilization completed at first follow up	-0.13 ()	0.40
Surgeon assessment of radiograph		0.50
Adequate healing	35 (21-56)	
Inadequate healing	34 (26-41)	

Correlation coefficients are reported for linear explanatory variables, mean (range) upper extremity scores for dichotomous variables; 95% CI: 95% Confidence Interval; * variables with p<0.1 included in multivariable regression analysis

Table 7. Final model of multivariable analysis of factors associated with upper extremity function as measured with the PROMIS Upper Extremity CAT

	Regression coefficient (95% CI)	p-value	Adjusted R^2
			0.38
Patient variables			
Male sex	5.2 (0.89-9.6)	<0.05*	
BMI	-0.38 (-0.69 to -0.065)	<0.05*	
Questionnaire Scores			
PROMIS Pain Interference CAT	-0.40 (-0.66 to -0.14)	<0.05*	

95% CI: 95% Confidence Interval; * statistically significant at p<0.05

DISCUSSION

Increasing evidence suggests that nondisplaced scaphoid waist fractures heal with less than the traditional 8-12 weeks of immobilization.[3–5,26] Surgeon reliance on unreliable measures of fracture union – including radiographs and pain intensity – may hinder the adoption of shorter immobilization times. This study investigated factors associated with surgeon decision to continue immobilization of a nondisplaced scaphoid waist fracture at the first visit where cast removal was being considered. Patients with perceived inadequate radiographic healing and patients with greater symptoms of depression were more likely to receive continued cast or splint immobilization. Pain during clinical examination was not associated with continued immobilization.

Strengths of this study include the prospective study design. It provides a comprehensive analysis of factors associated with additional immobilization. Weaknesses include the fact that our findings may apply best to our institution. However, we believe the protocol – including the use of radiographs to assess union– reflects common practice.[1,26,27] Secondly, only 17 out of 46 patients had MRI or CT at time of diagnosis. If one diagnoses a scaphoid waist fracture as non-displaced using CT or MRI, then one can count on a very high union rate even with relatively brief immobilization times.[4,5] In the absence of this some fractures may have been displaced, which could increase surgeon concerns about union and alter their behaviour. Thirdly, the relatively small sample size and floor effect of pain scores may have influenced the analysis. The small sample size also did not allow for a distinction to be made between factors associated with continued splint *versus* cast immobilization. In clinical practice, the distinction between splint or cast recommendation may be an important reflection of surgeons' interpretation of the extent of fracture healing, with splint immobilization representing an intermediate state of uncertainty. For the purposes of this study, we were interested in any expression of concern related to uncertainty as embodied in continuation of either splint or cast immobilization. Fourthly, there might be variation in how surgeons performed examination

manoeuvres, interpreted radiographs, and managed uncertainty. This may relate, in part, to experience. The variation in our study reflects daily clinical practice of our unit and likely others as well. There were too many clinicians involved for a meaningful analysis of these factors in this study, but we addressed them in a separate study. Furthermore, subjective surgeon attitude – including fear of litigation, was not investigated. Also, there could be variation among surgeons whether they consider time since injury or immobilization when assessing fracture healing. Variation in individual interpretation of the part of healing that occurs naturally and the part that is enhanced by a cast was not investigated and may affect decision-making. We did not address clinician factors in this study because the set-up of our fracture care makes this difficult with so many clinicians involved, but we do address these important factors in other studies. The difference between time of immobilization and time since injury was small, suggesting only a few patients had relatively delayed treatment. Due to scheduling conveniences, not every patient was seen after exactly 6 weeks of immobilization. Importantly, neither days since injury nor immobilization duration completed were associated with surgeon decision to continue immobilization. Lastly, surgeon decision-making may have been influenced by their awareness of the study (Hawthorne effect), potentially causing surgeons to be more cautious in their decision making.[27]

The observation that patients with perceived inadequate radiographic healing and greater symptoms of depression were more likely to receive continued immobilization, identifies important hindrances to adopting increasingly proposed shorter immobilization times for nondisplaced scaphoid waist fractures.[3-5,28] Radiographic appearance is influencing treatment recommendations in spite of the established fact that radiographs are unreliable and inaccurate for assessing scaphoid union 6-12 weeks after fracture.[7-9] CT is increasingly used to diagnose scaphoid union. Its reliability and accuracy may be better than radiographs, but are also limited.[29,30] It is not clear that the appearance of a scaphoid fracture on CT is associated with a benefit from additional immobilization. Buijze et al. documented union in all patients with a nondisplaced waist fracture who were allowed to mobilize after 10 weeks of immobilization regardless of CT appearance of union. This included patients with uncertain union (rated as 0-25% of bony bridging) on a 10-week CT.[2]

The finding that greater symptoms of depression were independently associated with a recommendation to continue splint or cast immobilization suggests that surgeons may misinterpret the known influence of psychological distress on illness behavior[10-12,14] leading to unhelpful continued immobilization. It is not that surgeons are aware of a score on a depression measure and use it to choose treatment. The association indicates that surgeons are reacting to some aspect of illness behaviour associated with symptoms of depression. For instance, one study of 117 people with a healing upper extremity fracture with no risk of nonunion, found greater pain on examination was correlated with less adaptive responses to pain and older age.[13] Another study found that misconceptions about pain mediated the degree to which pain intensity was associated with activity intolerance among 125 patients with a musculoskeletal illness.[14] A study of over 10,000

patients confirmed the correlation of symptoms of depression and activity intolerance.[31] There is compelling evidence that greater pain intensity, fracture tenderness, and activity intolerance may suggest important misconceptions or psychological distress independent of the degree of pathophysiology. Surgeons can account for this important aspect of human illness behaviour and thereby decrease the potential for unhelpful tests and treatments (e.g. continued cast immobilization). Further research regarding the relationship between patient mood and surgeon recommendations is merited.

The finding that pain interference has moderate correlation with pain intensity during clinical examination in bivariable analysis is consistent with prior research. It is not clear why it was not included in the multivariable analysis. Pain and tenderness tend to be associated with unhealthy thoughts in relation to nociception[10-14] and may therefore be an unreliable method for assessing union[13], although that was not evaluated in this study.

The finding that surgeon interpretation of radiographic healing was associated with duration of immobilization, but not duration since injury suggests that surgeon interpretation of radiographs may be influenced by context. For instance, surgeons may consider cast immobilization more important than time in the healing process, leading to more negative assessment of union with shorter immobilization times independent of the total time available for healing. Evidence of the effect of context on the interpretation of imaging is documented in studies like that of Becker et al. who found that patient factors are associated with variation in radiographic classification of trapeziometacarpal arthrosis.[32]

The observation that greater pain interference with daily activities was associated with greater limitations in upper extremity function during immobilization is consistent with previous studies.[33-35]

This study demonstrates that surgeon recommendation for additional immobilization of a nondisplaced waist fracture is associated with factors unlikely to be related to the probability of union such as radiographic appearance at the first visit where cast removal is being considered and likely illness behaviour associated with symptoms of depression. To give patients the option of shorter immobilization, surgeons may need to accept uncertainty of radiographic appearance and anticipate variations in patient illness behaviour.

REFERENCES

1. Bhat M, McCarthy M, Davis TR, Oni JA, Dawson S. MRI and plain radiography in the assessment of displaced fractures of the waist of the carpal scaphoid. *J Bone Joint Surg Br.* 2004;86(5):705-713.
2. Buijze GA, Goslings JC, Rhemrev SJ, et al. Cast immobilization with and without immobilization of the thumb for nondisplaced and minimally displaced scaphoid waist fractures: a multicenter, randomized, controlled trial. *J Hand Surg Am.* 2014;39(4):621-627.
3. Clementson M, Jorgsholm P, Besjakov J, Bjorkman A, Thomsen N. Union of Scaphoid Waist Fractures Assessed by CT Scan. *J Wrist Surg.* 2015;4(1):49-55.
4. Geoghegan JM, Woodruff MJ, Bhatia R, et al. Undisplaced scaphoid waist fractures: is 4 weeks' immobilisation in a below-elbow cast sufficient if a week 4 CT scan suggests fracture union? *J Hand Surg Eur Vol.* 2009;34(5):631-637.
5. Grewal R, Suh N, MacDermid JC. Is Casting for Non-Displaced Simple Scaphoid Waist Fracture Effective? A CT Based Assessment of Union. *Open Orthop J.* 2016;10:431-438.
6. Clementson M, Bjorkman A, Thomsen NOB. Acute scaphoid fractures: guidelines for diagnosis and treatment. *EFORT Open Rev.* 2020;5(2):96-103.
7. Dias JJ, Taylor M, Thompson J, Brenkel IJ, Gregg PJ. Radiographic signs of union of scaphoid fractures. An analysis of inter-observer agreement and reproducibility. *J Bone Joint Surg Br.* 1988;70(2):299-301.
8. Hannemann PF, Brouwers L, Dullaert K, van der Linden ES, Poeze M, Brink PR. Determining scaphoid waist fracture union by conventional radiographic examination: an analysis of reliability and validity. *Arch Orthop Trauma Surg.* 2015;135(2):291-296.
9. Singh HP, Forward D, Davis TR, Dawson JS, Oni JA, Downing ND. Partial union of acute scaphoid fractures. *J Hand Surg Br.* 2005;30(5):440-445.
10. Alokozai A, Eppler SL, Lu LY, Sheikholeslami N, Kamal RN. Can Patients Forecast Their Postoperative Disability and Pain? *Clin Orthop Relat Res.* 2019;477(3):635-643.
11. Cunningham DJ, Steele JR, Allen NB, Nunley JA, Adams SB. The Impact of Preoperative Mental Health and Depression on Outcomes After Total Ankle Arthroplasty. *J Bone Joint Surg Am.* 2021;103(2):131-138.
12. Lentz TA, George SZ, Manickas-Hill O, et al. What General and Pain-associated Psychological Distress Phenotypes Exist Among Patients with Hip and Knee Osteoarthritis? *Clin Orthop Relat Res.* 2020;478(12):2768-2783.
13. Gonzalez AI, Kortlever JTP, Crijns TJ, Ring D, Reichel LM, Vagner GA. Pain during physical examination of a healing upper extremity fracture. *J Hand Surg Eur Vol.* 2020:1753193420952010.
14. Cremers T, Zoulfi Khatiri M, van Maren K, Ring D, Teunis T, Fatehi A. Moderators and Mediators of Activity Intolerance Related to Pain. *J Bone Joint Surg Am.* 2020.
15. Ali SA, Kloseck M, Lee K, Walsh KE, MacDermid JC, Fitzsimmons D. Evaluating the design and reporting of pragmatic trials in osteoarthritis research. *Rheumatology (Oxford).* 2018;57(1):59-63.
16. Sedgwick P. Explanatory trials versus pragmatic trials. *BMJ.* 2014;349:g6694.
17. Stekhoven DJ, Buhlmann P. MissForest--non-parametric missing value imputation for mixed-type data. *Bioinformatics.* 2012;28(1):112-118.
18. Mallee WH, Henny EP, van Dijk CN, Kamminga SP, van Enst WA, Kloen P. Clinical diagnostic evaluation for scaphoid fractures: a systematic review and meta-analysis. *J Hand Surg Am.* 2014;39(9):1683-1691 e1682.
19. Parvizi J, Wayman J, Kelly P, Moran CG. Combining the clinical signs improves diagnosis of scaphoid fractures. A prospective study with follow-up. *J Hand Surg Br.* 1998;23(3):324-327.
20. Nicholas MK, McGuire BE, Asghari A. A 2-item short form of the Pain Self-efficacy Questionnaire: development and psychometric evaluation of PSEQ-2. *J Pain.* 2015;16(2):153-163.

21. Amtmann D, Cook KF, Jensen MP, et al. Development of a PROMIS item bank to measure pain interference. *Pain.* 2010;150(1):173-182.

22. Schalet BD, Pilkonis PA, Yu L, et al. Clinical validity of PROMIS Depression, Anxiety, and Anger across diverse clinical samples. *J Clin Epidemiol.* 2016;73:119-127.

23. Beckmann JT, Hung M, Voss MW, Crum AB, Bounsanga J, Tyser AR. Evaluation of the Patient-Reported Outcomes Measurement Information System Upper Extremity Computer Adaptive Test. *J Hand Surg Am.* 2016;41(7):739-744 e734.

24. Talaei-Khoei M, Ogink PT, Jha R, Ring D, Chen N, Vranceanu AM. Cognitive intrusion of pain and catastrophic thinking independently explain interference of pain in the activities of daily living. *J Psychiatr Res.* 2017;91:156-163.

25. Kortlever JT, Janssen SJ, van Berckel MM, Ring D, Vranceanu AM. What Is the Most Useful Questionnaire for Measurement of Coping Strategies in Response to Nociception? *Clin Orthop Relat Res.* 2015;473(11):3511-3518.

26. Wilkens SC, Lans J, Bargon CA, Ring D, Chen NC. Hand Posturing Is a Nonverbal Indicator of Catastrophic Thinking for Finger, Hand, or Wrist Injury. *Clin Orthop Relat Res.* 2018;476(4):706-713.

27. McCambridge J, Witton J, Elbourne DR. Systematic review of the Hawthorne effect: new concepts are needed to study research participation effects. *J Clin Epidemiol.* 2014;67(3):267-277.

28. Rhemrev SJ, van Leerdam RH, Ootes D, Beeres FJ, Meylaerts SA. Non-operative treatment of non-displaced scaphoid fractures may be preferred. *Injury.* 2009;40(6):638-641.

29. Hannemann PF, Brouwers L, van der Zee D, et al. Multiplanar reconstruction computed tomography for diagnosis of scaphoid waist fracture union: a prospective cohort analysis of accuracy and precision. *Skeletal Radiol.* 2013;42(10):1377-1382.

30. Buijze GA, Wijffels MM, Guitton TG, et al. Interobserver reliability of computed tomography to diagnose scaphoid waist fracture union. *J Hand Surg Am.* 2012;37(2):250-254.

31. Bernstein DN, Houck JR, Hammert WC. A Comparison of PROMIS UE Versus PF: Correlation to PROMIS PI and Depression, Ceiling and Floor Effects, and Time to Completion. *J Hand Surg Am.* 2019;44(10):901 e901-901 e907.

32. Becker SJ, Bruinsma WE, Guitton TG, et al. Interobserver Agreement of the Eaton-Glickel Classification for Trapeziometacarpal and Scaphotrapezial Arthrosis. *J Hand Surg Am.* 2016;41(4):532-540 e531.

33. Crijns TJ, Bernstein DN, Ring D, Gonzalez RM, Wilbur D, Hammert WC. Depression and Pain Interference Correlate With Physical Function in Patients Recovering From Hand Surgery. *Hand (N Y).* 2018:1558944718777814.

34. Ring D, Kadzielski J, Fabian L, Zurakowski D, Malhotra LR, Jupiter JB. Self-reported upper extremity health status correlates with depression. *J Bone Joint Surg Am.* 2006;88(9):1983-1988.

35. Das De S, Vranceanu AM, Ring DC. Contribution of kinesophobia and catastrophic thinking to upper-extremity-specific disability. *J Bone Joint Surg Am.* 2013;95(1):76-81.

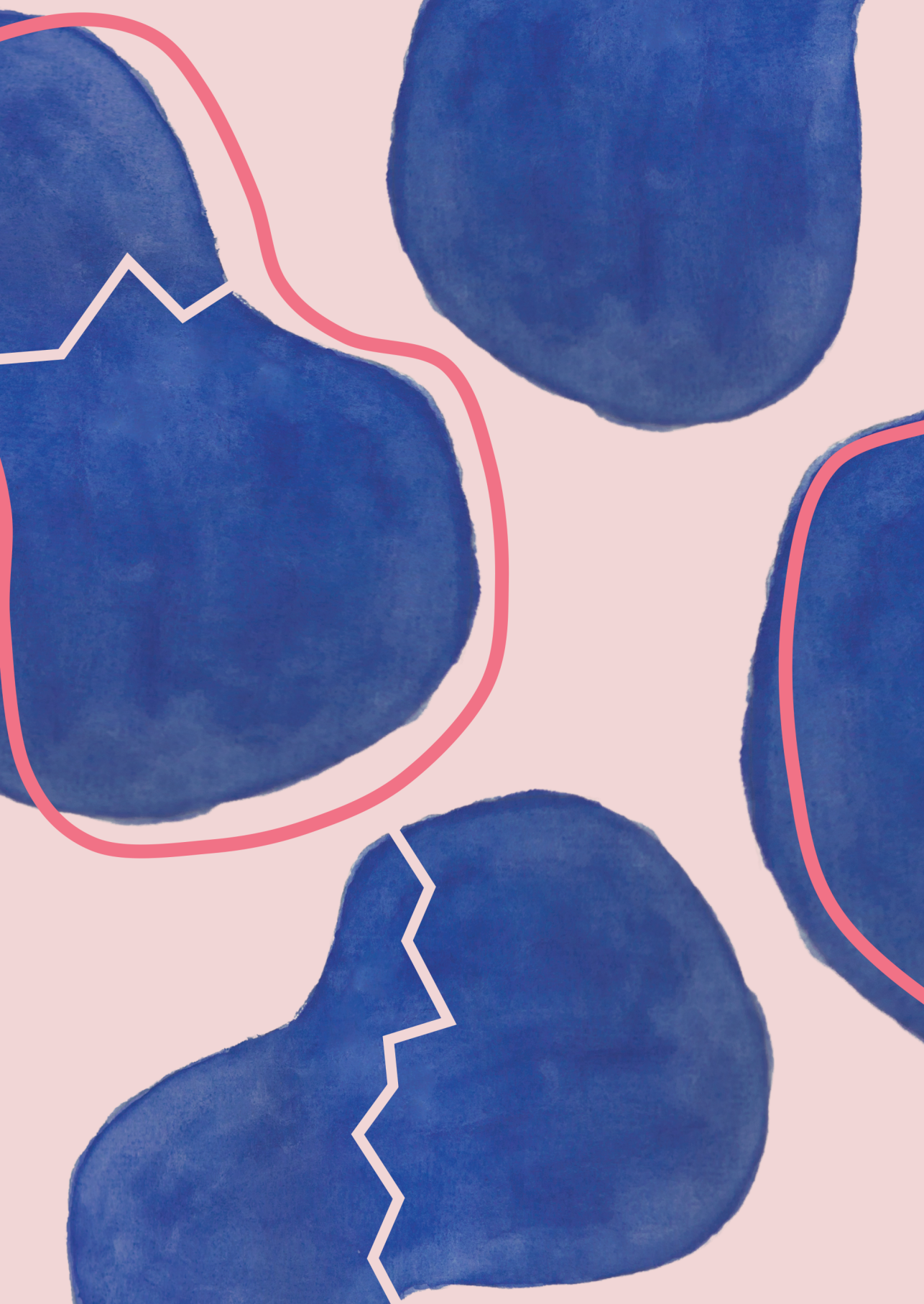

PART V

GENERAL DISCUSSION

CHAPTER 11

Summary

PART I – SCAPHOID FRACTURES: WHAT IS THE PROBLEM?

As described in **Chapter 1 (Part I),** in this thesis we investigated the overdiagnosis and overtreatment of (nondisplaced) scaphoid waist fractures. We aimed to increase diagnostic efficiency and treatment functionality in three parts:

1. Improve efficiency and accuracy of acute scaphoid fracture diagnosis (**Part II -** Diagnosis of the [Suspected] Scaphoid Fracture);

2. Differentiate fractures that heal predictably from those that are at an increased risk of nonunion (**Part III -** Scaphoid Fracture Characteristics);

3. Investigate surgeon decision making with regards to the recommendation for prolonged cast immobilization (**Part IV -** Immobilization Duration of a Nondisplaced Scaphoid Waist Fracture).

To understand the challenges in the diagnosis and treatment of scaphoid fractures, a thorough understanding of scaphoid anatomy is essential. In **Chapter 2** we presented a literature review of scaphoid anatomy. Great variability has been reported in literature on scaphoid osseous and ligamentous anatomy. Interindividual variations in both shape and ligament attachments are likely to result in distinct kinematic patterns. The difficult diagnosis of scaphoid fractures is typically attributed to its complex 'boat-shaped' form, its oblique orientation relative to the distal radius and the multiple articulations with adjacent bones. As such, CT reconstructions along the oblique axis of the scaphoid have proven more accurate for evaluating a scaphoid fracture than standard coronal, sagittal and axial sequences. The relatively high risk of nonunion is frequently attributed to the fragile retrograde blood supply.

The fear of symptomatic scaphoid nonunion largely accounts for the fear of undertreatment among surgeons. In **Chapter 3** risk factors and preferred management options for scaphoid nonunion and scaphoid nonunion advanced collapse (SNAC) were outlined through a systematic literature review. Proximal fracture location, displacement and delayed treatment were identified as risk factors for nonunion. Established nonunions (> 6 months) are typically treated with bone grafts and internal fixation. In the absence of avascular necrosis, vascularized bone grafts and non-vascularized bone grafts are equivalent in terms of union rate (88% versus 92%, respectively) and functional outcomes. In unstable nonunions with a humpback deformity, corticocancellous grafts allow for restoration of carpal alignment, resulting in better functional outcomes compared to non-structural cancellous grafts. There was insufficient evidence to support the use of adjunctive treatments such as pulsed electromagnetic field therapy, low intensity pulsed ultrasound or recombinant human bone morphogenetic proteins. In stage II-III SNAC wrists proximal row carpectomy (PRC) and 4 corner arthrodesis (4CA) yield comparable

results in terms of pain relief and range of motion. However, 4CA is associated with a higher complication rate (29%) compared to PRC (14%). Overall, the quality of the evidence on risk factors and management of scaphoid nonunion was low to moderate due to methodological limitations and heterogeneity among studies.

PART II – DIAGNOSIS OF A (SUSPECTED) SCAPHOID FRACTURE

In Part II of this thesis, we focussed on the diagnostic pathway of patients presenting with clinical signs of a scaphoid fracture. We investigated strategies to improve diagnostic accuracy of radiographs and MRI and reduce the number of patients undergoing advanced imaging.

In **Chapter 4** a clinical prediction rule was designed to selectively initiate advanced imaging in patients with a suspected scaphoid fracture. A Machine Learning (ML) algorithm was developed to estimate the probability of a scaphoid fracture, based on a combined cohort of 422 patients presenting with radial sided wrist pain after acute wrist trauma. The ML algorithm accurately predicted the probability of a scaphoid fracture based on 4 four simple and objective variables: pain in the anatomic snuffbox on ulnar deviation (<72 hours after injury), patient sex, age and mechanism of injury. The algorithm was incorporated in a clinical decision rule. This rule proposes to initiate advanced imaging (MRI or CT) in patients with clinical signs of a fracture but negative radiographs when the ML estimated probability of a scaphoid fracture is ≥10%. At this threshold, the ML algorithm yielded a 100% sensitivity and 38% specificity for the diagnosis of a scaphoid fracture in our cohort. Based on internal validation on the current study cohort, it was estimated that this rule has the potential of reducing the number of patients undergoing MRI or CT with a third (36%), with a very small risk of missing a fracture. External validation in a prospective setting is required prior to implementation.

In **Chapter 5** a convoluted neural network (CNN) was trained to detect scaphoid fractures on radiographs, based on 300 patients reviewed for a possible scaphoid fracture. The CNN yielded an area under the curve (AUC) of 0.77. The CNN correctly diagnosed 72 out of 100 patients (accuracy 72%). Forty-two out of 50 patients with an MRI or CT confirmed fracture were correctly identified (sensitivity: 84%). Twenty out of 50 patients without a fracture were incorrectly diagnosed as having a scaphoid fracture (specificity: 60%). Adding patient sex and age to the CNN derived probabilities of a fracture did not improve the ability to differentiate between patients with and without a fracture. Surgeons outperformed the CNN in terms of accuracy (84% [95%CI 81-88%]) versus 72% [95% CI 60-84%]) and specificity (93% [95% CI 87-99%] versus (60% [95% CI 46-74%]). Sensitivity was comparable for CNN (84% [95% CI 74-94%]) and human observers (76%; 95% CI 70-82%). Although our study demonstrates the potential for CNN detection of scaphoid fractures, the current model cannot replace human assessment.

In **Chapter 6** we evaluated patterns of signal change present among 267 MRI scans of patients with a clinically suspected scaphoid waist fracture. Signal changes were present in 34% of the scans. In 5.6% of the scans signal changes were categorized as "looks like a scaphoid waist fracture". Only four in this category (1.5%) were classified as "clearly a waist fracture". Fourteen percent (14%) of the MRI scans showed signal variation categorized as "might be confused for a scaphoid waist fracture". Fifteen percent (15%) was categorized as "clearly not a scaphoid waist fracture". The interobserver reliability of differentiating patterns was moderate to substantial (kappa: 0.55-0.62). Male patients were more likely to have signal changes that "look like a scaphoid waist fracture". Based on the following findings - 1) the high prevalence of signal changes that may be confused for a scaphoid waist fracture, 2) the low prevalence of signal changes that clearly represent a scaphoid waist fracture, 3) the moderate to substantial interobserver reliability of distinguishing between categories of signal change and 4) the low prevalence (i.e. low pre-test odds) of a true fracture among patients with a suspected scaphoid fracture – we conclude that MRI carries a notable risk of overdiagnosis and potentially overtreatment among patients with a suspected scaphoid fracture.

PART III – SCAPHOID FRACTURE CHARACTERISTICS

The correlation between fracture characteristics and clinical outcomes such as union rate has been well established. In Part III of this thesis, we aimed to identify recurring fracture patterns and investigate how they relate to displacement and comminution. This may aid in scaphoid fracture diagnosis and in recognizing and differentiating fractures that heal predictably from those that are at an increased risk of nonunion.

In **Chapter 7** 3DCT analysis revealed four dominant fracture patterns among 75 patients with an acute scaphoid fracture: proximal pole fractures (7%), transverse waist fractures (37%), oblique waist fractures (32%) and tubercle or distal pole fractures (12%). Comminution was present in 52% of the fractures. Sixty-four percent of the fractures were displaced. In this selected series of CT scans, transverse fractures of the waist had a significantly higher incidence of displacement (79%) compared to proximal pole (33%), oblique waist (63%) and distal pole fractures (1%). Oblique waist fractures showed a higher incidence of comminution (67%) versus proximal pole (17%), transverse waist (54%) and tubercle (13%) fractures. Ninety percent of the comminuted fractures were displaced. Distinguishing transverse and oblique waist fractures can be important as these fracture types may differ in terms of fracture stability and/or risk of displacement. Also, fracture plane orientation can determine fixation strategy.

Scaphoid fracture displacement is the most important predictor of nonunion. In **Chapter 8** we used 3DCT analysis to investigate the correlation between fracture configuration (fracture location and comminution) and displacement in 51 proximal pole and waist fractures. Fracture location was analysed in terms of the location of the cortical

breach on the volar and dorsal side of the scaphoid, corresponding to the fractures' "entry"- and "exit point", respectively.

The location of the cortical breach on the dorsal side of the scaphoid (i.e. "dorsal fracture location") and the presence of comminution were closely correlated to displacement pattern. As fracture location on the dorsal side of the scaphoid became more distal, translation (ulnar, proximal, volar) and angulation (flexion, pronation) of the distal fragment relative to the proximal fragment increased. Comminuted fractures had more displacement. The correlation between dorsal fracture location and displacement pattern can be attributed to the dorsal localization of the dorsal intercarpal (DIC) and dorsal scapholunate (dSL) ligaments as important stabilizers. As dorsal fracture location predictably dictates the direction of translation and angulation, surgeon attention to dorsal fracture location can help identify patterns of displacement. This may provide guidance in adequately reducing a displaced scaphoid fracture.

PART IV – IMMOBILIZATION DURATION OF A NONDISPLACED SCAPHOID WAIST FRACTURE

There is increasing evidence that CT-confirmed nondisplaced scaphoid waist fractures heal with shorter (<8 weeks) immobilization duration. In Part IV of this thesis, we identified potential barriers to adopting shorter immobilization times by investigating factors affecting surgeon decision making.

In **Chapter 9** we identified factors associated with surgeon recommendation for additional cast immobilization of a CT-confirmed nondisplaced scaphoid waist fracture through an international survey-based study. Two-hundred-and-eighteen (218) orthopaedic, trauma and (plastic) hand and wrist surgeons were asked to recommend for or against additional immobilization (>8 and >12 weeks) in 16 fictional scenarios. Unclear healing on radiographs, the presence of fracture tenderness and 8 weeks of completed immobilization (versus 12) were the most important factors associated with surgeon recommendation for additional immobilization. Female surgeons, surgeons not specialized in orthopaedic trauma or upper extremity surgery and surgeons practicing outside of Europe were more likely to recommend additional immobilization. The results of this study suggest that the adoption of shorter immobilization times may be hindered by surgeons' overreliance on fracture tenderness and radiographic appearance of fracture union. This is in conflict with evidence that diagnosis of scaphoid fracture union on radiographs is unreliable and that pain intensity is strongly related to psychosocial factors in patients with upper extremity injury. Furthermore, the lack of consensus among surgeons in this study, illustrates the need for evidence-based guidelines on cast duration.

In **Chapter 10** we identified clinical, radiological and psychosocial factors associated with continued immobilization of a nondisplaced scaphoid waist fracture among a prospective cohort of 46 patients. Inadequate radiographic healing, as rated by the

treating surgeon, and higher symptoms of depression were independently associated with continued immobilization after 6 weeks of completed cast wear. Contrarily to the findings in Chapter 9, pain on examination was not associated with continued immobilization. These findings confirm that surgeon recommendation for additional cast immobilization is associated with factors unlikely to be related to the probability of union. This includes radiographic appearance and likely illness behaviour associated with symptoms of depression. To give patients the option of shorter immobilization duration, surgeons may need to accept uncertainty of radiographic appearance and anticipate variations in patient illness behaviour.

CHAPTER 12

Discussion and Future Perspectives

DISCUSSION AND FUTURE PERSPECTIVES

When evaluating a patient with a (suspected) scaphoid fracture, the restrictions and potential harm imposed by unnecessary diagnostics and treatment must be weighed against the risks of a missed or undertreated fracture. This thesis provided insights into the barriers to adopting more efficient diagnostic and treatment protocols. The overall objective was to identify strategies to reduce unhelpful (advanced) imaging and immobilization in patients with a suspected or confirmed scaphoid waist fracture.

PART I – SCAPHOID FRACTURES WHAT IS THE PROBLEM?

Surgeons' fear of undertreatment may lead to overdiagnosis and overtreatment of patients with a (suspected) scaphoid fracture. The potential risk of a symptomatic nonunion - and possibly the fear of medicolegal consequences - largely account for this fear.

Traditionally, nonunion rates up to 34% have been reported.[1,2] Given the increasing and compelling evidence on the relation between fracture displacement and the risk of nonunion, one may speculate that the nonunion reported in older series primarily concern displaced scaphoid fractures. Unfortunately, many of the older series did not diagnose displacement or used radiographs to diagnose displacement. Evidence on the risk of nonunion in an untreated nondisplaced scaphoid fracture that is *not visible* on radiographs is lacking. Similarly, our knowledge on the natural history – and thus incidence of nonunion - among untreated fractures is lacking. This is largely because only patients with a symptomatic nonunion are evaluated.[3] The correlation between symptoms and disease in nonunions therefore remains unclear. As a result, some of our decision making may be based more on tradition and habit rather than on scientific data.

PART II - DIAGNOSIS OF A TRUE SCAPHOID FRACTURE

Diagnosing a true scaphoid waist fracture is the first and perhaps most vexing challenge when evaluating a patient with a suspected scaphoid fracture. The findings of this thesis confirm the two core obstacles in acute scaphoid fracture diagnosis. Firstly, the absence of a consensus reference standard and secondly, the low prevalence of true fractures among suspected scaphoid fractures - 5.6% in this thesis. Based on a 5% prevalence of true fractures among patients evaluated for a clinically suspected scaphoid fracture and a 99% sensitivity and 94% specificity of MRI; the odds that a patient with a positive MRI has a true scaphoid fracture is only 46% (according to Bayes Theorem).[4,5] In other words, it is more likely that a patient with a positive MRI does *not* have a fracture and is treated unnecessarily with 6 weeks of cast immobilization.[4,5]

This thesis presented innovative strategies aiming to improve diagnostic accuracy and increase the prevalence of true scaphoid waist fractures among patients with a

clinically suspected fracture. The first strategy, a ML-decision rule, demonstrated the potential to reduce the number of patients undergoing costly imaging such as CT or MRI with a third (36%). Unfortunately, the prevalence of true fractures among patients with a suspected fracture remained as low as 8.7% among the selected group of patients identified as 'high risk' by the ML-algorithm. As such, the decision rule appears effective at reducing the use of costly diagnostic modalities such as MRI and CT. However, in its current form, it is unlikely to further increase diagnostic accuracy of MRI or CT by increasing the pre-test odds. Better results may be yielded by training the algorithm on larger datasets, focussing on patients with negative radiographs only. Furthermore, the clinical decision rule needs to be externally validated in a prospective setting before it can be implemented in clinical practice.

As a second strategy, a Convolutional Neural Network (CNN) was developed to improve the diagnosis of scaphoid fractures on radiographs. This may potentially reduce the need for advanced imaging. The diagnostic performance of the algorithm did not exceed human observers (orthopaedic surgeons) and is currently not able to replace human assessment. While this may suggest that deep learning may be more suitable for the diagnosis of more obvious fractures instead of radiographically subtle (or invisible) fractures, it is possible that performance may improve when trained on a larger dataset. Also, techniques such as attention regularization through annotation may improve diagnostic accuracy.[6] Annotation techniques allow the attention of the algorithm to be guided to the area of interest by annotating this area (i.e. scaphoid waist area). In a follow up study of our group, annotation methods increased accuracy from 76% to 83%.[6] Overall, while CNN may not replace human observers altogether, its potential as an adjunct to human assessment is promising.

Although MRI and CT are considered the best available imaging modalities for scaphoid fractures[7], our analysis of MRIs confirmed important limitations. The evaluation of MRI signal changes among patients with a suspected scaphoid waist fracture, suggests that MRI carries a notable risk of overdiagnosis. Furthermore, the reliability in distinguishing between patterns of MRI signal change was limited. To increase the reliability and accuracy of scaphoid fracture diagnosis on MRI, future research should focus on establishing and validating a consensus definition of the signal changes that represent a scaphoid waist fracture. To date, conflicting definitions continue to exist of what constitutes a scaphoid fracture on MRI. While some consider a zone of bone marrow oedema a fracture[8], others require the presence of a cortical or trabecular fracture line.[9] The characterization of signal changes presented in this thesis may aid in establishing a consensus definition.

Despite their limitations, the innovative strategies presented in this thesis lay the foundation for a new and promising field of research employing ML for scaphoid fracture diagnosis. Ideally, algorithms are used in conjunction, combining demographic, clinical and radiographic data to improve risk stratification. Whether a CNN can be used for pattern recognition of MRI signal changes and ultimately differentiate non fractures from fractures merits further investigation.

PART III - FRACTURE CHARACTERISTICS

Fracture characteristics correlate closely to the risk of nonunion and therefore largely determine treatment. For instance, displaced[10,11] and proximal pole fractures[1,12] are at a higher risk of nonunion and therefore benefit from surgical fixation. Conversely, CT confirmed nondisplaced scaphoid waist fractures are known to heal reliably with cast immobilization.[10,11,13,14] Recognizing fracture types associated with a higher risk of nonunion - and differentiating those from fractures that heal predictably - is therefore important to allow for more patient specific treatment options.

The four dominant fracture patterns established in this thesis- 1) proximal pole- ; 2) transverse waist- ; 3) oblique waist- and 4) tubercle fracture - largely correspond to the frequently used Herbert classification[15] Our finding that waist fractures can be divided into transverse and oblique waist fractures, contradict the results by Luria et al. who described waist fractures to be horizontal oblique rather than transverse.[16] We also found that transverse waist fractures were more frequently displaced than oblique waist fractures. This suggests that these fracture types may indeed be two separate entities, behaving in different manners.

Fracture displacement - the biggest risk factor for scaphoid nonunion - can be challenging to diagnose on radiographs and even CT.[17,18] Using 3DCT we investigated how fracture characteristics correlate to displacement. The finding that the location of the cortical breach on the dorsal side of the scaphoid (i.e. the fracture's "exit point") predictably dictates the pattern of displacement, can aid surgeons in recognizing displacement. It also reinforces the previous observation that transverse waist fractures – typically exiting distal to the scaphoid apex - were most frequently displaced. The correlation between dorsal fracture location and displacement can be attributed to the dorsal localization of important ligamentous stabilizers of the scaphoid. Oblique waist and proximal pole fractures have a more proximal dorsal fracture location. These fractures largely propagate proximal to the attachments of the dorsal intercarpal- (DIC) and dorsal scapholunate (dSL) ligament. By contrast, transverse waist fractures have a more distal dorsal fracture location. These fractures propagate largely distal to these ligamentous attachments, accounting for the greater degree of translation and angulation observed.

While the studies in this thesis are limited by their selection bias of patients that had CT, they emphasize the importance of carefully considering fracture characteristics when evaluating a patient with a scaphoid fracture. We therefore recommend CT in all patients with an (established) scaphoid fracture to accurately assess fracture characteristics. Elaborating on the findings in this thesis, the next steps are, firstly, to investigate whether fracture patterns correlate with clinical outcome and can therefore be used to guide treatment. For example, can dorsal fracture location be used to determine which patients benefit most from surgery? Secondly, we need to establish whether dorsal fracture location can be reliably assessed on readily available modalities such as two-dimensional CT. Another important knowledge gap is how fracture displacement and stability relate. While displaced fractures are considered unstable, some nondisplaced fractures have

equally proven unstable intra-operatively.[17] The correlation between dorsal fracture location in relation to ligamentous attachments may provide insights into fracture stability in (non)displaced fractures.

PART IV - CAST DURATION

The increased understanding of the link between displacement and the risk of scaphoid nonunion has allowed us to consider shorter immobilization times for CT-confirmed nondisplaced scaphoid waist fractures. Among studies investigating CT- or MRI-confirmed nondisplaced scaphoid waist fractures, the union rate was found to be near 100% (99.4%) following nonoperative treatment.[10,11,14,19] It is therefore notable that in this thesis, 47% and 21% of the surgeons recommended cast duration beyond 8 and 12 weeks, respectively.

Through an international survey based- and prospective cohort study we found that surgeon decision making is influenced by factors that are unlikely to be associated with the probability of union: fracture tenderness upon examination and radiographic appearance of fracture union. This is in spite of the evidence that radiographs are unreliable and inaccurate for assessing scaphoid union 6-12 weeks after fracture.[20] Similarly, fracture tenderness may not be a helpful measure of fracture union, given the compelling evidence that pain intensity is strongly associated with symptoms of depression and less effective coping strategies among patients with upper extremity injury.[21,22] Also, patients recovering from a scaphoid fracture are likely to experience some residual tenderness. The finding that patients with greater symptoms of depression were more likely to be prescribed additional cast immobilization, suggests that surgeons are responding to some aspects of illness behaviour that are related to symptoms of depression. Further research into how patient illness behaviour affects surgeon decision making is merited. This may aid surgeons in accounting for variations in illness behaviour in their decision making and possibly reduce overtreatment. Furthermore, it may reveal targets to enhance recovery in patients recovering from a scaphoid waist fracture.

The variation in recommendation for cast duration among surgeons of different (sub) specialties, nationalities and gender emphasizes the lack of evidence-based decision-making. We are therefore in need of clearer guidelines with regards to mobilization time, and how, or if, union can reliably be assessed within 4 to 8 weeks after injury. While there is an increase in the use of CT to assess union, it is not clear whether CT appearance of union correlates well with the need for additional immobilization.[19] This finding suggests that a shorter duration of immobilization will only be possible if surgeons are influenced less by radiographic appearance and rely more on the evidence that a CT-confirmed nondisplaced scaphoid fracture heals predictably, even with relatively short immobilization. Ideally, studies investigating 6 or 8 weeks of immobilization regardless of radiographic appearance of union are to be pursued. To safely reduce immobilization times, the need for CT to reliably rule out displacement must be emphasized.

CONCLUSION AND RECOMMENDATION FOR CLINICAL PRACTICE

In this thesis we have identified barriers to adopting more efficient diagnostic and functional treatment protocols when treating a patient with a (suspected) scaphoid fracture. Strategies proposed to reduce overdiagnosis and overtreatment of patients with a (suspected) scaphoid fracture included 1) a ML-decision rule to selectively identify patients that benefit from advanced imaging; 2) a CNN to improve the diagnosis of scaphoid fractures on radiographs; 3) characterization of patterns of scaphoid MRI signal change to facilitate recognition of a true scaphoid fracture; 4) identification of fracture patterns to recognize fractures that are associated with a higher risk of nonunion and differentiate those from fractures that heal predictably using 3DCT; 5) insights into surgeon recommendation for prolonged cast immobilization. Evidently, most strategies in this thesis require further validation or investigation prior to implementation. Figure 1 presents a preliminary workflow regarding the recommendations proposed in this thesis

Following the rapid innovations in technology, it may be appealing to rely solely on sophisticated techniques - such as deep learning and 3DCT - for scaphoid fracture diagnosis and to guide us in treatment decisions. However, it is important to realize that the modalities presented in this thesis can only provide us with more accurate probability estimates. Therefore, to successfully implement strategies that reduce overdiagnosis and overtreatment, a paradigm shift amongst those caring for patients with a (suspected) scaphoid fracture may be required. Surgeons may need to acknowledge and accept that in scaphoid fracture diagnosis we continue to deal in probabilities. In this complex situation, involving patients in decision making is paramount, to be able to offer treatment options that best correspond to their values and preferences. Furthermore, to give patients the option of shorter immobilization, surgeons may need to trust the evidence that CT-confirmed nondisplaced scaphoid waist fractures heal predictably with a shorter period of immobilization. This involves accepting uncertainty of radiographic appearance and anticipating variations in patient illness behaviour when assessing scaphoid union.

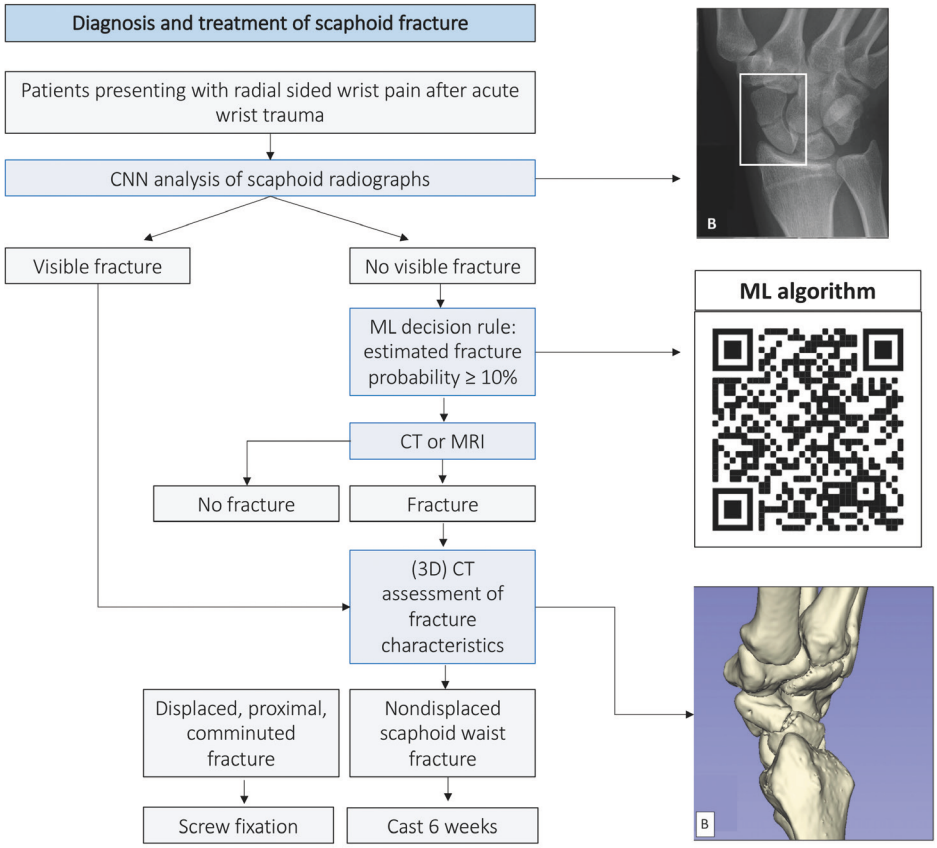

Figure 1. Preliminary workflow for the (suspected) scaphoid fracture

REFERENCES

1. Eastley N, Singh H, Dias JJ, Taub N. Union rates after proximal scaphoid fractures; meta-analyses and review of available evidence. *J Hand Surg Eur Vol.* 2013;38(8):888-897.
2. Merrell GA, Wolfe SW, Slade JF, 3rd. Treatment of scaphoid nonunions: quantitative meta-analysis of the literature. *J Hand Surg Am.* 2002;27(4):685-691.
3. Buijze GA, Ochtman L, Ring D. Management of scaphoid nonunion. *J Hand Surg Am.* 2012;37(5):1095-1100; quiz 1101.
4. Ring D, Lozano-Calderon S. Imaging for suspected scaphoid fracture. *J Hand Surg Am.* 2008;33(6):954-957.
5. Henry SL, Ring D. Chapter 1 - Using Evidence to Manage Scaphoid Fractures. In: Buijze GA, Jupiter JB, eds. *Scaphoid Fractures: Evidence-Based Management.* Elsevier; 2018:1-5.
6. Boxel van MF, Liao Z, Bulstra AE, et al. Improving the Performance of a Convolutional Neural Network in Detecting Scaphoid Fractures by Attention Regularization with Minimal Effort Annotation. *Submitted to J Bone Joint Surg Am.* 2022.
7. Mallee WH, Wang J, Poolman RW, et al. Computed tomography versus magnetic resonance imaging versus bone scintigraphy for clinically suspected scaphoid fractures in patients with negative plain radiographs. *Cochrane Database Syst Rev.* 2015(6):CD010023.
8. Mallee W, Doornberg JN, Ring D, van Dijk CN, Maas M, Goslings JC. Comparison of CT and MRI for diagnosis of suspected scaphoid fractures. *J Bone Joint Surg Am.* 2011;93(1):20-28.
9. Memarsadeghi M, Breitenseher MJ, Schaefer-Prokop C, et al. Occult scaphoid fractures: comparison of multidetector CT and MR imaging--initial experience. *Radiology.* 2006;240(1):169-176.
10. Bhat M, McCarthy M, Davis TR, Oni JA, Dawson S. MRI and plain radiography in the assessment of displaced fractures of the waist of the carpal scaphoid. *J Bone Joint Surg Br.* 2004;86(5):705-713.
11. Geoghegan JM, Woodruff MJ, Bhatia R, et al. Undisplaced scaphoid waist fractures: is 4 weeks' immobilisation in a below-elbow cast sufficient if a week 4 CT scan suggests fracture union? *J Hand Surg Eur Vol.* 2009;34(5):631-637.
12. Grewal R, Lutz K, MacDermid JC, Suh N. Proximal Pole Scaphoid Fractures: A Computed Tomographic Assessment of Outcomes. *J Hand Surg Am.* 2016;41(1):54-58.
13. Clementson M, Jorgsholm P, Besjakov J, Thomsen N, Bjorkman A. Conservative Treatment Versus Arthroscopic-Assisted Screw Fixation of Scaphoid Waist Fractures--A Randomized Trial With Minimum 4-Year Follow-Up. *J Hand Surg Am.* 2015;40(7):1341-1348.
14. Grewal R, Suh N, MacDermid JC. Is Casting for Non-Displaced Simple Scaphoid Waist Fracture Effective? A CT Based Assessment of Union. *Open Orthop J.* 2016;10:431-438.
15. Herbert TJ, Fisher WE. Management of the fractured scaphoid using a new bone screw. *J Bone Joint Surg Br.* 1984;66(1):114-123.
16. Luria S, Schwarcz Y, Wollstein R, Emelife P, Zinger G, Peleg E. 3-dimensional analysis of scaphoid fracture angle morphology. *J Hand Surg Am.* 2015;40(3):508-514.
17. Buijze GA, Jorgsholm P, Thomsen NO, Bjorkman A, Besjakov J, Ring D. Diagnostic performance of radiographs and computed tomography for displacement and instability of acute scaphoid waist fractures. *J Bone Joint Surg Am.* 2012;94(21):1967-1974.
18. Lozano-Calderon S, Blazar P, Zurakowski D, Lee SG, Ring D. Diagnosis of scaphoid fracture displacement with radiography and computed tomography. *J Bone Joint Surg Am.* 2006;88(12):2695-2703.
19. Buijze GA, Goslings JC, Rhemrev SJ, et al. Cast immobilization with and without immobilization of the thumb for nondisplaced and minimally displaced scaphoid waist fractures: a multicenter, randomized, controlled trial. *J Hand Surg Am.* 2014;39(4):621-627.

20. Hannemann PF, Brouwers L, Dullaert K, van der Linden ES, Poeze M, Brink PR. Determining scaphoid waist fracture union by conventional radiographic examination: an analysis of reliability and validity. *Arch Orthop Trauma Surg.* 2015;135(2):291-296.

21. Gonzalez AI, Kortlever JTP, Crijns TJ, Ring D, Reichel LM, Vagner GA. Pain during physical examination of a healing upper extremity fracture. *J Hand Surg Eur Vol.* 2020:1753193420952010.

22. Vranceanu AM, Bachoura A, Weening A, Vrahas M, Smith RM, Ring D. Psychological factors predict disability and pain intensity after skeletal trauma. *J Bone Joint Surg Am.* 2014;96(3):e20.

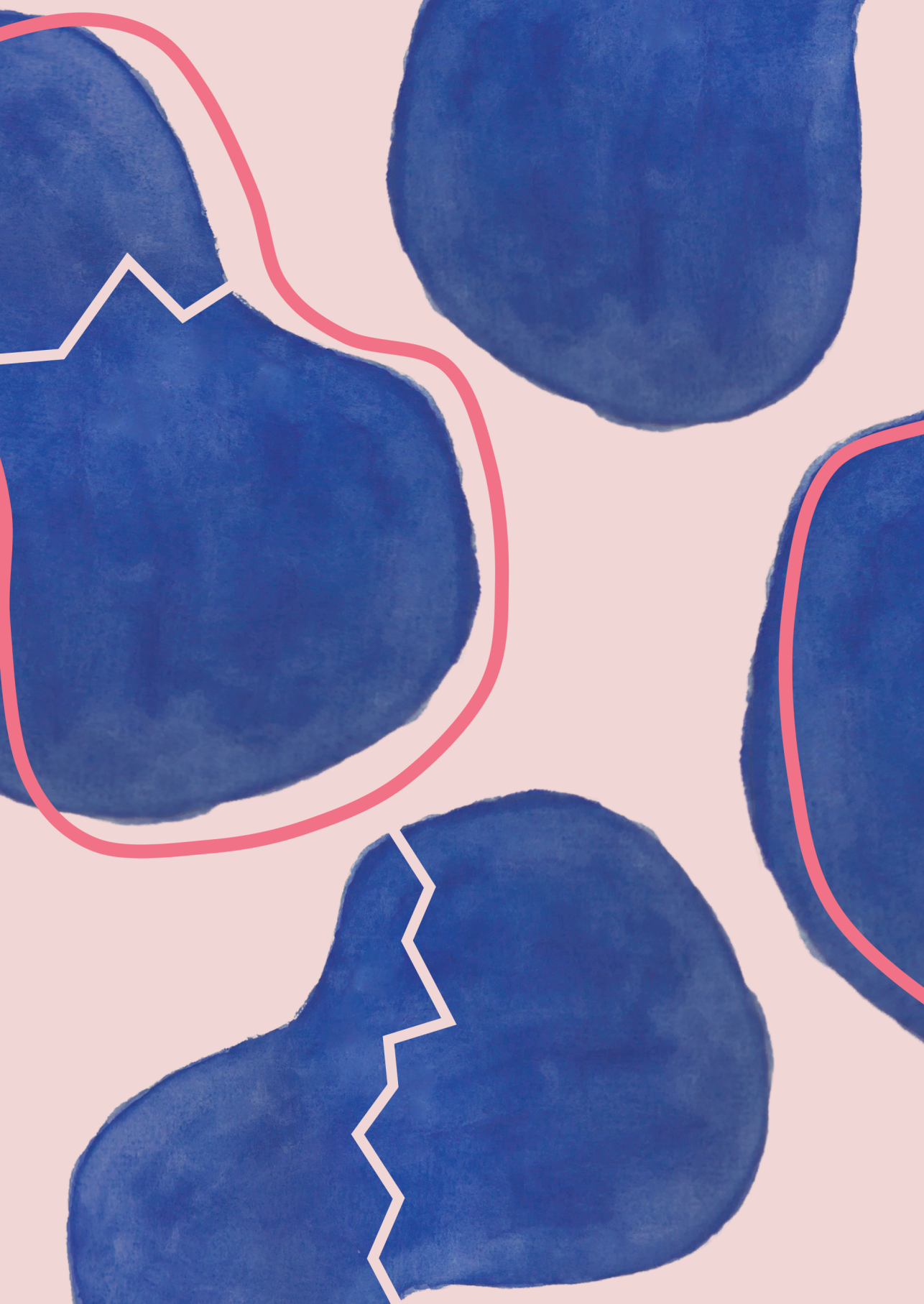

PART VI

APPENDICES

NEDERLANDSE SAMENVATTING

DEEL I – SCAPHOÏDFRACTUREN: WAT IS HET PROBLEEM?

Een scaphoïdfractuur is een breuk van het scheepsvormige handwortelbeentje (os scaphoïdeum) van het polsgewricht. Het is een veel voorkomende breuk die meestal optreedt na een val op uitgestrekte hand. Een breuk van het scaphoïd is moeilijk te diagnosticeren. Ongeveer 1 op de 5 breuken wordt bij de initiële presentatie gemist op röntgenonderzoek. Ook is dit type breuk van oudsher berucht vanwege het risico op pseudoartrose (een zogenaamde 'nonunion') wanneer de diagnose gemist wordt, of wanneer de breuk inadequaat behandeld wordt. Pseudoartrose kan in sommige gevallen leiden tot pijn en een verminderde beweeglijkheid van de pols. De vrees onder artsen voor een gemiste diagnose en het 'onderbehandelen' van een scaphoïdfractuur, leidt veelal tot een defensief beleid.

Patiënten met symptomen van een scaphoïdfractuur zonder aantoonbare breuk op röntgenonderzoek, worden met gips behandeld totdat herhaald of aanvullend onderzoek wordt verricht. In de praktijk omvat dit vaak twee weken gipsimmobilisatie waarna het röntgenonderzoek herhaald wordt. Het resultaat van dit beleid is, dat ongeveer 4 op de 5 patiënten met een klinische verdenking op een scaphoïdfractuur – zonder aantoonbare breuk op röntgenonderzoek – onnodig met gips worden behandeld tot nadere diagnostiek verricht wordt. Daarnaast worden patiënten met een bewezen breuk tot wel 8 tot 12 weken met gips geïmmobiliseerd. Dit is in strijd met toenemend bewijs dat 4 tot 6 weken gipsbehandeling voldoende is voor simpele niet-gedisloceerde breuken van de schacht.

Zoals wordt toegelicht in **Hoofdstuk 1 (Deel I)**, richt dit proefschrift zich op de overbehandeling en overdiagnostiek van scaphoïdfracturen. De doelstelling van het proefschrift was om de doelmatigheid van de diagnostiek en behandeling van patiënten met een (verdenking op een) scaphoïdfractuur te verbeteren middels drie pijlers.

In **Deel II -** *Diagnostiek bij een verdenking op een scaphoïdfractuur* **-** streefden we naar het verbeteren van de diagnostische efficiëntie en nauwkeurigheid.

In **Deel III** – *Fractuurkarakteristieken* - werd getracht onderscheid te maken tussen breuken die probleemloos genezen met een niet-operatieve behandeling, en breuken met een hoger risico op het ontwikkelen van pseudartrose en derhalve een eventuele operatie-indicatie hebben.

In **Deel IV** - *Duur van gipsimmobilisatie van de niet-gedisloceerde scaphoïd schachtfractuur* - onderzochten we de besluitvorming van chirurgen met betrekking tot het aanbevelen van een verlengde gipsduur.

Anatomische kennis van het scaphoïd en aanhechtende ligamenten is essentieel om de uitdagingen rondom de diagnostiek en behandeling van scaphoïdfracturen te doorgronden. **Hoofdstuk 2** was gericht op de anatomie van het scaphoïd middels een

uiteenzetting van anatomische studies. Er bestaat veel variatie in zowel de ossale als ligamentaire anatomie van het scaphoïd. Het is aannemelijk dat deze anatomische variaties resulteren in verschillende bewegingspatronen. De moeizame diagnose van scaphoïdfracturen op röntgenonderzoek wordt veelal gewijd aan de complexe vorm, de schuine oriëntatie ten opzichte van de radius en de multipele articulaties met de radius en carpalia. Daardoor, zijn CT-reconstructies in de schuine as van het scaphoïd accurater gebleken dan standaard CT-opnames in coronale, sagittale en transversale richtingen. Het relatief hoge risico op pseudoartrose na een scaphoïdfractuur is te wijten aan de fragiele retrograde bloedtoevoer van het scaphoïd.

In **Hoofdstuk 3** werden de risicofactoren en behandelopties voor pseudartrose van het scaphoïd en de zogenaamde SNAC-pols (Scaphoid Nonunion Advanced Collaps) onderzocht middels een systematische review. Als een scaphoïdfractuur 6 maanden na trauma nog niet geconsolideerd is, is er sprake van pseudartrose. Fracturen van de proximale pool en fracturen met dislocatie hebben een hoger risico op het ontwikkelen van pseudoartrose, evenals fracturen die pas na 4 weken of langer na het trauma behandeld worden. Patiënten met pseudartrose worden meestal behandeld middels interne fixatie in combinatie met een bottransplantaat. In de afwezigheid van avasculaire necrose van het scaphoïd, bleken gevasculariseerde en niet-gevascullariseerde bottransplantaten gelijkwaardig wat betreft het helingspercentage (respectievelijk, 88% en 92%) en functionele uitkomsten. In het geval van een instabiele pseudoartrose waarbij het scaphoïd inzakt (een zogenaamde 'humpback' deformiteit), kan het gebruik van een corticale spaan als bottransplantaat de vorm herstellen. Dit resulteert in een meer anatomisch herstel van het carpale gewricht en betere functionele uitkomsten ten opzichte van een niet-structureel, oftewel enkel spongieus, bottransplantaat. Er was onvoldoende bewijs om het gebruik van aanvullende therapieën zoals elektromagnetische-, ultrasone geluidsgolf-therapie of botgroeifactoren te ondersteunen. Voor de behandeling van een stadium II en III SNAC-pols, boden een proximale rij carpectomie (PRC) en carpale ('4 corner') arthrodese (4CA) gelijkwaardige resultaten wat betreft pijnverlichting en bewegingsvrijheid. 4CA is echter complicatiegevoeliger (29%) dan PRC (14%). Aanbevelingen en conclusies wat betreft de risicofactoren en behandeling van pseudartrose van het scaphoïd werden beperkt door de matige kwaliteit van onderzoeken.

DEEL II – DIAGNOSTIEK BIJ EEN VERDENKING OP EEN SCAPHOÏDFRACTUUR

In deel twee van dit proefschrift streefden we ernaar de doelmatigheid en nauwkeurigheid van het diagnostische proces van patiënten met een klinische verdenking op een scaphoïdfractuur te verbeteren. De doelstelling was om strategieën te ontwikkelen om de nauwkeurigheid van röntgen- en MRI-onderzoek te verbeteren en het aantal patiënten dat aanvullende diagnostiek ondergaat te verminderen.

In **Hoofdstuk 4** werd een klinische beslisregel ontwikkeld om te bepalen welke patiënten met klinische symptomen van een scaphoïdfracturen baat hebben bij aanvullend CT- of MRI-onderzoek. Op basis van een cohort van 422 patiënten met een klinische verdenking op een scaphoïdfractuur, werd een 'Machine Learning' (ML)-algoritme ontwikkeld om de kans op een scaphoïdfractuur te voorspellen. Het ML-algoritme kon met goede accuratesse de kans op een fractuur voorspellen op basis van 4 eenvoudig en objectieve variabelen: pijn ter plaatse van de tabatière anatomique bij ulnair deviatie van de pols, patiënt leeftijd, geslacht en ongevalsmechanisme. Het algoritme werd toegepast in een klinische beslisregel. Hierin werd aanbevolen dat patiënten met een klinische verdenking op een scaphoïdfractuur, negatief röntgenonderzoek én een ML-berekende fractuurkans van ≥ 10% een MRI- of CT-scan dienen te ondergaan. In het huidige studiecohort leverde het algoritme een sensitiviteit van 100% en een specificiteit van 38% op voor de diagnose van een scaphoïdfractuur. Ook werd er geschat dat het toepassen van deze beslisregel, het aantal patiënten dat aanvullend onderzoek ondergaat kan verminderen met een derde (36%), met slechts een zeer geringe kans op een gemiste scaphoïdfractuur. De beslisregel dient gevalideerd te worden in een extern, en bij voorkeur prospectief cohort, voordat deze geïmplementeerd kan worden.

In **Hoofdstuk 5** werd op basis van 300 patiënten met een verdenking op een scaphoïdfractuur een 'deep learning' algoritme ontwikkeld om scaphoïdfracturen te diagnosticeren op röntgenonderzoek. De 'Area Under the Receiver Operating Characteristic [ROC] Curve', oftewel AUC, van het algoritme bedroeg 0.77. Het algoritme diagnosticeerde 72 van de 100 patiënten correct (accuratesse 72%). Tweeënveertig van de 50 patiënten met een middels MRI of CT bevestigde fractuur werden correct geïdentificeerd (sensitiviteit: 84%). Twintig van de 50 patiënten zonder fractuur werden ten onrechte gediagnosticeerd met een scaphoïdfractuur (specificiteit: 60%). Het toevoegen van patiënt leeftijd en geslacht in de analyse, verbeterde de diagnostische waarde van het algoritme niet. In vergelijking met het algoritme, scoorden orthopedische traumachirurgen beter in het vaststellen van de aan- of afwezigheid van een scaphoïdfracturen wat betreft de accuratesse (84% [95% CI 81-88%]) versus 72% [95% CI 60-84%]) en specificiteit (93% [95% CI 87-99%] versus (60% [95% CI 46-74%]). De sensitiviteit was vergelijkbaar tussen orthopedische traumachirurgen en het algoritme (respectievelijk, 76%; [95% CI 70-82%] en 84% [95% CI 74-94%]). Alhoewel onze studie de potentiële bijdrage van 'deep learning' algoritmen in de diagnostiek van scaphoïdfracturen aantoont, is het huidige model nog niet in staat om menselijke beoordeling van röntgenonderzoek te vervangen.

MRI wordt in toenemende mate gebruikt om een scaphoïdfractuur te diagnosticeren. Echter, de mogelijkheid om met MRI subtiele veranderingen in signaalintensiteit vast te stellen, verhoogt ook de kans op fout positieve diagnosen. In **Hoofdstuk 6** onderzochten we patronen van signaalintensiteit op MRI-scans van patiënten met een klinische verdenking op een scaphoïdfractuur. Van de 267 scans toonde 34% van de scans veranderingen in signaalintensiteit van het scaphoïd. Slechts 5.6% van deze signalen konden geduid worden als mogelijk passend bij een scaphoïdfractuur en slechts 1.5% als evidente scaphoïdfractuur. In 14% van de scans werden er veranderingen in

signaalintensiteit waargenomen die verward zouden kunnen worden met de aanwezigheid van een scaphoïdfractuur. De lage prevalentie van scaphoïdfracturen onder patiënten met een klinische verdenking op een scaphoïdfractuur en de hoge prevalentie van veranderingen in signaalintensiteit op MRI, duiden erop dat het gebruik van MRI om een scaphoïdfractuur vast te stellen kan leiden tot overdiagnostiek en mogelijk -behandeling. Strategieën om de a priori kans van een scaphoïdfractuur te verhogen – zoals een klinische beslisregel – kunnen de accuratesse van MRI helpen te verhogen.

DEEL III – FRACTUURKARAKTERISTIEKEN

Fractuureigenschappen van het scaphoïd zoals fractuurlocatie en dislocatie correleren met belangrijke klinische uitkomsten zoals het genezingspercentage. In **Deel III** van dit proefschrift worden fractuurpatronen onderzocht, evenals hun correlatie met belangrijke voorspellers van genezing zoals dislocatie en comminutie. Een beter inzicht in deze patronen kan helpen om te voorspellen welke breuken genezen en welke een groter risico hebben op het ontwikkelen van pseudoartrose.

In **Hoofdstuk 7** werd gebruikt gemaakt van driedimensionale CT-analyse om fractuurpatronen te analyseren van 75 patiënten met een acute scaphoïdfractuur. Er werden vier dominante fractuurpatronen vastgesteld: fracturen van de proximale pool (7%), dwarse fracturen van de schacht (37%), schuin verlopende fracturen van de schacht (32%) en fracturen van het tuberculum of de distale pool (12%). Twee-en-vijftig procent (52%) van de fracturen waren comminutief. Dislocatie was aanwezig in 64% van de fracturen. In de geanalyseerde reeks van CT-scans kwam dislocatie significant vaker voor bij dwarse fracturen van de schacht (79%), ten opzichte van fracturen van de proximale pool (33%), schuine fracturen van de schacht (63%) en fracturen van de distale pool (1%). Comminutie kwam het meeste voor bij schuine fracturen van de schacht (67%); ten opzichte van proximale pool- (17%), dwarse schacht- (54%) en distale pool- (13%) fracturen. Negentig procent (90%) van de comminutieve fracturen waren tevens gedisloceerd. Het onderscheiden van verschillende typen fracturen – inclusief dwars of schuin verlopende breuken van de schacht - kan van belang zijn, aangezien deze fractuurpatronen mogelijk leiden tot verschillen in stabiliteit en het risico op dislocatie. Bovendien, dient de oriëntatie van het breukvlak in acht te worden genomen bij de operatieve behandeling van scaphoïdfracturen.

Fractuurdislocatie is de belangrijkste voorspeller voor het optreden van pseudoartrose. In **Hoofdstuk 8** werd het verband tussen fractuurlocatie, comminutie en dislocatie onderzocht middels driedimensionale CT-analyse van 51 fracturen van de schacht en proximale pool. Fractuurlocatie werd bestudeerd aan de hand van de hoogte van de corticale onderbreking aan de volaire en dorsale zijde van het scaphoïd. Het typische traumamechanisme in acht nemend – een val op de uitgestrekte hand – zou dit beschouwd kunnen worden als het zogenaamde intrede- (volaire zijde) en

uittredepunt (dorsale zijde) van de breuk. De locatie van de breuk aan de dorsale zijde van het scaphoïd (oftewel, het uittredepunt) en de aanwezigheid van comminutie waren nauw gecorreleerd met het dislocatie patroon.

Naarmate de fractuurlocatie aan de dorsale zijde van het scaphoïd meer distaal werd, nam translatie (in ulnaire, proximale en volaire richting), evenals angulatie (flexie en pronatie) van het distale fragment ten opzichte van het proximale fragment toe. Comminutieve fracturen toonden een grotere mate van dislocatie. De correlatie tussen de fractuurlocatie aan de dorsale zijde van het scaphoïd en het dislocatiepatroon, kan worden toegeschreven aan de dorsale lokalisatie van belangrijke carpale stabilisatoren: het dorsale intercarpale- (DIC) en dorsale scapholunaire (dSL) ligament. Aangezien fractuurlocatie het dislocatiepatroon direct beïnvloed, kan het aandachtig beoordelen van fractuurlocatie helpen bij het herkennen en reduceren van gedisloceerde fracturen.

DEEL IV – DUUR VAN GIPSIMMOBILISATIE VAN DE NIET-GEDISLOCEERDE SCAPHOÏD SCHACHTFRACTUUR

Er is toenemend bewijs dat simpele fracturen van de scaphoïd schacht, zonder dislocatie op CT, genezen met minder dan de traditionele 8 weken gipsimmobilisatie. Een verkorte gipsduur draagt niet alleen bij aan patiëntcomfort, arbeidsproductiviteit en kosteneffectiviteit, maar reduceert ook het relatieve voordeel van operatieve interventie (i.e. snellere werkhervatting). In de praktijk, worden echter vaak nog lange periodes (> 6-8 weken) van gipsimmobilisatie gehanteerd. In **Deel 4** van dit proefschrift werd de besluitvorming van artsen omtrent de duur van gipsimmobilisatie onderzocht.

In **Hoofdstuk 9** werd onderzocht welke klinische-, patiënt- en chirurg-gerelateerde factoren het besluit om gipsimmobilisatie na 8 of 12 weken te verlengen beïnvloeden. Tweehonderd-en-achttien (218) orthopedische, trauma- en (plastische) hand- en polschirurgen werden gevraagd om aanvullende immobilisatie (>8 en>12 weken) aan te bevelen of af te raden op basis van 16 fictieve scenario's van patiënten met een niet-gedisloceerde scaphoïd schachtfractuur. Gemiddeld 47% en 21% van de chirurgen adviseerden gipsduur te verlengen na respectievelijk, 8 en 12 weken. Onduidelijke consolidatie op röntgenonderzoek, pijn bij lichamelijk onderzoek en een voltooide gipsduur van 8 weken (versus 12 weken), waren de belangrijkste patiënt-gerelateerde factoren die verband hielden met de aanbeveling voor verlengde immobilisatie. Vrouwelijke chirurgen, chirurgen niet gespecialiseerd in traumachirurgie of de bovenste extremiteit en niet-Europese chirurgen, adviseerden vaker aanvullende gipsimmobilisatie. De resultaten van dit onderzoek impliceren dat de toepassing van een verkorte gipsduur mogelijk wordt verhinderd doordat chirurgen hun besluitvorming te veel baseren op lichamelijk- en röntgenonderzoek. Dit is in strijd met wetenschappelijk bewijs dat genezing van een scaphoïdfractuur niet goed te beoordelen is op röntgenonderzoek, en dat pijnintensiteit sterk afhankelijk is van psychosociale factoren bij patiënten met

letsel van de bovenste extremiteit. Bovendien, illustreert het gebrek aan consensus onder chirurgen de behoefte aan wetenschappelijk onderbouwde richtlijnen over de immobilisatieduur van CT-bewezen niet-gedisloceerde scaphoïd schachtfracturen.

In **Hoofdstuk 10** werd middels een prospectieve cohortstudie onder 46 patiënten onderzocht welke klinische, radiologische, en psychosociale factoren een verband hielden met verlengde gipsimmobilisatie. Inadequate consolidatie op röntgenonderzoek en een grotere mate van depressieve symptomen, waren beiden geassocieerd met een verlengde gipsduur van meer dan 6 weken. In tegenstelling tot de bevindingen van Hoofdstuk 9, werd er geen verband aangetoond tussen pijn bij lichamelijk onderzoek en de gipsduur. De resultaten van deze studie suggereren dat chirurgen hun besluit om gipsimmobilisatie te verlengen na 6 weken baseren op factoren die waarschijnlijk geen verband houden met de genezingskans van de fractuur. Dit omvat het röntgenologische aspect van de breuk, evenals ziektegedrag van patiënten dat zich mogelijk uit in symptomen van depressie. Om een kortere periode van gipsimmobilisatie in de praktijk te kunnen bewerkstelligen, moeten chirurgen onzekerheid over het radiologische aspect wellicht accepteren en kunnen anticiperen op interindividuele variaties in ziektegedrag van patiënten.

LIST OF PUBLICATIONS

Publications part of this thesis

Bulstra AEJ, Doornberg JN, Buijze GA, Bain GI. Anatomy of the Scaphoid Bone and Ligaments. *In: Buijze GA, Jupiter JB, eds. Scaphoid Fractures: Evidence-Based Management.* Elsevier; 2017:21-34.

Bulstra AEJ and Turow A, Oldhoff M, Hayat B, et al. 3D mapping of scaphoid fractures and comminution. *Skeletal Radiol.* 2020;49(10):1633-1647.

Langerhuizen DWG, Bulstra AEJ, Janssen SJ, et al. Is Deep Learning On Par with Human Observers for Detection of Radiographically Visible and Occult Fractures of the Scaphoid? *Clin Orthop Relat Res.* 2020;478(11):2653-2659

Bulstra AEJ, Al-Dirini RMA, Turow A, et al. The influence of fracture location and comminution on acute scaphoid fracture displacement: three-dimensional CT analysis. *J Hand Surg Eur Vol*. 2021;46(10):1072-1080.

Bulstra AEJ, Doornberg JN, Obdeijn MC, Buijze GA. Scaphoid Nonunion. *In: Bhandari M, ed. Evidence Based Orthopedics.* John Wiley and Sons; 2021:883-888.

Bulstra AEJ, Crijns TJ, Janssen SJ, et al. Factors associated with surgeon recommendation for additional cast immobilization of a CT-verified nondisplaced scaphoid waist fracture. *Arch Orthop Trauma Surg*. 2021;141(11):2011-2018.

Bulstra AEJ, Hendrickx LAM, Sierevelt IN, et al. Prospective Cohort Study to Investigate Factors Associated With Continued Immobilization of a Nondisplaced Scaphoid Waist Fracture. *J Hand Surg Am*. 2021;46(8):685-694.

Bulstra AEJ, Machine Learning C. A Machine Learning Algorithm to Estimate the Probability of a True Scaphoid Fracture After Wrist Trauma. *J Hand Surg Am.* 2022: 47(8):709-718.

Bulstra AEJ, van Boxel MF, Crijns TJ, Kelly J, Obdeijn MC, Kerkhoffs GMMJ, Doornberg JN, Ring D, Jaarsma RL. Routine MRI Among Patients With a Suspected Scaphoid Fracture Risks Overdiagnosis. *Clin Orthop Relat Res. 2023; 10.1097/CORR.0000000000002851* (online ahead of print)

Publications outside of this thesis

van Leeuwen MC, Bulstra AEJ, van Leeuwen PA, Niessen FB. A new argon gas-based device for the treatment of keloid scars with the use of intralesional cryotherapy. *J Plast Reconstr Aesthet Surg*. 2014;67(12):1703-1710.

van Leeuwen MCE, Stokmans SC, Bulstra AEJ, Meijer OWM, van Leeuwen PAM, Niessen FB. High-dose-rate brachytherapy for the treatment of recalcitrant keloids: a unique, effective treatment protocol. Plast Reconstr Surg. 2014;134(3):527-534.

van Leeuwen MC, Bulstra AEJ, Ket JC, Ritt MJ, van Leeuwen PA, Niessen FB. Intralesional Cryotherapy for the Treatment of Keloid Scars: Evaluating Effectiveness. *Plast Reconstr Surg Glob Open*. 2015;3(6):e437.

van Leeuwen MC, Bulstra AEJ, van der Veen AJ, Bloem WB, van Leeuwen PA, Niessen FB. Comparison of two devices for the treatment of keloid scars with the use of intralesional cryotherapy: An experimental study. *Cryobiology.* 2015;71(1):146-150.

van Leeuwen MCE, van der Wal MBA, Bulstra AEJ, Galindo-Garre, F, Molier, J, van Zuijlen PPM, van Leeuwen PAM, Niessen FB. Intralesional cryotherapy for treatment of keloid scars: a prospective study. *Plast Reconstr Surg*. 2015;135(2):580-589.

van Leeuwen MC, Stokmans SC, Bulstra AEJ, Meijer OW, Heymans MW, Ket JC, Ritt, MJ

van Leeuwen PAM, Niessen, FB. Surgical Excision with Adjuvant Irradiation for Treatment of Keloid Scars: A Systematic Review. *Plast Reconstr Surg Glob Open*. 2015;3(7):e440.

Fricke TA, Bulstra AEJ, Naimo PS, Bullock A, Robertson T, d'Udekem Y, Brizard CP, Konstantinov, IE. Excellent Long-Term Outcomes of the Arterial Switch Operation in Patients With Intramural Coronary Arteries. *Ann Thorac Surg*. 2016;101(2):725-729.

Fricke TA, Bulstra AEJ, Loyer BR, Weintraub RG, d'Udekem Y, Brizard, CP, Konstantinov, IE, Outcomes of the Arterial Switch Operation in Children Less Than 2.5 Kilograms. *Ann Thorac Surg*. 2017;103(3):840-844.

Hendrickx LAM, Sobol GL, Langerhuizen D, Bulstra AEJ, Hreha J, Sprague S, Sirkin MS, Ring D, Kerkhoffs GMMJ, Jaarsma RL, Doornberg JN; Machine Learning Consortium A Machine Learning Algorithm to Predict the Probability of (Occult) Posterior Malleolar Fractures Associated with Tibial Shaft Fractures to Guide "Malleolus First" Fixation. *Journal of Orthopaedic Trauma.* 2019. 34(3):131-138

Bergsma M, Bulstra AEJ, Morris D, Janssen M, Jaarsma R, Doornberg J. A Prospective Cohort Study on Accuracy of Dorsal Tangential Views to Avoid Screw Penetration With Volar Plating of Distal Radius Fractures. *J Orthop Trauma*. 2020;34(9):e291-e297.

Oosterhoff JHF, Doornberg JN, Machine Learning Consortium. Artificial intelligence in orthopaedics: false hope or not? A narrative review along the line of Gartner's hype cycle. *EFORT Open Rev*. 2020;5(10):593-603.

Machine Learning Consortium, on behalf of the SPRINT and FLOW Investigators. A Machine Learning Algorithm to Identify Patients with Tibial Shaft Fractures at Risk for Infection After Operative Treatment. *J Bone Joint Surg Am. 2021*;103(6):532-540.

Machine Learning Consortium, on behalf of the SPRINT and FLOW Investigators. A Machine Learning Algorithm to Identify Patients at Risk of Unplanned Subsequent Surgery After Intramedullary Nailing for Tibial Shaft Fractures. *J Orthop Trauma. 2021;*35(10):e381-e388.

Bulstra AEJ, Vidovic AJ, Doornberg JN, Jaarsma RL, Buijze GA. Scaphoid Length Loss Following Nonunion Is Associated with Dorsal Intercalated Segment Instability. *J Wrist Surg. 2023;* 10.1055/s-0043-1760753

Cohen A, van Boxel MF, Bulstra AEJ, Doornberg JN, Colaris JW, on behalf of the Machine Learning Consortium. Can we safely discharge patients with a Machine Learning probability calculated low risk for an occult scaphoid fracture at the emergency department? An external validation study. *Submitted to Clin Orthop Relat Res 2023.*

PORTFOLIO

PHD TRAINING		ECTS
Seminars, workshops and masterclasses		
2018-19	Weekly research meetings Orthopaedic & Trauma surgery Unit Flinders Medical Centre	4.0
2019-19	Weekly grand rounds Orthopaedic & Trauma surgery Unit Flinders Medical Centre	3.0
2018-19	Monthly upper limb research meetings Orthopaedic & Trauma Surgery Unit Flinders Medical Centre	1.0
2018	Wrist arthroscopy workshop led by prof. Greg Bain and dr. Scott Wolfe	0.3
Supervising		
2018	M.G.E. Oldhoff Master's Student Biomedical Engineering Delft University of Technology.	2.0
Other		
2018	Observership at Hand & Arm Service Mass General's Department of Orthopaedic Surgery (under supervision of dr. Neal Chen)	1.5

PODIUM PRESENTATIONS		ECTS
Bulstra AEJ and Turow AT, Oldhoff MG, Hayat B, Jaarsma RL, Doornberg JN, Bain GI; *3D Mapping of Scaphoid Fractures and Comminution.*		
2018	South Australian Hand Surgery Society (SAHSS), Annual Meeting, Adelaide, Australia.	0.5
2018	Australian Orthopaedic Association SA/NT Meeting, Adelaide, Australia	0.5
2018	Australian Orthopaedic Association, Annual Scientific Meeting, Australia (presented by A. Turow).	0.5
2019	International Federation of Societies for Surgery of the Hand (IFSSH), Berlin, Germany	0.5
2019	Traumadagen, Amsterdam, the Netherlands.	0.5
2019	Nederlandse Vereniging van Plastische Chirurgie (NVPC) Wetenschappelijke Vergadering, Amsterdam, the Netherlands.	0.5
Bulstra AEJ, Crijns T, Jansen S, Buijze GA, Ring D, Jaarsma RL, Kerkhoffs GMMJ, Obdeijn MC, Doornberg JN, Science of Variation Group. *Factors Associated With Surgeon Recommendation for Additional Cast Immobilization of a Nondisplaced Scaphoid Waist Fracture*		
2018	South Australian Hand Surgery Society (SAHSS), Annual Meeting, Adelaide, Australia.	0.5
2019	Australian Orthopaedic Association, Annual Scientific Meeting, Canberra, Australia.	0.5
2018	Australian Orthopaedic Association SA/NT Meeting, Adelaide, Australia	0.5
2019	International Federation of Societies for Surgery of the Hand (IFSSH), Berlin, Germany	0.5
2019	Nederlandse Vereniging van Plastische Chirurgie (NVPC) Wetenschappelijke Vergadering, Amsterdam, the Netherlands.	0.5

Bulstra AEJ, Kelly J, Kerkhoffs GMMJ, Ring D, Obdeijn MC, Doornberg JN, Jaarsma RL. *Efficacy of MRI in Patients with Suspected Scaphoid Fractures*		
2018	Australian Orthopaedic Association, Annual Scientific Meeting, Perth, Australia	0.5
2018	Australian Orthopaedic Trauma Society, Noosa, Australia (presented by J. Kelly)	0.5
Bulstra AEJ, on behalf of the Machine Learning Consortium. *A Machine Learning Algorithm to Estimate the Probability of a True Scaphoid Fracture After Wrist Trauma.*		
2019	Symposium Experimenteel Onderzoek Heelkundige Specialismen (SEOHS), Amsterdam, the Netherlands	0.5
2019	Australian Orthopaedic Association, Annual Scientific Meeting, Canberra, Australia	0.5
2019	Australian Orthopaedic Association SA/NT Meeting, Serafino, Australia	0.5
2019	South Australian Hand Surgery Society (SAHSS), Annual Meeting, Adelaide, Australia (*best presentation Award)*	0.5
2020	Federation of European Societies for the Surgery of the Hand, (FESSH), virtual oral presentation FESSH (ON)line congress due to COVID-19.	0.5
2020	Nederlandse Vereniging van Plastische Chirurgie (NVPC) Wetenschappelijke Vergadering, Amsterdam, the Netherlands, Top 8 Abstracts selected for online oral presentation due to COVID.	0.5
Bulstra AEJ, Hendrickx LAM, Buijze GA, Ring D, Kerkhoffs GMMJ, Jaarsma RL, Doornberg JN**.** *Prospective Cohort Study to Investigate Factors Associated with Continued Immobilization of a Nondisplaced Scaphoid Waist Fracture*		
2020	Federation of European Societies for the Surgery of the Hand, (FESSH), virtual oral presentation FESSH (ON)line congress due to COVID-19.	0.5
Bulstra AEJ, Al-Dirini RMA, Turow A, Oldhoff MGE, Bryant K, Obdeijn MC, Doornberg JN, Jaarsma RL. *The Influence of Fracture Location and Comminution on Acute Scaphoid Fracture Displacement: Three-Dimensional CT Analysis*		
2019	South Australian Hand Surgery Society (SAHSS), Annual Meeting, Adelaide, Australia	0.5

POSTER PRESENTATIONS		**ECTS**
Bulstra AEJ, Kelly J, Kerkhoffs GMMJ, Ring D, Obdeijn MC, Doornberg JN, Jaarsma RL. *Efficacy of MRI in Patients with Suspected Scaphoid Fractures - a Retrospective Imaging Study of 244 Patients*		
2018	American Society of Surgery of the Hand (ASSH), Annual Meeting, Boston, United States	0.5
Bulstra AEJ, Crijns T, Janssen S, Buijze GA, Ring D, Jaarsma RL, Kerkhoffs GMMJ, Obdeijn MC, Doornberg JN, Science of Variation Group. *Factors Associated With Surgeon Recommendation for Additional Cast Immobilization of a Nondisplaced Scaphoid Waist Fracture.*		0.5
2019	American Society of Surgery of the Hand (ASSH), Annual Meeting, Las Vegas, United States	0.5

Bulstra AEJ and Turow AT, Oldhoff MGE, Hayat B, Jaarsma RL, Doornberg JN, Bain GI. *Three-Dimensional Computed Tomography Analysis of Acute Scaphoid Fracture Patterns*		
2019	American Society of Surgery of the Hand (ASSH), Annual Meeting, Las Vegas, United States	0.5
Bulstra AEJ, on behalf of the Machine Learning Consortium. *A Machine Learning Algorithm to Estimate the Probability of a True Scaphoid Fracture After Wrist Trauma.*		
2019	Traumadagen, Amsterdam, the Netherlands.	0.5
Bulstra AEJ, Al-Dirini R, Turow A, Oldhoff MGE, Jaarsma RL, Doornberg JN, MC Obdeijn, Bain GI *The Effect of Fracture Location and Comminution on Displacement of Acute Scaphoid Fractures – Three-Dimensional Computed Tomography Analysis*		
2020	Federation of European Societies for the Surgery of the Hand (FESSH), (ON) line-week due to COVID-19	0.5
Langerhuizen DWG, Bulstra AEJ, Janssen SJ, Ring D, Kerkhoffs GMMJ, Jaarsma RL, Doornberg JN. *Detection Of Radiographically Visible And Occult Fractures Of The Scaphoid Using Deep Transfer Learning*		
2020	21st Vienna European federation of National Associations of Orthopaedics and Traumatology (EFORT), Vienna, Austria.	0.5
Bulstra AEJ, Hendrickx LAM, Buijze GA, Ring D, Kerkhoffs GMMJ, Jaarsma RL, Doornberg JN**.** *Prospective Cohort Study to Investigate Factors Associated with Continued Immobilization of a Nondisplaced Scaphoid Waist Fracture*		
2020	American Society of Surgery of the Hand (ASSH), Annual Meeting, San Antonio, United States	0.5

(INTER)NATIONAL CONFERENCES		**ECTS**
2018	American Society of Surgery of the Hand (ASSH), Annual Meeting, Boston, United States	1.5
2018	Australian Orthopaedic Association SA/NT Meeting, Adelaide, Australia	0.3
2018	Australian Orthopaedic Association, Annual Scientific Meeting, Perth, Australia	0.3
2018 2019	South Australian Hand Surgery Society (SAHSS), Annual Meeting, Adelaide, Australia.	0.6
2019	International Federation of Societies for Surgery of the Hand (IFSSH), Berlin, Germany	1.5
2019	Traumadagen, Amsterdam, the Netherlands.	0.5
2019	Australian Orthopaedic Association, Annual Scientific Meeting, Canberra, Australia.	0.3
2019	Symposium Experimenteel Onderzoek Heelkundige Specialismen (SEOHS), Amsterdam, the Netherlands	0.3
2019	Australian Orthopaedic Association SA/NT Meeting, Serafino, Australia	0.3
2019- 2020	Nederlandse Vereniging van Plastische Chirurgie (NVPC) Wetenschappelijke Vergadering, Amsterdam, the Netherlands.	0.6

SPECIAL ITEMS (PODCAST / INTERVIEW)		ECTS
2022	Journal of Hand Surgery Podcast Episode 77. Interview by Editor in Chief Dr. Graham on the August 2022 lead article *"A Machine Learning Algorithm to Estimate the Probability of a True Scaphoid Fracture After Wrist Trauma"*.	0.3
2021	Journal of Hand Surgery Podcast July 2021 editor's Choice Audio Abstracts "Prospective Cohort Study to Investigate Factors Associated With Continued Immobilization of a Nondisplaced Scaphoid Waist Fracture"	0.3

PARAMETERS OF ESTEEM	
Grants	
2019	Hospital Research Foundation Statewide Travel Grant – Flinders Medical Centre
2019	Prins Bernhard Cultuurfonds Studiebeurs
2019	Stichting Prof. Michaël-van Vloten Fonds
2019	Flinders University Student Association Development Grant
2018	Anna Fonds Reisbeurs
2018	KNAW van Leersum Beurs
2018	Jo Kolk Studiefonds
2018	Marti-Keuning Eckhardt Stichting
2018	Flinders University Scholarship Tuition Fee Waiver
2018	Flinders University Student Association Development Grant
Awards and Prizes	
2018	Dodridge Prize Best Presentation – South Australian Hand Surgery Society Annual Meeting (presented by Arthur Turow)
2019	Dodridge Prize Best Presentation - South Australian Hand Surgery Society Annual Meeting

ABBREVIATIONS

3D	three dimensional
4CA	four corner arthrodesis
ANOVA	analysis of variance
AUC	area under the receiver operating characteristic curve
AVN	avascular necrosis
BMI	body mass index
CAT	computer adaptive test
CI	confidence interval
CNN	convolutional neural network
CT	computed tomography
CT-distance	distance between the capitate and triquetrum
DIC	dorsal intercarpal
DICOM	digital imaging and communications in medicine
DISI	dorsal intercalated segment instability
DRC	dorsal radiocarpal
dSL(L)	dorsal scapholunate (ligament)
ED	emergency department
LIPUS	low-intensity pulsed ultrasound
LRL	long radiolunate
MFC	medial femoral condyle
ML	machine learning
MOI	mechanism of injury
MPR	multiplanar reconstructions
MRI	magnetic resonance imaging
NSAID	nonsteroidal anti-inflammatory drugs
NVBG	non vascularized bonegraft
PACS	picture archiving and communication system
PEMF	pulsed electromagnetic field therapy
PI	pain interference
PRC	proximal row carpectomy
PROMIS	Patient-Reported Outcomes Measurement Information System

PSEQ	pain self-efficacy questionnaire
pSL(L)	palmar scapholunate (ligament)
RC	radiocapitate
RCT	randomized controlled trial
rhBMP	recombinant human bone morphogenetic proteins
ROC	receiver operating characteristics curve
RS	radioscaphoid
RSC	radioscaphocapitate
RSL	radioscapholunate
ScC	scaphocapitate
ScTd	scaphotrapezoid
ScTm	scapotrapezium
SD	standard deviation
SL	scapholunate
SLIO	scapholunate interosseous ligament
SNAC	scaphoid nonunion advanced collapse
SOVG	Science of Variation Group
STL	stereolithography files
STROBE	Strengthening the Reporting of Observational Studies in Epidemiology
STT(J)	scaphoid-trapezio-trapezoid (joint)
TCL	transverse carpal ligament
TRIPOD	Transparent Reporting of multivariable Prediction models for individual Prognosis Or Diagnosis
VBG	vascularized bone graft
VGG	visual geometry group
vScTq	volar scaphotriquetral

DANKWOORD

Heel graag wil ik iedereen bedanken die op wat voor manier dan ook heeft geholpen om dit proefschrift een realiteit te maken: collega's, patiënten, familie en vrienden. Naast mijn dank aan alle patiënten die aan onderzoeken hebben deelgenomen, wil ik in het bijzonder bedanken:

Prof. dr. R. Jaarsma, beste Ruurd, ontzettend veel dank voor de prachtige tijd in Adelaide, waar jij ons zowel binnen als buiten het ziekenhuis met veel warmte en enthousiasme hebt ontvangen. Dankzij jouw nuchtere, pragmatische Nederlandse blik, 'with a touch of Aussie calmness' verliet ik jouw kantoor of research meeting nooit zonder oplossing of gerustgesteld hart. Jouw diplomatieke en empathische begeleiding waren onmisbaar tijdens mijn onderzoek.

Prof. dr. G. Kerkhoffs, beste Gino, heel veel dank dat ik ook als 'plasticus' op jouw vertrouwen en altijd snelle feedback en begeleiding kon rekenen, ook aan de andere kant van de wereld. Dat we onze onderzoekservaringen en het leven buiten het ziekenhuis tijdens jouw bezoek aan Adelaide konden delen was een mooi hoogtepunt!

Prof. dr. J. Doornberg, beste Job, jouw aanstekelijke enthousiasme was het startsein en de brandstof voor ruim twee waanzinnige onderzoeksjaren in Australië. Alles kon en alles mocht. Ik bewonder jouw energie en vermogen om mensen bijeen te brengen. Zonder jou was dit boekje er niet geweest. Jouw 'the sky is the limit' en 'champagne session' mentaliteit hebben ervoor gezorgd dat ik mijn tijd in Australië als één groot avontuur heb beleefd. Naast alles wat ik vanaf het begin op onderzoeksvlak van jou heb mogen leren, zullen bovenal deze levenslessen mij bijblijven. Heel veel dank voor alles!

Dr. M. Obdeijn, beste Miryam, alhoewel onze samenwerking veelal 'trans-pacific' emailwisselingen en bliksembezoeken in Nederland omvatte, kon ik altijd rekenen op jouw nauwkeurige feedback en loopbaan adviezen. Nu ik met mijn opleiding ben gestart, zij het in een andere regio, hoop ik ook op klinisch vlak nog van jou te mogen leren.

Overige leden van de promotiecommissie, **prof. dr. M.J.P.F. Ritt, dr. H.A. Rakhorst, prof. dr. M. Maas, dr. C.M. Lameijer, prof. dr. B.J. van Royen, prof. dr. J.A.M. Bramer**, hartelijk dank voor uw interesse in en het beoordelen van mijn proefschrift.

Prof. dr. Bain, thank you for sharing your passion for upper extremity surgery and research with me. You taught me to approach challenging concepts with a creative and open mind, always leaving me with new questions to answer and paths to explore. If I can maintain only a fraction of your curiosity and enthusiasm, I know I will never experience a boring day in my career.

Prof. dr. Ring, dear David, I cannot thank you enough for your mentorship and perseverance in many of my projects. Your devotion to research and improving patient care by investigating and promoting concepts that are off the beaten track are really inspiring. You have taught me the essentials of research, and most importantly not be discouraged by a setback.

Dr. G. Buijze, beste Geert, 'big shoes to fill' (en 'hóeveel kan je publiceren over dat éne botje?') waren mijn eerste gedachten toen ik mij, net als jij, mocht gaan vastbijten in het scaphoïd. Ontzettend veel dank voor de vliegende start en kansen die jij mij, altijd met mijn belang voorop, hebt gegund. Zowel jouw wetenschappelijke als klinische loopbaan zijn een groot voorbeeld.

Dr. Rami Al-Dirini, thank you for all your time and effort invested in translating our clinical ideas into mindblowing codes and algorithms. Our 3D analysis of scaphoid fracture displacement would not have been possible without your expertise.

Raphael Garcia, thank you for welcoming us into the inspiring 3D-lab at Tonsley and sharing your knowledge, time and patience with us, clinicians and technology newbies.

To all surgeons, residents, nurses and other staff at the **Flinders Medical Centre Trauma Clinic**, thank you for helping me include all patients for our prospective study. From putting up with endless 'scaphoid tests' to a dazzling number of post-its all over clinic, the completion of this study would not have been possible without you.

All **co-authors,** thank you for your collaboration and valuable input and expertise in all studies that constitute this thesis. This thesis would not have been possible without you.

Lieve **Jetske**, samen onderzoek doen in Australië was het begin van onze vriendschap. Van de genadeloze 'backwash' en minstens even genadeloze 'journal revisions', tot waanzinnige trips, the Australian Open, jouw promotie en vandaag die van mij: het was en is geweldig om al deze hoogte- en dieptepunten met jou te kunnen delen! Sindsdien weet ik dat ik altijd op je kan rekenen. Ik ben ontzettend blij dat ik jou sinds Australië zo'n dierbaar vriendinnetje kan noemen én dat jij vandaag als paranimf naast mij staat!

Lieve **Sophie**, alhoewel onze gezamenlijke roots in Groningen en collegezaal 1 van het AMC liggen, hebben wij elkaar tijdens onze co-schappen en vooral tijdens alle leuke dingen in het leven daarbuiten, zoveel beter leren kennen! Ontelbaar mooie en grappige herinneringen aan onze ziekenhuisavonturen, vakanties, kookavonden met fijne gesprekken en onze kortdurende overlap in Australië! Je weet me altijd aan het lachen te maken, ook wanneer de last-minute-rode-vlekken-deadline-stress de overhand heeft over onze zo gewilde 'hang loose' mentaliteit. Zo leuk om vandaag met jou als paranimf te vieren!

De **'Cotutelles', Jetske, Annelise, David, Robin, Bram, Minke, Batur**, **Mads,** dank jullie wel voor de samenwerking en de mooie avonturen die we met elkaar hebben beleefd. Van alle strand- en surfdagen, kampeertrips en BBQ's tot aan congresdagen en eindeloze Tonsley sessies!

Dutchies in Adelaide, **familie Jaarsma, familie Doornberg** en **familie Janssen**, wat was het heerlijk om met regelmaat aan jullie warme Nederlandse familietafels aan te mogen schuiven! Surfweekends in Middleton, BBQ's in West Lake Shores en eindeloze borrelsessies in Henley Beach behoren tot mijn mooie herinneringen aan Australië. En laten we jullie voorbeeldfunctie voor een aantal pretty kick-ass life-goals niet vergeten!

Taran, Katharina, Sylvia, thank you for welcoming us in Adelaide and Flinders Medical Centre. Theo's coffee breaks were always a great kick start of the day! **Kim,** thank you for your support and guidance through many research and logistic puzzles.

Ellen Rolleman, zonder jouw hulp en ondersteuning hadden we de eindsprint naar de finishline nooit kunnen inzetten. Veel dank daarvoor!

Plastische chirurgie OLVG, dank jullie wel voor de leuke en leerzame tijd, eerst als semi-arts en daarna als ANIOS. Mede door jullie was de keuze voor de plastische chirurgie onbetwist.

Plastische chirurgie Isala, ontzettend leuk om deze mijlpaal met jullie te vieren, en ik kijk enorm uit naar de rest van mijn opleiding met dit mooie team!

Lieve, attente en trouwe vriendinnetjes: zonder jullie interesse, steun en altijd welkome afleiding had ik dit proefschrift nooit tot een succesvol einde kunnen brengen! **Ils,** onze gehele studie hebben wij zij aan zij voltooid. Van liters cola light op het voetenplein tot witte wijn op de Molukkenstraat; van AH maaltijdsalades in tentamenweek tot overheerlijke pasta vongole aan jouw vertrouwde keukentafel. Jij staat altijd voor me klaar met integer advies, een goede portie cynische humor en onuitputtelijke support middels lieve berichtjes en attente, creatieve brievenbusverrassingen. **Stien,** van de peuterspeelzaal tot het studentenhuis, er zijn weinig mensen die mij beter kennen dan jij. Voor een luisterend oor of memorabele avond, als één van mijn oudste vriendinnetjes kan ik altijd op jou bouwen. Dank voor je engelengeduld en interesse wanneer de onderzoeks- en ziekenhuispraat-plaat weer eens werd aangezwengeld. **Mies**, jouw oprechte enthousiasme en interesse in alles en iedereen om jou heen – inclusief deze gezapige +200 pagina's - maken je zo'n fijn mens en ontzettend dierbare vriendin. Met jou kan ik altijd lachen. Ik hoop dat we nog jaren samen dansjes zullen wagen en de slappe lach zullen hebben. **Eem,** van samen in de wieg, tot aan de andere kant van het land of wereldbol, de flauwe grappen zullen altijd blijven en onze paden zullen elkaar altijd blijven kruisen! **Char,** een opgetogen en energiek 'early-bird' belletje naar Down

Under - nog vóór jouw chirurgie overdracht - bracht mij vaak weer de hele onderzoeksdag door. Eén van de vele voorbeelden van hoe lief en trouw jij als vriendinnetje bent! **Har,** vertrok ik als brave Hendrik om 8u naar college, bleef jij als gezelligheidsdier na een logeerpartij nog even met de rest in huis hangen. Geen verrassing, dat we later écht huisgenoten werden en ik altijd bij je terecht kon voor een portie van jouw positiviteit onder het genot van een kop thee. Na vandaag volgen er hopelijk weer meer dinertjes in Rotterdam en Amersfoort! **Kim,** er zijn er weinig zo attent als jij. Ik mis onze rondjes door het Vondelpark of op de Jaap Eden Baan, waarin jij vol energie mijn hoofd weer wist te legen en elk probleem werd opgelost. Naast de locatie, laat ik zowel de activiteit als het niveau daarvan maar in het midden, wanneer beginnen we aan de volgende hobby? **Myrth,** met jou kan ik lachen en werkelijk alles bespreken. Ik hecht enorm veel waarde aan jouw eerlijkheid en adviezen, welke je altijd met een goede dosis humor en met een integer inzicht uit elk gesprek weet te destilleren. Naast ons overlappende verlof, kijk ik ook naar onze langverwachte kapiteins carrière! Lieve **jaargenootjes**, tijdens mijn eerste studentenjaren hebben jullie deze Zwitserse studiebol gelukkig vaak genoeg uit de studiebanken weten te trekken. Veel dank voor alle leuke avonden, dinertjes en vakanties! Dear **Swisses,** I'm glad that after spending a few years spread out all across the globe, our paths have started to cross again. I'm looking forward to our next get together. Hands up for organizing the next wedding, anyone?

Lieve **familie Hendrickx,** dank jullie wel dat ik Ran zo lang van jullie mocht stelen in Australië. Jullie werden gemist! Bernadette en René, wat was het bijzonder om jullie te mogen verwelkomen in Adelaide en om samen een deel van het land te ontdekken! De herinneringen aan onder andere Kangaroo Island zijn enorm dierbaar.

Lieve **Reinier en Diederick,** jullie staan altijd voor me klaar. Als jongste van de drie kijk ik enorm naar jullie op en heb ik veel bewondering voor hoe jullie in het leven staan. Zonder de portie relativeringsvermogen en humor van mijn oudere broers, had ik dit proefschrift niet (of in ieder geval niet in 'good sanity') kunnen afronden. Zo fijn dat ik voor de kleine dingen - van een 'mind numbingly proofread' tot een creatieve spoedklus - maar bovenal voor de grote dingen in het leven altijd op jullie kan rekenen! Lieve **Léo en Dickie**, al zo lang onderdeel van de familie, zonder jullie nooit compleet. Thanks for keeping us all sane!

Lieve **oma**, er zijn er weinig zo geïnteresseerd en betrokken bij mijn opleiding en onderzoek als u. Lang waren wij de oudste en de jongste van de familie en ik had mij geen beter voorbeeld kunnen wensen. Ik hoop dat ik op uw leeftijd nog net zo positief, geïnteresseerd en open in het leven sta. Ik heb u lang laten wachten, maar wat ben ik blij dat ik deze dag samen met u op de eerste rij mag vieren!

Lieve **pap en mam**, dit boekje is voor jullie, want zonder jullie onvoorwaardelijke steun was het er nooit geweest! Ik kan jullie niet genoeg bedanken voor alles wat jullie van kleins

af aan voor mij hebben gedaan. Niets was en is voor jullie te gek! Dat jullie altijd achter mijn beslissingen staan en op alle mogelijke manieren voor mij klaar staan, betekent alles voor me. Met jullie als voorbeeld, heb ik geleerd door te zetten, met een open blik nieuwe avonturen aan te gaan en de écht belangrijke dingen in het leven te vieren en te koesteren.

Lieve **Ran,** jou wil ik het meeste bedanken. Daar gingen we dan, als verliefde studenten op avontuur naar Australië. Opeens was je naast mijn vriend ook mijn collega, surf instructeur, statistisch adviseur, therapeut ten tijde van promotiestress, maar bovenal, altijd mijn steun en toeverlaat. Ik had dit onvergetelijke avontuur met niemand anders willen delen. Ik ben mega trots op alles wat jij hebt gepresteerd en kan je niet genoeg bedanken voor jouw onvoorwaardelijke steun! Ik kan niet wachten op de volgende avonturen die we nog gaan beleven, want met jou naast mij, is alles in het leven mooier.

CURRICULUM VITAE

Anne Eva Bulstra was born on October 12th 1991 in Apeldoorn. After spending her early childhood years in Brunei and Groningen, she moved to Switzerland at the age of 13. In 2009 she graduated from the International School of Geneva where she obtained her International Baccalaureate. Prior to commencing university, she spent several months in Ghana doing volunteer work in a children's orphanage and local hospital. In the operating theatre in Ghana her interest in surgical specialties was first elicited.

In 2010 Anne Eva returned to the Netherlands to study Medicine at the University of Amsterdam (UvA). Her interest in plastic- and reconstructive surgery was soon sparked and later confirmed through research projects at the department of plastic and reconstructive surgery at the VU Medical centre and clinical rotations in plastic surgery in OLVG and the Royal Free Hospital, London.

After completing her medical degree Cum Laude in 2017, Anne Eva was accepted into the Cotutelle PhD program, an official collaboration between the UvA, the Netherlands, and Flinders University, Adelaide Australia. She was rewarded multiple grants allowing her to work as a PhD candidate in hand- and wrist surgery at Flinders Medical Centre, Adelaide, Australia, under guidance of prof. dr. Ruurd Jaarsma, prof. dr. Job Doornberg, prof. Gino Kerkhoffs and dr. Miryam Obdeijn. She presented multiple papers at international conferences in Australia, Boston (ASSH) and Berlin (FESSH).

After two exciting years in Australia Anne Eva returned to the Netherlands in 2020 to gain (ANIOS) experience in general surgery at the Rode Kruis Ziekenhuis, Beverwijk and plastic surgery at OLVG Hospital, Amsterdam. In 2021 she started her training as a resident (AIOS) in plastic-, reconstructive- and hand- and wrist surgery in Isala, Zwolle under supervision of dr. Michiel Tellier and dr. Joris Franken.